

# University of Alberta

## Examining the Structure, Function and Mode of Action of Bacteriocins from Lactic Acid Bacteria

by

Leah Alina Martin-Visscher

A thesis submitted to the Faculty of Graduate Studies and Research  
in partial fulfillment of the requirements for the degree of

Doctor of Philosophy

Department of Chemistry

©Leah Alina Martin-Visscher  
Spring, 2010  
Edmonton, Alberta

Permission is hereby granted to the University of Alberta Libraries to reproduce single copies of this thesis and to lend or sell such copies for private, scholarly or scientific research purposes only. Where the thesis is converted to, or otherwise made available in digital form, the University of Alberta will advise potential users of the thesis of these terms.

The author reserves all other publication and other rights in association with the copyright in the thesis and, except as herein before provided, neither the thesis nor any substantial portion thereof may be printed or otherwise reproduced in any material form whatsoever without the author's prior written permission.

## **Examining Committee**

Dr. John C. Vederas (Supervisor)  
*Department of Chemistry*

Dr. Christopher W. Cairo  
*Department of Chemistry*

Dr. David R. Bundle  
*Department of Chemistry*

Dr. John S. Klassen  
*Department of Chemistry*

Dr. Hasan Uludag  
*Department of Chemical & Materials Engineering*

Dr. Michael D. Burkart (External)  
*Department of Chemistry & Biochemistry*  
*University of California at San Diego*

# **Dedication**

*For my family*

## Abstract

Carnocyclin A (CclA) is a remarkably stable, potent bacteriocin produced by *Carnobacterium maltaromaticum* UAL307. Elucidation of the amino acid and genetic sequences revealed that CclA is a circular bacteriocin. Preliminary structural studies (dynamic light scattering, NMR, circular dichroism, stereochemical analysis) indicated that CclA is monomeric and alpha-helical in aqueous conditions and composed of L-residues. The 3D structure of [<sup>13</sup>C,<sup>15</sup>N]CclA was solved by NMR, revealing a compact arrangement of four helices. To examine the structure of the precursor peptide (pCclA) several fusion proteins were constructed and overexpressed; however, pCclA could not be isolated. To investigate the requirements for cyclization, several internally hexahistidine-tagged (His<sub>6</sub>) pCclA mutants were constructed. Expression conditions are underway.

PisI was heterologously expressed and confirmed to impart protection against piscicolin 126 (PisA). Labeled and unlabeled PisA and PisI were purified following overexpression as maltose-binding protein fusions (MalE-fusions) and Factor Xa cleavage. NMR studies indicated that PisI and PisA do not physically interact. The 3D structure of PisI was solved by NMR, confirming that the four-helix bundle is a conserved motif for the immunity proteins of type IIa bacteriocins. The putative receptor proteins for these bacteriocins were cloned and overexpressed as His<sub>6</sub>-fusion proteins. Experiments are underway to optimize the expression and purification of these membrane proteins.

The peptidase domain of the ABC-transporter protein (CbnTP) for carnobacteriocin B2 (CbnB2) was overexpressed as a His<sub>6</sub>-fusion protein. Active protease could not be purified from inclusion bodies, but was obtained as soluble protein following low-temperature overexpression. The CbnB2 precursor pCbnB2 (and a truncated derivative pCbnB2<sub>-RP</sub>) was purified following overexpression as a MalE-fusion and Factor Xa cleavage. pCbnB2 was incubated with CbnTP and MALDI-TOF and activity testing confirmed that CbnTP cleaved the leader peptide from pCbnB2. Five Cys→Ser CbnTP mutants were constructed. Crystallographic studies of CbnTP are underway.

Six bacteriocins (nisin, gallidermin, lacticin 3147, CclA, PisA, enterocin 710C) were tested against Gram-negative bacteria (*E. coli* DH5 $\alpha$ , *Pseudomonas aeruginosa* ATCC 14207, *Salmonella typhimurium* ATCC 23564) in the absence and presence of EDTA. PisA and lacticin 3147 exhibited minimal activity, whereas the other bacteriocins killed at least one strain, in the presence of EDTA.

## Acknowledgements

The work presented in this thesis was made possible by the support, encouragement and enthusiasm of many different people. Foremost, I am thankful to my supervisor, Professor John Vederas. Thank-you for you providing me with the opportunity to do this research – for your endless guidance, commitment, insight, and encouragement. I am thankful to all the members of the Vederas group whom I have been privileged to work with. You have created a stimulating and enjoyable work environment. Whether through scientific discussions, group dinners, cocktails and make-up nights, free babysitting, or mindless lunchtime chitchat, I am thankful for the numerous ways in which you have encouraged and helped me. Special thanks to WISEST and summer students Anna King (2008), Michael Kreuzer (2008) and Erika Steels (2009) for their help and contributions to this work. I am particularly grateful to Clarissa Sit and Dr. Marco van Belkum for their assistance in proofreading this manuscript and offering many useful suggestions. To Christine Otter, thank-you for always being on top of things and making sure that details were always taken care of. You are a tremendous asset to our group. There are many others who have been instrumental in helping me over the past five years. I am especially grateful to Dr. Randy Whittal and Jing Zheng for their help with mass spectrometry, and to Wayne Moffat for performing circular dichroism experiments. I extend a tremendous amount of thanks to Dr. Albin Otter, Mark Miskolzie, Dr. Ryan McKay and Dr. Tara Sprules for their help with NMR. To Tara, thank-you for teaching me how to interpret biomolecular NMR data and moreover, for your continued encouragement over the years. I am

particularly thankful to Gareth Lambkin, Dr. Jean Percy, Dr. Sandra Marcus and Dr. Marco van Belkum for their help with numerous biological and genetic experiments. To Marco, I am tremendously grateful for all your help. Although I will never be as dexterous as you, I am thankful for everything you have taught me. You have been a wonderful (and patient) teacher, as well as a friend. For funding, thanks to the University of Alberta, the Natural Sciences and Engineering Research Council of Canada, Alberta Heritage Foundation for Medical Research and the Advanced Foods and Materials Network.

I am indebted to my family for their constant love. They have been an invaluable source of strength and support throughout the duration of my graduate work. To Mom and Dad, I am so grateful for your encouragement, hugs, endless (and free) babysitting and constant reminder of what really is important in life. To Nathaniel, thank-you for being such an awesome big brother – your advice has helped me make it through the last five years, even when the challenges seemed insurmountable. To Bronwyn, thank-you for always knowing what I needed. To Nigel, you will never know how much wisdom you have shown me. Thank-you for being the quiet, calming presence that you always were. I will forever miss you. To my dearest Darcy and Maia, thank-you for everything. Maia, you have been such a wonderful source of joy and delight. I hope and pray that you will grow up with a sense of wonder at this marvelous creation. To Darcy, thank-you for your love and patience over the past five years. You have made tremendous sacrifices for my sake and I cannot describe in words how appreciative I am. Thank-you.

## Table of Contents

<b>Chapter 1. Bacteriocins from Lactic Acid Bacteria</b> .....	1
<b>1.1. Introduction</b> .....	1
1.1.1. Bacteriocins from lactic acid bacteria .....	1
1.1.2. Classification of LAB bacteriocins .....	2
<b>1.2. Lantibiotics</b> .....	4
1.2.1. General characteristics .....	4
1.2.2. Biosynthesis.....	6
1.2.3. Mode of action.....	8
<b>1.3. Non-lantibiotics: The type IIa bacteriocins</b> .....	15
1.3.1. General characteristics .....	15
1.3.2. Biosynthesis.....	15
1.3.3. Mode of action.....	17
<b>1.4. Circular bacteriocins</b> .....	18
1.4.1. General characteristics .....	18
1.4.2. Biosynthesis.....	19
1.4.3. Mode of action.....	21
<b>1.5. Commercial Applications of LAB Bacteriocins</b> .....	21
1.5.1. Biopreservatives.....	21
1.5.2. Therapeutic agents .....	23
<b>1.6. Overview of Projects</b> .....	24

<b>Chapter 2. Structural studies of carnocyclin A</b> .....	26
<b>2.1. Background</b> .....	26
2.1.1. The circular bacteriocins .....	26
2.1.2. The structure of enterocin AS-48.....	28
2.1.3. Objectives .....	29
<b>2.2. Results &amp; Discussion</b> .....	30
2.2.1. Purification of CclA .....	30
2.2.2. Elucidation of the amino acid sequence of CclA.....	31
2.2.3. Characterization and mode of action of CclA .....	36
2.2.3.a. Antimicrobial spectrum of CclA .....	36
2.2.3.b. Stability studies .....	37
2.2.3.c. Mode of action.....	37
2.2.4. Preliminary structural studies .....	39
2.2.4.a. Stereochemical analysis .....	39
2.2.4.b. Secondary structure determination via CD and <sup>15</sup> N HSQC .....	42
2.2.4.c. Oligomeric state of CclA .....	42
2.2.5. 3D NMR solution structure of CclA .....	44
2.2.5.a. Chemical shift assignments and structure calculations.....	44
2.2.5.b. Structural features.....	46
2.2.5.c. Comparison to AS-48 .....	48
2.2.5.d. Homology modeling of the other circular bacteriocins .....	50
2.2.5.e. Fluorine NMR studies.....	54
2.2.6. Examining the linear precursor of CclA (pCclA) .....	56

2.2.6.a.	Construction and overexpression of Mal.pCclA .....	57
2.2.6.b.	Construction and expression of His <sub>6</sub> -tagged pCclA .....	58
2.2.7.	Mutational analysis of CclA .....	60
2.2.7.a.	Construction of internally tagged His <sub>6</sub> mutants .....	62
2.2.7.b.	Expression of the His <sub>6</sub> mutants .....	65
<b>2.3.</b>	<b>Conclusion &amp; Future Directions</b> .....	<b>66</b>
<b>Chapter 3.</b>	<b>The type IIa bacteriocins: Immunity and mode of action</b> .....	<b>68</b>
<b>3.1.</b>	<b>Background</b> .....	<b>68</b>
3.1.1.	The type IIa bacteriocins .....	68
3.1.2.	Immunity proteins for the type IIa bacteriocins .....	71
3.1.3.	Mode of action of the type IIa bacteriocins .....	77
3.1.4.	Objectives .....	79
<b>3.2.</b>	<b>Results &amp; Discussion</b> .....	<b>80</b>
3.2.1.	Construction of pMG36e.PisI & heterologous expression of PisI... ..	80
3.2.2.	Expression and purification of PisA and [ <sup>15</sup> N]PisA .....	82
3.2.3.	Expression and purification of PisI, [ <sup>13</sup> C, <sup>15</sup> N]PisI and [ <sup>15</sup> N]PisI .....	83
3.2.4.	Interaction of PisA and PisI .....	84
3.2.4.a.	Circular dichroism .....	85
3.2.4.b.	Titration of [ <sup>15</sup> N]PisA with PisI .....	85
3.2.5.	NMR solution structure of PisI .....	86
3.2.5.a.	Chemical shift assignments and structure calculations .....	86
3.2.5.b.	Structural features of PisI .....	90

3.2.5.c. Comparison of Pisl to the other immunity proteins .....	92
3.2.6. Cloning and expression of the man-PTS system .....	95
3.2.6.a. Construction of expression systems for the IIC & IID subunits .....	95
3.2.6.b. Construction of an expression system for the IIAB subunit .....	96
3.2.6.c. Pilot expression of the IIC and IID membrane proteins .....	96
<b>3.3. Conclusion &amp; Future Directions.....</b>	<b>100</b>

## **Chapter 4. *In vitro* Studies of the Peptidase Domain of CbnT: Cleavage of pCbnB2 by CbnTP .....**

<b>4.1. Background .....</b>	<b>102</b>
4.1.1. Prebacteriocins and leader peptides of the Gly-Gly motif .....	102
4.1.2. Maturation and secretion of bacteriocins .....	105
4.1.3. Objectives .....	108
<b>4.2. Results &amp; Discussion .....</b>	<b>109</b>
4.2.1. Purification of pCbnB2 .....	109
4.2.2. Purification of CbnTP .....	111
4.2.2.a. Purification of CbnTP from inclusion bodies .....	112
4.2.2.b. Purification of CbnTP from soluble protein .....	113
4.2.3. Peptidase activity of CbnTP .....	115
4.2.4. Construction of Cys→ Ser mutants of CbnTP .....	116
<b>4.3. Conclusions &amp; Future Directions .....</b>	<b>119</b>

<b>Chapter 5. Testing the activity of LAB bacteriocins against Gram-negative pathogens</b> .....	121
<b>5.1. Background</b> .....	121
5.1.1. Drawbacks to the utility of LAB bacteriocins in food preservation and as human therapeutics .....	121
5.1.2. Gram-negative bacteria and LAB bacteriocins.....	121
5.1.3. The bacteriocins of Gram-negative organisms .....	127
5.1.4. Objectives .....	131
<b>5.2. Results &amp; Discussion</b> .....	132
5.2.1. Bacteriocins used in this study.....	132
5.2.2. Testing strategy .....	135
5.2.3. Testing results .....	136
<b>5.3. Conclusions &amp; Future Directions</b> .....	141
<b>Chapter 6. Experimental Procedures</b> .....	142
<b>6.1. General methods for protein production and purification</b> .....	142
6.1.1. Plasmids, bacterial strains and culture conditions .....	142
6.1.2. Centrifugation .....	143
6.1.3. General approach for the expression of recombinant proteins .....	143
6.1.4. Cell lysis .....	143
6.1.4.a. Freeze thaw & sonication.....	143
6.1.4.b. Cell disrupter.....	144
6.1.5. Spot-on-lawn activity assays .....	144
6.1.6. Protein purification.....	145

6.1.6.a.	Amylose XAD-16.....	145
6.1.6.b.	Megabond C <sub>18</sub> solid-phase extraction .....	146
6.1.6.c.	RP-HPLC .....	146
6.1.6.d.	Cation exchange chromatography.....	146
6.1.6.e.	Size exclusion chromatography.....	147
6.1.6.f.	Amylose affinity chromatography.....	147
6.1.6.g.	Ni-NTA affinity chromatography .....	148
6.1.7.	Factor Xa digestion .....	148
6.1.8.	Protein electrophoresis .....	149
6.1.8.a.	SDS-PAGE.....	149
6.1.8.b.	Tris-Tricine SDS-PAGE.....	150
6.1.8.c.	Western blots.....	150
6.1.9.	Protein quantification.....	151
6.1.9.a.	Spectrophotometric quantification .....	151
6.1.9.b.	BCA colorimetric analysis.....	151
6.1.10.	Protein characterization.....	152
6.1.10.a.	Mass spectrometry.....	152
6.1.10.b.	Circular dichroism.....	152
6.1.10.c.	NMR .....	153
<b>6.2.</b>	<b>General methodologies for genetic manipulations.....</b>	<b>153</b>
6.2.1.	Plasmids, bacterial strains and culture conditions .....	153
6.2.2.	Reagents and stock solutions .....	154
6.2.3.	Polymerase chain reaction (PCR).....	155

6.2.4.	Agarose gel electrophoresis.....	157
6.2.5.	Quantification of DNA.....	157
6.2.6.	Purification of DNA following PCR or restriction digest reactions.....	157
6.2.7.	Isolation of crude DNA for use as a template for PCR.....	158
6.2.8.	Purification of plasmid DNA on a mini-preparative scale .....	158
6.2.9.	Large scale purification of plasmid DNA .....	160
6.2.10.	Preparation of competent <i>E. coli</i> cells.....	162
6.2.10.a.	Electrocompetent cells ( <i>E. coli</i> JM109).....	162
6.2.10.b.	Heat-shock competent cells .....	162
6.2.10.c.	Chemically competent cells .....	163
6.2.11.	Preparation of electrocompetent <i>Carnobacterium</i> spp.....	163
6.2.12.	Transformation of <i>E. coli</i> .....	163
6.2.12.a.	Electroporation .....	163
6.2.12.b.	Heat-shock .....	164
6.2.12.c.	Chemical treatment.....	164
6.2.13.	Transformation of <i>Carnobacterium</i> spp.....	165
6.2.14.	Screening for desired clones.....	165
6.2.15.	DNA sequencing.....	166
<b>6.3.</b>	<b>Experimental procedures for the structural studies of carnocyclin A.....</b>	<b>167</b>
6.3.1.	Plasmids, bacterial strains and culture conditions .....	167
6.3.2.	Isolation and purification of CclA .....	168
6.3.3.	Isolation and purification of [ <sup>13</sup> C, <sup>15</sup> N]CclA .....	170

6.3.4.	Confirming the purity and antimicrobial activity of CclA .....	170
6.3.5.	Antimicrobial spectrum of CclA.....	170
6.3.6.	Stability of CclA .....	171
6.3.6.a.	Effect of temperature .....	171
6.3.6.b.	Effect of pH.....	171
6.3.6.c.	Effect of proteolytic enzymes .....	171
6.3.7.	Amino acid sequence of CclA .....	172
6.3.7.a.	Edman sequencing.....	172
6.3.7.b.	Tandem mass spectrometry.....	172
6.3.8.	Circular dichroism of CclA .....	174
6.3.9.	Stereochemical analysis of CclA .....	174
6.3.9.a.	Hydrolysis and derivatization of CclA .....	174
6.3.9.b.	Preparation of standards .....	175
6.3.9.c.	GC-MS .....	175
6.3.10.	Oligomeric state of CclA.....	176
6.3.10.a.	NMR studies.....	176
6.3.10.b.	Dynamic light scattering (DLS).....	176
6.3.11.	NMR spectroscopy of [ <sup>13</sup> C, <sup>15</sup> N]CclA.....	177
6.3.12.	Structure calculations .....	178
6.3.13.	Fluorine NMR.....	178
6.3.14.	Examining the lysine side chains of CclA by NMR .....	179
6.3.15.	Secondary structure analysis and homology modeling of the other circular bacteriocins .....	179
6.3.16.	Purification of pCclA as a MalE fusion protein.....	181

6.3.16.a.	Construction of pMAL.FXA.pCclA .....	181
6.3.16.b.	Overexpression and purification of MalE.pCclA .....	182
6.3.16.c.	Factor Xa digestion of MalE.pCclA .....	183
6.3.17.	Purification of pCclA as His <sub>6</sub> -tagged fusion protein.....	185
6.3.17.a.	Construction of pQE60.FXA.pCclA.....	186
6.3.17.b.	Construction of pQE60.pCclA .....	187
6.3.17.c.	Pilot expression of clone 16.5 (His <sub>6</sub> .FXa.pCclA).....	188
6.3.17.d.	Pilot expression of clone 17.4 (His <sub>6</sub> .pCclA).....	189
6.3.18.	Construction of internally tagged His <sub>6</sub> pCclA mutants .....	189
6.3.18.a.	pMG36e.pCclA.M1 – His <sub>6</sub> between I6 and A7.....	189
6.3.18.b.	pMG36e.pCclA.M4 – His <sub>6</sub> between Q52 and G53 .....	191
6.3.18.c.	pMG36e-pCclA.M2 – His <sub>6</sub> between L22 and T23.....	192
6.3.18.d.	pMG36e-pCclA.M3 – His <sub>6</sub> between G33 and V34.....	193
6.3.19.	Pilot expression of pCclA mutants.....	194
<b>6.4.</b>	<b>Experimental procedures for the investigation of the type IIa bacteriocins, their immunity proteins &amp; mode of action.....</b>	<b>195</b>
6.4.1.	Plasmids, bacterial strains and culture conditions .....	195
6.4.2.	Heterologous expression of Pisl .....	196
6.4.2.a.	Construction of pMG36e.Pisl .....	196
6.4.2.b.	Activity testing .....	198
6.4.3.	Construction of fusion proteins.....	198
6.4.3.a.	pMAL-PisA.....	198
6.4.3.b.	pMAL-Pisl .....	199

6.4.4.	Purification of PisI, [ <sup>13</sup> C, <sup>15</sup> N]PisI and [ <sup>15</sup> N]PisI .....	199
6.4.4.a.	Overexpression and purification of Male-PisI.....	199
6.4.4.b.	Digestion with Factor Xa .....	201
6.4.4.c.	Cation exchange .....	201
6.4.4.d.	RP-HPLC .....	202
6.4.5.	Purification of PisA and [ <sup>15</sup> N]PisA.....	202
6.4.5.a.	Overexpression and purification of Male-PisA .....	202
6.4.5.b.	Digestion with Factor Xa.....	203
6.4.5.c.	RP-HPLC .....	203
6.4.6.	Circular dichroism.....	204
6.4.7.	NMR spectroscopy of [ <sup>15</sup> N]PisI and [ <sup>13</sup> C, <sup>15</sup> N]PisI .....	204
6.4.8.	Structure calculations .....	205
6.4.9.	Titration of [ <sup>15</sup> N]PisA with PisI.....	206
6.4.9.a.	Aqueous conditions .....	206
6.4.9.b.	50% TFE.....	206
6.4.10.	Construction of pMV24.....	207
6.4.11.	Construction of pQE60.mptAB .....	209
6.4.12.	Pilot studies on the overexpression of IIC and IID.....	211
<b>6.5.</b>	<b>Experimental procedures for the <i>in vitro</i> studies of the peptidase domain of CbnT.....</b>	<b>212</b>
6.5.1.	Plasmids, bacterial strains and culture conditions .....	212
6.5.2.	Purification of pCbnB2 .....	213
6.5.2.a.	Overexpression and purification of Male-pCbnB2.....	213
6.5.2.b.	Factor Xa Digestion of Male-pCbnB2 .....	214

6.5.2.c.	RP-HPLC purification .....	215
6.5.3.	Purification of CbnTP from inclusion bodies.....	216
6.5.3.a.	Overexpression conditions.....	216
6.5.3.b.	Purification of inclusion bodies .....	217
6.5.3.c.	Refolding attempts.....	218
6.5.3.d.	Activity of CbnTP isolated from inclusion bodies.....	220
6.5.4.	Purification of CbnTP as soluble protein .....	220
6.5.4.a.	Overexpression conditions .....	220
6.5.4.b.	Purification of soluble protein.....	221
6.5.4.c.	Activity of CbnTP isolated as soluble protein .....	222
6.5.5.	Construction of CbnTP mutants.....	222
6.5.5.a.	Construction of pQE60.CbnTP.M1 .....	222
6.5.5.b.	Construction of pQE60.CbnTP.M2.....	224
6.5.5.c.	Construction of pQE60.CbnTP.M3 .....	224
6.5.5.d.	Construction of pQE60.CbnTP.M4.....	225
6.5.5.e.	Construction of pQE60.CbnTP.M5 .....	226
6.5.6.	Pilot Expression of CbnTP Mutants.....	226
<b>6.6.</b>	<b>Experimental procedures for testing the activity of LAB bacteriocins against Gram-negative pathogens .....</b>	<b>227</b>
6.6.1.	Reagents, bacterial strains and culture conditions .....	227
6.6.2.	Preparation of bacteriocin testing solutions.....	227
6.6.2.a.	General description of testing solutions.....	227
6.6.2.b.	CclA.....	228
6.6.2.c.	Enterocin 710C (Ent7A & Ent7B) .....	229

6.6.2.d. Gallidermin .....	229
6.6.2.e. Lacticin 3147.....	229
6.6.2.f. Nisin A .....	232
6.6.2.g. PisA .....	232
6.6.2.h. Subtilosin A.....	232
6.6.3. Testing procedure.....	233
6.6.3.a. In-solution testing.....	233
6.6.3.b. Colony counting method.....	234
6.6.4. Analysis of cfu data.....	235
<b>Chapter 7. References .....</b>	<b>237</b>
<b>Appendix A. NMR Solution structure of ColV .....</b>	<b>283</b>
<b>A.1. Background .....</b>	<b>283</b>
<b>A.2. Results &amp; Discussion .....</b>	<b>285</b>
A.2.1. Purification of ColV .....	285
A.2.2. NMR spectroscopy of ColV .....	285
<b>A.3. Conclusions.....</b>	<b>287</b>
A.4. Experimental Procedures.....	288
A.4.1. Plasmids, bacterial strains and culture conditions .....	288
A.4.2. Preparation of [ <sup>13</sup> C, <sup>15</sup> N]ColV .....	289
A.4.2.a. Overexpression and purification of Male-ColV .....	289

A.4.2.b. Factor Xa digestion.....	290
A.4.2.c. RP-HPLC purification .....	290
A.4.3. NMR spectroscopy of [ <sup>13</sup> C, <sup>15</sup> N]CoIV .....	291
<b>A.5. References.....</b>	<b>292</b>

## List of Tables

<b>TABLE 1.</b> Classification of LAB bacteriocins.....	3
<b>TABLE 2.</b> Spectrum of activity of CclA .....	36
<b>TABLE 3.</b> Structural statistics for CclA .....	45
<b>TABLE 4.</b> Peptides with similar structural folds to CclA .....	50
<b>TABLE 5.</b> Primers used for the construction of internal His <sub>6</sub> -tagged pCclA mutants.....	64
<b>TABLE 6.</b> Structural statistics for PisI .....	88
<b>TABLE 7.</b> Primers used for site-directed mutagenesis of CbnTP.....	118
<b>TABLE 8.</b> The efficacy of LAB bacteriocins against Gram-negative pathogens .....	126
<b>TABLE 9.</b> The microcins produced by enterobacteria: their modifications, recognition and import into target cells, and mode of action. ....	130
<b>TABLE 10.</b> Plasmids and bacterial strains used in the study of CclA .....	168
<b>TABLE 11.</b> Plasmids and bacterial strains used for the study of PisA, PisI and the EII <sub>t</sub> <sup>man</sup> permease.....	195
<b>TABLE 12.</b> Plasmids and bacterial strains used for the study of CbnTP and CbnTP mutants.....	213
<b>TABLE 13.</b> Concentrations of the various bacteriocin test solutions.....	228
<b>TABLE 14.</b> Layout of well-plate and testing solutions for in-solution bacteriocin testing against Gram-negative pathogens .....	234
<b>TABLE A.1.</b> Plasmids and bacterial strains used for investigation of ColV .....	288

## List of Figures

<b>FIG. 1.</b> The chemical structures of lanthionine, methyllanthionine and other unusual amino acids found in lantibiotics. ....	5
<b>FIG. 2.</b> Genes required for the biosynthesis of nisin.....	6
<b>FIG. 3.</b> Structure of the Gram-positive cell wall.....	9
<b>FIG. 4.</b> Chemical structure of lipid II, the docking molecule for many lantibiotics.....	10
<b>FIG. 5.</b> Structures of nisin, lactacin 314, gallidermin and mersacidin.....	14
<b>FIG. 6.</b> Genes required for the biosynthesis of piscicolin 126 (PisA).....	16
<b>FIG. 7.</b> Genes required for the biosynthesis of enterocin AS-48.....	19
<b>FIG. 8.</b> Characterization of CclA by MALDI-TOF MS, gel electrophoresis and activity testing.....	31
<b>FIG. 9.</b> Elucidation of the linear sequence of CclA by Edman degradation and MS/MS sequencing.....	33
<b>FIG. 10.</b> Determining the relative position of amino acid sequences within a circular sequence.....	34
<b>FIG. 11.</b> Elucidation of the circular structure of CclA: from linear sequence, to genetic sequence, to confirmation of the circular structure.....	35
<b>FIG. 12.</b> Chiral GC-analysis of hydrolyzed and derivatized CclA and (L)- and (D)-amino acid standards.....	41
<b>FIG. 13.</b> Secondary structural analysis of CclA by circular dichroism and <sup>15</sup> N HSQC.....	42
<b>FIG. 14.</b> Examining the effect of NaCl and pH on the backbone and sidechain amide resonances of CclA by <sup>15</sup> N HSQC.....	43
<b>FIG. 15.</b> Overlay of the 20 lowest energy conformers of CclA.....	45
<b>FIG. 16.</b> Structural characteristics of CclA.....	48
<b>FIG. 17.</b> Structural and sequence alignment of CclA and AS-48.....	49

<b>FIG. 18.</b> Sequence alignment, predicted secondary structures and homology modeling of the circular bacteriocins.....	53
<b>FIG. 19.</b> <sup>19</sup> F-NMR spectra of NaF titrated against CclA (1 mM in 90% H <sub>2</sub> O:10% D <sub>2</sub> O, pH 3.8).....	56
<b>FIG. 20.</b> The internally His <sub>6</sub> -tagged CclA mutants.....	61
<b>FIG. 21.</b> Schematic representation of recombinant PCR.....	63
<b>FIG. 22.</b> 3D structure of various type IIa bacteriocins.....	69
<b>FIG. 23.</b> Sequence alignment and subgrouping of various type IIa bacteriocins.....	70
<b>FIG. 24.</b> Sequence alignment of various immunity proteins.....	73
<b>FIG. 25.</b> Structures of the group A and C immunity proteins.....	75
<b>FIG. 26.</b> Heterologous expression of PisI.....	81
<b>FIG. 27.</b> MALDI-TOF of piscicolin 126.....	83
<b>FIG. 28.</b> MALDI-TOF of piscicolin 126 immunity protein.....	84
<b>FIG. 29.</b> CD spectra of PisA and PisI.....	85
<b>FIG. 30.</b> <sup>15</sup> N HSQC of PisA when titrated with PisI.....	86
<b>FIG. 31.</b> <sup>15</sup> N HSQC of PisI in 20 mM sodium phosphate (pH 5.9) at 25°C and 800 MHz.....	87
<b>FIG. 32.</b> Overlay of the 20 lowest energy conformers of PisI.....	88
<b>FIG. 33.</b> Edmundson helical wheel diagram of PisI.....	89
<b>FIG. 34.</b> Electrostatic surface potential of PisI.....	91
<b>FIG. 35.</b> Hydrophobic surface of PisI.....	91
<b>FIG. 36.</b> Overlay of PisI (blue) with ImB2, Mun-im, EntA-im and PedB.....	92
<b>FIG. 37.</b> SDS-PAGE analysis of the overexpression of IIC and IID with different concentrations of IPTG.....	98
<b>FIG. 38.</b> Overexpression of IIC at 37°C with different concentrations of IPTG.....	99

<b>FIG. 39.</b> NMR solutions structures of CbnB2 and pCbnB2 in membrane-mimicking conditions. ....	104
<b>FIG. 40.</b> Helical wheel diagram of pCbnB2 and conserved residues of the Gly-Gly type leader peptides.....	105
<b>FIG. 41.</b> Schematic of the ABC-transporters for bacteriocins with Gly-Gly type leader peptides.....	108
<b>FIG. 42.</b> MALDI-TOF of the cleavage of MalE-pCbnB2 by Factor Xa under different digestion conditions.....	110
<b>FIG. 43.</b> Sequence alignment of the N-terminal domain of CbnT with other ABC-transporters.....	111
<b>FIG. 44.</b> Purification of CbnTP as soluble protein.....	114
<b>FIG. 45.</b> MALDI-TOF and activity testing to determine the proteolytic activity of CbnTP toward pCbnB2. ....	116
<b>FIG. 46.</b> Cys→Ser mutants of CbnTP.....	117
<b>FIG. 47.</b> 15% SDS-PAGE analysis of expression of CbnTP and mutants (M1-M5).. ....	119
<b>FIG. 48.</b> The cell wall of Gram-negative bacteria and the chemical structure of Kdo <sub>2</sub> -lipid A, the fundamental LPS constituent of Gram-negative bacteria... ..	122
<b>FIG. 49.</b> Structures of various siderophores, used by bacteria to complex iron..	128
<b>FIG. 50.</b> The effect of LAB bacteriocins on the growth of Gram-negative bacteria in the absence and presence of 20 mM EDTA.. ....	137
<b>FIG. 51.</b> Predicting the secondary structure of the circular bacteriocins and allowing for structural elements to encompass the N- and C- termini.....	180
<b>FIG. 52.</b> Pilot expression of clone 16.5 to examine the effect of different growth temperatures and IPTG concentrations.....	188
<b>FIG. 53.</b> MALDI-TOF traces of purified lactacin 3147.....	231
<b>FIG. A.1.</b> Alignment of the amino acid sequences of ColV and MccL. ....	284
<b>FIG. A.2.</b> <sup>15</sup> N HSQC spectra of ColV in aqueous and membrane-mimicking conditions.....	286

## List of Abbreviations

<b><math>\alpha</math></b>	alpha-helix
<b>A or Ala</b>	alanine
<b>aa</b>	amino acid
<b>ABC</b>	ATP-binding cassette
<b>AEBSF</b>	4-(2-aminoethyl) benzenesulfonyl fluoride hydrochloride
<b>amp</b>	ampicillin
<b>APT</b>	all purpose tween
<b>ATP</b>	adenosine triphosphate
<b>C or Cys</b>	cysteine
<b>CbnB2</b>	carnobacteriocin B2 (bacteriocin)
<b><i>cbnB2</i></b>	carnobacteriocin B2 gene
<b>CbnT</b>	ABC-transporter for CbnB2
<b><i>cbnT</i></b>	gene for ABC-transporter for CbnB2
<b>CbnTP</b>	164 N-terminal amino acids of CbnT (peptidase domain)
<b>CbnTP.M1</b>	C15S mutant of CbnTP
<b>CbnTP.M2</b>	C15S, C19S mutant of CbnTP
<b>CbnTP.M3</b>	C15S, C19S, C55S mutant of CbnTP
<b>CbnTP.M4</b>	C15S, C19S, C55S, C63S mutant of CbnTP
<b>CbnTP.M5</b>	C15S, C19S, C63S mutant of CbnTP
<b>CclA</b>	carnocyclin A (bacteriocin)
<b><i>cclA</i></b>	carnocyclin A structural gene

<b>CD</b>	circular dichroism
<b>cfu</b>	colony forming units
<b>ColV</b>	colicin V (bacteriocin) – see also MccV
<b><i>colV</i></b>	colicin V structural gene
<b>CSI</b>	chemical shift index
<b>D or Asp</b>	aspartic acid / aspartate
<b><i>d</i><sub>3</sub>-TFE</b>	deuterated trifluoroethanol (CF <sub>3</sub> CD <sub>2</sub> OD)
<b>dATP</b>	deoxyadenosine triphosphate
<b>dCTP</b>	deoxycytidine triphosphate
<b>dGTP</b>	deoxyguanosine triphosphate
<b>DLS</b>	dynamic light scattering
<b>DNA</b>	deoxyribonucleic acid
<b>dNTP</b>	deoxynucleotide triphosphate
<b>DSS</b>	2,2-dimethyl-2-silapentane-5-sulfonate sodium salt
<b>DTT</b>	± dithiothreitol
<b>dTTP</b>	deoxythymidine triphosphate
<b>E or Glu</b>	glutamic acid / glutamate
<b>EDTA</b>	ethylenediaminetetraacetic acid
<b>EII<sup>man</sup></b>	mannose permease complex of the man-PTS system
<b>EntA-im</b>	enterocin A immunity protein
<b>EtBr</b>	ethidium bromide
<b>EtOH</b>	ethanol
<b>F or Phe</b>	phenylalanine

<b>FXA</b>	Factor Xa cleavage site
<b>G or Gly</b>	glycine
<b>GC-MS</b>	gas chromatography mass spectrometry
<b>GlcNAc</b>	N-acetylglucosamine
<b>GRAS</b>	generally regarded/recognized as safe
<b>H or His</b>	histidine
<b>HCCA</b>	$\alpha$ -cyano-4-hydroxycinamic acid
<b>His<sub>6</sub></b>	hexahistidine tag (His-His-His-His-His-His)
<b>HSQC</b>	heteronuclear single quantum coherence
<b>I or Ile</b>	isoleucine
<b>ImB2</b>	carnobacteriocin B2 immunity protein
<b>IPA</b>	2-propanol / isopropyl alcohol
<b>IPTG</b>	isopropyl- $\beta$ -D-thiogalactopyranoside
<b>K or Lys</b>	lysine
<b>kan</b>	kanamycin
<b>Kdo</b>	3-deoxy-D-manno-octulosonic acid
<b>L or Leu</b>	leucine
<b>LAB</b>	lactic acid bacteria
<b>LB</b>	Luria-Bertani
<b>LC-MS</b>	liquid chromatography mass spectrometry
<b>LC-MS/MS</b>	liquid chromatography tandem mass spectrometry
<b>LeuA</b>	leucocin A
<b>LPS</b>	lipopolysaccharide

<b>LRF</b>	log reduction factor
<b>M or Met</b>	methionine
<b>MALDI-TOF</b>	matrix assisted laser desorption ionization time of flight
<b><i>malE</i></b>	maltose binding protein gene
<b>MalE-CoIV</b>	maltose binding protein colicin V fusion protein
<b>man-PTS</b>	mannose phosphotransferase system
<b>MccV</b>	colicin V (bacteriocin) – see also CoIV
<b>MeCN</b>	acetonitrile
<b><i>mptAB</i></b>	structural gene for the IIAB protein of the $EII_t^{\text{man}}$ permease
<b><i>mptC</i></b>	structural gene for the IIC protein of the $EII_t^{\text{man}}$ permease
<b><i>mptD</i></b>	structural gene for the IID protein of the $EII_t^{\text{man}}$ permease
<b>MRSA</b>	methicillin resistant <i>Staphylococcus aureus</i>
<b>MS/MS</b>	tandem mass spectrometry
<b>Mun-im</b>	mundtacin immunity protein
<b>MurNAc</b>	N-acetylmuramic acid
<b>MW</b>	molecular weight
<b>MWCO</b>	molecular weight cut-off
<b>N or Asn</b>	asparagine
<b>NMR</b>	nuclear magnetic resonance
<b>NOE</b>	nuclear Overhauser effect / enhancement
<b>NOESY</b>	NOE spectroscopy
<b>OD<sub>600</sub></b>	optical density measured at 600 nm
<b>OM</b>	outer membrane

<b>P or Pro</b>	proline
<b>PAGE</b>	polyacrylamide gel electrophoresis
<b>pCbnB2</b>	precarnobacteriocin B2 (precursor)
<b>pCbnB2<sub>-RP</sub></b>	precarnobacteriocin B2 missing R65, P66 (truncated precursor)
<b>pCclA</b>	carnocyclin A (precursor)
<b>PCR</b>	polymerase chain reaction
<b>PedB</b>	pediocin PP-1 immunity protein
<b>PisA</b>	piscicolin 126 (bacteriocin)
<i><b>pisA</b></i>	piscicolin 126 structural gene
<b>PisI</b>	piscicolin 126 immunity protein
<i><b>pisI</b></i>	piscicolin 126 immunity protein gene
<b>Q or Gln</b>	glutamine
<b>R or Arg</b>	arginine
<b>rmsd</b>	root mean square deviation
<b>RP-HPLC</b>	reverse phase high performance liquid chromatography
<b>rpm</b>	revolutions per minute
<b>RT</b>	room temperature
<b>S or Ser</b>	serine
<b>SA</b>	sinapinic acid
<b>SDS</b>	sodium dodecyl sulfate
<b>SDS-PAGE</b>	sodium dodecyl sulfate poly acrylamide gel electrophoresis
<b>T or Thr</b>	threonine
<b>TBE</b>	tris-borate EDTA

<b>TBS</b>	tris-buffered saline
<b>TFA</b>	trifluoroacetic acid
<b>TFE</b>	trifluoroethanol
<b>TOCSY</b>	total correlation spectroscopy
<b>Tris-Cl</b>	tris(hydroxymethyl)aminomethane hydrochloride
<b>TSB</b>	tryptic soy broth
<b>UDP</b>	undecaprenyl
<b>V or Val</b>	valine
<b>VRE</b>	vancomycin resistant enterococci
<b>W or Trp</b>	tryptophan
<b>Y or Tyr</b>	tyrosine

# Chapter 1. Bacteriocins from Lactic Acid Bacteria

## 1.1. Introduction

### 1.1.1. Bacteriocins from lactic acid bacteria

Lactic acid bacteria (LAB) are a heterogeneous group of Gram-positive bacteria. They are non-sporulating rod or cocci organisms, with a GC content of less than 50% (1). As implied by their name, LAB produce lactic acid upon fermentation of glucose and other carbohydrates, and are classified as either homofermentative (lactic acid is sole by-product) or heterofermentative (lactic acid is major by-product) (1, 2). Although LAB are non-respiring, many strains are either aerotolerant or facultative anaerobes (3). LAB are found in a variety of ecological niches and are commonly isolated from plants, food products (particularly dairy and meats) (1, 2), and from the oral, gastrointestinal and urogenital tracts of animals (1, 4).

For centuries, LAB have been used in the production of fermented foods, such as dairy products, cheeses and alcoholic beverages (5, 6). Many of the beneficial effects of LAB derive from their metabolic by-products. The production of lactic acid and other organic acids, as well as hydrogen peroxide and diacetyl, inhibits the growth of many food-spoilage organisms (1, 5, 7-9). However, in addition to these small molecules, LAB also produce a vast array of antimicrobial peptides that specifically kill other bacteria. These peptides are ribosomally synthesized and are referred to as bacteriocins (10). It is believed that > 99% of all bacteria produce at least one bacteriocin (11). The ability to produce these peptide weapons allows bacteria to compete for nutrients and space, and is a

key component in bacterial warfare. In addition to LAB, many other bacteria, including Gram-negative strains such as *E. coli*, are known to produce bacteriocins (4, 6, 9, 12).

### 1.1.2. Classification of LAB bacteriocins

Over the years, numerous classification schemes have been proposed to categorize the LAB bacteriocins according to a variety of characteristics, such as size, primary sequence, structure, mode of action and biosynthesis (1, 6, 12, 13). As new bacteriocins are identified and knowledge of existing bacteriocins is refined, the classification of these remarkably diverse peptides is continually evolving. Nevertheless, two main families of LAB bacteriocins have emerged: the lantibiotics (class I) and the non-lantibiotics (class II). The identity of the class III and class IV bacteriocins has undergone the greatest revision in recent years. The class III bacteriocins are large proteins (> 30 kDa), however, whether they truly belong to the bacteriocins has recently been called into question (6, 12). Previously, the class IV bacteriocins were described as proteins that required lipid or carbohydrate moieties to exert their activity. As no members of this class have fully been characterized, they have been removed from many of the current classification schemes (6). The newly emerging circular bacteriocins (which were formerly considered to be class II bacteriocins) have now subsumed that position (12, 14). Table 1 lists the commonly accepted classification of the LAB bacteriocins, as put forth by Nes *et al.* (12).

**TABLE 1.** Classification of LAB bacteriocins according to Nes *et al.* (12)

Class	Characteristics	Examples (reference)
<b>Class I. Lantibiotics</b>		
<i>Extensively post-translationally modified to contain either lanthionine (Lan) or methylanthionine (MeLan) and may contain other unusual amino acids (such as Dha, Dhb, D-Ala). Traditionally, classified into two subgroups, but recently, as many as 11 different subgroups have been proposed.</i>		
Type A	Elongated, flexible, cationic peptides	Nisin (15) Gallidermin (16) Lacticin 3147 A2 (17, 18)
Type B	Globular, rigid, anionic or neutral peptides	Mersacidin (19, 20) Lacticin 3147 A1 (17, 18) Cinnamycin (21)
<b>Class II. Non-lantibiotics</b>		
<i>Non-lanthionine containing peptides; aside from cleavage of the leader peptide, these peptides do not undergo post-translational modifications.</i>		
Type IIa (Pediocin-like)	Highly anti-listerial, conserved “Pediocin-box” motif in the N-terminus (YGNV)	Leucocin A (22) Pediocin PA-1 (23) Piscicolin 126 (24, 25)
Type IIb	Two-component bacteriocins – full antimicrobial activity depends on the presence of both peptides	Lactococcin G (26) Plantaricin EF (27)
Type IIc	Miscellaneous peptides (do not easily fit into the other categories)	Lactococcin A (28)
Type IId	Leaderless peptides	Enterocin L50 (29) Enterocin Q (30)
Type IIe	Bacteriocins derived from the fragmentation of larger proteins	HP (31) Propiocin F (32)
<b>Class III</b> <i>Large, heat-labile bacteriocins</i>		Helveticin J (33) Enterolysin A (34-36)
<b>Class IV. Circular</b>		
<i>The N- and C- termini of the peptide are linked via a peptide bond</i>		
Class i	Low sequence homology, high pI (~10)	Enterocin AS-48 (37) Circularin A (38)
Class ii	High sequence homology, low pI (~6)	Gassericin A / reuterin 6 (39) Acidocin B (putative) (40)

Despite attempts to fully classify the bacteriocins from Gram-positive organisms (particularly LAB), there are some bacteriocins that are not adequately represented in this classification scheme. For example, subtilisin A, which is produced by *Bacillus subtilis* (a non-LAB bacterium), is backbone cyclized, yet also contains unique thioether bridges (41-44). Recently, several other

bacteriocins that likely contain these unusual thioether bridges have been discovered (45, 46) and it has been proposed that bacteriocins with these modifications comprise yet a new class of bacteriocins (43). The following sections will discuss the general features, biosynthesis and proposed mode of action of the lantibiotics, type IIa non-lantibiotics and the circular bacteriocins.

## **1.2. Lantibiotics**

### **1.2.1. General characteristics**

The lantibiotics are small (< 5 kDa), heat-stable peptides that undergo extensive posttranslational modifications and contain the unusual amino acids lanthionine (Lan) or  $\beta$ -methylanthionine (MeLan) (5, 6, 9, 12). These amino acids are formed by the dehydration of either serine or threonine residues to 2,3-dehydroalanine (Dha) and 2,3-dehydrobutyryne (Dhb) residues, respectively, followed by the intramolecular Michael addition of a thiol group from a cysteine onto the dehydrated residue. Both the dehydration and cyclization steps are enzyme mediated. The presence of Lan or MeLan residues imparts the polycyclic structure of the lantibiotics. Numerous other unusual amino acids have been identified within the lantibiotics, including D-Ala, 2-oxobutyrate and S-[(Z)-2-aminovinyl]-(3S)-3-methyl-D-cysteine (AviMeCys) (6, 12, 47), as illustrated in Fig. 1. To date, 17 different types of unusual amino acids have been discovered within the lantibiotics (48).

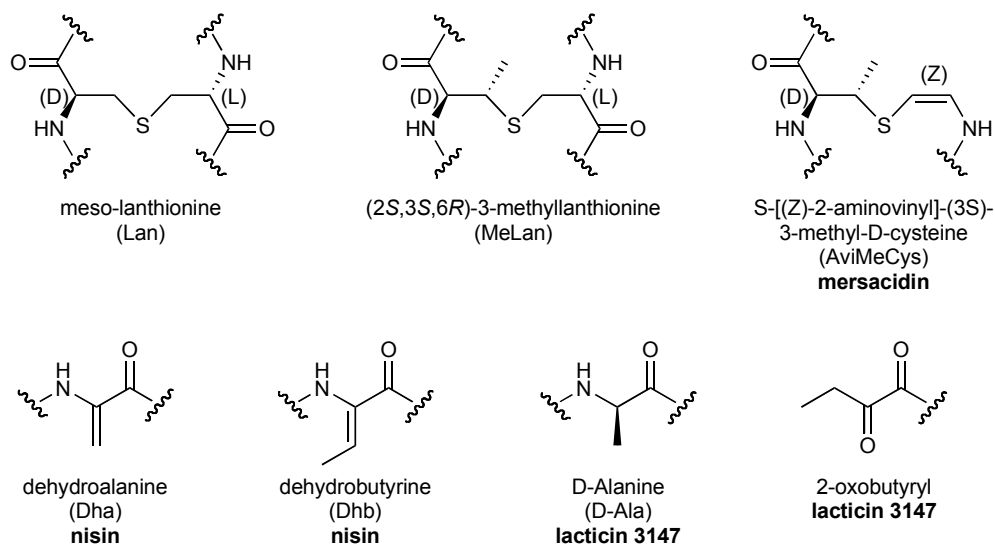


**FIG. 1.** The chemical structures of lanthionine, methyllanthionine and other unusual amino acids found in lantibiotics. The name of the amino acid (and its abbreviation) is listed, along with a representative lantibiotic incorporating that amino acid.

The lantibiotics are further subdivided, according to a variety of characteristics, including primary sequence, structure, biosynthesis, and mode of action (47-50). Typically, they are classified as either type A or type B. The type A lantibiotics are elongated, flexible and cationic peptides that are known to elicit pore formation. The type B lantibiotics are globular, rigid and neutral or anionic peptides that inhibit cell wall biosynthesis (6, 12, 48, 50, 51). Currently however, this sub classification has been called into question, as some lantibiotics appear to fit into both categories. For example, lactacin 3147 is comprised of two peptides (LtnA1 and LtnA2). LtnA2 is elongated and characteristic of the type A lantibiotics, whereas LtnA1 is globular and would thus appear to be a type B lantibiotic. In addition, it is now known that many type A lantibiotics (such as nisin, subtilin, and gallidermin) inhibit cell wall biosynthesis, in addition to their

pore forming abilities (52, 53). Recently, it has been suggested that the lantibiotics be divided into 11 different classes (51).

### 1.2.2. Biosynthesis

The genes encoding for lantibiotic production are located on plasmids, conjugative transposons or on the chromosome, and are typically organized in operon-like structures. The generic identifiers “*lan*” and “Lan” are used to represent the genes and proteins involved in lantibiotic biosynthesis (47, 48, 54). To help illustrate the genes required for the biosynthesis of lantibiotics, the operon encoding for the production of nisin is depicted in Fig. 2.

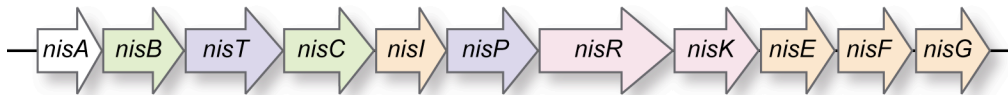


**FIG. 2.** Genes required for the biosynthesis of nisin. The white gene (*nisA*) encodes for the precursor peptide. The green genes (*nisB*, *nisC*) are involved in peptide modification (dehydration and cyclization). The blue genes (*nisT*, *nisP*) are required for secretion and maturation of the bacteriocin. The orange genes (*nisI*, *nisEFG*) are involved in immunity. The pink genes (*nisR*, *nisK*) are involved in regulation of nisin production.

Lantibiotics are synthesized as precursor peptides, encoded by the *lanA* gene. The precursor peptides contain an N-terminal extension. It is believed that the leader peptide keeps the bacteriocin in an inactive state, and helps direct the prepeptide to the enzymes responsible for modification, and also secretion of the bacteriocin (55).

The typical post-translational modifications for the lantibiotics are dehydration of serine and threonine, and cyclization of cysteines onto the dehydrated residues. These processes may be done by two independent enzymes

(LanB which performs the dehydration and LanC which is responsible for the cyclization) or by a single bifunctional enzyme (LanM). The lantibiotics are classified as being type I if they use LanB and LanC enzymes, or type II if they use a LanM enzyme (47-50). The designation type I or type II is unrelated to the type A or B classification. As seen in Fig. 2, nisin is a type I lantibiotic, since it uses separate NisB and NisC enzymes for these modifications.

The modified precursor peptide is then exported out of the cell, with concomitant removal of the leader peptide, yielding the mature bacteriocin. For the type I lantibiotics, two separate genes are required: *lanT* and *lanP*. *lanT* encodes for a dedicated ABC-transporter which secretes the precursor out of the cell, powered by the hydrolysis of ATP. The leader peptide is then cleaved off by a serine protease, encoded by *lanP*. Alternatively, for the type II lantibiotics, this maturation and secretion step is performed by one protein, LanT, which is a dedicated ABC-transporter that contains a cytoplasmic, N-terminal peptidase domain (6, 9, 54). This mechanism of maturation and secretion is very similar to that used by the majority of non-lantibiotic bacteriocins (56).

In order to protect themselves, lantibiotic producers also synthesize immunity proteins. Two different modes of immunity have been described and lantibiotics may utilize one or both of these mechanisms (48, 57). The *lanI* gene encodes for a dedicated immunity protein, which is located extracellularly (either as a membrane associated lipoprotein or as a lipid-free protein) and sequesters the bacteriocin. In the case of nisin, the NisI immunity protein is known to exist in both forms: some NisI is anchored to the extracellular side of the cytoplasmic

membrane via lipid modification (58, 59), whereas some NisI is lipid-free and found in the growth medium (59, 60). Both forms of NisI bind nisin, thus protecting the cytoplasmic membrane of a nisin-producing cell (61). The *lanEFG* genes encode for a dedicated ABC-transporter that is thought to actively pump out bacteriocin that may have entered the producer cell. As shown in Fig. 2, nisin uses both mechanisms of immunity.

For many lantibiotics, bacteriocin production is a regulated process. The *lanK* and *lanR* genes encode for a bacteriocin-specific histidine protein kinase (HPK) and a response regulator (RR). In some cases, an additional gene, *lanF*, is present which encodes for a peptide pheromone called an induction factor (IF). The induction factor is also synthesized with an N-terminal leader sequence, which is proteolytically removed during the secretion out of the cell by the ABC-transporter. In other cases, such as with nisin, the bacteriocin itself is autoinducing. Extracellular IF or bacteriocin is recognized by the membrane associated HPK, which triggers autophosphorylation of the HPK at a conserved histidine residue. The phosphoryl group is then transferred to the RR, which in turn stimulates bacteriocin production (9, 48, 50, 54).

### **1.2.3. Mode of action**

Traditionally, it was thought that lantibiotics either formed pores (type A) or interfered with cell wall biosynthesis (type B). However, in recent years, it has become evident that the killing effect of many lantibiotics is a complex phenomenon and many lantibiotics display dual modes of action. To understand

how the lantibiotics interact with their target cells, it is crucial to examine the structure of the Gram-positive cell wall.

The cytoplasmic membrane of both Gram-positive and Gram-negative bacteria is protected by an outer layer of peptidoglycan. Peptidoglycan is a polymeric network of alternating amino sugars, N-acetylglucosamine (GlcNAc) and N-acetylmuramic acid (MurNAc). Pentapeptide chains with the sequence (L-Ala)-( $\gamma$ -D-Glu)-(L-Lys or *m*-diaminopimelate)-(D-Ala)-(D-Ala) are attached to the MurNAc sugar. The glycan polymers are cross-linked by the enzymatic coupling of a D-Ala residue to the diamino (DA) residue on an adjacent chain (Fig. 3). Approximately 20 layers of peptidoglycan encompass the Gram-positive cytoplasmic membrane, providing structural integrity to the cell. In contrast, only a thin layer (about 1.5 layers thick) of peptidoglycan surrounds the cytoplasmic membrane of Gram-negative cells (62-65). However, these organisms have an outer membrane that provides protection, as will be discussed in chapter 5.

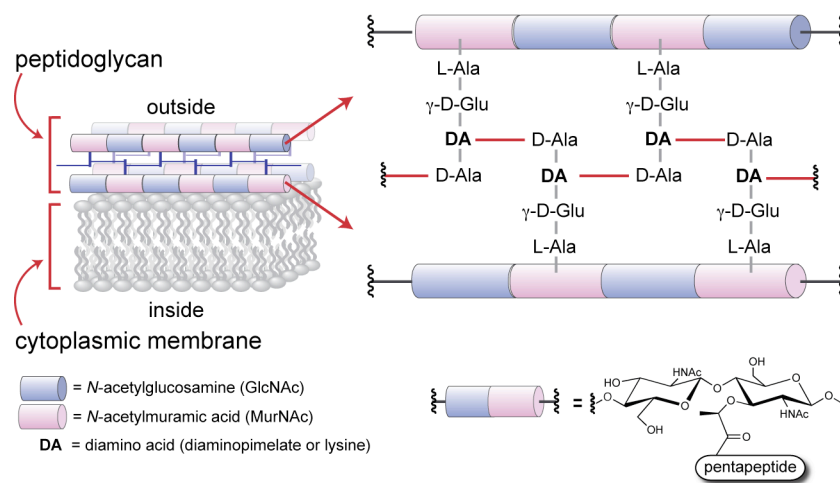


**FIG. 3.** Structure of the Gram-positive cell wall. A thick layer of peptidoglycan surrounds the cytoplasmic membrane, providing structural integrity. The peptidoglycan monomers are covalently linked via the pendant peptide chains, attached to the MurNAc sugars.

Lipid II is the building block of peptidoglycan. In addition to the sugar moieties and the pentapeptide chain, lipid II also contains a C<sub>55</sub> undecaprenyl (UDP) lipid tail, which is attached to the MurNAc sugar via a pyrophosphate linker (Fig. 4) (62-64). Lipid II is assembled in the cytosol and is then translocated across the cytoplasmic membrane. The UDP tail anchors lipid II in the bilayer, after which transglycosylation and transpeptidase enzymes couple the sugar moieties and pentapeptide chain onto the peptidoglycan framework.

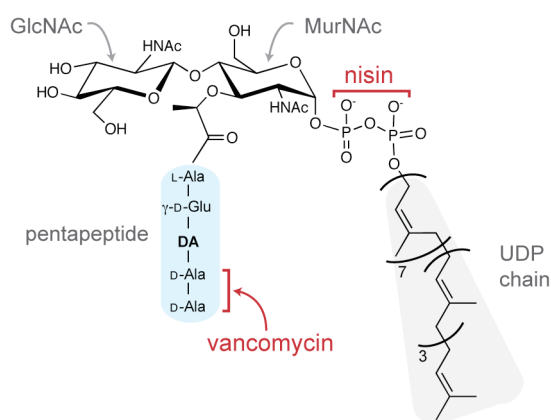


**FIG. 4.** Chemical structure of lipid II, the docking molecule for many lantibiotics. The pentapeptide and UDP chain are shaded in blue and grey, respectively and labeled. The GlcNAc and MurNAc sugars are labeled. The sites of interaction of both nisin and vancomycin with lipid II are indicated.

Vancomycin is an important antibiotic used to combat serious and persistent bacterial infections. This glycopeptide is known to interact with lipid II by binding to the (D-Ala)-(D-Ala) residues of the pentapeptide chain (Fig. 4) and thereby inhibiting peptidoglycan biosynthesis (66-69). However, numerous strains of vancomycin resistant superbugs have emerged. A simple mutation of the

terminal D-Ala residue to D-lactate prevents the binding of vancomycin with lipid II, rendering this “drug of last resort” impotent (62-64).

Many lantibiotics also utilize lipid II as a docking molecule, but with a different mode of binding. The NMR structure of nisin in complex with lipid II reveals that the N-terminal portion of nisin forms a cage-like structure around the pyrophosphate moiety of lipid II (70). The A and B rings of nisin are critical for this interaction. It has also been shown that truncated nisin derivatives, which include the A and B rings, are antagonists to nisin: they compete for binding with lipid II (71). The binding of nisin onto lipid II thus inhibits cell wall biosynthesis by preventing the incorporation of peptidoglycan subunits into the cell wall. Recently, it has been shown that many other lantibiotics, including lactacin 3147, epidermin and gallidermin (Fig. 5) also interfere with peptidoglycan biosynthesis and likely use lipid II as a docking molecule (53, 72-74).

The traditional type B lantibiotics, such as mersacidin and cinnamycin, are small, globular peptides and inhibit cell wall biosynthesis. Mersacidin (Fig. 5) has also been shown to bind to lipid II, but in a different manner than nisin does. The interaction between mersacidin and lipid II includes the terminal GlcNAc sugar (20, 75, 76). Sequence homology between residues 12-18 of mersacidin and several other type B lantibiotics suggests that binding to lipid II and inhibition of peptidoglycan biosynthesis is likely a common mode of action (64).

As mentioned earlier, the type A lantibiotics were traditionally described as elongated and flexible peptides that killed sensitive cells by pore formation. These peptides insert into the cytoplasmic membrane of sensitive cells, inducing leakage

of ions, or low-molecular weight solutes from the cell, dissipation of the proton motive force, hydrolysis of ATP and eventually, cell death. However, it has been shown that many type A lantibiotics are capable of killing sensitive cells by binding to lipid II (thus inhibiting), as well as pore formation. These lantibiotics are described as having a dual mode of action, whereby the lantibiotic first docks onto lipid II and then inserts into the membrane. This mechanism helps explain the extremely potent activity of the lantibiotics, which typically display MIC values in the nanomolar range (6, 47, 48, 54, 62, 77).

For example, it was originally thought that nisin's major mode of action was pore formation. However, as significantly higher concentrations of nisin are required to permeate artificial membranes (devoid of lipid II), compared to the nanomolar concentrations of nisin that kill sensitive cells *in vivo* (52), it became apparent that nisin's mode of action could not be adequately explained solely by pore formation (52). In the past decade, numerous studies have investigated the interaction between nisin and lipid II, revealing that nisin's antimicrobial activity is intimately linked to lipid II (70, 74, 77-81). It is now accepted that upon binding to lipid II, the C-terminus of nisin inserts into the cytoplasmic membrane and forms oligomers with other complexes of lipid II and nisin (78-80). This ultimately results in the formation of stabilized pores, composed of eight nisin molecules and four lipid II molecules (78). As such, the potent activity of nisin requires an interaction with lipid II, and results in both pore formation and inhibition of cell wall biosynthesis.

As mentioned previously, lacticin 3147 is a two-component lantibiotic, comprised of LtnA1 and LtnA2. Individually, the peptides exhibit marginal (LtnA1) or very low (LtnA2) antimicrobial activity; however, in combination, a highly potent synergistic effect is observed (82). In 2004, our group reported the NMR solution structure of lacticin 3147 (17), revealing that LtnA1 assumes a compact globular structure, whereas LtnA2 is more flexible and elongated. Subsequent mode of action studies have shown that the activity of lacticin 3147 is intimately linked to an interaction with lipid II. In 2006, Wiedemann *et al.* (72) investigated the effects of LtnA1 and LtnA2 (individually or in combination, in the absence and presence of lipid II) on intact cells, liposomes, and planar lipid bilayers. Their results suggested that lacticin 3147 forms a high-affinity three component complex with lipid II. Initially, LtnA1 interacts with the cell membrane and complexes with lipid II. This coordination is believed to induce a conformational change in LtnA1, which exposes a binding site for LtnA2. Furthermore, lipid II helps stabilize the intermolecular interaction between LtnA1 and LtnA2. Upon binding of LtnA2 onto LtnA1, the complex penetrates deep into the cytoplasmic membrane, resulting in pore formation (72). Thus, inhibition of cell wall biosynthesis and cell permeation requires the interaction between lipid II, LtnA1 and LtnA2.

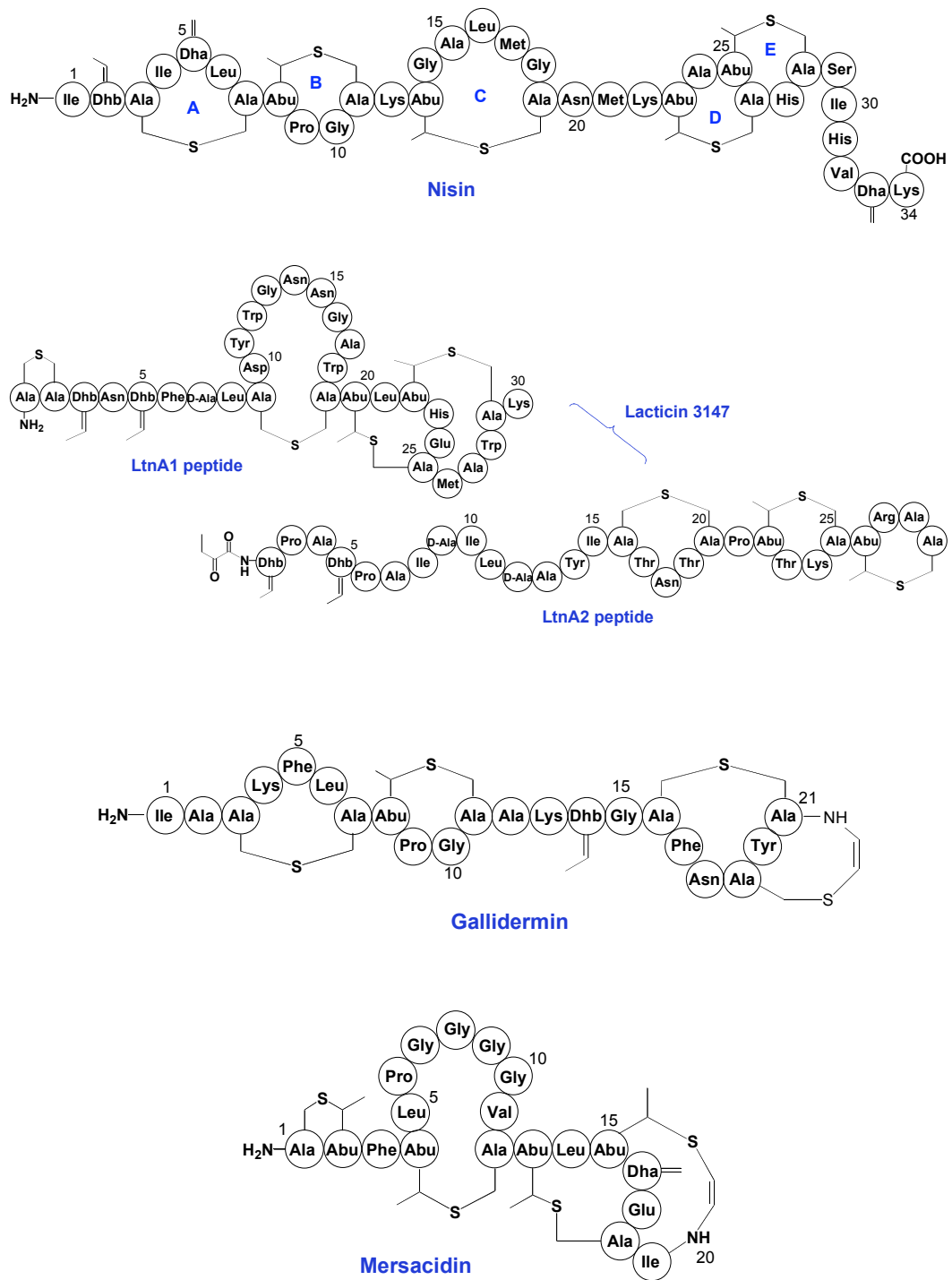


FIG. 5. Structures of nisin, lactacin 3147, gallidermin and mersacidin.

### **1.3. Non-lantibiotics: The type IIa bacteriocins**

#### **1.3.1. General characteristics**

The class II bacteriocins are small (< 10 kDa), heat-stable peptides that do not undergo posttranslational modifications other than cleavage of a leader peptide and possible disulfide bond formation. Interestingly, a number of leaderless bacteriocins have also been identified in this grouping. Within the class II bacteriocins, the type IIa or pediocin-like bacteriocins are the most studied. These heat-stable peptides are small (37 to 48 residues), cationic, and display potent activity against *Listeria monocytogenes*. There is high sequence homology in the N-terminal domain of these peptides, characterized by the consensus sequence YGNGVXC and a conserved disulfide bridge (1, 6, 8, 9, 12, 83, 84). Chapters 3 and 4 will describe many features of these bacteriocins in greater detail, including their three-dimensional structures, immunity and mode of action (Chapter 3), and biosynthesis (Chapter 4).

#### **1.3.2. Biosynthesis**

Like the lantibiotics, the genes involved in production of the type IIa bacteriocins are located on the chromosome, plasmids or conjugative transposons, and are typically clustered in operons. In general, four genes are required for the production of the type IIa bacteriocins and encode for the bacteriocin precursor, a dedicated ABC-transporter, an accessory protein, and a dedicated immunity protein. In some cases, bacteriocin production is regulated and additional genes encoding for an induction factor (IF), histidine protein kinase (HPK) and response

regulator (RR) are also present (1, 83). The operon for piscicolin 126 (PisA) (24) is shown in Fig. 6 and this operon will be used as an example in the following discussion to help illustrate the biosynthesis of the type IIa bacteriocins.

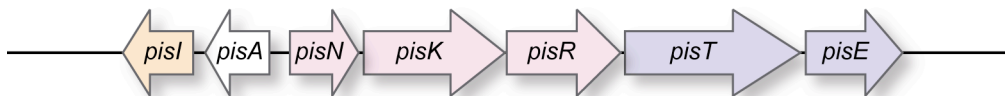


**FIG. 6.** Genes required for the biosynthesis of piscicolin 126 (PisA). The white gene (*pisA*) encodes for the precursor peptide. The blue genes (*pisT*, *pisE*) are required for maturation and secretion of the bacteriocin. The orange gene (*pisI*) is required for immunity. The pink genes (*pisN*, *pisR*, *pisK*) are involved in regulation of bacteriocin production.

The structural gene (*pisA*) for a type IIa bacteriocin encodes for a precursor peptide, with an N-terminal extension. Nearly all type IIa bacteriocins have leader peptides of the double-glycine type. The prepeptide is then secreted out of the producer cell by a dedicated ABC-transporter (encoded by *pisT*), with concomitant cleavage of the leader peptide. For bacteriocins with the Gly-Gly processing site in their leaders, cleavage of the leader peptide is performed by the N-terminal peptidase domain of the ABC-transporter, as will be described in Chapter 4. Hydrolysis of ATP provides the energy required for transport of the bacteriocin out of the cell. An accessory protein (encoded by *pisE*) is also required for secretion, although the function of this protein is currently unknown (1, 8, 12, 83). There are a few type IIa bacteriocins that do not have Gly-Gly type leader peptides and are not exported by dedicated secretion proteins. Rather, these bacteriocins contain an N-terminal signal sequence that targets them for secretion via the cell's general secretion pathway (1).

A highly specific, dedicated immunity protein (encoded by *pisI*) protects the producer organisms from the deadly effects of its own bacteriocin. Unlike the lantibiotics, the immunity proteins for the type IIa bacteriocins are located almost exclusively in the cytoplasm, with less than 1% associated with the membrane (85, 86). Despite the remarkable specificity that immunity proteins have, it does not appear that they interact directly with their cognate bacteriocins. Currently, the mechanism of immunity for these bacteriocins is unknown (12, 83, 87). Chapter 3 will discuss the structural features of these immunity proteins.

The biosynthesis of many type IIa bacteriocins is regulated by a quorum-sensing signal-transduction system. The producer organism constitutively expresses an induction factor, or IF, encoded by *pisN*. This IF is also a small peptide, with an N-terminal leader sequence containing a Gly-Gly processing site. It is recognized and transported out of the producer cell by the ABC-transporter. The IF is recognized by the membrane-associated HPK (encoded by *pisK*) and at a certain threshold concentration, triggers phosphorylation of the HPK, which then phosphorylates the RR (encoded by *pisR*). This in turn stimulates transcription of genes involved in bacteriocin production (1, 83, 84).

### **1.3.3. Mode of action**

The type IIa bacteriocins display potent antimicrobial activity, especially against *Listeria*. Mutational studies have revealed that the C-terminal domain of the peptide controls the antimicrobial specificity. The type IIa bacteriocins permeabilize the cytoplasmic membrane of sensitive cells, resulting in the

formation of non-selective pores, dissipation of the proton motive force and depletion of ATP. The type IIa bacteriocins are attracted to the anionic surface of the cytoplasmic membrane via electrostatic interactions. The hydrophobic / amphiphilic C-terminal domains of the peptides can then insert into the membrane, resulting in pore formation (1, 12, 83, 84, 88).

Like the lantibiotics, it is likely that the type IIa bacteriocins utilize a specific receptor, or docking molecule. It is believed that this receptor is the  $EII_t^{\text{man}}$  permease of the mannose-phosphotransferase system (6, 12, 83, 84). However, details regarding the interaction of the type IIa bacteriocins with this receptor remain elusive. This will be discussed in depth in Chapter 3.

## **1.4. Circular bacteriocins**

### **1.4.1. General characteristics**

The circular bacteriocins are a newly emerging class of bacteriocins. Previously, they were categorized with the class II bacteriocins (1, 6, 13). However, since the circular bacteriocins must undergo a unique post-translational modification to construct the circular backbone, several groups have recently suggested that the circular bacteriocins be moved to their own class (class IV) (12, 14, 89). These peptides are typically larger than other LAB bacteriocins (58-70 aa) and are remarkably stable to variation in pH, temperature and exposure to proteases (14). Chapter 2 will discuss the circular bacteriocins in greater detail.

### 1.4.2. Biosynthesis

The operons for several of the circular bacteriocins have been discovered (90-95); however, in comparison to the lantibiotics and class IIa bacteriocins, relatively little is known about the biosynthesis of the circular bacteriocins. For several of these peptides, various genes required for immunity have been identified, as well as numerous accessory proteins that appear to be essential for the production and export of these peptides. Many of these genes encode for basic and hydrophobic proteins. In addition, many of these proteins are predicted to contain multiple transmembrane domains and are likely membranous proteins (14). Of the circular bacteriocins, enterocin AS-48 has been the most thoroughly studied, from both a biochemical and genetic perspective. The gene cluster encoding for production of enterocin AS-48 is depicted in Fig. 7.

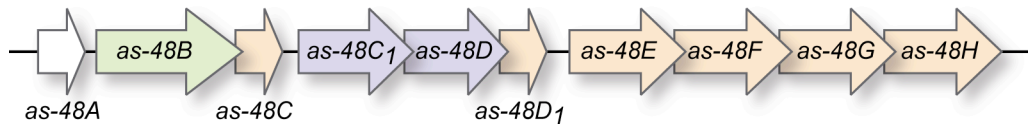


**FIG. 7.** Genes required for the biosynthesis of enterocin AS-48. The white gene (*as-48A*) encodes for the precursor peptide. The blue genes (*as-48C<sub>1</sub>D*) are required for maturation and secretion of the bacteriocin. The green gene (*as-48B*) is implicated in processing. The orange genes (*as-48C<sub>D</sub><sub>1</sub>EFGH*) are required for immunity.

Like the other LAB bacteriocins, the circular bacteriocins are also synthesized as precursor peptides. However, the leader peptides for these bacteriocins are diverse, with little sequence homology. Some are intriguingly short (2 aa for lactocyclin Q), while others are long (35 aa for enterocin AS-48). It is not known how or when the leader peptide is removed from the bacteriocin,

or what role it plays in the cyclization of the backbone. The genes for a putative ABC-transporter have been identified in the AS-48 gene cluster (*as-48C<sub>1</sub>D*) and are likely involved in transporting the bacteriocin out of the cell. While enterocin AS-48 does not utilize a quorum-sensing mechanism to regulate bacteriocin production, other circular bacteriocins (such as uberolysin) have genes encoding for a putative response regulator (14, 95, 96).

AS-48 has several genes required for immunity. One gene appears to encode for a small protein (*as-48D<sub>1</sub>*), another for an auxiliary protein (*as-48C*), whereas other genes likely encode for proteins that are involved in the formation of a dedicated ABC-transporter (*as-48EFGH*). All of these gene products appear to have transmembrane domains and are likely associated with the cytoplasmic membrane (14). The mechanism of immunity for the circular bacteriocins is unknown, but may be similar to that of the lantibiotics that utilize the two-fold immunity mechanism, encoded by *lanI* and *lanEFG* genes.

The circular bacteriocins are post-translationally modified in order to covalently link their N- and C- termini. In the case of enterocin AS-48, it was found that the *as-48B* gene is required for complete production of the bacteriocin. This gene encodes for a large, hydrophobic protein, with 12 predicted transmembrane domains (14). Currently, it is not clear what role this protein plays in the biosynthesis of AS-48. Without biochemical characterization of the genes required for the biosynthesis of these peptides, it is difficult to fully understand the mechanism behind the construction, export and immunity of the circular bacteriocins.

### 1.4.3. Mode of action

Like many other bacteriocins produced by LAB, the circular bacteriocins appear to be pore-forming toxins. Enterocin AS-48 permeabilizes the cell membrane and forms non-selective pores that permit leakage of ions and low molecular weight solutes and dissipation of the proton motive force, ultimately resulting in cell death (97). Interestingly, it has been reported that enterocin AS-48 is also active against various Gram-negative bacteria, including strains of *E. coli*, *Shigella sonnei*, *Rhizobium* and *Myxococcus xanthus*, albeit it at much higher concentrations (98). The broad spectrum of activity, in combination with its stability, makes AS-48 a potential candidate for use in food preservation (37, 89, 97).

## 1.5. Commercial Applications of LAB Bacteriocins

### 1.5.1. Biopreservatives

In recent years, there has been an increase in consumer demand for foods that are safe, minimally-processed and contain few chemical additives. The use of bacteriocins in food preservation is a natural response to such demand (2, 5-7, 9, 83, 99, 100). As already mentioned, LAB have been used for centuries in the biopreservation of fermented foods since they inhibit the growth of food-spoilage and pathogenic bacteria. Today, many different LAB are used as starter cultures in numerous cheese and dairy industries (4, 6, 9). In addition, many strains of LAB are used as probiotics (1, 4). The widespread use of LAB in the food

industry has garnered them, and their products, GRAS status (generally regarded as safe).

There are many potential benefits to the use of bacteriocins as biopreservatives. In general, bacteriocins have shown very little, if any, toxicity toward eukaryotic cells. Many bacteriocins are pH and heat tolerant and as such, can withstand the various processing, packaging and storage treatments currently used for food preservation. As well, the addition of bacteriocins during food processing and preparation can help reduce the overall processing required for the food. This enhances the organoleptic properties of the food and reduces costs associated with processing. Furthermore, the potent activity of numerous LAB bacteriocins against many serious food pathogens, such as *Bacillus*, *Listeria* and *Clostridia*, makes them ideal candidates for use in food safety. Lastly, since bacteriocins display varied spectra of activity, they can be used selectively to target specific pathogens, unlike the indiscriminate effects that other food processing techniques exert (2, 5-7, 9, 83, 100-103).

Despite these advantages, the direct application of either purified or semi-purified bacteriocin extracts to food has been limited. To date, only nisin and pediocin (marketed as Nispalin™ and Alta™ 2431, respectively) are used commercially as semi-purified growth extracts, and only nisin has received regulatory approval from both the World Health Organization (in 1969) and the U.S. Food and Drug Administration (in 1988) to be added as a purified compound (5, 6, 9). Nonetheless, extensive research continues to explore the utility of bacteriocins as safe and natural additives to be used in food preservation.

### 1.5.2. Therapeutic agents

There is also great potential for the application of bacteriocins as therapeutic agents. As bacterial resistance to conventional antibiotics continues to emerge, there is an urgent need to develop novel approaches to combat bacterial infection. In addition to being non-toxic to eukaryotic cells, there are several other characteristics that make bacteriocins attractive therapeutics. First, bacteriocins are typically much more potent than conventional antibiotics. Second, different bacteriocins display different spectra of activity: this allows for a tailored therapeutic approach. Third, many bacteriocins are active against known superbugs, including various strains of methicillin resistant *Staphylococcus aureus* (MRSA) and vancomycin resistant *enterococci* (VRE). Lastly, many bacteriocins kill their target cells by causing pore formation and permeation of the cytoplasmic membrane. Unlike conventional antibiotics that typically target specific enzymes, the mode of action of bacteriocins is diverse, ranging from pore formation to inhibition of cell wall biosynthesis, and as previously described, some bacteriocins are capable of exerting dual modes of action. As such, the killing effect of bacteriocins is complex, making it much more difficult for pathogens to develop resistance (4, 6, 48, 51, 104-106).

Nisin is currently used in veterinary medicine to treat bovine mastitis, a common and persistent bacterial infection of the udder that afflicts dairy cows. Research has indicated that lactacin 3147 can also be used to treat such infections (6). Numerous animal model studies have shown that various lantibiotics can be used to treat oral infections, such as tooth decay and gingivitis, as well as skin

infections (6, 51, 107). Recently, the spermicidal activity of various bacteriocins has also been investigated (108). It is likely that as bacterial resistance continues to threaten the effectiveness of current antibiotics, bacteriocins will emerge as exciting, new therapeutic agents.

## 1.6. Overview of Projects

The projects described in this thesis are focused on the characterization of bacteriocins, examining the biosynthesis and mode of action of bacteriocins from a structural perspective, and expanding the spectra of activity of various bacteriocins.

Chapter 2 will describe the isolation and characterization of carnocyclin A (CclA), a member of the newly emerging class of circular bacteriocins. The primary sequence of this peptide was solved by a combination of techniques, including Edman degradation, *de novo* MS/MS sequencing and genetic analysis. The 3D structure of this bacteriocin was solved using a variety of multi-dimensional, heteronuclear NMR experiments. The stability, spectrum of activity and mode of action of CclA will also be described. In addition, on-going research to investigate the role of the leader peptide in bacteriocin structure and activity will be discussed.

Chapter 3 will focus on the type IIa bacteriocins, particularly their immunity proteins. In this chapter, the characterization and structural elucidation of PisI, the immunity protein for piscicolin 126, will be described. Furthermore, studies towards the overexpression and purification of the membrane-bound IIC

and IID subunits of the  $EII_t^{\text{man}}$  permease of the man-PTS system membrane proteins will be discussed. This preliminary work sets the stage for future studies aimed at exploring the interaction of the type IIa bacteriocins, and their immunity proteins, with their receptor.

Chapter 4 will also examine the type IIa bacteriocins, but will focus on the role of the ABC-transporter in the maturation of these bacteriocins. As mentioned previously, the leader peptides of the type IIa bacteriocins are cleaved off by the peptidase domain of their ABC-transporters. The overexpression and purification of pCbnB2 (carnobacteriocin B2 with its leader peptide) and of CbnTP (the peptidase domain of the ABC-transporter for this peptide) will be discussed. In addition, the preparation of various Cys→Ser mutants of CbnTP, to facilitate crystallographic studies, will be described.

Chapter 5 will highlight some of the current limitations of LAB bacteriocins, particularly their inability to kill Gram-negative pathogens. However, under certain conditions, the efficacy of LAB bacteriocins can also be extended to these bacteria. In this study, the efficacy of six different bacteriocins toward *E. coli*, *Pseudomonas* and *Salmonella*, was evaluated.

Lastly, Appendix A will describe attempts to solve the 3D structure of colicin V (ColV), a bacteriocin produced by the Gram-negative bacterium *E. coli*. The overexpression and purification of ColV will be discussed. A variety of multi-dimensional, heteronuclear NMR experiments were performed and analysis of the results indicated that ColV was random coil.

## Chapter 2. Structural studies of carnocyclin A

### 2.1. Background

Much of the following chapter has been adapted from our recent publications on the sequence (109), mode of action (110) and structure of CcIA (111).

#### 2.1.1. The circular bacteriocins

The circular bacteriocins are a unique group of bacteriocins from LAB, characterized by an amide bond linking the N- and C-termini of the peptide. They exhibit enhanced stability to pH and temperature variation, and are resistant to numerous proteases, in contrast to many linear bacteriocins. This stability derives, in part, from the cyclic structure of the peptide (14, 112-114). Interestingly, circular peptides are not unique to bacteria: they have also been discovered in plants and animals, and exhibit a diverse range of bioactivities. Typically, the circular peptides from these higher organisms are shorter in length and contain at least one disulfide bond, further enhancing their structural integrity (112, 114).

Prior to this study, seven other circular bacteriocins had been reported. These include enterocin AS-48 (37), butyrivibriocin AR10 (90), circularin A (38), gassericin A / reuterin 6 (which were initially thought to be diastereomers) (92, 115), subtilisin A (41, 43), uberolysin (95), and most recently, lactocyclicin Q (116). Acidocin B is considered a putative circular protein, as it shows 98% sequence identity to gassericin A, but its circular nature has not been confirmed

(40). Of these bacteriocins, subtilisin A is atypical: it is significantly shorter (35 amino acids), anionic and contains unique thioether bridges linking cysteine sulfurs to the  $\alpha$ -carbon of other residues (42-44). As such, subtilisin A represents a unique class of bacteriocins (43) and will not be included in the present discussion of the other circular bacteriocins, which typically range from 58 – 70 amino acids in length, are cationic and contain a large number of hydrophobic residues (14). All of the known circular bacteriocins are synthesized as precursor peptides, with an N-terminal extension and a free C-terminus. There is no apparent sequence homology between the leader peptides, some of which are very short (2, 3, 6 and 8 aa for lactocyclin Q (116), circularin A (38), uberolysin (95) and subtilisin A (44), respectively) while others are much longer (22, 33 and 35 aa for butyriovibriocin AR10 (90), gassericin A (92), and AS-48 (94), respectively).

Currently, the mechanism of backbone cyclization is a mystery. It is believed that cyclization occurs after loss of the N-terminal leader peptide and nucleophilic attack of the resultant amine onto the C-terminus of the peptide. It is unknown how the C-terminus is activated to facilitate this attack. In contrast, the cyclotides (circular peptides produced by plants) are synthesized as precursor peptides with both N- and C-terminal extensions (113, 117, 118). In most cyclotides, this C-terminal extension begins after a conserved Asn or Asp residue and mutations to this position appear to prevent the excision of the C-terminus and cyclization of the peptide (117, 119). After loss of the N-terminal leader, it is believed that a cysteine protease recognizes the C-terminal extension and cleaves

it from the cyclotide chain (120). The “new” C-terminus of the cyclotide remains bound to the enzyme active site, as a thioester intermediate. Rather than water hydrolyzing the thioester, it is believed that the N-terminus of the cyclotide enters the active site. The amine attacks the thioester, thus regenerating the free enzyme and releasing the now cyclized peptide (117, 120).

### **2.1.2. The structure of enterocin AS-48**

Prior to this study, the structure of only one circular bacteriocin had been reported. In 2000, González *et al.* (121) described the NMR solution structure of AS-48, revealing that it consists of five helices encompassing a compact hydrophobic core. The covalent bond linking the N- and C- termini of the peptide was found to reside within the fifth helix. In 2003, crystallographic studies supported the proposal that at physiological pH AS-48 exists as a water soluble dimer, in which the hydrophobic faces of the individual monomers are in contact and polar interactions with the aqueous solvent are maximized (122). However, upon interaction with a membrane, this dimer undergoes a conformational change, exposing its hydrophobic faces and facilitating insertion into the membrane. The 3D structure of AS-48 shows a significant charge separation across the molecule, as a cluster of lysines at one end of the molecule imparts a high degree of positive charge on the surface of the peptide (121, 122). This charge localization is believed to be crucial for insertion of the peptide into the membrane through a mechanism known as molecular electroporation (89, 121, 123). Functional studies of AS-48 have shown that this peptide causes non-selective pore formation in

lipid bilayers, thereby allowing for the free diffusion of ions and low molecular weight solutes across the membrane (97). A similar mode of action has been reported for gassericin A / reuterin 6 (124).

### 2.1.3. Objectives

*Carnobacterium maltaromaticum* UAL307, a heterofermentative LAB, was isolated from fresh pork. This strain displays remarkably high activity toward many *Listeria* species, prompting us to investigate the bacteriocins produced by this organism. Initial studies by Dr. Sylvie Garneau revealed that *C. maltaromaticum* UAL307 produces at least three unique bacteriocins. Through a combination of Edman degradation, MS/MS sequencing and genetic analysis, Dr. Sylvie Garneau identified two of these bacteriocins as piscicolin 126 and carnobacteriocin BM1, which are both type IIa bacteriocins that have previously been reported (24, 25, 125). The focus of this project was the characterization of the third bacteriocin, which we have named carnocyclin A (CclA).

In particular, this project had three main goals. First, it was necessary to determine the primary amino acid sequence of CclA. Secondly, we wanted to characterize the antimicrobial activity of CclA, including its spectrum of activity, stability profile and mode of action. Third, we wanted to elucidate the three dimensional structure of CclA by solution NMR. As will be described, all of these goals were achieved. In addition, an on-going project will be presented, which focuses on the cyclization of CclA. The construction of overexpression systems

for the precursor peptide (pCclA), as well as various pCclA mutants, and initial expression studies will be described.

## 2.2. Results & Discussion

### 2.2.1. Purification of CclA

The bacteriocins produced by *C. maltaromaticum* UAL307 were isolated from overnight culture supernatant by hydrophobic interaction chromatography. In the first step of the purification, the supernatant was loaded onto Amberlite XAD-16 resin. The bacteriocins PisA and CbnBM1, as well as CbnB1 (an oxidized form of CbnBM1) were separated from CclA by washing the resin with 40% IPA. CclA was then eluted with 70% IPA, pH 2. The CclA fraction was further purified via solid-phase extraction, using a Megabond C<sub>18</sub> cartridge. The addition of a 30% MeCN wash during this step significantly improved the subsequent HPLC purification. From 1 liter of cell culture, an average yield of 2 mg of carnocyclin A was obtained.

The identity and purity of carnocyclin A was assessed by mass spectrometry and gel electrophoresis. MALDI-TOF MS indicated that CclA has a molecular mass of 5862 Da (Fig. 8A). The results of SDS-PAGE showed that the bacteriocin was pure; however, it migrated with an apparent molecular mass of 3,900 Da (Fig. 8B). This anomalous behavior on SDS-PAGE has been reported for other bacteriocins, including several circular bacteriocins (38, 95, 115, 126), and is attributed to their highly compact, globular structures. Gel electrophoresis followed by *in situ* activity testing showed that the purified peptide displayed

antimicrobial activity (Fig. 8B), confirming that we had indeed successfully purified the bacteriocin.

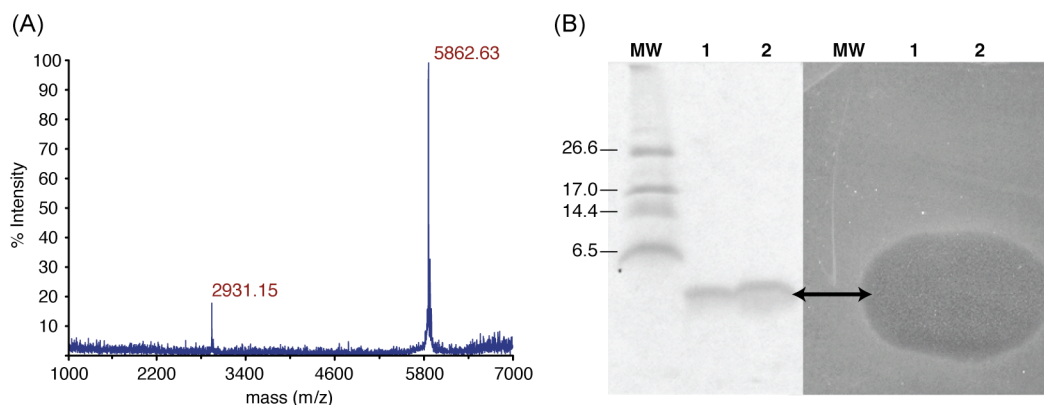


**FIG. 8.** Characterization of CclA by MALDI-TOF MS, gel electrophoresis and activity testing. (A) MALDI-TOF spectrum of CclA, showing the singly and doubly charged species. (B) 16.5% Tris-Tricine gel and activity testing of CclA against *C. divergens* LV13. The activity test was performed by overlaying soft agar (containing the indicator organism) onto the gel. Lanes 1 and 2 contain 7  $\mu$ g and 14  $\mu$ g of purified CclA, respectively, and lane MW contains molecular weight markers. The double-headed arrow indicates the position of CclA. Molecular weights are listed (in kDa).

### 2.2.2. Elucidation of the amino acid sequence of CclA

CclA was refractory to both Edman degradation and MS/MS sequencing, which led us to speculate that perhaps it had a circular backbone. To generate linear fragments, CclA was digested with trypsin and  $\alpha$ -chymotrypsin. The resulting fragments were then analyzed by Edman degradation and extensive *de novo* MS/MS sequencing (performed by Dr. Randy Whittal and Jing Zheng). Several key linear sequences were elucidated, and overlapping of these segments provided a putative amino acid sequence comprised of 60 residues (Fig. 9A). Fragment 1 was sequenced by Edman degradation and hence, Leu and Ile residues

were unambiguously assigned. The remaining fragments (2-9) were sequenced by *de novo* MS/MS sequencing and definitive identification of Leu and Ile residues was not possible. The identity of several leucines was predicted on the basis of the  $\alpha$ -chymotrypsin fragments as follows: since  $\alpha$ -chymotrypsin cleaves at the C-terminus of Leu but not Ile, if the mass difference at the C-termini of these fragments was indicative of Leu/Ile and an intense peak was observed, then the residue was presumed to be leucine. In order to differentiate between Lys and Gln residues, exact mass measurements were obtained by Fourier transform ion cyclotron resonance (FTICR) for fragments 2, 3, 8, and 9. From the 60 aa sequence, the molecular mass of CclA was calculated to be 5,880 Da, 18 units higher than the observed molecular mass. As suspected, this difference could be explained by the loss of a water molecule, due to an N-to-C cyclization and the formation of a new peptide bond. Thus, the sequence data, combined with the failed attempts to sequence the intact peptide, strongly suggested that CclA is a circular peptide.

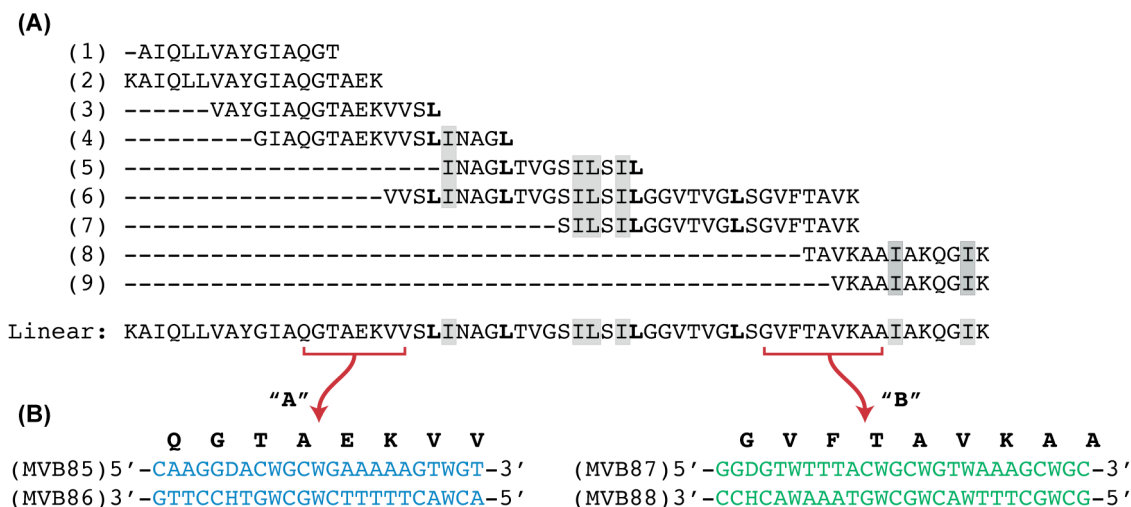


**FIG. 9.** Elucidation of the linear sequence of CclA by Edman degradation and MS/MS sequencing. (A) Amino acid sequences of various peptide fragments and the deduced total linear sequence of CclA. Leucine and isoleucine residues that were not definitively assigned are shaded grey. Leucines that are bolded were observed as the C-terminal residue following digestion with  $\alpha$ -chymotrypsin and hence, presumed to be leucine. Peptide fragment 1, trypsin digest followed by Edman sequencing; peptide fragments 2, 6, and 7, trypsin digest followed by *de novo* MS/MS sequencing; peptide fragments 3, 4, 5, 8, and 9,  $\alpha$ -chymotrypsin digest followed by *de novo* MS/MS sequencing. (B) Nucleotide sequences of degenerate primers used to amplify the internal part of the structural gene of CclA. The nucleotide bases D, H, and W indicate a mixture A/G/T, A/C/T and A/T nucleotides, respectively.

Although the sequence data suggested that CclA was circular, it could not reveal where the point of cyclization occurred. To fully confirm the circular structure of the peptide, and identify the N- and C- termini, it was necessary to isolate the *cclA* structural gene. This work was performed by Dr. Marco van Belkum. Two sets of degenerate primers (MVB85/MVB86 and MVB87/MVB88) were designed, based on two regions of the primary sequence (QGTAEKVV and GVFTAVKAA, regions “A and “B” respectively) displaying the least amount of codon degeneracy (Fig. 9B). If CclA was indeed cyclic, the relative position of these two regions had to be determined. As depicted in Fig. 10A, if region A was N-terminal to region B, then primer pair MVB85/MVB88 would yield a PCR

product. On the other hand, if region B were N-terminal to region A, then primer pair MVB87/MVB88 would generate a PCR product (Fig. 10B). Of course, there also existed the unlucky possibility that either region contained the point of cyclization (Fig. 10C,D). If this were the case, likely no PCR products would be generated.

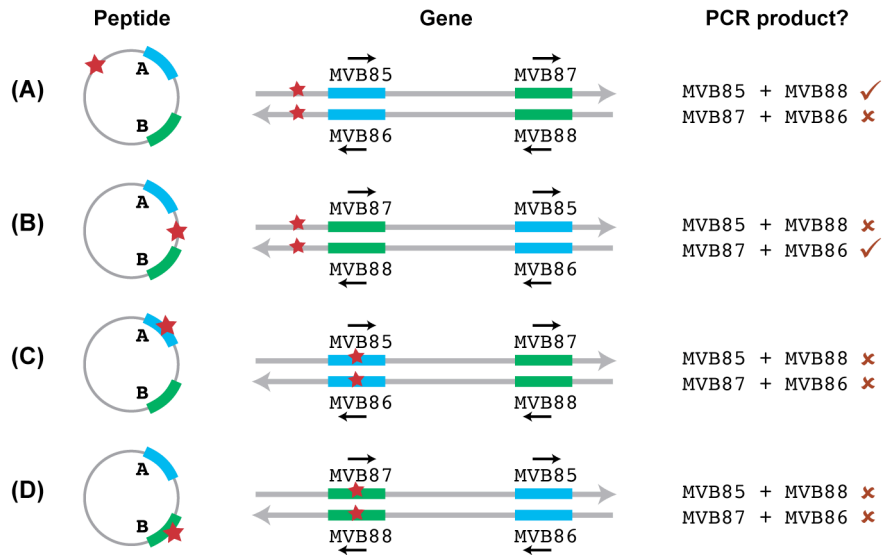


**FIG. 10.** Determining the relative position of amino acid sequences within a circular sequence. The red star indicates the start of the N-terminus of the CclA peptide and the *cclA* structural gene. (A) In this scenario, fragment A is N-terminal to B and primer pair MVB85/MVB88 would yield a PCR product. (B) In this scenario, fragment B is N-terminal to A and primer pair MVB87/MVB86 would yield a PCR product. (C, D) In these situations, the point of cyclization lies within either fragment A or B and no PCR product would be observed.

Using total genomic DNA from *C. maltaromaticum* UAL307 as a template, only primer pair MVB85/MVB88 generated a PCR product, which upon sequencing, corresponded to the nucleotide sequence from region A to B. This sequence data was then used to design specific primers, and with inverse PCR, the whole sequence of *cclA* was obtained. Analysis of the nucleotide sequence revealed that *cclA* encoded for a 64 aa peptide. By comparing the predicted amino

acid sequence based on the nucleotide sequence to the known linear sequence, it was clearly demonstrated that CclA is a circular peptide, with a head-to-tail cyclization between leucine-60 and leucine-1. The identities of the ambiguous Ile and Leu residues were confirmed, with the revision of only one Leu. Moreover, it was shown that CclA is synthesized as a precursor peptide, with a four amino acid leader peptide (MLYE). These findings are illustrated in Fig. 11.

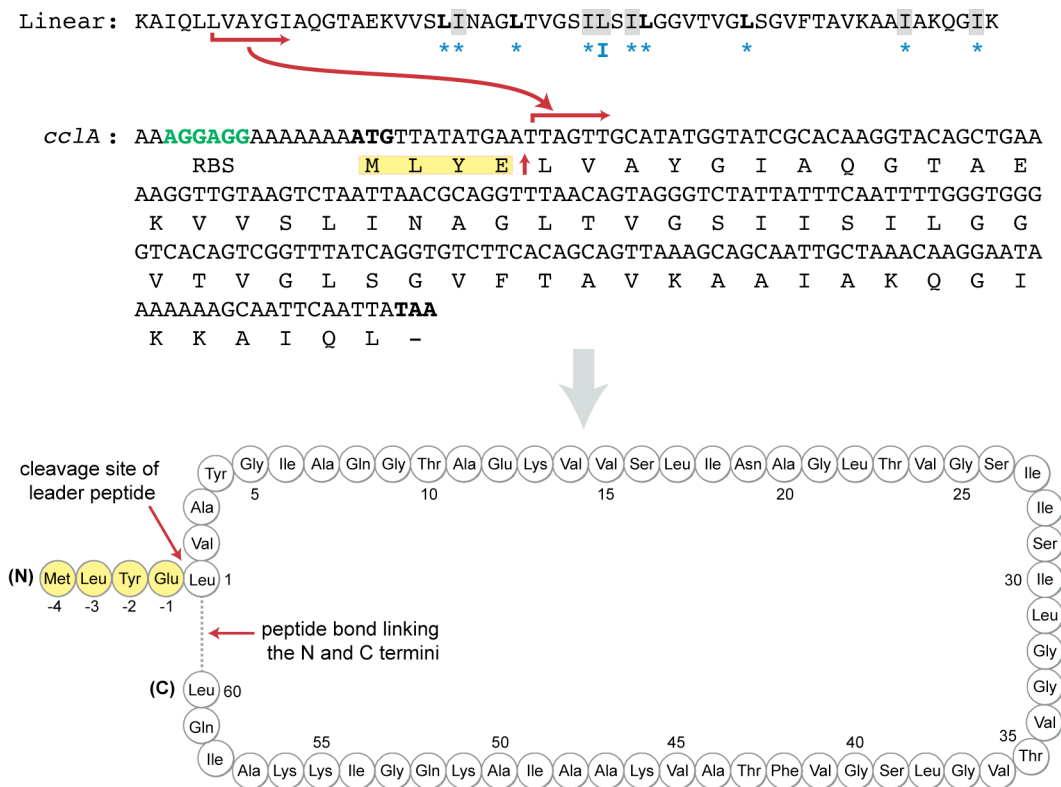


**FIG. 11.** Elucidation of the circular structure of CclA: from linear sequence, to genetic sequence, to confirmation of the circular structure. The blue asterisks beneath the linear sequence confirm the predicted aa identity of that position, where as the blue Ile denotes the revision, based on the genetic sequence. The ribosomal binding site (RBS) for *cclA* is highlighted in green. The leader sequence is highlighted in yellow and the cleavage point indicated with a red arrow. The start and stop codons for *cclA* are bolded. The bead-on-string diagram shows the complete primary structure.

### 2.2.3. Characterization and Mode of action of CclA

#### 2.2.3.a. Antimicrobial spectrum of CclA

To determine the spectrum of activity of CclA, a variety of Gram-positive and Gram-negative organisms were tested, using spot-on-lawn assays. CclA exhibited a broad spectrum of activity and was active against all of the Gram-positive strains tested, including pathogens such as *Listeria* and *S. aureus*. No activity was observed against the Gram-negative strains that were tested. Results are listed in Table 2.

**TABLE 2.** Spectrum of activity of CclA

Indicator strain	Results <sup>a</sup>	Ref. or source
<i>C. maltaromaticum</i> UAL26	+	(24)
<i>C. maltaromaticum</i> LV17	+	(127)
<i>C. divergens</i> LV13	+	(128)
<i>Brochothrix campestris</i> ATCC 43754	+	ATCC <sup>b</sup>
<i>Brochothrix thermosphacta</i> ATCC 11509	+	ATCC
<i>Enterococcus faecalis</i> ATCC 7080	+	ATCC
<i>Enterococcus faecium</i> ATCC 19434	+	ATCC
<i>Ent. faecium</i> BFE900	+	(129)
<i>Lactococcus lactis</i> spp. <i>lactis</i> ATCC 11454	+	ATCC
<i>Lc. lactis</i> ssp. <i>cremoris</i> ATCC 11602	+	ATCC
<i>Lc. lactis</i> subsp. <i>lactis</i> DPC3147	+	(130)
<i>Lactobacillus sakei</i> 706	+	(131)
<i>Lb. sakei</i> UAL1218	+	Lab collection
<i>Leuconostoc mesenteroides</i> Y105	+	(132)
<i>Pediococcus acidilactici</i> PAC1.0	+	(133)
<i>Listeria monocytogenes</i> ATCC 15313	+	ATCC
<i>L. monocytogenes</i> H7762	+	CDC <sup>c</sup>
<i>L. monocytogenes</i> ATCC 43256	+	ATCC
<i>L. monocytogenes</i> HPB 642	+	Health Canada
<i>L. monocytogenes</i> UAFM 1	+	Lab collection
<i>L. monocytogenes</i> UAFM 15	+	Lab collection
<i>Staphylococcus aureus</i> ATCC 25923	+ f	ATCC
<i>S. aureus</i> ATCC 6538	+ f	ATCC
<i>S. aureus</i> ATCC 29213	+	ATCC
<i>Escherichia coli</i> JM109	–	(134)
<i>E. coli</i> BF2	–	Lab collection
<i>E. coli</i> DH5 $\alpha$	–	Invitrogen
<i>Pseudomonas aeruginosa</i> ATCC 14207	–	ATCC
<i>P. aeruginosa</i> ATCC 15442	–	ATCC
<i>Salmonella typhimurium</i> ATCC 23564	–	ATCC
<i>S. typhimurium</i> ATCC 13311	–	ATCC

<sup>a</sup> +, inhibition; +f, faint inhibition; – no inhibition of the indicator strain at 250  $\mu$ M CclA;

<sup>b</sup>American Type Culture Collection; <sup>c</sup>Centre for Disease Control and Prevention

### **2.2.3.b. Stability studies**

When exposed to temperatures between  $-80^{\circ}\text{C}$  and  $75^{\circ}\text{C}$  for 1 h, carnocyclin A retained its activity. In addition, autoclaving the peptide ( $121^{\circ}\text{C}$  for 15 min) had no effect on activity, but when it was boiled at  $100^{\circ}\text{C}$  for 1 h (1 atm), a 32-fold reduction of activity was observed. Thus, it appears that the peptide is able to withstand heat treatment without aeration for a limited period of time, after which it begins to lose activity. No loss in activity was detected when the bacteriocin was treated for 24 h at pH values ranging from 2 to 12 at  $4^{\circ}\text{C}$ .

CclA was also remarkably stable in the presence of various proteases. CclA was unaffected by chymopapain, endoproteinase Glu-C, endoproteinase Asp-N, and papain (a non-specific protease). However, treatment with trypsin, pepsin, and protease VIII resulted in a complete loss of antimicrobial activity. MALDI-TOF analysis of the reaction mixtures revealed that the peptide had been digested into several smaller fragments. This was also observed when CclA was incubated with  $\alpha$ -chymotrypsin and thermolysin. This proteolytic stability suggests that CclA has a highly compact three-dimensional structure, which helps prevent proteolysis of its peptide bonds.

### **2.2.3.c. Mode of action**

In collaboration with Drs. Marek Duszyk and Xiandi Gong (Department of Physiology, University of Alberta), the pore forming properties of CclA were investigated. Liposomes containing CclA were prepared and reconstituted into lipid bilayers. The effect of CclA on the bilayer conductance, under a variety of

conditions, was then investigated using single channel recording techniques. All experiments and analysis of data was performed by Dr. Xiandi Gong and are described in our recent publications on the ion channel properties (110) and 3D structure (111) of CclA. A brief summary of the results are provided below.

The results of lipid bilayer studies revealed that CclA forms ion channels in lipid bilayers. Interestingly, these channels are anion selective, with a preference for transporting nitrate and chloride, as well as fluoride. It was found that while pH did not affect the conformation of the channel, it did affect the stability of the CclA pore: under acidic conditions, greater conductance across the membrane was observed, suggesting that the CclA ion channel was stabilized and anion permeation was facilitated. At neutral pH, the five lysine sidechains of CclA would be protonated, imparting a localized, positive charge on the molecule. At lower pH, the side chain of Glu-12 would also be protonated, further enhancing the net positive charge of the molecule. This net positive charge is likely a key component in both attracting CclA to the anionic lipid membrane and facilitating membrane insertion via molecular electroporation (135). In addition, channel activation was found to be strongly voltage dependent. Channel formation required the presence of a negative membrane potential and the channels were completely deactivated upon membrane depolarization. However, channel gating was voltage-independent. Since CclA was able to interact directly with the lipid bilayer, its mode of action is likely not receptor mediated.

According to these results, the following model has been proposed to describe the mode of action of CclA against target cells. After approaching the

surface of a bacterial cell, due to electrostatic interactions, CclA is exposed to the highly negative membrane potential of the bacterial cell (-100 mV) (136). At this potential difference, CclA creates anion selective pores across the membrane and channel activation occurs. As anions flow through the channel, depolarization occurs, leading to the inactivation of the CclA channel.

Interestingly, the ion channel properties of CclA are different than those of enterocin AS-48. Investigations of the effect of AS-48 on bacterial cells, membrane vesicles and lipid bilayers report that AS-48 forms voltage-independent, non-selective pores, which result in the diffusion of ions and small solutes across the membrane and ultimately, collapse of membrane potential (97). In contrast, the ion channels formed by CclA are anion selective, and highly stable, remaining in the open state for several minutes. Furthermore, the interaction of CclA with the bilayer and channel activation was strongly voltage dependent. Ultimately, both AS-48 and CclA permeate the cytoplasmic membrane of their target cells. However, the differences in ion channel characteristics for these two bacteriocins may help explain the different spectra of activity that each display.

## **2.2.4. Preliminary structural studies**

### **2.2.4.a. Stereochemical analysis**

Prior to initiating structural studies, a stereochemical analysis of CclA was performed, as it had been reported that two other circular bacteriocins (gassericin A and reutericin 6) contained (D)-residues (124). Very recently, however, it has

been revealed gassericin A and reutericin 6 do *not* contain (D)-amino acids and are in fact, identical to each other (unpublished data, correspondence with senior investigator). Summer student Michael Kreuzer was involved in the preparation of samples (CclA and amino acid standards), and the subsequent stereochemical analysis of the samples.

After acid hydrolysis of CclA, the constituent amino acids were derivatized to their pentafluoropropanamide isopropyl esters. Sets of (L)- and (D)-amino acid standards were also prepared. Chiral GC-MS revealed that CclA contains only (L)-amino acids, as the chromatogram for CclA overlaid perfectly with that of the (L)- standards (Fig. 12A). Furthermore, when CclA was spiked with the (L)- standards, no new peaks were observed. It should be noted that when a mixture of the (L)- and (D)- standards was analyzed by GC-MS, the enantiomers of each residue except Asn/Asp were well resolved (Fig. 12B). When the standards were analyzed individually, the Asn/Asp peak was narrow, but when the standards were mixed, this peak exhibited broadening. When CclA was spiked with the (L)-standards, this peak did not display broadening, suggesting that the Asn of CclA is the (L)- amino acid. In addition, when the (L)- and (D)- standards were mixed, L-Thr and D-Val co-eluted, as did L-Leu and D-Ser (see inset in Fig. 12B). When CclA was analyzed, mass spectrometry indicated that only L-Thr and L-Leu were present in these two peaks, indicating that neither D-Val nor D-Ser were present.

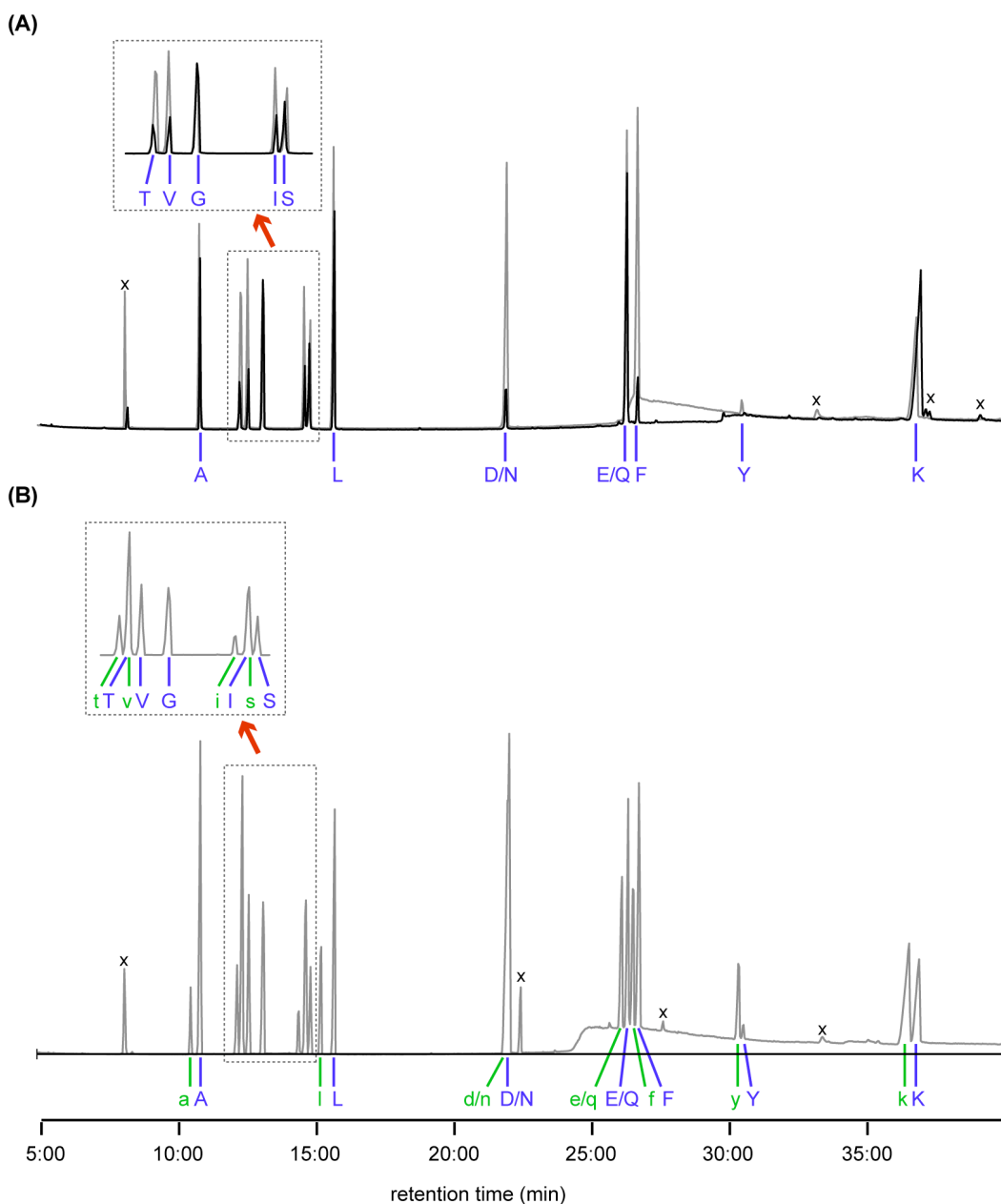


**FIG. 12.** Chiral GC-analysis of hydrolyzed and derivatized CcIA and (L)- and (D)- amino acid standards. (A) Overlay of CcIA's chromatogram (in black) with the set of (L)- standards (in grey). (B) Chromatogram of mixed (L)- and (D)- standards. The inset shows the overlapping L-Thr/D-Val, and L-Leu/D-Ser peaks. The identity of each peak is indicated. Capitalized, blue letters refer to (L)-amino acids and lower case green letters refer to (D)- amino acids. Contaminants are indicated with an x.

### 2.2.4.b. Secondary structure determination via CD and $^{15}\text{N}$ HSQC

Circular dichroism (CD) was performed to determine if CclA had defined secondary structural elements (Fig. 13A). Under aqueous conditions, CD indicated that CclA contains helical structures (approximately 36%). Upon addition of TFE, a membrane-mimicking solvent (137), this helicity was enhanced (up to 52%). In contrast, the type IIa bacteriocins are almost entirely random coil in aqueous conditions and TFE must be added to induce helicity (137-140). The  $^{15}\text{N}$  HSQC spectrum of CclA showed good spectral dispersion, with 58 out of the 60 amides displaying unique chemical shifts, suggesting the presence of defined secondary structure (Fig. 13B).

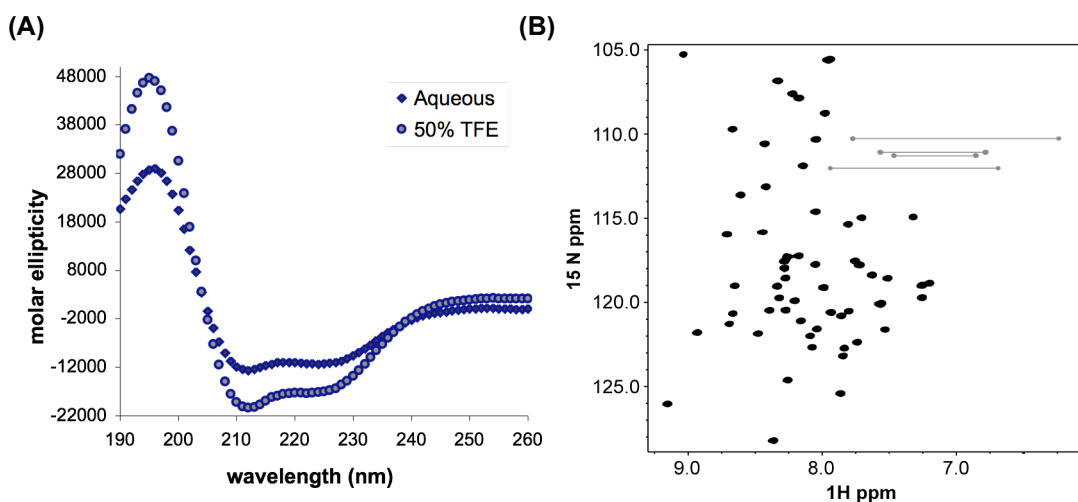


**FIG. 13.** Secondary structural analysis of CclA by circular dichroism and  $^{15}\text{N}$  HSQC. (A) CD spectra of CclA in aqueous and membrane-mimicking conditions. (B)  $^{15}\text{N}$ -HSQC of CclA. Sidechain NH resonances (from Gln and Asn) are colored grey.

### 2.2.4.c. Oligomeric state of CclA

To determine the oligomeric state of CclA under different pH and salt conditions, a combination of dynamic light scattering (DLS) and NMR

experiments were performed. Results from DLS indicated that CclA is monomeric at all pH values tested (from pH 3 to 8), at a protein concentration of  $\sim 1$  mM. Increasing the salt concentration (up to 500 mM NaCl) had virtually no effect on the backbone structure of CclA, as monitored by  $^{15}\text{N}$  HSQC (Fig. 14A), whereas varying the pH resulted in slight chemical shift perturbations (Fig. 14B).

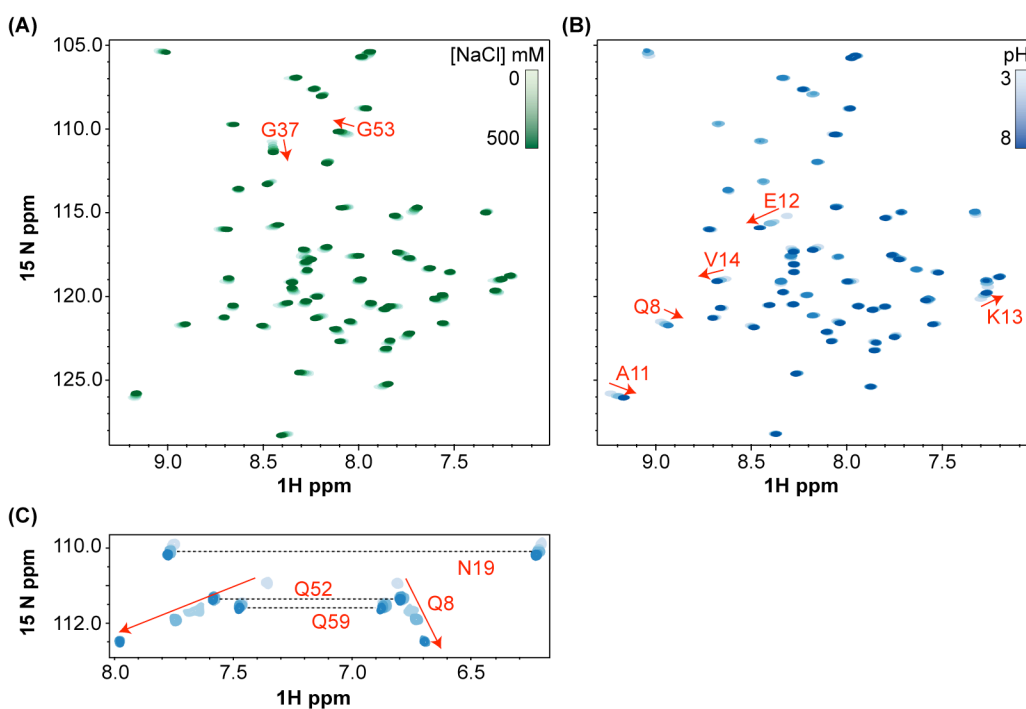


**FIG. 14.** Examining the effect of NaCl and pH on the backbone and sidechain amide resonances of CclA by  $^{15}\text{N}$  HSQC. (A) Effect of NaCl, (from 0 to 500 mM) on the backbone amide resonances of CclA. (B) Effect of pH (from 3 to 8) on the backbone amide resonances of CclA. (C) Effect of pH on the Gln and Asn sidechain amides resonances of CclA.

The greatest changes were observed for glutamate-12 and the side chain of glutamine-8, with minor changes to the backbone resonances of glutamine-8, alanine-11, lysine-13 and valine-14 (Fig. 14C). Chemical shift assignments will be described in a subsequent section. At high pH, the side chain of E12 likely hydrogen bonds with the amide side chain of Q8. As the pH decreases, the side

chain of E12 becomes protonated and hydrogen bonding with Q8 is disrupted, resulting in a slight reorganization of the nearby residues. Taken together, our results indicated that, in contrast to AS-48, CclA is monomeric under physiological conditions, and across a broad range of pH and ionic strengths.

## 2.2.5. 3D NMR solution structure of CclA

### 2.2.5.a. Chemical shift assignments and structure calculations

To facilitate NMR studies, a [ $^{13}\text{C}$ , $^{15}\text{N}$ ]-labeled sample of CclA was prepared by growing the producer organism in isotopically enriched complex media. The doubly-labeled CclA was purified in the same manner as described above (section 2.2.1). The backbone resonances ( $^{15}\text{N}$ ,  $^{13}\text{C}\alpha$  and H) of CclA were assigned using a suite of three-dimensional, triple resonance experiments. Complete side chain chemical shift assignments were achieved through a combination of homonuclear and heteronuclear multidimensional experiments. Chemical shift index (CSI) analysis (141) of the  $\alpha$ -carbons suggested that CclA contains four distinct helices separated by short loops, and that both the N- and C-termini of CclA are involved in helical segments.

The structure of CclA was calculated with CYANA 2.1 (142), using a combination of manually and automatically assigned distance constraints generated from NOE experiments, and angle constraints from the HNHA experiment and the program TALOS (143). A family of 20 structures, representative of the solution structure of CclA, was obtained. This ensemble of structures is well superimposed (Fig. 15). The structural statistics for this

ensemble of structures are listed in Table 3. CclA contains four helices, comprised of residues Q8–A20 ( $\alpha$ 1), V24–L31 ( $\alpha$ 2), L38–Q52 ( $\alpha$ 3) and I54–Y4 ( $\alpha$ 4). The linkage between the N- and C-termini of CclA is located within  $\alpha$ 4.

**TABLE 3.** Structural statistics for CclA<sup>a</sup>

Parameter	Value
NOE restraints	657
short range ( $ i - j  \leq 1$ )	388
medium range ( $1 <  i - j  < 5$ )	144
long range ( $ i - j  \geq 5$ )	125
Dihedral angle restraints ( $\Phi$ and $\Psi$ ) <sup>b</sup>	98
Coupling constants ( $^3J_{\text{HNH}\alpha}$ )	43
Ramachandran plot (residues 1..60)	
$\Phi/\Psi$ in most favored region	94.0 %
$\Phi/\Psi$ in additionally allowed region	6.0 %
$\Phi/\Psi$ in generously allowed region	0.0 %
$\Phi/\Psi$ in disallowed region	0.0 %
Atomic rmsd ( $\text{\AA}$ )	
backbone atoms (1..60)	$0.62 \pm 0.16$
backbone atoms (1..32, 38..60)	$0.53 \pm 0.12$
heavy atoms (1..60)	$1.02 \pm 0.13$
heavy atoms (1..32, 38..60)	$0.93 \pm 0.09$

<sup>a</sup> 20 lowest energy structures;

<sup>b</sup> Generated with TALOS.

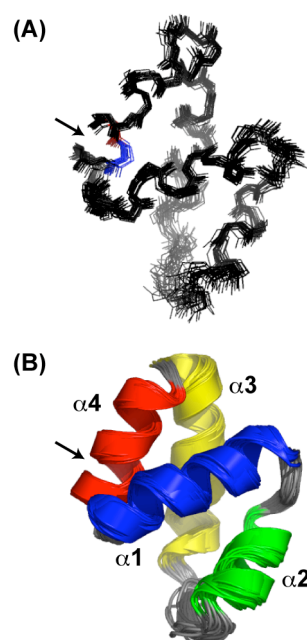


**FIG. 15.** Overlay of the 20 lowest energy conformers of CclA. (A) backbone and (B) cartoon rendering. The helices are colored and labeled. The N- to C- linkage is indicated with an arrow.

In general, the helices are connected by short, well-defined loops. However, a longer, more flexible loop is located between helices 2 and 3. This region, spanning G32 to G37, contains three glycines and exhibits the highest degree of flexibility in the structure. When these six residues are excluded from the rmsd calculation, the rmsd of the ensemble decreases from  $0.62 \text{ \AA}$  to  $0.53 \text{ \AA}$ . Coordinates for CclA have been deposited in the PDB data bank (code 2KJF) and

chemical shift assignments have been deposited in the BioMagRes Bank (code 16319).

#### **2.2.5.b. Structural features**

Many of the hydrophobic side chains (Leu, Ile, Val, Phe) of CclA point toward the core of the structure (Fig. 16A). However, there are also several solvent exposed hydrophobic residues (Fig. 16B), resulting in a hydrophobic strip that runs along the interface of  $\alpha 1$  and  $\alpha 2$ . The crystal structure of AS-48 exhibits similar features: at physiological pH, AS-48 exists as a water-soluble dimer due to interactions between hydrophobic residues on the surfaces of  $\alpha 1$  and  $\alpha 2$  (122). However, our results show that in solution, CclA is monomeric across a broad pH range and likely does not form a water-soluble dimer like AS-48. Rather than dimer formation, the hydrophobic patches on the surface of CclA may facilitate its interaction with the lipophilic portion of the target membrane. CclA also has a hydrophobic cleft encircling the turns connecting  $\alpha 4/\alpha 1$  and  $\alpha 2/\alpha 3$ . This region may be crucial for recognition and interaction with the enzyme(s) responsible for the cyclization of the N- and C-termini of CclA. The cyclization of CclA requires the loss of a 4 aa leader sequence (MLYE) and the covalent union of two leucine residues, located within  $\alpha 4$ . The point of linkage is surrounded by this cleft and as such, the hydrophobic nature of the cleft may facilitate interaction of the linear pre-CclA with the cyclization enzyme(s), help bring the termini of the peptide into close proximity and stabilize the hydrophobic residues that must contact each other.

In addition to hydrophobic patches, the surface of CclA exhibits a prominent positive region, located along  $\alpha 3$  and  $\alpha 4$  (Fig. 16C). CclA contains five lysine residues, four of which are located within this stretch (K46, K51, K55, K56). Again, a similar situation is reported for AS-48, wherein seven lysines reside in this section (121). In the case of AS-48, it has been suggested that this positive charge is essential for membrane insertion through a mechanism known as molecular electroporation (89, 121). According to this mechanism, when a peptide carrying sufficient charge density binds to the surface of a membrane, the local electric field associated with the peptide causes destabilization of the membrane, allowing for insertion of the peptide (135). However, it has also been shown that that this region alone is not sufficient for antibacterial activity. In 2005, Jiménez *et al.* reported that a fragment of AS-48, bearing these charges and adopting a similar helical conformation to the native peptide, did not exhibit antibacterial activity (123). As such, this charged region of the peptide must act in concert with other parts of the bacteriocin in order to kill susceptible bacteria.

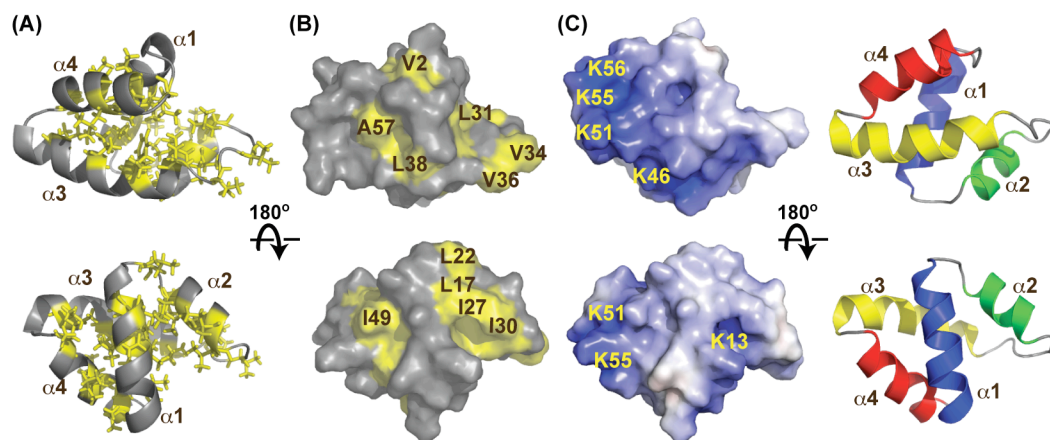


**FIG. 16.** Structural characteristics of CclA. (A) Ribbon diagram, depicting the compact, hydrophobic core of CclA. Hydrophobic sidechains are drawn as sticks. (B) Surface plot illustrating solvent exposed hydrophobic residues. Yellow indicates hydrophobicity from I, L, V and F. (C) Electrostatic surface potential of CclA. Blue and red indicate positive and negative charge, respectively. Key residues are labeled. The helical diagrams show the orientation of CclA.

### 2.2.5.c. Comparison to AS-48

The structure of CclA (60 aa) is remarkably similar to that of AS-48 (70 aa), even though their sequences share only 30% identity. Both structures reveal highly compact, globular peptides, comprised of four or five helices enclosing a hydrophobic core. The two structures align surprisingly well, with an rmsd of  $\sim 3.0$  Å across the entire sequence (Fig. 17). The superposition of CclA and AS-48 shows that in general, the helices are similar in length and assume similar orientations. For both structures,  $\alpha 1$  and  $\alpha 2$  are closely aligned, as are  $\alpha 4$  of CclA and  $\alpha 5$  of AS-48. In both molecules, the covalent linkage between the N- and C-termini resides in the last helix, at approximately the same three-dimensional location. In addition to having a similar architecture, CclA shares many surface features with AS-48, particularly the hydrophobic and cationic sections discussed above.

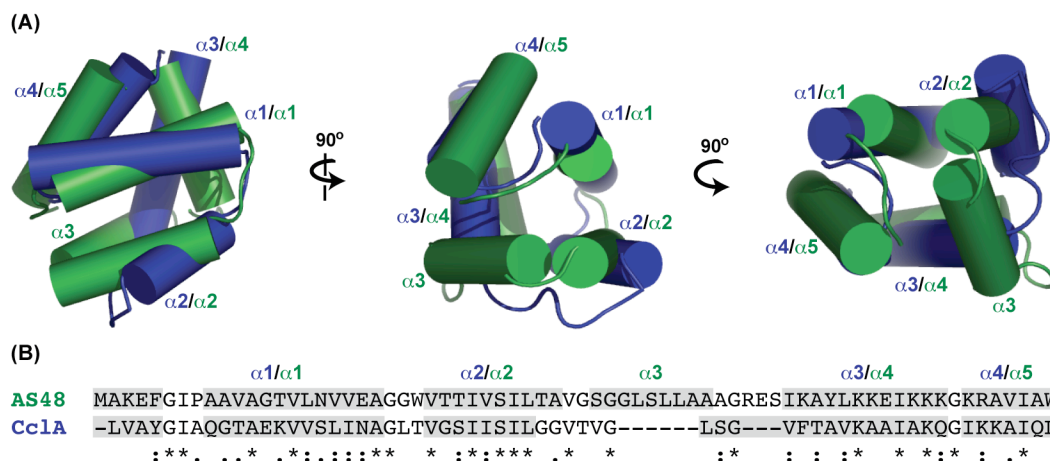


**FIG. 17.** Structural and sequence alignment of CclA and AS-48. (A) Structural alignment of the two bacteriocins. CclA is blue and AS-48 is green. The helices of each are labeled accordingly. (B) Sequence alignment of CclA and AS-48, according to Clustal W (144). Residues shaded in grey represent helical regions. Conserved residues are denoted with an asterisk, conservative substitutions with a colon and semi-conservative substitutions with a period.

The most notable difference between CclA and AS-48 is that the latter contains an additional helix. Alignment of their structures illustrates that  $\alpha 3$  of AS-48 and the extended loop of CclA occupy the same relative location. Since CclA is shorter than AS-48 by ten residues (Fig. 17B), it is unable to form a well-defined helix at this site. Other differences can be observed between  $\alpha 3$  of CclA and  $\alpha 4$  of AS-48. In particular,  $\alpha 3$  of CclA is longer, has a slight bend and its N-terminal portion does not overlay well with  $\alpha 4$  of AS-48. As can be seen from the overlay, the extended loop and kink in  $\alpha 3$  allows the shorter CclA to maintain its overall alignment with AS-48.

The program DALI (145) was used to identify other proteins with similar structural folds to CclA. As expected, the highest similarity was with AS-48. In addition, several linear saposin and saposin-like peptides, were also identified. Saposins A and C (146), which interact with the cell membrane and act as

sphingolipid activator proteins (SAPs) to facilitate the degradation of glycosphingolipids, were found to be remarkably similar to CclA, despite very low sequence similarity. In addition, the saposin-like peptides amoebapore A (147) and NK-lysin (148), which lyse bacterial and eukaryotic cells, also displayed high structural similarity to CclA. The  $Z_{\text{score}}$  and rmsd calculations for the structural alignments of CclA with these peptides are listed in Table 4.

**TABLE 4.** Peptides with similar structural folds to CclA, as determined by DALI (145)

Peptide (# aa)	PDB code	sequence identity	$Z_{\text{score}}^a$	rmsd
AS-48 (70 aa)	1E68	30%	6.9	2.7 Å across 58 residues
Saposin A (83 aa)	2DOB	6%	4.5	2.4 Å across 53 residues
Saposin C (83 aa)	2GTG	4%	3.9	2.4 Å across 50 residues
Amoebapore A (77 aa)	1OF9	7%	4.2	2.9 Å across 54 residues
NK-lysin (78 aa)	1NKL	2%	3.2	2.6 Å across 51 residues

<sup>a</sup>  $Z_{\text{score}} > 2$  represent significant matches and are indicative of similar structural folds.

#### 2.2.5.d. Homology modeling of the other circular bacteriocins

It has been suggested that the circular bacteriocins be divided into two subclasses according to their sequence (6). Group i contains the disparate bacteriocins (CclA, lactocyclin Q, AS-48, circularin A and uberolysin) whereas the highly homologous bacteriocins (gassericin A / reuterin 6 and butyrivibriocin AR10) comprise group ii. Our results reveal that even though CclA and AS-48 have low sequence identity, their three dimensional structures are remarkably similar. In addition, CD studies of gassericin A / reuterin 6, and sequence analysis of lactocyclin Q, indicate that these bacteriocins also contain helical secondary structure elements (116, 124). We hypothesized that both

groups of circular bacteriocins share the common overall structural motif of a saposin fold (148). To investigate this, we examined their potential structures through a combination of secondary structure prediction (using the Jpred3 (149) and PSIPred (150) servers) and homology modeling. The results are illustrated in Fig. 18.

For the group i circular bacteriocins, sequence alignment revealed that the greatest similarity exists among the N-terminal domain of these peptides and this region is predicted to contain two distinct helices, ranging approximately from residues 8-20 and 24-34. For both CclA and lactocyclin Q a stretch of six or seven residues with a high number of helix breaking residues (glycines and prolines) is found after  $\alpha_2$ , followed by a long, helical section. Indeed, this prediction matches the observed structure of CclA in which a long, extended loop separates  $\alpha_2$  from  $\alpha_3$  and a short, tight loop demarks  $\alpha_3/\alpha_4$ . For the longer bacteriocins AS-48, circularin A and uberolysin, an additional helical segment is predicted. As can be seen from the sequence alignment and the superposition of CclA with AS-48, this extra helix is located after  $\alpha_2$ . Thus, it is likely that circularin A and uberolysin contain five helices (like AS-48), whereas the shorter circular bacteriocins have four helices. Homology modeling was then performed on the group i bacteriocins. Lactocyclin Q was modeled after CclA, whereas circularin A and uberolysin were modeled after AS-48. For comparison, we also predicted the structure of CclA by threading it onto AS-48. The resulting model of CclA matched well to the experimental NMR solution structure, with very slight differences in the orientation of the four helices. Results of homology modeling

indicate that the other group i bacteriocins display similar structural and surface features to those of CclA and AS-48. All the bacteriocins have a nonpolar core with hydrophobic patches on their surfaces (Fig. 18C). In addition, they exhibit substantial positive patches on their surfaces, though in slightly different locations. Inspection of the aligned primary sequences (Fig. 18A) shows that CclA, AS-48 and circularin A have a high density of basic residues toward the end of their C-terminal domains ( $\alpha3/\alpha4$  for CclA and  $\alpha4/\alpha5$  for AS-48 and circularin A), whereas the sequence of uberolysin shows several basic residues in both the extreme N- and C- termini ( $\alpha5/\alpha1$ ). Lactocyclin Q differs from the other bacteriocins in this regard. Its basic residues are more uniformly distributed along the sequence of this peptide, with only a small positively charged patch located at the turn connecting  $\alpha3/\alpha4$ . The homology model of lactocyclin Q also shows several negatively charged patches on the surface of this bacteriocin.



similarity to the group i bacteriocins. Furthermore, the physical properties of this subgroup are different, as these peptides contain many more acidic residues and have predicted isoelectric points (pI ~5) much lower than those of subgroup i (pI ~10) (151). Nonetheless, it appears likely that the overall structure of this group of bacteriocins closely matches that of CclA, with four helices enclosing a compact hydrophobic core with an overall saposin fold.

#### **2.2.5.e. Fluorine NMR studies**

As described in section 2.2.3.c, CclA forms anion selective channels in lipid bilayers and transports anions, including fluoride. We decided to use NMR to probe this interaction. In an initial set of experiments, CclA was titrated with NaF and the chemical shift of the fluoride was monitored by  $^{19}\text{F}$ -NMR. The results revealed at least two modes of binding between fluoride and CclA (Fig. 19). Prior to the addition of exogenous fluoride, a small peak at -156.9 ppm was present in the spectrum. This endogenous fluoride likely originated from exposure to Teflon®, which is known to produce small amounts of fluoride ion in aqueous solution (152). Upon addition of NaF (0.5, 1.0 molar equivalents) another peak appeared at -156.3 ppm. Further addition of NaF (1.5, 2.0 and 3.0 molar equivalents) yielded a third peak at -155.2 ppm. This third peak had a chemical shift equivalent to that observed for fluoride anion in the absence of CclA (pH 3.8) and likely represents unbound fluoride. Thus, the results suggest that there are at least two different binding modes between CclA and fluoride. At low concentrations of anion, fluoride assumes one particular mode of binding; this

mode is then replaced by another as the concentration of the anion increases and exceeds a molar equivalent.

Since the interaction between fluoride and CclA could be observed by  $^{19}\text{F}$ -NMR, the effect of fluoride on the backbone amides and lysine side chains of CclA was examined by NMR spectroscopy. Upon addition of 0.5 molar equivalents of NaF, no changes in the backbone amides of CclA were observed in the regular  $^{15}\text{N}$  HSQC spectrum. Using an upfield  $^{15}\text{N}$ -HSQC experiment, three of the five lysine  $\epsilon$ -amino groups were detected and the identity of these groups was assigned with a  $^{15}\text{N}$ -TOCSY-HSQC spectrum. However, no significant changes in the spectra of these side chains were detected when fluoride was added. This is not surprising as CclA binds and transports different anions, including acetate, and presumably, trifluoroacetate. Purified CclA contains trifluoroacetate as its counterion from the HPLC purification, which can be seen by a large peak at -78 ppm in the  $^{19}\text{F}$  NMR spectrum. Hence, prior to addition of NaF, the residues involved in fluoride binding are likely already held in an anion-binding conformation due to interaction with trifluoroacetate and no significant structural rearrangement of CclA occurs. Similarly, the effect of other anions (phosphate and chloride) on the backbone structure of CclA did not result in any detectable changes by  $^{15}\text{N}$ -HSQC, as evidenced by our previous studies on the oligomeric state of CclA (see Fig. 14). Taken together, the results suggest that the two different peaks observed by  $^{19}\text{F}$ -NMR for fluoride bound to CclA may be due to different hydrogen-bonding ligands (e.g. water, protonated  $\epsilon$ -amino groups of lysine) attached to this anion.

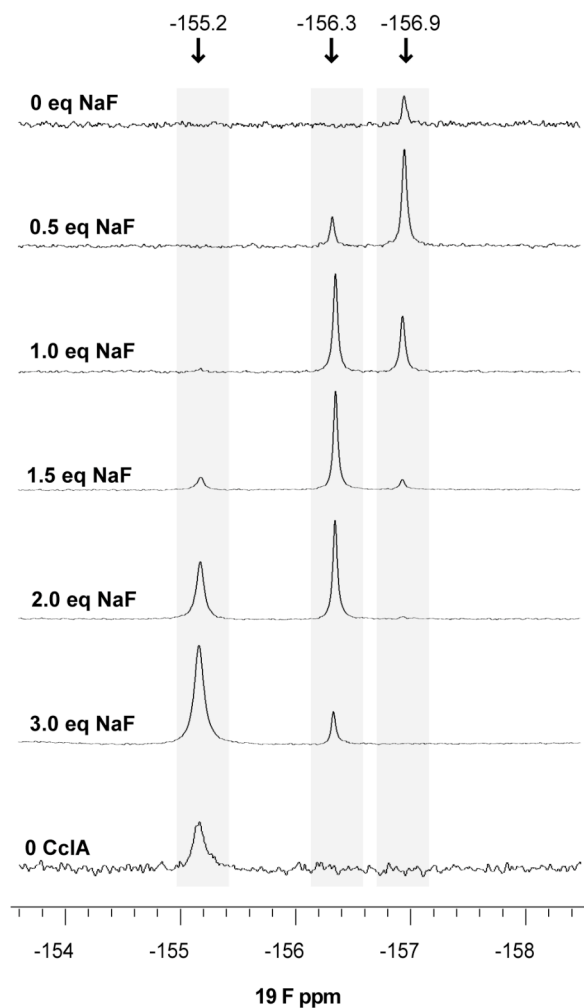


**FIG. 19.**  $^{19}\text{F}$ -NMR spectra of NaF titrated against CclA (1 mM in 90%  $\text{H}_2\text{O}$ :10%  $\text{D}_2\text{O}$ , pH 3.8). Spectra were recorded on a 500 MHz Varian VNMR5 spectrometer. The fluoride signal present in the 0 eq NaF spectrum is due to endogenous fluoride interacting with CclA.

### 2.2.6. Examining the linear precursor of CclA (pCclA)

As mentioned in Chapter 1, almost all bacteriocins are synthesized as precursor peptides with N-terminal extensions. In general, it is believed that the function of the leader peptide is to render the bacteriocin inactive, as well as target the bacteriocin to its secretion machinery (1, 56, 83, 153, 154). The function and proteolytic removal of common leader peptides will be further described in Chapter 4. The leader peptide of CclA, comprised of four amino

acids, is unusually small. Three other circular bacteriocins (lactocyclin Q, circularin A and uberolysin) also have short leader peptides. We were therefore interested in exploring the effect of these four residues on the antimicrobial activity and structure of CclA. In addition, we were hoping that the structure of the precursor peptide might reveal clues regarding the cyclization of the backbone. As such, several fusion proteins, expressing the 64 amino acid linear precursor, pCclA, were prepared.

#### **2.2.6.a. Construction and overexpression of MalE-pCclA**

Initially, pCclA was overexpressed as a maltose-binding protein fusion. With assistance of WISEST student Anna King, the *cclA* structural gene (encoding for the 64 aa linear precursor) was amplified by PCR and cloned into the *SacI* and *BamHI* site of the pMAL™-c2X expression vector. This vector uses the PTAC / *lacI<sup>q</sup>* promoter to control expression and upon addition of IPTG, produces high levels of fusion protein, located in the cytoplasm. A Factor Xa recognition sequence (IEGR) was also incorporated, in between the *malE* and *cclA* structural genes. The fusion protein was heterologously expressed in *E. coli* JM109 and BL21 cells. Following cell lysis, the fusion protein was purified by amylose affinity chromatography. MalE-pCclA was properly expressed in *E. coli* JM109 (i.e.: major product was ~48.7 kDa), but from *E. coli* BL21, large amounts of truncated fusion protein were also obtained, as evidenced by SDS-PAGE analysis of the amylose purification.

The fusion protein (overexpressed in *E. coli* JM109) was then digested with Factor Xa to cleave the MalE affinity tag (42 kDa) from pCclA (6417 Da). However, MALDI-TOF analysis revealed that pCclA was rapidly overdigested by Factor Xa: rather than the expected m/z of 6418, two smaller fragments (m/z of 2862 and 3547) were consistently observed. Occasionally, a very small peak indicative of pCclA was seen. Even at low protease concentrations (0.25 – 0.5 %, w/w), and reduced temperatures (4°C), overdigestion was observed within 1 h. Overdigestion by Factor Xa has been reported for proteins that are either unstable, or in partially unfolded states. To circumvent this possibility, 50% TFE was added to the Factor Xa digestion buffer to induce helicity in pCclA. However, this resulted in complete inhibition of the cleavage.

Despite the problems, a large-scale digestion was performed (aqueous conditions), with the hope that at least some pCclA could be obtained by RP-HPLC purification. After digestion of the fusion protein for 1 h, the mixture was subjected to HPLC purification. Although MalE gave a definite elution profile, no peaks indicative of pCclA were observed. Five minute fractions were collected over the duration of the purification and after lyophilizing, all fractions were analyzed by MALDI-TOF. However, pCclA could not be detected in any fractions.

#### **2.2.6.b. Construction and expression of His<sub>6</sub>-tagged pCclA**

Since we were unable to isolate pCclA following cleavage of the MalE-fusion protein, we decided to overexpress pCclA as a His<sub>6</sub>-tagged protein (on the

N-terminus) with the pQE60 expression vector. This vector uses the T5 promoter and a double *lac* operator repression module to tightly regulate gene expression, which is induced with IPTG. Two different fusion proteins were constructed: one that included a Factor Xa recognition sequence between the His<sub>6</sub>-tag and the start of pCclA (named <sup>Met</sup>His<sub>6</sub>.FXA.pCclA), and the other without the cleavage site (named <sup>Met</sup>His<sub>6</sub>.pCclA).

The *cclA* structural gene was amplified by PCR using forward primers that included either an N-terminal His<sub>6</sub>-tag (for <sup>Met</sup>His<sub>6</sub>.pCclA) or an N-terminal His<sub>6</sub>-tag followed by the Factor Xa recognition sequence (for <sup>Met</sup>His<sub>6</sub>.FXA.pCclA). The same reverse primer was used in both cases. The PCR inserts were then cloned into the *EcoRI* and *HindIII* sites of the pQE60 expression vector. The fusion proteins were heterologously expressed in *E. coli* JM109.

A series of pilot experiments were performed to investigate the effect of temperature and inducer concentration on the expression of the two fusion proteins. However, no fusion protein could be detected from any of the pilot experiments, by either Tris-Tricine gel electrophoresis or Western blot analysis. It is unclear why the fusion proteins were not expressed. It may be that they were severely degraded *in vivo*. If so, it is likely that very small fragments, including the His<sub>6</sub>-tags would migrate off the gel during gel electrophoresis and elude detection by Western blotting. Future work will involve dot blot analysis and allowing the expression to proceed for longer periods of time (i.e.: up to 20 h).

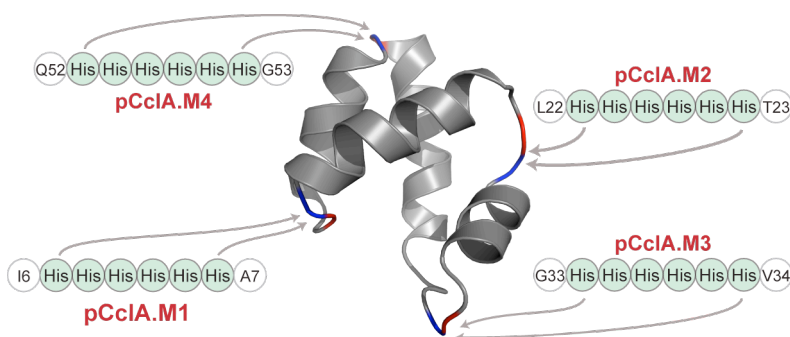
### 2.2.7. Mutational analysis of CclA

To date, only one study has been reported that describes the mutational analysis of a circular bacteriocin from LAB. In 2008, Sánchez-Hidalgo *et al.* described the preparation and characterization of four Glu→Ala mutants of enterocin AS-48 (155). These mutants were prepared by site-directed mutagenesis and a gene replacement strategy in a two-step fashion. Initially, a plasmid bearing the *as-48* structural gene was used as the template for amplification. The *as-48* mutation was incorporated with appropriate primers and the plasmid was amplified, after which the parental DNA was digested (with *DpnI*). In the second step, the mutated structural gene was cut out of the amplified plasmid and inserted into a second plasmid, harbouring the entire *as-48* gene cluster, in which the original AS-48 structural gene had been cut out. This plasmid was then transferred to a host for heterologous expression.

At this time, our ability to perform mutational analysis of CclA remains limited. Recently, Dr. Marco van Belkum in our group has discovered the operon responsible for production of CclA. However, heterologous expression has not yet been successful. Without a functioning system for heterologous expression, it is not trivial to explore the effect of mutations on the processing (i.e.: removal of leader peptide and cyclization events), bioactivity and structure of the carnocyclin mutants.

Therefore, we devised an alternate approach to examine the effect of mutations on the processing and cyclization of CclA. Since we did not have access to a heterologous expression system, we decided to clone the *cclA* mutants

into the constitutive expression vector pMG36e (regulated by the P32 promoter), and then use the CclA producer strain (*C. maltaromaticum* UAL307) to process, cyclize and secrete our mutants, as well as provide immunity. However, since the producer strain would also produce wild-type CclA, we needed a facile method for the detection and purification of our CclA-mutants. As such, we decided to insert His<sub>6</sub>-tags into the *cclA* structural gene to explore if the resulting mutants would be processed, cyclized and secreted. The presence of the His<sub>6</sub>-tag would allow for easy detection by dot blot or Western blot analysis, visualized with anti-His<sub>6</sub>-peroxidase, as well as providing a route to Ni-NTA affinity purification. Four internally His<sub>6</sub>-tagged mutants were designed, based on the 3D structure of CclA. The His<sub>6</sub>-tag was inserted at the loop regions connecting adjacent helices. This corresponded to insertion of His<sub>6</sub> between I6/A7 (pCclA.M1), L22/T23 (pCclA.M2), G33/V34 (pCclA.M3) and Q52/G53 (pCclA.M4), where the numbering refers to the CclA bacteriocin, not the precursor (Fig. 20). It was not known how the insertion of six histidine residues would affect the production and processing of CclA.

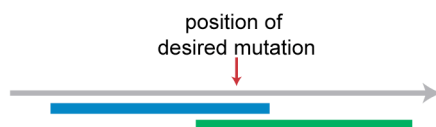
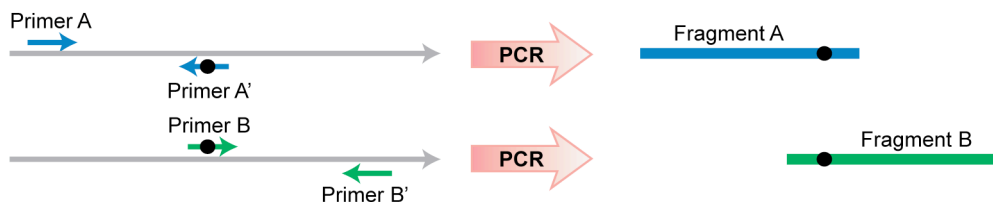


**FIG. 20.** The internally His<sub>6</sub>-tagged CclA mutants

### 2.2.7.a. Construction of internally tagged His<sub>6</sub> mutants

The primers used to construct the mutants are listed in Table 5. To construct pCclA.M1, the *cclA* structural gene was amplified by PCR, using forward primer LAM6 and reverse primer LAM7. Primer LAM6 introduced the His<sub>6</sub>-tag at the appropriate position (between I6 and V7 of CclA). pCclA.M4 was constructed in a similar fashion, except that forward primer LAM14 and reverse primer LAM15 were used. Primer LAM15 introduced the His<sub>6</sub>-tag (between Q52 and G53 of CclA).

Recombinant PCR was used to construct pCclA.M2 and pCclA.M3. A schematic explanation of recombinant PCR is provided in Fig. 21. With this technique, the gene of interest is first PCR amplified as two separate, overlapping fragments (A and B), using forward and reverse primers for each fragment (A/A' and B/B'). The reverse primer for fragment A (primer A') incorporates the desired mutation, as does the forward primer for fragment B (primer B) (Fig. 21 A,B). Following PCR, fragments A and B are gel purified to remove template DNA. The two fragments are then mixed together and amplified by PCR, without the addition of primers. The two fragments will anneal in their region of overlap and act as primers to each other. Chain extension (for just a few cycles) will provide the complete gene, with incorporation of the desired mutation, thus creating a full-length template for additional PCR cycles. The forward primer for fragment A (primer A) and reverse primer for fragment B (primer B') are added in and PCR is continued (for 35 cycles) (Fig. 21C). Recombinant PCR allows for the insertion, deletion or change of numerous residues within a given stretch.

**(A) Divide the gene of interest into fragments A (blue) and B (green)****(B) Design primers for each fragment, with desired mutation (●); run 2 PCR reactions****(C) Mix fragments A and B and do PCR with primers A and B'**

**FIG. 21.** Schematic representation of recombinant PCR. (A) The gene of interest is divided into two overlapping fragments, A and B, which encompass the position of the desired mutation (B) Forward and reverse primers are designed for each fragment (primers A/A' and B/B'), with the mutation encoded in primers A' and B. Two PCR reactions are performed to amplify fragments A and B separately. (C) The two fragments are mixed together and PCR is performed with primers A and B' to produce the full length gene, with incorporation of the desired mutation.

To construct pCclA.M2 by recombinant PCR, the *cclA* structural gene was initially designed as two overlapping fragments: M2.A and M2.B. In the second step of recombinant PCR, forward and reverse primers were designed for each fragment (A/A' and B/B'). The two fragments were then amplified in separate PCR reactions, as follows. To prepare fragment M2.A, the *cclA* structural gene was amplified using LAM8/LAM9 as the forward and reverse primers (A/A'). Primer LAM8 incorporated a *Pst*I restriction site and primer LAM9 introduced the His<sub>6</sub> mutation. Fragment M2.B was prepared in a similar fashion, but with LAM10/LAM11 as the forward and reverse primers (B/B'). LAM10 incorporated

the His<sub>6</sub>-mutation and LAM11 incorporated a *Hind*III restriction site. The two fragments M2.A and M2.B were purified by gel extraction. In the last step of recombinant PCR, fragments M2.A and M2.B were mixed together and amplified over seven cycles to prepare the full-length *cclA* gene, with the internal His<sub>6</sub>-mutation. Then, primers LAM8 and LAM11 were added to the PCR mixture, to act as the forward primer (A) and reverse primer (B') for complete amplification of the mutated *cclA* gene, and PCR was continued for an additional 35 cycles. pCclA.M3 was prepared in a similar fashion, except that primers LAM12 and LAM13 were used in place of primers LAM9 and LAM10, in order to shift the position of overlap and location of the His<sub>6</sub>-insertion.

**TABLE 5.** Primers used for the construction of internal His<sub>6</sub>-tagged pCclA mutants

Primer	Sequence <sup>a</sup>	Purpose
LAM6	5' –ATATCTGCAGAGGAGGAAAAAAAAATGTTATATGAAT TAGTTGCATATGGTATCC <b>CATCACCATCACCATC</b> CAG CACAAGGTACAGCTGAAAAGGTT–3'	Forward primer for pCclA.M1
LAM7	5' –ATATAAGCTTTTATAAATTGAATTGCTTTTTTTTA TTCC–3'	Reverse primer for pCclA.M1
LAM8	5' –ATATCTGCAGAGGAGGAAAAAAAAATGTTATAT–3'	Forward (A) primer for pCclA.M2 and pCclA.M3
LAM9	5' –TGT <b>GTGATGGT</b> GTATGGT <b>GTATG</b> TAAACCTGCGTTAAT TAGACTTAC–3'	Reverse (A') primer for pCclA.M2
LAM10	5' –TT <b>CATCACCATCACCATC</b> ACAGTAGGGTCTATT ATTTCAATT–3'	Forward (B) primer for pCclA.M2
LAM11	5' –ATATAAGCTTTTATAAATTGAATTGCTTTTTTT–3'	Reverse (B') primer for pCclA.M2 and pCclA.M3
LAM12	5' –GAC <b>GTGATGGT</b> GTATGGT <b>GTATG</b> CCCAACCAAAATTGA AATAATAGA–3'	Reverse (A') primer for pCclA.M3
LAM13	5' –GGG <b>CATCACCATCACCATC</b> AGTACAGTCGGTTTA TCAGGTGTC–3'	Forward (B) primer for pCclA.M3
LAM14	5' –ATATCTGCAGAGGAGGAAAAAAAAATGTTATATGAA–3'	Forward primer for pCclA.M4
LAM15	5' –ATATAAGCTTTTATAAATTGAATTGCTTTTTTTTATTC <b>CGT</b> GTATGGT <b>GTATG</b> TTGTTTAGCAATTGCTG CTTTAAC–3'	Reverse primer for pCclA.M4

<sup>a</sup> The *Pst*I (CTGCAG) and *Hind*III (AAGCTT) restriction sites are underlined and nucleotides encoding His<sub>6</sub> are bolded.

After the four mutant *cclA* structural genes had been constructed, they were cloned into the *Pst*I and *Hind*III site of the pMG36e vector. The plasmids were propagated in *E. coli* JM109 and the clones were sequenced to ensure that the desired mutation had been incorporated. No successful clones for pCclA.M1 were obtained. The plasmids incorporating pCclA.M2, pCclA.M3 and pCclA.M4 were then transferred into *C. maltaromaticum* UAL307.

#### **2.2.7.b. Expression of the His<sub>6</sub> mutants**

In an initial set of experiments, the producer strain and the three mutants were cultured and both the supernatant and cell pellets were analyzed. For the producer, it is known that pCclA is processed to remove the leader peptide, then cyclized and exported outside the cell. However, it was not known if the mutant pCclA peptides would be processed, or cyclized, or excreted. The supernatant from each culture was partially purified by hydrophobic interaction chromatography and analyzed by MALDI-TOF. In each case, wild-type CclA was observed. For the three mutants, no obvious peaks corresponding to either cyclized His<sub>6</sub>-mutants (expected m/z of 6686), or linear His<sub>6</sub>-mutants (expected m/z of 6704) were observed. The cell pellets of both the producer strain and the mutants were analyzed by Tris-Tricine gel electrophoresis, but the protein bands were very faint and results were inconclusive. It may be that the protein levels were well below the detection limits of the Coomassie stain. However, analysis by Western blot did not indicate the presence of His<sub>6</sub>-tagged peptides.

We had hoped that the incorporation of an internal His<sub>6</sub>-tag would not disrupt the biosynthesis of CclA and would allow for facile detection of the mutants via immunoblotting. However, the addition of six extra residues may adversely affect the structure and stability of the precursor peptide *in vivo*, preventing its processing, cyclization and secretion. Ultimately, a system for the heterologous expression of CclA is required to probe the effect of mutations on the production and bioactivity of this unique bacteriocin.

### 2.3. Conclusion & Future Directions

In this study, we isolated and characterized a new member of the circular bacteriocins. CclA is a highly stable peptide, with a broad spectrum of activity. The structure of this peptide was elucidated by a variety of techniques, including stereochemical analysis, circular dichroism and NMR. The results reveal that CclA shares many structural similarities to enterocin AS-48, despite limited sequence homology. Furthermore, analysis of the primary sequences of the other circular bacteriocins, coupled with homology modeling, indicates that the circular bacteriocins likely share a conserved structural motif, which is remarkably similar to that of the saposin-like peptides.

In addition to the characterization and structural elucidation of CclA, preliminary studies to explore the function of the leader peptide, and the requirements for cyclization were described. Additional studies to purify the precursor peptide (pCclA) and to examine the biosynthesis and activity of the pCclA mutants are required. For the circular bacteriocins, it is not known what

role the leader peptides play, nor are there any details regarding the cyclization event. We are keen to understand, and potentially exploit, the mechanisms governing the cyclization of these peptides. Such knowledge may allow for the engineering of new circular bacteriocins that may act as highly stable antimicrobial agents for use in food preservation and as human therapeutics, or as stable scaffolds for drug delivery.

## **Chapter 3. The type IIa bacteriocins: Immunity and mode of action**

### **3.1. Background**

Much of the following chapter has been adapted from our publication on the three-dimensional structure of PisI, the piscicolin 126 immunity protein (156).

#### **3.1.1. The type IIa bacteriocins**

The type IIa bacteriocins are an important class of antimicrobial peptides produced by LAB. They have been extensively studied and there are numerous reviews describing this class of bacteriocins (1, 3, 5, 6, 8, 9, 12, 83, 84, 88, 99, 157, 158). The first type IIa bacteriocin to be purified and fully characterized was leucocin A (22). To date, more than 30 type IIa bacteriocins have been identified (12). These heat stable peptides are small (37- 48 residues), cationic and highly anti-listerial. There is high sequence homology in the N-terminal domain of these peptides, characterized by the consensus sequence YGNGVXC and a conserved disulfide bridge, typically between C9 and C14 (1, 8, 12, 83). In addition, the N-terminal domains contain numerous hydrophilic and cationic residues. Less homology is observed across the C-terminal domains of these peptides. Studies involving mutations to this class of bacteriocins, as well as hybrid or chimeric bacteriocins, have shown that antimicrobial specificity is governed by the C-terminal domain of the bacteriocin (137, 159-163).

The three-dimensional solution structures of several type IIa bacteriocins (leucocin A, carnobacteriocin B2, sakacin P and curvacin A) have been reported

(138-140, 164). These structures reveal that in membrane mimicking environments the cationic N-terminus assumes a three-stranded, antiparallel  $\beta$ -sheet structure, whereas the hydrophobic / amphiphilic C-terminal end of the peptide is  $\alpha$ -helical. The far C-terminus folds back over the helix, forming a hairpin-like loop (Fig. 22). The two domains of the bacteriocin are connected by a hinge region, which allows them to move relative to each other (12, 83, 138-140). Circular dichroism and modeling studies of a variety of other type IIa bacteriocins have confirmed this structural pattern amongst the type IIa bacteriocins (137, 165). It has been shown that the N-terminal domain of these peptides interacts with the membrane interface via electrostatic interactions, while the C-terminal domain is involved in pore formation (83, 88, 166, 167).

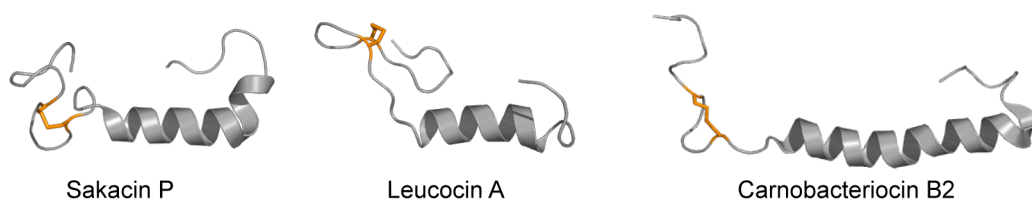


**FIG. 22.** 3D structure of various type IIa bacteriocins. Disulfide bridges are shown in orange.

The type IIa bacteriocins are subdivided into three groups, according to sequence alignment (Fig. 23). The group 1 peptides contain an additional disulfide bond or a conserved tryptophan in their C-terminal domain. The group 2 peptides have a shorter C-terminal domain, but also contain the additional disulfide or tryptophan. It is believed that these features help stabilize the hairpin



Generally, the type IIa bacteriocins are synthesized as precursor peptides, with a Gly-Gly type leader peptide, which is a common feature of the class II bacteriocins. The leader peptide is recognized and cleaved off by a dedicated ABC-transporter, which, along with an accessory protein, secretes the bacteriocin outside of the producer cell. Chapter four will describe this maturation and secretion mechanism in greater detail. A handful of type IIa bacteriocins (such as listeriolysin 743A (175), bacteriocin 31 (170) and enterocin P (179)) do not have the Gly-Gly type leaders and instead, utilize the *sec*-dependent pathway for translocation.

### **3.1.2. Immunity proteins for the type IIa bacteriocins**

Bacteriocins are generally co-expressed with their cognate immunity proteins (1, 8, 12, 83, 84, 87, 88). The gene for a type IIa bacteriocin immunity protein is typically, but not always, located on the same operon and downstream of the structural gene for the bacteriocin. Since expression of the dedicated immunity protein is coupled to bacteriocin expression, it has been noted that when a producer strain is not actively producing bacteriocin, it displays sensitivity when challenged with its own bacteriocin (87). Several “orphan” immunity proteins have also been discovered, whose regulation is independent of bacteriocin production (87, 125, 181, 182). It is believed that these orphan immunity proteins provide generic, basal protection against a variety of type IIa bacteriocins (87). Although some cross immunity has been observed (87, 183), most dedicated

immunity proteins are highly specific ensuring that the producer organism is protected from its own bacteriocin (1, 12, 83, 87).

While there is high sequence homology between the type IIa bacteriocins, the same is not true for their immunity proteins. The type IIa immunity proteins range in size from 81-115 amino acids and sequence identity varies from 5% to 85% (87). As with the bacteriocins, studies on hybrids of the type IIa immunity proteins suggest that the C-terminal domain of the protein confers immunity and is involved in specific recognition with its cognate bacteriocin (163, 165). The type IIa immunity proteins have been classified into 3 groups, according to sequence similarity (87) (Fig. 24).

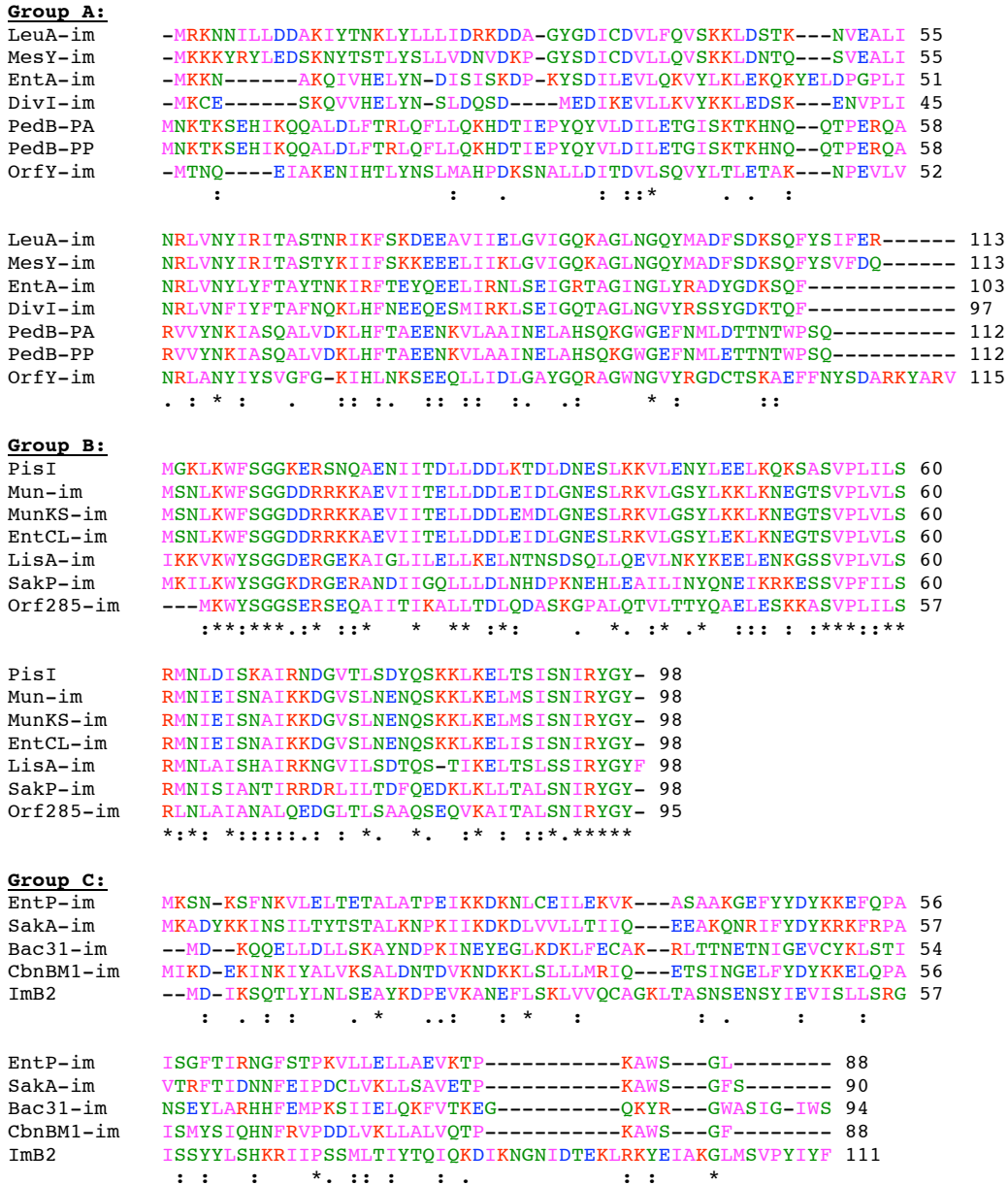


**FIG. 24.** Sequence alignment of various immunity proteins. Sequences were aligned using ClustalW (168) and arranged into groups according to Fimland *et al.* (160). Group A: immunity proteins for leucocin A (22), mesentericin Y105 (176), enterocin A (184), divercin V41 (181), pediocin PA-1 (23) and pediocin PP-1 (185) and orphan immunity protein OrfY-im (186). Group B: immunity proteins for piscicolin 126 (24), muntidicin (187), muntidicin KS (171), enterocin CRL35 (188), listeriocin 743A (175), sakacin P (174), and orphan immunity protein Orf285-im (182). Group C: immunity proteins for enterocin P (179), sakacin A (189), bacteriocin 31 (170), carnobacteriocin BM1 and carnobacteriocin B2 (125). Residues are colored according to physicochemical properties: blue for acidic, red for basic, magenta for hydrophobic and green for polar (and glycine). Conserved residues within are denoted with an asterisk, conservative substitutions with a colon and semi-conservative substitutions with a period.

In 2004, our group published the NMR solution structure of ImB2, a group C immunity protein (Fig. 25A) (190). This work revealed that in aqueous conditions this protein assumes a well-defined structure with an antiparallel four-helix bundle. The helices are nearly parallel with each other, resulting in tight packing and the formation of a hydrophobic core in the centre of the protein. A large, flexible loop connects  $\alpha 3$  and  $\alpha 4$ . The C-terminus contains a fifth helix and an extended strand, which runs perpendicular to  $\alpha 3$  and  $\alpha 4$  (190). Subsequently, the X-ray crystal structures of two group A immunity proteins (EntA-im and PedB, Fig. 25B,C) were reported (185, 191). Like ImB2, these proteins contain an antiparallel four-helix bundle. However, in EntA-im and PedB the loop between  $\alpha 3$  and  $\alpha 4$  is more clearly defined. Residues from this loop are incorporated into the hydrophobic core and  $\alpha 3$  and  $\alpha 4$  acquire a triangular relationship relative to each other, whereas in ImB2, these same helices are nearly parallel to each other. In the absence of a fifth helix and extended C-terminus, the third helices of EntA-im and PedB are straight, rather than kinked (as observed for  $\alpha 3$  in ImB2) (185). As will be described shortly, this project was aimed at solving the structure of a group B immunity protein (PisI), to determine if the four-helix bundle was a conserved structural motif for the immunity proteins of the type IIa bacteriocins. Subsequent to our publication of PisI, the structure of another group B immunity protein (Mun-im) has also been reported (187).

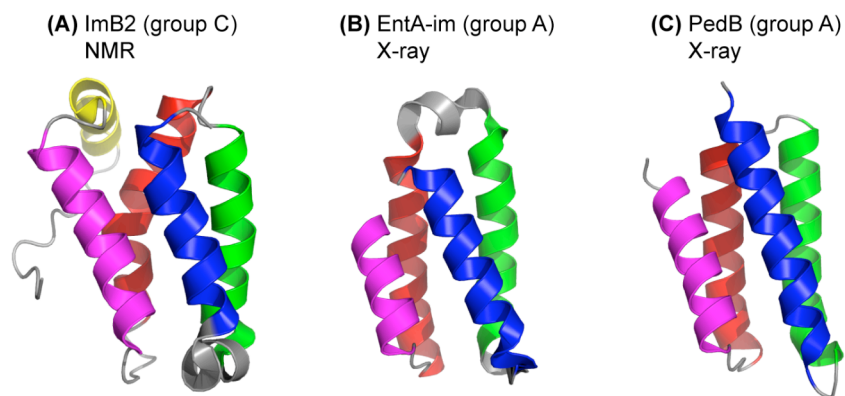


**FIG. 25.** Structures of the group A and C immunity proteins. Helices 1-4 are colored blue, green, red and magenta, respectively. The additional fifth helix of ImB2 is colored yellow. The grouping for each immunity protein, and how its structure was solved, is listed.

The mechanism of immunity for the type IIa bacteriocins is not fully understood. Despite the highly specific relationship between an immunity protein and its bacteriocin, no direct, physical connection between the two has yet been discovered. Various experimental approaches have been used to probe this interaction. Quadri *et al.* detected no binding between ImB2 and microtiter plates coated with CbnB2 (85). Several groups have observed that the extracellular addition of immunity protein in the presence of bacteriocin did not confer protection to sensitive strains, whereas heterologous expression of the immunity protein resulted in complete protection (85, 87, 157, 163). Immunity proteins are located intracellularly, with a very small proportion (~1%) associated with the cell membrane (85, 86). CD studies of EntA-im and LeuA-im showed that these proteins are  $\alpha$ -helical in water and exposure to membrane mimicking environments did not increase helicity, implying that the type IIa immunity proteins do not interact strongly with membranes (165). Since no direct, physical interaction between an immunity protein and its bacteriocin has yet been reported,

it is likely that they interact via a membrane bound receptor. The following section (3.1.3) will discuss the putative receptor for the type IIa bacteriocins, as well as describe the possible interaction of the immunity proteins with this receptor.

It should be noted that the mechanism of immunity for other types of bacteriocins has been established. For several lantibiotics two modes of immunity have been described: a dedicated immunity protein and a dedicated ABC-transporter (5, 9, 57, 165). It has been found that different lantibiotics may utilize both, or just one of these systems. The mechanism of immunity for several lantibiotics have been well studied, and recently reviewed (57). As described in chapter one, the dedicated immunity protein for nisin, NisI, is exported out of the cell. Some NisI remains anchored to the cytoplasmic membrane by the attachment of lipids (58, 59), whereas other NisI is free (59, 60). In either case, NisI has been shown to physically interact with and sequester nisin, thereby preventing pore formation (61). Nisin also makes use of a dedicated ABC-transporter to actively pump out nisin that may have crossed the cytoplasmic membrane (61).

For the colicins produced by enterobacteria, the immunity proteins interact directly with the colicin. For pore forming colicins, the immunity protein is located at the inner membrane, where it interacts with the colicin, thus blocking pore formation (192). For colicins with nuclease-type activity, the cognate immunity proteins form high affinity complexes with the colicin, thus preventing the colicin from performing its lethal actions. The complex dissociates only in the presence of a target cell (192, 193). Interestingly, the 3D structures of the

immunity proteins for the type IIa bacteriocins are intriguingly similar to some of the immunity proteins for the nuclease-type colicins (194-196).

### 3.1.3. Mode of action of the type IIa bacteriocins

The remarkable specificity and potency of the type IIa bacteriocins strongly suggest that these peptides target a particular receptor, rather than indiscriminate attack of the cell membrane. In 2000, our group synthesized the enantiomer of leucocin A (ent-LeuA) and compared its antimicrobial activity to that of the natural, LeuA. Surprisingly, ent-LeuA was devoid of activity, thus revealing that chiral recognition (most likely mediated by a protein receptor) is required for bacteriocin activity (197). Many studies have indicated that this receptor is part of the mannose phosphotransferase system (198-203).

In bacterial cells, the mannose phosphotransferase system (man-PTS) is involved in the import and phosphorylation of mannose and glucose. This system is comprised of three components: enzyme I (EI), HPr, and the mannose specific enzyme II permease ( $EII_t^{\text{man}}$ ). The  $EII_t^{\text{man}}$  permease consists of three domains: the cytoplasmic IIAB domain, and the membrane bound IIC and IID domains. The IIC and IID subunits form a complex, which recognize and transport mannose (and glucose) into the cell. EI and HPr are involved in the transfer of a phosphoryl group from phosphoenolpyruvate (PEP) to the IIAB domain of  $EII_t^{\text{man}}$ , where phosphorylation of the sugar ultimately occurs (204, 205).

Several correlations between the activities of type IIa bacteriocins and the man-PTS system, in particular the  $EII_t^{\text{man}}$  permease, have been reported. Studies

have shown that high level resistance to bacteriocins is linked to mutations that either decrease expression of the man-PTS system (206-208), or to mutations that directly affect the *mpt* genes (198, 200, 201, 203). In addition, heterologous expression of a man-PTS system (from a sensitive strain) in an otherwise insensitive strain induced sensitivity to the type IIa bacteriocins (209). Recently, a phylogenetic analysis of the IIC and IID subunits from 86 different man-PTS systems from various bacteria (some sensitive and some insensitive to type IIa bacteriocins) revealed that these systems could be clustered into three different groups (I, II and III) (202). The authors noted that bacteriocin sensitivity was only linked to group I man-PTS systems. Their findings suggested that genetic analysis of a man-PTS system is a predictor of bacteriocin sensitivity (202). To test this, they heterologously expressed seven different group I man-PTS systems in an insensitive host and upon exposure to bacteriocin, saw that sensitivity had been conferred to six of the transformants (202). Furthermore, sequence alignment of the IIC and IID subunits from the group I man-PTS systems revealed three conserved regions, all of which are located on the extracellular side of the cytoplasmic membrane and likely play a role in bacteriocin recognition (202).

It has also been hypothesized that the immunity proteins interact with the  $EII_t^{\text{man}}$  permease of the man-PTS system, either by preventing the bacteriocin from binding to it or by blocking pore formation (87, 190, 199, 210). Recently, Nes and coworkers used immunoprecipitation experiments to demonstrate that the immunity protein for lactococcin A (a type IIc bacteriocin) complexes with the IIC and IID components of  $EII_t^{\text{man}}$  only in the presence of externally applied

lactococcin A. In a similar manner, they explored the interaction of enterocin P and sakacin A with their respective immunity proteins and also observed that the immunity proteins complexed with  $EII_t^{\text{man}}$  upon exposure to bacteriocin (199). This supports the hypothesis that the IIC and IID components of the man-PTS  $EII_t^{\text{man}}$  permease play a key role in the mechanism by which immunity proteins protect cells against their bacteriocins. However, without structural data to fully illustrate the interaction of a bacteriocin with its receptor, it is difficult to rationalize the specificity and mechanistic details governing the relationship between the type II bacteriocins, their targets, and their immunity proteins.

#### 3.1.4. Objectives

The type IIa bacteriocins have been intensively studied. Much is known about their biosynthesis, structural features and pore forming activity toward sensitive cells. The immunity proteins for these bacteriocins have also been characterized, through mutational analysis as well as structural studies. However, details regarding the receptor mediated mode of action, and immunity, of these bacteriocins is still a mystery. The projects described in this chapter were aimed at resolving these questions. The first project that will be discussed focuses on the characterization of PisI, the putative immunity protein for piscicolin 126 (PisA). The characterization required: (1) heterologous expression of PisI to confirm its function as an immunity protein; (2) examining the interaction between PisI and PisA by NMR; and (3) elucidating the 3D structure of PisI by NMR. The second project that will be described is the on-going exploration of the IIC and IID

membrane proteins of the man-PTS system, which are believed to be involved in both bacteriocin recognition and immunity. Specifically, the construction of overexpression systems for these proteins and initial efforts towards their expression will be described.

## 3.2. Results & Discussion

### 3.2.1. Construction of pMG36e.PisI and heterologous expression of PisI

Piscicolin 126 is a type IIa bacteriocin that has been isolated from two different producer strains, *Carnobacterium maltaromaticum* JG126 (25) and *C. maltaromaticum* UAL26 (24). Interestingly, bacteriocin production differs between the two strains, and several nucleotide differences between the two operons have been identified (24). In both cases, a putative immunity protein, PisI, has been proposed. The two immunity proteins are identical, except for amino acid 52. This residue is either a glycine (PisI from *C. maltaromaticum* JG126) or a serine (PisI from *C. maltaromaticum* UAL26). In either case, the PisI protein belongs to the group B immunity proteins, according to sequence alignment (Fig. 24). When this study was initiated, no group B immunity protein had yet been structurally characterized, thus we elected to study PisI. To confirm that PisI is indeed the immunity protein for piscicolin 126 (PisA), PisI was heterologously expressed in two PisA-sensitive hosts. This required cloning the *pisI* gene into the constitutive expression vector pMG36e, transferring the plasmid into two different host strains, and testing the activity of PisA against the newly transformed hosts.

Using crude DNA isolated from *C. maltaromaticum* UAL26, the *pisI* gene was amplified by PCR and cloned into the *Pst*I and *Hind*III site of the pMG36e vector. The recombinant plasmid was transferred to *E. coli* JM109 by electroporation and transformants were sequenced to ensure that *pisI* had successfully been cloned. The recombinant plasmid was subsequently transferred to two PisA-sensitive organisms, *C. divergens* LV13 and *C. maltaromaticum* LV17C, by electroporation. To test if *pisI* conferred immunity to PisA, spot-on-lawn activity testing was performed. Serial two-fold dilutions of PisA (purification described below, in section 3.2.2) were spotted onto agar plates that had been overlaid with soft agar containing either the wild-type strains (*C. divergens* LV13 or *C. maltaromaticum* LV7C) or the strains harbouring the plasmid pMG36e.PisI. As illustrated in Fig. 26, both the wild-type strains were sensitive to PisA, at all the concentrations tested. However, when the strains expressed the *pisI* gene, they displayed immunity toward PisA, confirming that PisI is the immunity protein for PisA.

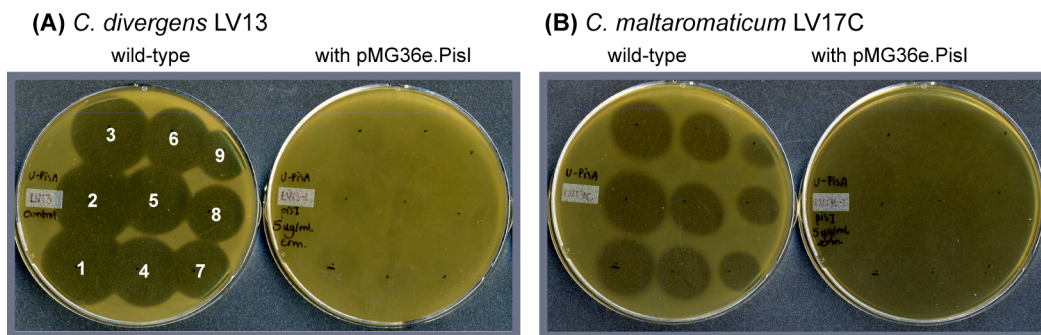


**FIG. 26.** Heterologous expression of PisI. (A) Activity of PisA against *C. divergens* LV13, as the wild-type strain, or transformed with plasmid pMG36e.PisI. (B) Activity of PisA against *C. maltaromaticum* LV17C, as the wild-type strain or transformed with plasmid pMG36e.PisI. Two-fold serial dilutions of PisA (starting with 250  $\mu$ M) were prepared and 10  $\mu$ L of each solution was spotted onto the plates (spots 1-9), as indicated in the left-most image.

### 3.2.2. Expression and purification of PisA and [<sup>15</sup>N]PisA

In order to obtain relatively large amounts of labeled PisA for structural studies, it was necessary to develop a heterologous expression system for PisA. As such, PisA was overexpressed as a maltose-binding protein fusion (MalE-PisA), with a Factor Xa recognition sequence linking MalE and PisA. The construct was prepared by Dr. Lucas Gursky (24) and then transferred into *E. coli* BL21(DE3). To prepare unlabelled protein, the fusion protein was overexpressed in LB media. To prepare isotopically enriched <sup>15</sup>N protein, the fusion protein was overexpressed in M9 minimal media, containing (<sup>15</sup>NH<sub>4</sub>)<sub>2</sub>SO<sub>4</sub> as the sole nitrogen source. In either case, the fusion protein was purified via affinity chromatography, using amylose resin. To remove the MalE affinity tag, the fusion protein was digested with Factor Xa. This digestion was somewhat troublesome, as the liberated PisA tended to precipitate out of solution, and was also subject to secondary cleavage by Factor Xa. Precipitation of the peptide was minimized by increasing the ionic strength of the buffer. To prevent secondary cleavage, digestions were allowed to proceed for ~ 8 h, after which a serine protease inhibitor (AEBSF) was added to irreversibly inhibit Factor Xa. PisA was subsequently purified by RP-HPLC. Both MALDI-TOF and SDS-PAGE revealed that PisA had been successfully purified. Fig. 27 shows the MALDI-TOF traces for PisA and [<sup>15</sup>N]PisA.

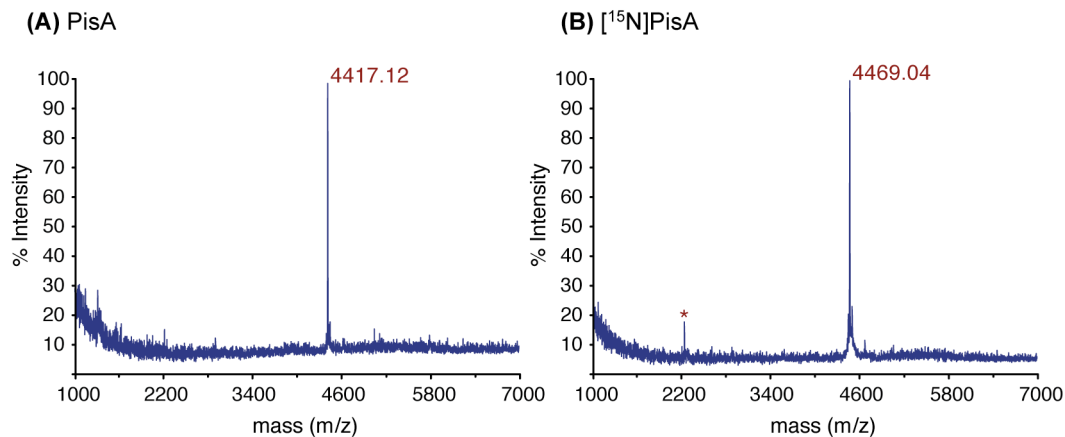


**FIG. 27.** MALDI-TOF of piscicolin 126. (A) Overexpressed and purified from unlabelled media. (B) Overexpressed and purified from M9 minimal media, supplemented with  $(^{15}\text{NH}_4)_2\text{SO}_4$ . Doubly charged species are indicated with an asterisk.

### 3.2.3. Expression and purification of PisI, $[^{13}\text{C}, ^{15}\text{N}]\text{PisI}$ and $[^{15}\text{N}]\text{PisI}$

PisI was also overexpressed as a maltose-binding fusion protein (MalE-PisI) and grown in either LB media for unlabelled protein, or  $[^{13}\text{C}, ^{15}\text{N}]$  or  $[^{15}\text{N}]$  enriched media for labeled protein. In either case, the fusion protein was purified over an amylose column and subsequently cleaved with Factor Xa. PisI was purified by cation exchange chromatography, followed by RP-HPLC. MALDI-TOF and SDS-PAGE confirmed the identity and purity of the protein. The MALDI-TOF traces for PisI are illustrated in Fig. 28. It should be noted that once purified, PisI was not stable in solution for extended periods of time. This caused many problems during the acquisition of NMR data, as degradation products interfered with and complicated data analysis. In total, five separate preparations of  $[^{13}\text{C}, ^{15}\text{N}]\text{PisI}$  were required in order to obtain the NMR data necessary for complete structural characterization.

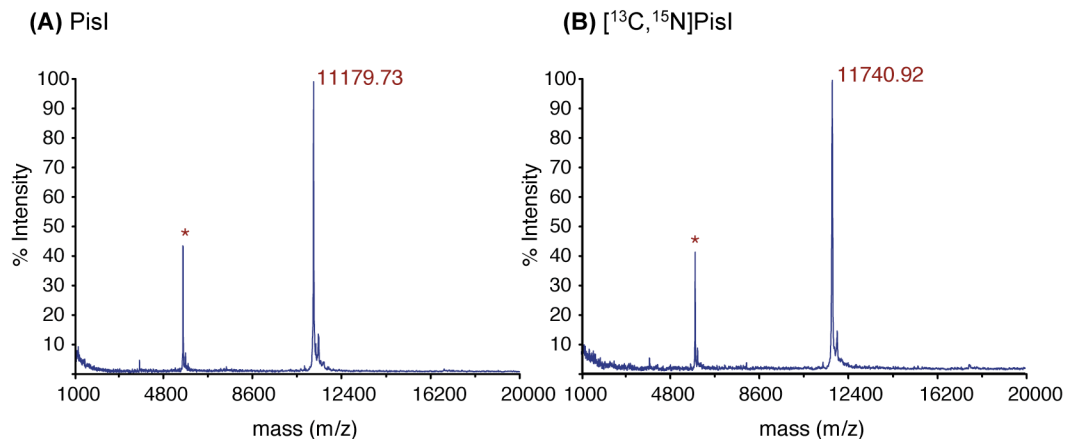


**FIG. 28.** MALDI-TOF of piscicolin 126 immunity protein. (A) Overexpressed and purified from unlabelled media. (B) Overexpressed and purified from M9 minimal media, supplemented with  $(^{15}\text{NH}_4)_2\text{SO}_4$  and  $^{13}\text{C}$ -glucose. Doubly charged species are indicated with an asterisk.

### 3.2.4. Interaction of PisA and PisI

As mentioned previously (section 3.1.2), no direct, physical interaction between a type IIa bacteriocin and its immunity protein has been observed. Previously in our group, NMR was used to explore the potential interaction between an immunity protein and its cognate bacteriocin by titrating  $[^{15}\text{N}]\text{ImB2}$  with 1.5 molar equivalents of CbnB2. The  $^{15}\text{N}$  HSQC of ImB2 before and after the addition of CbnB2 showed no changes, thus implying that there was no direct binding between the immunity protein and its bacteriocin (190). It has been suggested that a direct interaction may only occur once the bacteriocin is membrane bound and hence structured (87, 190). In this study we again used NMR to search for an interaction, but this time we monitored the  $^{15}\text{N}$  HSQC of the bacteriocin, rather than the immunity protein, as it was more likely to observe structural changes in the small, random coil peptide, as opposed to the large, highly structured immunity protein.

### 3.2.4.a. Circular dichroism

Initially, CD experiments were performed to analyze the secondary structural elements of PisA and PisI in both aqueous and membrane-mimicking environments. As expected, PisA was unstructured in aqueous conditions but assumed some helicity when TFE was added (Fig. 29A). The structure of PisI was virtually identical in both systems (Fig. 29B).

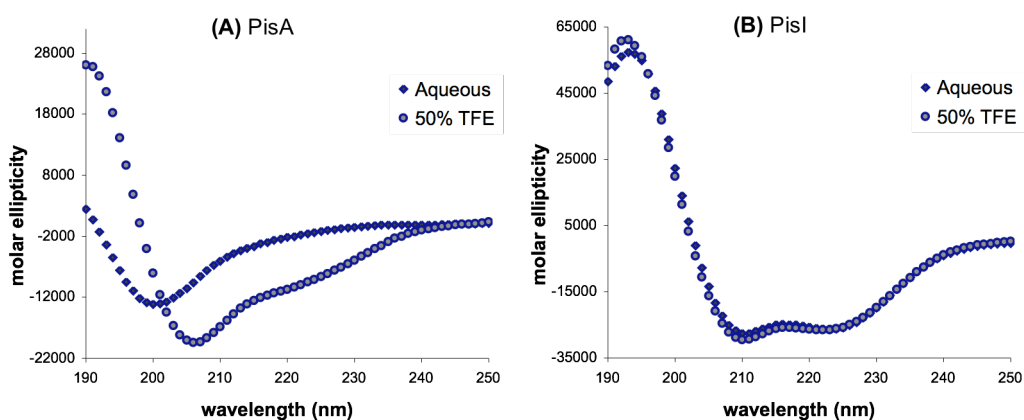


**FIG. 29.** CD spectra of PisA and PisI in aqueous and membrane-mimicking environments. (A) PisA. (B) PisI

### 3.2.4.b. Titration of [ $^{15}\text{N}$ ]PisA with PisI

NMR was subsequently used to determine if PisA underwent structural changes upon addition of PisI. Using a  $^{15}\text{N}$  HSQC experiment, the backbone resonances of [ $^{15}\text{N}$ ]PisA were monitored while unlabelled PisI was titrated against PisA. No significant changes in the spectral dispersion of NH resonances were observed, indicating that there is no significant interaction between bacteriocin and immunity protein (Fig. 30A).

The experiment was repeated under membrane mimicking conditions. Upon addition of 50% TFE, the backbone resonances of PisA showed a dramatic

change, as the peptide assumed a helical structure (Fig. 30B, blue spectrum). However, upon addition of PisI, no additional changes were observed (Fig. 30B, black spectrum). These results suggest that even when the bacteriocin is in the vicinity of the membrane and has assumed secondary structure, there is no significant interaction with its immunity protein that leads to further structuring of the bacteriocin.

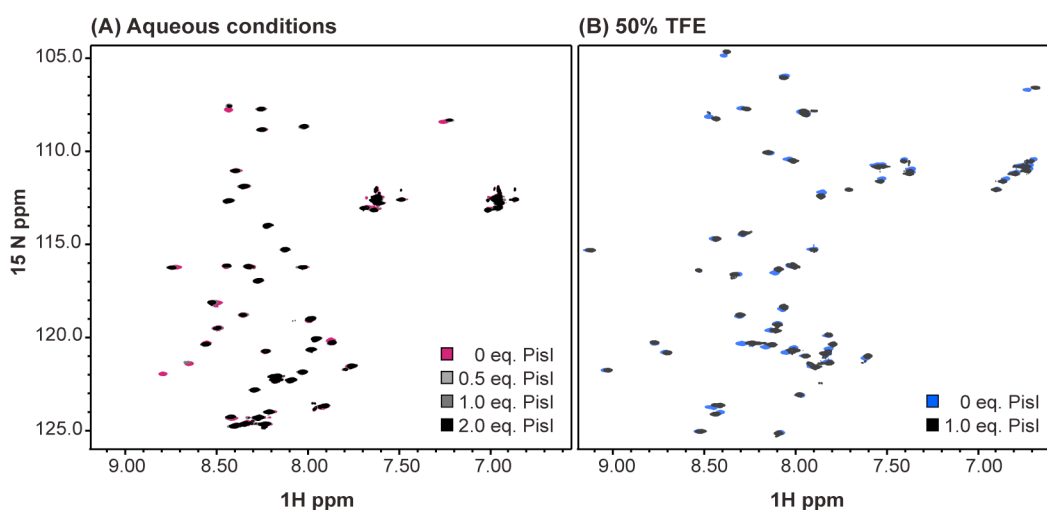


**FIG. 30.**  $^{15}\text{N}$  HSQC of PisA when titrated with PisI. (A) Titration under aqueous conditions. (B) Titration under membrane-mimicking conditions. The amount of PisI that has been added is indicated in the legend. The Trp sidechains are not shown.

### 3.2.5. NMR solution structure of PisI

#### 3.2.5.a. Chemical shift assignments and structure calculations

PisI is a 98 amino acid protein, of which there are 15 leucines, 7 isoleucines, 12 lysines and 11 serines (comprising 46% of the protein). The amide crosspeaks in the  $^{15}\text{N}$  HSQC spectrum of PisI were relatively well dispersed, despite the high degree of multiplicity. Although there was some overlap, all of

the expected amide protons could be assigned (Fig. 31), except for the first two residues, which were not observed (due to rapid exchange with solvent). Sequential backbone and C $\alpha$ , C $\beta$  chemical shift assignments for PisI were obtained by analysis of HNCACB and CBCA(CO)NH spectra. Further side chain assignments were made by analysis of CCONH,  $^{15}\text{N}$  TOCSY-HSQC,  $^{13}\text{C}$  HCCH-TOCSY and  $^{13}\text{C}$  HSQC experiments. Nearly complete backbone and side chain  $^1\text{H}$ ,  $^{15}\text{N}$  and  $^{13}\text{C}$  assignments were obtained (~99%, with 96 out of 98 residues fully assigned). Chemical shift analysis of the assigned  $\alpha$  and  $\beta$  carbons indicated that PisI was highly structured and likely contained four distinct helices (141).

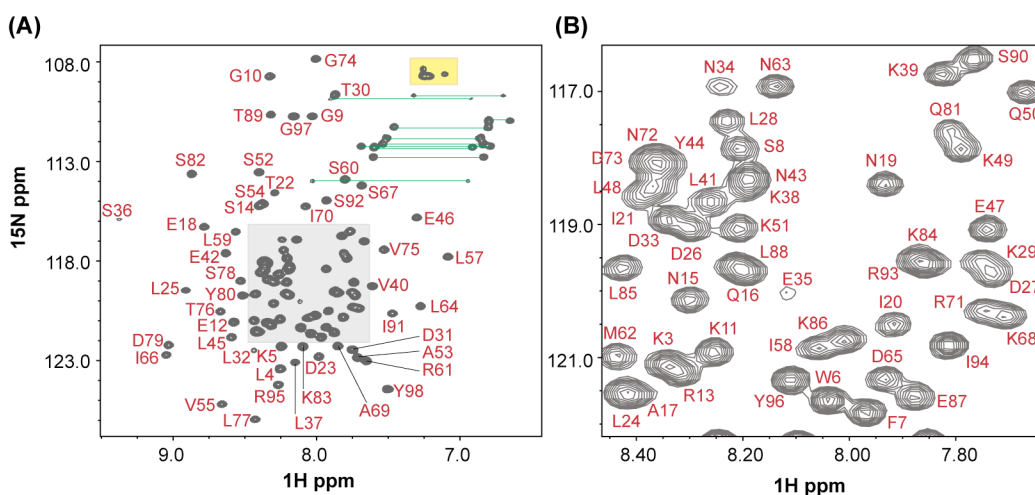


**FIG. 31.**  $^{15}\text{N}$  HSQC of PisI in 20 mM sodium phosphate (pH 5.9) at 25°C at 800 MHz. (A) Full spectrum of PisI. Crosspeaks from Asn and Gln side chains are indicated with horizontal lines and those from Arg are shaded in yellow while the Trp side chain is not shown. All other crosspeaks are labeled by residue number. The grey box is enlarged in panel (B).

A family of 20 structures, representative of the solution structure of PisI, was obtained using CYANA 2.1 (142). The structural statistics characterizing these structures are summarized in Table 6. As shown in figure 32, the final ensemble of 20 structures is well defined between residues R13 and N92. PisI

consists of a four-helix bundle, flanked by a flexible N-terminus and slightly more rigid C-terminus. Heteronuclear NOE data shows an average NOE of 0.75 from residues S14–S91, as would be expected for a structured, globular protein. This value is slightly less for certain residues in the loops connecting the helices, but overall, the loops are also relatively rigid. The N-terminus of the protein is quite mobile, as evidenced by negative NOE values for residues K3-K5, and values < 0.5 for residues W6-K13.

**TABLE 6.** Structural statistics for PisI<sup>a</sup>

Parameter	Value
NOE restraints	1725
short range ( $ i-j  \leq 1$ )	995
medium range ( $1 <  i-j  < 5$ )	444
long range ( $ i-j  \geq 5$ )	286
$\phi$ angles <sup>b</sup>	76
Average target function value	$1.83 \pm 0.14$
Atomic rmsd (Å) (13..92)	
backbone	$0.56 \pm 0.10$
heavy atoms	$1.03 \pm 0.12$
Ramachandran plot (13..92)	
$\Phi/\Psi$ in most favored region	83.9 %
$\Phi/\Psi$ in additionally allowed region	16.1 %
$\Phi/\Psi$ in generously allowed region	0
$\Phi/\Psi$ in disallowed region	0

<sup>a</sup> 20 lowest energy structures

<sup>b</sup> from analysis of the HNHA experiment

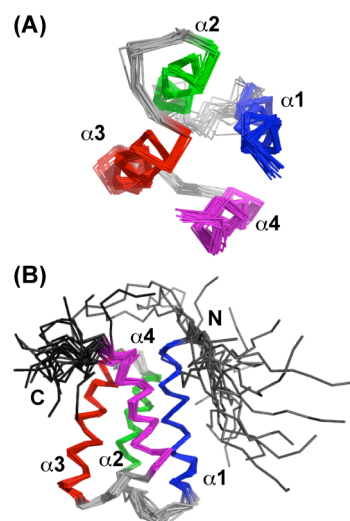


**FIG. 32.** Overlay of the 20 lowest energy conformers of PisI. Helices 1-4 are colored blue, green, red and magenta, respectively. (A) Looking down the axis of the helix. The N and C termini have been omitted for clarity; (B) Side view of the structure. The N and C termini are labeled and colored grey.

The helices of PisI are relatively straight and range in length from 12 to 19 amino acids.  $\alpha 1$  is formed by residues R13–K29,  $\alpha 2$  is formed by residues

K38–K49,  $\alpha_3$  is formed by residues V55–D73 and  $\alpha_4$  is formed by residues D79–I92. Angles of  $28^\circ$ ,  $7^\circ$ ,  $32^\circ$  and  $15^\circ$  are found between the pairs formed by  $\alpha_1/\alpha_2$ ,  $\alpha_2/\alpha_3$ ,  $\alpha_3/\alpha_4$  and  $\alpha_4/\alpha_1$ , respectively. The helices are largely amphiphilic, as illustrated with an Edmundson helical wheel diagram (Fig. 33). Most of the hydrophobic side chains pack tightly into the interior, forming a hydrophobic core, while most of the polar and hydrophilic residues face the aqueous exterior. The helices of the other immunity proteins for which structural data are known (ImB2, EntA-im, PedB and Mun-im) are also highly amphiphilic.

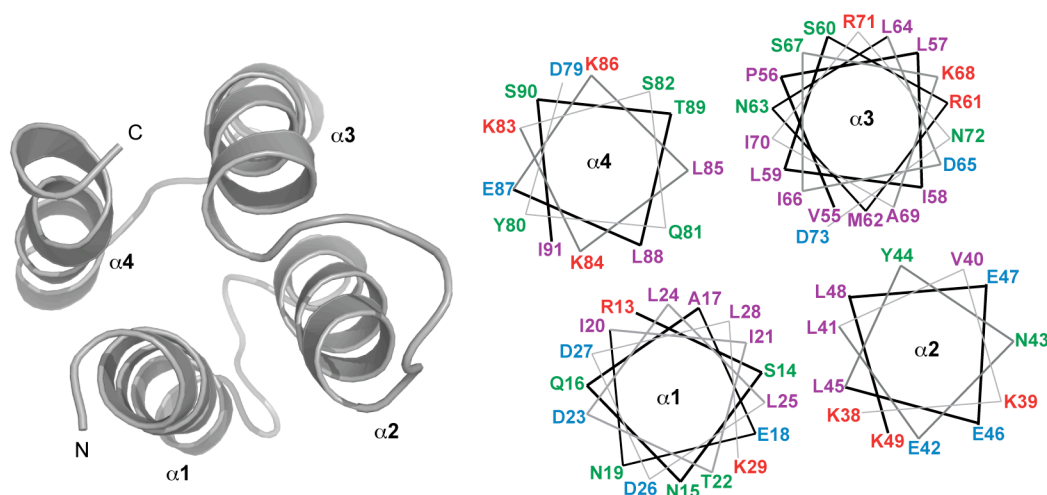


**FIG. 33.** Edmundson helical wheel diagram of PisI. A cartoon representation of PisI is provided, to show the relative orientation of the four helices. Residues are labeled and colored as follows: blue for acidic, red for basic, magenta for hydrophobic and green for polar (and glycine).

### 3.2.5.b. Structural features of PisI

PisI has both negatively and positively charged regions on its surface. A large, negatively charged groove is formed by residues in  $\alpha 1$  (E18, D23, D26, D27) and  $\alpha 4$  (D79, E87) and extends down to the loop between  $\alpha 1$  and  $\alpha 2$  (D31, D33, E35) (Fig. 34A). Many of these residues are conserved amongst the group B immunity proteins (Fig. 24). Indeed, the recently published X-ray structure of Mun-im also displays a negatively charged patch, in approximately the same position (187). The positively charged patch is located at the junction of the N-terminus of  $\alpha 1$  (K11, R13), the loop connecting  $\alpha 2$  and  $\alpha 3$  (K51), R61 of  $\alpha 3$ , and the C-terminus of  $\alpha 4$  (R95) (Fig. 34A). Like the negatively charged region, several of these residues are also conserved within the group B immunity proteins, particularly R13, R61 and R95 (Fig. 24).

PisI also has a small, hydrophobic pocket, located near the connecting loop of  $\alpha 3$  and  $\alpha 4$  (Fig. 35). This pocket is comprised of I66, I70, V75, L77 and L85. All of these residues are very highly conserved in the group B immunity proteins (Fig. 24). Since protein-protein interactions generally involve hydrophobic contacts, this region may be involved in the interaction between the immunity protein and its receptor. Interestingly, several basic residues surround this pocket, including R/K71, K83 and K86, which are conserved across the group B immunity proteins (Fig. 24). A recent study of several mutants of Mun-im has revealed that a K86E mutation profoundly diminished the capability of the protein to provide immunity against its cognate bacteriocin, although mutating position

71 had no such effect (187). As such, it has been suggested that these basic residues may play a key role in immunity.

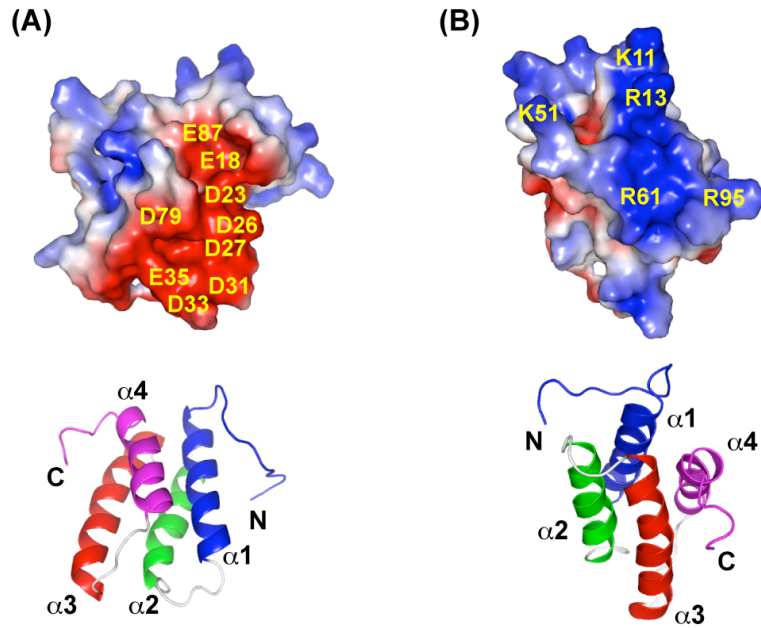


**FIG. 34.** Electrostatic surface potential of PisI. A ribbon diagram is shown for reference and the termini and helices are colored and labeled. (A) Viewing the negatively charged region; (B) Viewing the positively charged region. Blue indicates positive charge and red indicates negative charge. Key residues are identified.

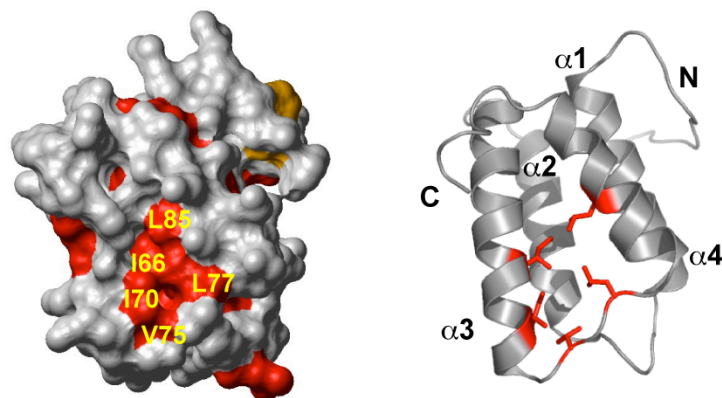


**FIG. 35.** Hydrophobic surface of PisI. A ribbon diagram is shown for reference and the termini and helices are labeled. In the surface plot, red indicates hydrophobicity from Ile, Leu and Val. Key residues are labeled on the surface plot and illustrated as red sticks in the ribbon diagram.

### 3.2.5.c. Comparison of PisI to the other immunity proteins

By comparing the structure of PisI (and Mun-im) to ImB2 (group C), and EntA-im or PedB (group A), it is apparent that there are both similarities and differences between these three subgroups. Clearly, the four-helix bundle is a conserved motif amongst the type IIa immunity proteins. Despite the low sequence homology between PisI and the other group A and C immunity proteins, the structures overlap remarkably well. There are slight variations in the position of charged and exposed hydrophobic residues between the three subgroups, but overall, the architecture of the four-helix bundles are very similar. Fig. 36 illustrates the overlay of PisI with the group A, B and C immunity proteins. The rmsd values between backbones of the four-helix bundles for the alignment of PisI with the other structures, as determined with DALI-LITE (145), is also listed.

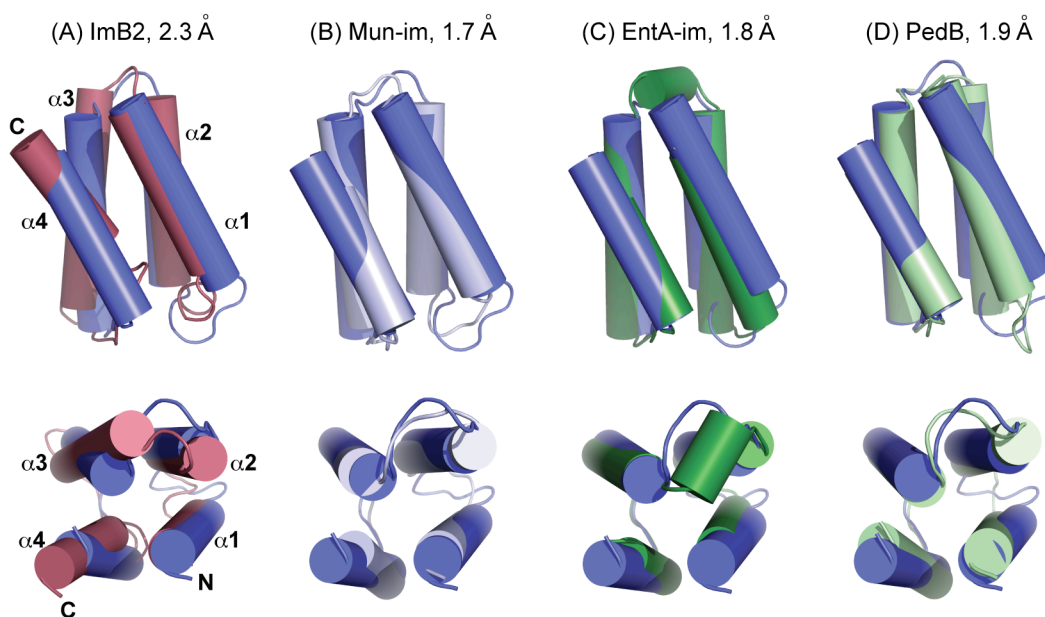


**FIG. 36.** Overlay of PisI (blue) with ImB2 (A), Mun-im (B), EntA-im (C) and PedB (D). The diagrams in the top panel show side view and the diagrams on the bottom panel depict the view down the axis of the bundle. All overlays are aligned the same way, so the N and C termini and helices are labeled in only one diagram. The rmsd between the two structures is listed.

There are many similarities in the surface features of the group A, B and C immunity proteins. Like PisI the structure of EntA-im is reported to have a negatively charged patch (191). Although the participating residues are slightly different, the relative location of this patch is very similar to PisI. Structural models for several other group A immunity proteins, including two hybrid proteins, are also predicted to display this negative region (191). The positively charged region is also common to all three subgroups. For the group A immunity proteins (EntA-im and PedB), this region is formed by residues in  $\alpha 2$  and  $\alpha 3$  and the connecting loop between these helices (185, 191). For the group C immunity protein ImB2, this region is located in the flexible loop connecting  $\alpha 3$  and  $\alpha 4$  (190). Although the position of this patch varies between the three subclasses, the presence of such a region is conserved, and in all cases is located in the C-terminal half of the protein. It has been suggested that this region may be involved in attracting the immunity protein to the surface of the cell membrane (190).

As previously discussed, PisI has a small hydrophobic pocket. The group C immunity protein, ImB2, also displays such a patch, albeit in a different location. In ImB2, this pocket is formed by hydrophobic residues in  $\alpha 2$  and  $\alpha 3$ . Sequence alignment shows that the group A immunity proteins have hydrophobic residues corresponding to the same location in ImB2 and therefore, likely display a hydrophobic pocket in this region. It has been suggested that this hydrophobic patch may mediate protein-protein interaction between the immunity protein and its putative receptor (190). Since all three subclasses exhibit this hydrophobic patch, this region may be critical for imparting immunity.

The most prominent difference between PisI and the other type IIa immunity proteins is the length and flexibility of both the N- and C- termini. PisI has a longer, more flexible N-terminus compared to the group A and C immunity proteins. On the other hand, the C-terminus of PisI is significantly shorter. Both the N- and C- termini of PisI contain several polar or charged residues that are well conserved within the group B immunity proteins. Studies involving hybrid immunity proteins (87, 163), and shortened variants of PedB (185), suggest that the C-terminal portion (extreme C-terminus in the case of PedB) of the protein is involved in specific recognition. However, this work has only used immunity protein and hybrids derived from subgroup A. Since PisI shows such a marked difference in its N-terminus, this region may also be involved in recognition. In fact, two residues in the N-terminus (K11 and R13) contribute to the positively charged patch of the protein. If this patch helps attract the protein to the cell membrane, then the N-terminus of the protein may also be crucial for recognition. Sequence alignment of the group B immunity proteins shows that this region is highly conserved. Recent mutational analysis of Mun-im only examined the effect of mutations in the C-terminal half of the protein (187). In order to investigate the importance of the N-terminus, the effect of mutations to the N- termini of the group B immunity proteins will need to be studied. Alternatively, hybrid proteins involving the group B immunity proteins may shed light on the role of the N-terminus.

### 3.2.6. Cloning and expression of the man-PTS system

The second major objective of this project was the preparation of overexpression systems for the IIAB, IIC and IID subunits of the  $EII_t^{\text{man}}$  permease of the man-PTS system. As described earlier in this chapter, the man-PTS system is believed to be the receptor for the type IIa bacteriocins, as well as their immunity proteins. Our ultimate goal is to perform crystallographic studies of the IIC and IID membrane components of the  $EII_t^{\text{man}}$  permease, complexed with a bacteriocin, and also with its immunity protein. Such a discovery would help uncover the mechanistic mysteries that govern the specificity of the type IIa bacteriocins and their immunity proteins. Thus, efforts were focused on the construction of His<sub>6</sub>-tagged fusion proteins of the IIC and IID membrane proteins, as well as the IIAB cytoplasmic protein. Although the IIAB subunit is not believed to be involved in bacteriocin recognition (or immunity), it may be required to help complex and stabilize the IIC and IID subunits in the membrane.

#### 3.2.6.a. Construction of expression systems for the IIC and IID subunits

The *mptC* structural gene was amplified by PCR, using primers that introduced a C-terminal His<sub>6</sub>-tag. The PCR product was then cloned into the *NcoI* and *HindIII* site of the pQE60 expression vector. The recombinant plasmid was named pMV24. The *mptD* gene was also cloned into the pQE60 vector, as C-terminal His<sub>6</sub>-tagged fusion protein by Dr. Marco van Belkum. The resulting plasmid was named pMV12. Genetic manipulations and plasmid propagation were done using *E. coli* JM109 as a host strain. For heterologous expression, the

plasmids were transferred to *E. coli* M15[pREP4]. The pREP4 plasmid constitutively expresses the *lac* repressor protein and thus, tightly regulates protein expression. Since both the IIC and IID proteins are membrane proteins, there was the potential for them to be toxic to the producer cell. Thus, we chose to use this tightly regulated expression system.

### **3.2.6.b. Construction of an expression system for the IIAB subunit**

The *mptAB* structural gene was amplified by PCR, using primers that introduced a C-terminal His<sub>6</sub>-tag. The *Nco*I restriction site was not compatible with the *mptAB* structural gene, so instead, a *Bsp*HI restriction site was introduced. Upon digestion with the *Bsp*HI endonuclease, this generated a sticky end that was complimentary to that produced by digestion with *Nco*I. Thus, the PCR insert was cloned into the *Nco*I and *Hind*III site of the pQE60 vector. However, no successful transformants were isolated. In total, 96 *E. coli* transformants were screened, but none contained the *mptAB* gene. Attempts to prepare this construct were halted.

### **3.2.6.c. Pilot expression of the IIC and IID membrane proteins**

To determine if the IIC and IID membrane proteins would be expressed, a series of pilot experiments were conducted. The expected masses of the His<sub>6</sub>-tagged IIC and IID fusion proteins are 28.2 kDa and 34.2 kDa, respectively. In an initial set of experiments, it was found that after induction with IPTG, *E. coli* cells harbouring the pMV24 plasmid (expressing IIC) continued to grow, as evidenced

by an increase in OD<sub>600</sub>. However, for *E. coli* cells with the pMV12 plasmid (expressing IID), the OD<sub>600</sub> post-induction decreased, indicating that the expressed protein is toxic to the cells. Pre-induction and post-induction protein samples from both experiments were analyzed by SDS-PAGE gel and are illustrated in Fig. 37. In both cases, a clear overexpression band was not visible, suggesting that overexpression levels are low. For the overexpression of IIC, a small band at ~33 kDa was visible (Fig. 37A). Interestingly, this band corresponds to the expected molecular mass of the IID protein. To rule out that the plasmids were accidentally mislabeled, they were resequenced, but it was confirmed that pMV24 contains the *mptC* gene.

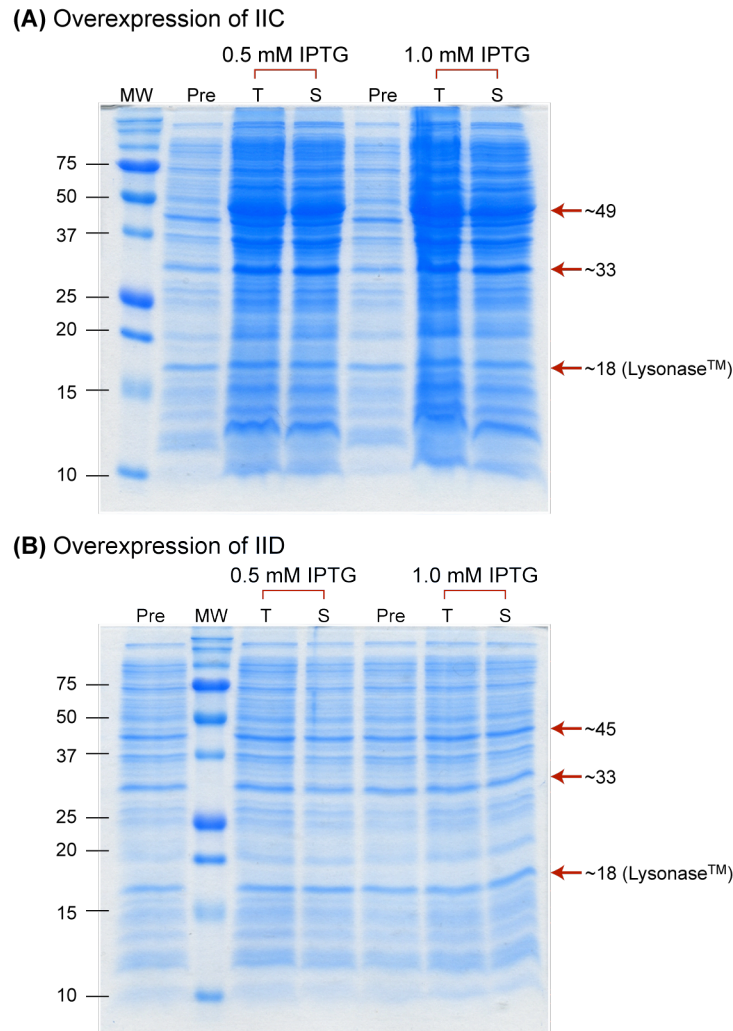


**FIG. 37.** SDS-PAGE analysis of the overexpression of IIC (A) and IID (B) with different concentrations of IPTG. The lane indicators MW, Pre, T, S and P refer to molecular weight markers, pre-induction, total protein, soluble protein, and pelleted protein, respectively. Molecular weights (kDa) are listed.

Additional pilot experiments were conducted only with pMV24 to determine if the expression of IIC could be enhanced at lower temperatures, or with varying concentrations of inducer. As such, *E. coli* cells with plasmid pMV24 were grown at either 30°C or 37°C and induced with various IPTG concentrations (0.1 mM, 0.3 mM, 0.5 mM and 1.0 mM). The different expression conditions were analyzed by SDS-PAGE and Western blot analysis. No

significant effect on protein expression resulting from either temperature or inducer concentration was observed. The Western blot for cells grown at 37°C and induced with either 0.5 mM or 1.0 mM IPTG is illustrated in Fig. 38.

Western blot indicated the presence of a His<sub>6</sub>-tagged protein at ~33 kDa (Fig. 38). Although this mass is higher than expected for IIC, it matches what we had previously observed on SDS-PAGE for the overexpression of IIC. Although some protein is visible in the pelleted fraction (indicative of inclusion bodies), it appears as though most of the protein is soluble. However, Western blot also revealed the presence of the His<sub>6</sub>-tagged protein in the pre-induction sample, suggesting that there is leaky expression. This is surprising, since a tightly regulated host strain was used. The addition of glucose to the growth media may help repress protein expression in the absence of IPTG.

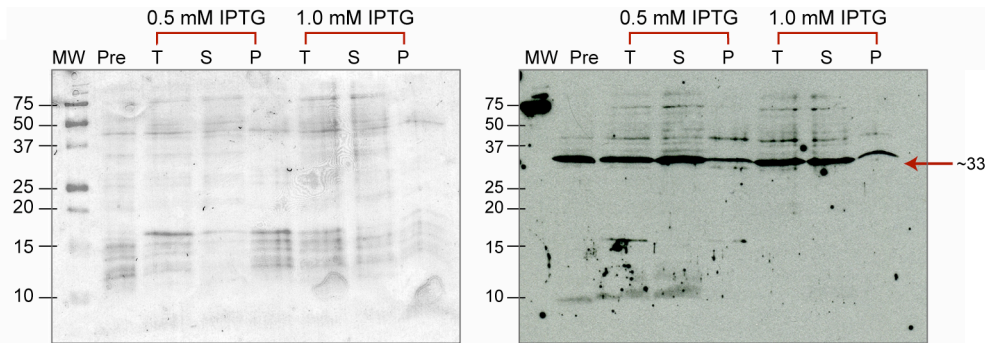


**FIG. 38.** Overexpression of IIC at 37°C with different concentrations of IPTG. The lane indicators MW, Pre, T, S and P refer to molecular weight markers, pre-induction, total protein, soluble protein, and pelleted protein, respectively. The image on the left shows the Ponceau stain of the resolved gel and the image on the right shows the Western blot. Molecular weights (kDa) are listed.

These initial experiments to probe the expression of the IIC membrane protein are promising and indicate that IIC is likely expressed as soluble protein. Future work will involve the large-scale expression and purification of the IIC membrane protein. Additional studies regarding the overexpression of the IID protein are required.

### **3.3. Conclusion & Future Directions**

This project focused on examining various aspects of the mechanisms of immunity and mode of action of the type IIa bacteriocins. Through heterologous expression of PisI, it was confirmed that this protein is indeed the immunity protein that provides protection against piscicolin 126 (PisA), a type IIa bacteriocin. Both PisI and PisA were overexpressed as maltose-binding proteins and successfully purified. Using NMR, it was determined that the structure of PisA does not change in the presence of PisI, suggesting that the type IIa bacteriocins do not interact directly with their immunity proteins in the absence of a receptor.

The 3D structure of PisI, a group B immunity protein, was solved using a combination of multidimensional, heteronuclear NMR experiments. The structure revealed that the group B immunity proteins share the same overall architecture as the group A and group C immunity proteins, confirming that the four-helix bundle is indeed a conserved motif for the proteins that confer immunity to the type IIa bacteriocins.

Lastly, preliminary studies to investigate the mode of action of the type IIa bacteriocins were initiated. It is widely accepted that the  $EII_t^{\text{man}}$  permease of the mannose phosphotransferase system is the receptor for the type IIa bacteriocins and is likely also involved in immunity. As such, the IIC and IID subunits of  $EII_t^{\text{man}}$  were cloned and initial experiments to overexpress these membrane proteins were conducted. Results suggest that the IIC subunit is overexpressed as soluble protein. More studies are required to examine the overexpression of the IID subunit. Future work will focus on the purification of these membrane proteins and crystallographic analysis. Undoubtedly, solving the structure of this receptor and examining its interaction with a type IIa bacteriocin, and its immunity protein, will help reveal the remarkable specificity that these bacteriocins have for their targets and how it is that their immunity proteins provide such specific protection.

## **Chapter 4. *In vitro* Studies of the Peptidase Domain of CbnT: Cleavage of pCbnB2 by CbnTP**

### **4.1. Background**

#### **4.1.1. Prebacteriocins and leader peptides of the Gly-Gly motif**

Most bacteriocins are synthesized as prepeptides with an N-terminal extension, or leader peptide. In the final stages of bacteriocin biosynthesis, these leader peptides are cleaved off and the bacteriocin is secreted outside of the cell (1, 6, 12, 56, 83, 84, 154). There has been much speculation regarding the biosynthetic function of the leader peptide. It is believed that the leader peptide keeps the bacteriocin in an inactive form, as many prebacteriocins exhibit diminished activity compared to the mature bacteriocin (153, 211). It is also accepted that leader peptides act as recognition signals that direct the prebacteriocins to the enzymes or protein complexes that are involved in their maturation and secretion (1, 212-215). This concept will be discussed in greater detail in the following section. In the case of lantibiotics, which undergo post-translational modification prior to secretion, it has been suggested that leader peptides function as recognition scaffolds for the modification enzymes (216-218), although it has recently been shown that for lacticin 481, posttranslational processing still occurs in the absence of the leader peptide (55). Aside from the leaderless bacteriocins, most LAB bacteriocins contain leader peptides ranging in length from 15-30 aa, that terminate with two glycine residues. These leaders are referred to as the double-glycine-type (Gly-Gly type) leaders. Some bacteriocins contain an N-terminal signal peptide and use the general secretion pathway (1).

Leader peptides of the Gly-Gly type are very similar. Sequence alignment, as well as numerous mutational studies have revealed the necessity for hydrophobic residues at positions (-4), (-7), (-12) and (-15), a Glu or Asp at position (-8), Gly at position (-2), and either Gly or Ala at position (-1) (219). Mutations to these positions result in substantial loss of bacteriocin production (212, 214, 220-223), suggesting that these positions are crucial for recognition of the precursor with its maturation and secretion enzymes. Typically, hydrophilic residues are found at positions (-5), (-6), (-9), (-11), (-13) and (-14), although mutations to these positions do not have a dramatic effect on bacteriocin production (221, 222).

In 2004, the first 3D structure of a prebacteriocin, pCbnB2, was published (153). pCbnB2 is the precursor peptide for carnobacteriocin B2 (CbnB2), a 48 aa type IIa bacteriocin whose NMR solution structure had also been published in 1999 (140). pCbnB2 contains an N-terminal 18 aa leader sequence. Analogous to the structure of CbnB2 and other type IIa bacteriocins (138-140, 164), pCbnB2 was shown to be random coil in aqueous conditions, but assumed secondary structure in the presence of membrane-mimicking conditions. The conserved  $\alpha$ -helix in the C-terminal domain of the type IIa bacteriocins was also present in the structure of pCbnB2. Interestingly, the leader peptide of pCbnB2 (residues -15 to -5, relative to the bacteriocin) also consisted of an amphipathic  $\alpha$ -helix. Although no long-range NOEs between the two helices were detected, it was hypothesized that the two helices could come into close contact with each other. As such, the leader peptide could effectively “block” the bacteriocin from exerting its pore

forming functions, thereby diminishing its antimicrobial activity (190). Fig. 39 shows the structures of CbnB2 and pCbnB2, as well as the overlay of the ensemble of structures. CbnB2 and pCbnB2 align very well in their C-terminal  $\alpha$ -helices. The mobile leader peptide of pCbnB2 is able to assume many orientations, relative to CbnB2.

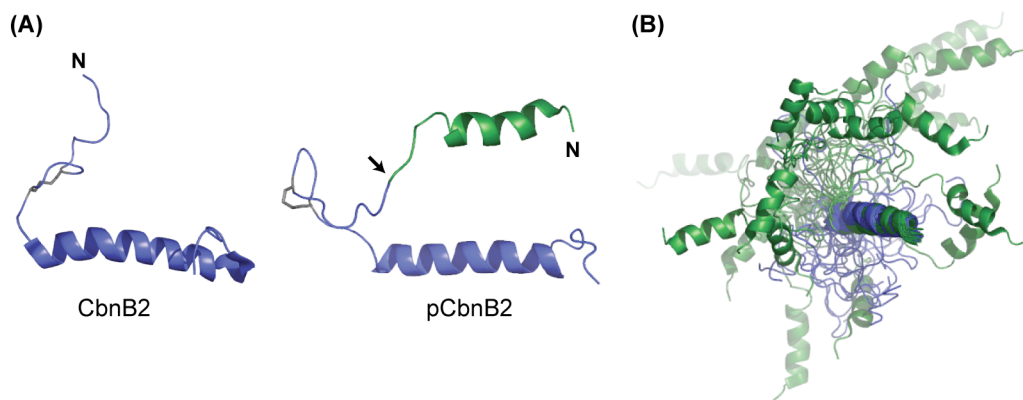


**FIG. 39.** NMR solutions structures of CbnB2 and pCbnB2 in membrane-mimicking conditions. (A) Single models of CbnB2 and pCbnB2 are depicted. The cleavage point of pCbnB2 is indicated with an arrow. (B) Overlay of pCbnB2 with CbnB2 (last 10 residues not shown). The ensemble of 20 structures representative of each peptide is shown. In both panels, the bacteriocin region is colored blue and the leader peptide is colored green.

In light of the structure of pCbnB2, the homology observed amongst the Gly-Gly type leader peptides can be understood from a structural perspective. As described above, the leader peptide of pCbnB2 was shown to contain a helical section. Looking down this helix, it is immediately apparent that the conserved hydrophobic residues, as well as Glu(-8), form one face of the helix (Fig. 40A). The sequences of several Gly-Gly type leaders are listed in Fig. 40C. The conserved hydrophobic residues at positions (-4), (-7), (-12) and (-15) all occupy the same position of helical wheel diagram (Fig. 40B). Since mutations to these residues profoundly affect bacteriocin production, it is highly likely that this face

of the helix interacts intimately with the enzyme(s) involved in maturation and secretion of the bacteriocin.

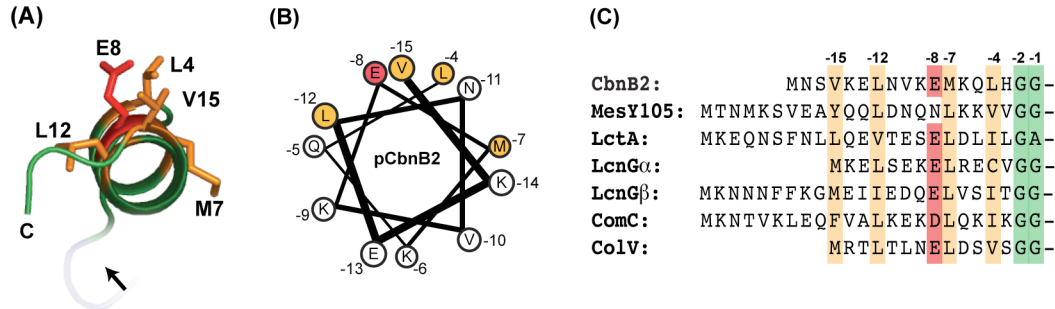


**FIG. 40.** Helical wheel diagram of pCbnB2 and conserved residues of the Gly-Gly type leader peptides. (A) Looking down the leader peptide helix of pCbnB2. The C-terminus is labeled and the site of cleavage is indicated with an arrow. Conserved residues are drawn as sticks. (B) Helical wheel diagram, based on pCbnB2. (C) Sequence alignment of various leader peptides. Conserved residues are highlighted and numbered. Orange and red refer to hydrophobic and acidic residues, respectively. Green residues denote the Gly-Gly/Ala sequence.

#### 4.1.2. Maturation and secretion of bacteriocins

Maturation and secretion of bacteriocins involves removal of the leader peptide and export outside the cell. Two different pathways for the maturation and secretion of bacteriocins have been identified: (1) use of a dedicated ABC-transporter and an accessory protein, and (2) the general secretion (*sec*-dependent) pathway (1, 83, 84). In recent years, several leaderless bacteriocins have also been discovered. While in the cytosol, they are likely complexed with an immunity protein to keep them inactive, and are then secreted out of the producer cell by a dedicated ABC-transporter (12, 29, 224). Most bacteriocins utilize the first pathway and the genes encoding both the ABC-transporter and accessory protein are typically located in the same operon as the bacteriocin gene (1). Although the

function of the accessory protein is unknown, the ABC-transporters have been studied in detail.

ABC-transporters constitute a super-family of membrane transporters. Both prokaryotic and eukaryotic cells rely on these systems to transport a wide range of substrates (such as sugars, amino acids, peptides, protein and inorganic ions) across membranes (225, 226). “ABC” refers to “ATP-binding cassette” and indeed, it is the hydrolysis of ATP that provides the energy for substrate transport. ABC-transporters consist of at least two domains: (1) a conserved cytoplasmic C-terminal ATP-binding domain; and (2) an integral membrane domain, typically consisting of six transmembrane helices (225, 226). These domains may be expressed as separate proteins, or together as a single polypeptide, as is the case for most bacterial ABC-transporters (56). Functional ABC-transporters exist as homodimers (56).

In 1995, Håvarstein *et al.* (56) discovered that the ABC-transporters for bacteriocins with Gly-Gly type leaders contain an additional, N-terminal domain. These transporters are typically 100-200 aa longer than the transporters used by bacteriocins that had leader peptides different than the Gly-Gly type (as is the case with several lantibiotics). Sequence alignment of several bacteriocin ABC-transporters containing this extra N-terminal domain revealed high levels of homology. In particular, two conserved motifs within the N-terminal domain were identified, in which a Gln, Cys, His and Asp were 100% conserved. These residues are characteristic of a cysteine protease. Furthermore, the ABC-transporter for ColV (a Gram-negative bacteriocin), as well as ComC (a quorum

sensing peptide produced by *Streptococcus pneumoniae*) also displayed this extra N-terminal domain. Interestingly, both ColV and ComC are also synthesized as precursor peptides with a Gly-Gly type leader. Thus, it was hypothesized that for bacteriocins (and other peptides) with a Gly-Gly type leader, the N-terminal domain of the dedicated ABC-transporter is responsible for the recognition and cleavage of the leader peptide (56). To test this hypothesis, Håvarstein *et al.* performed *in vitro* studies to examine the proteolytic activity of an ABC-transporter (56). Using lactococcin G (a two component bacteriocin comprised of lactococcin G $\alpha$  and G $\beta$ ) as their model system, the N-terminal domain of the ABC-transporter (LagD) was overexpressed, as was the precursor peptide of lactococcin G $\alpha$  (LagA). It was found that this truncated LagD successfully cleaved LagA, yielding active lactococcin G $\alpha$ .

Subsequently, many groups examined the connection between leader peptides and ABC-transporters. Using a “mix-and-match” approach, it was shown that different bacteriocins could be processed and secreted using the leader peptide and transport machinery of other bacteriocins (154, 213, 214). For example, by replacing the signal peptide of divergicin A (which normally utilizes the *sec*-dependent pathway for maturation and secretion), with the Gly-Gly type leader peptides of either leucocin A or ColV, divergicin A was secreted by the dedicated ABC-transporters for either leucocin A or ColV (154). In 1999, it was confirmed that this N-terminal, peptidase domain was located on the cytoplasmic side of the membrane (227). The topology of a typical bacteriocin ABC-transporter (monomer) is illustrated in Fig. 41.

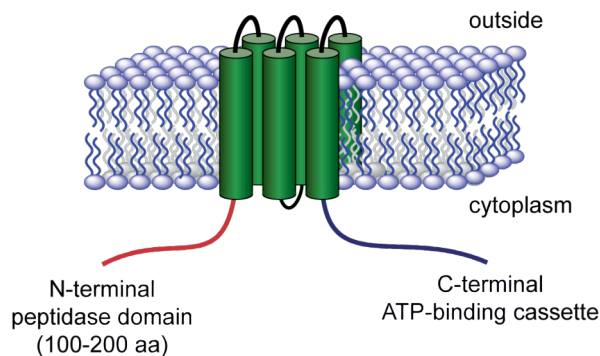


**FIG. 41.** Schematic of the ABC-transporters for bacteriocins with Gly-Gly type leader peptides.

Although many *in vivo* studies have been performed, only four other *in vitro* investigations have been reported. In 2004, the N-terminal domain of the ColV ABC-transporter (CvaB) was purified and shown to cleave the ColV prepeptide (228). Through mutational analysis, this study also confirmed that CvaB acted as a cysteine protease (228). In 2005, MesDp, the N-terminal domain of the ABC-transporter for the bacteriocin mesenterocin Y105 (MesY105) was purified and shown to cleave the precursor peptide of MesY105 (220). In 2006 and 2007, the proteolytic activity of several ABC-transporters (ComA) for various ComC molecules was also demonstrated (212, 223). In addition, it was shown the ComC prepeptide was random coil in aqueous conditions, but assumed helicity when incubated with the peptidase domain (PEP) of ComA (223). In 2008, the proteolytic activity of the ABC-transporter (LctT) for lacticin 481, a lantibiotic with the Gly-Gly type leader, was also demonstrated (222).

#### 4.1.3. Objectives

Despite the tremendous amount of work that has examined the interaction of leader peptides and ABC-transporters in the maturation of bacteriocins, there is

currently no structural information to depict this exquisite interaction. Since our group had already investigated the 3D structures of both CbnB2 and pCbnB2, our next goal was obtain an X-ray crystal structure of pCbnB2 with its protease. Thus, this project focused on the preparation of proteins for crystallographic studies. In particular, there were four main objectives for this project: (1) purify pCbnB2; (2) overexpress and purify CbnTP, the putative protease for pCbnB2; (3) establish the proteolytic activity of CbnTP; and (4) prepare Cys→Ser mutants of CbnTP.

## 4.2. Results & Discussion

### 4.2.1. Purification of pCbnB2

Using the plasmid pLQP, previously constructed by Dr. Luis Quadri (211), pCbnB2 was overexpressed as a maltose-binding protein fusion (MalE-pCbnB2) in *E. coli* BL21(DE3) cells. The fusion protein was purified via affinity chromatography using amylose resin, with a yield of ~110 mg/L. To remove the MalE affinity tag from pCbnB2, the fusion protein was treated with Factor Xa (1% w/w) for 12 h, as described in the literature (153, 211). However, it was discovered that under these conditions, pCbnB2 suffered significant secondary cleavage, as multiple fragments were observed by MALDI-TOF (Fig. 42A). This complicated subsequent purification as neither cation exchange nor RP-HPLC could successfully separate the peptide fragments. Hence, a pilot study was performed to examine digestion conditions. It was discovered that by reducing the amount of Factor Xa to 0.5% (w/w) and reducing the digestion time to 4 h, pCbnB2 did not undergo significant secondary cleavage (Fig. 42B). It should be

noted that in addition to pCbnB2, a truncated version (named pCbnB2<sub>RP</sub>) in which the two C-terminal amino acid (R65 and P66) were missing was also observed. Although Quadri *et al.* (211) never reported this derivative, it was the only species observed and purified by Sprules *et al.* (153). Factor Xa is known to promote secondary cleavage immediately following Gly-Arg sequences, as well as at other basic residues (229, 230). Indeed, the C-terminal residues of pCbnB2 are G63–R64–R65–P66, and as such, loss of the last two residues is to be expected. Interestingly, it has been reported that Factor Xa will not cleave at a site followed by an arginine (230), however, such cleavage was observed in this study. After establishing adequate conditions, a large-scale digestion of MalE-pCbnB2 was performed, and pCbnB2 / pCbnB2<sub>RP</sub> were purified by RP-HPLC. Although it had been reported that pCbnB2 was susceptible to degradation when stored as a lyophilized powder or in aqueous conditions (at -20°C) (153), no degradation of the purified sample was observed.

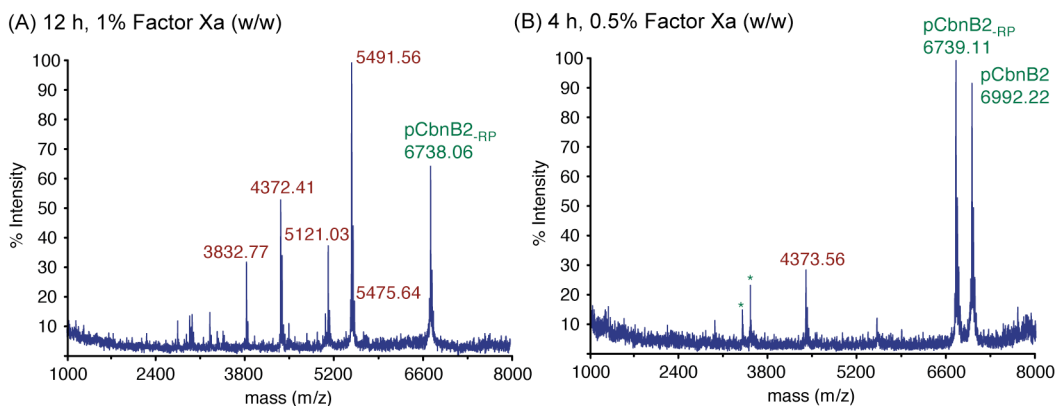


**FIG. 42.** MALDI-TOF of the cleavage of MalE-pCbnB2 by Factor Xa under different digestion conditions. (A) Digestion according to literature procedures (153, 211). Extensive overdigestion of CbnB2 is observed. (B) Digestion of MalE-pCbnB2 with reduced amounts of enzyme and digestion times. The desired pCbnB2 peaks are labeled in green while fragments are labeled in red. In panel B, asterisks denote the doubly charged ions of pCbnB2 / pCbnB2<sub>RP</sub>.

### 4.2.2. Purification of CbnTP

Part of the *cbnT* gene, corresponding to the N-terminal 164 aa was cloned into the pQE60 expression vector, as a C-terminal His<sub>6</sub>-tagged fusion protein (named CbnTP), by Dr. Marco van Belkum. Sequence alignment of CbnT with the other ABC-transporters that have been examined *in vitro* suggested that this region corresponds to a cysteine protease domain (Fig. 43). For CbnT, the conserved residues implicated in peptidase activity are Q9, C15, H94 and D110.

```

LagD   3 KIIYQQDEKDCGVACIAMILK-(64)-QKYQHYYVVVYKVKGDEIWIADPAKGKIRKTI 118
CvaB  22 PVIHQETETAECGLACLAMICG-(58)-WDFSHFVVLVSVKRNRYVLHDPARGIRYISR 131
MesD  12 DYISQVDERDCGVAALAMILA-(64)-GKYPHYVYVYGMKGDQLLIADPDNTVVGKTKM 127
ComA   7 HYRPQVDQMDCGVASLAMVFG-(64)-GKLLHYVYVVTGQDKDSIHIADPDPGVKLTKL 122
LctT   6 QNNEQDCLLACYSMILGYFGR-(59)-WNDNHFVVVTKIYRKNVTLIDPAIGVKYNY 116
CbnT   5 SFVQQQDEKDCGVACIAMILK-(64)-KTYMHYVYVYGVKENKLLIADPAEGMKKSI 120

```

**FIG. 43.** Sequence alignment of the N-terminal domain of CbnT with other ABC-transporters. The catalytic triad (Cys, His, Asp/Glu) and the oxyanion hole Gln are highlighted in yellow. The first and last numbers indicate the amino acid positions, while those in brackets denote the number of excluded residues. LagD, CvaB, MesD, ComA, LctT and CbnT refer to the ABC-transporters for lactococcin G, colicin V, mesenterocin Y105, ComC signaling peptides, lactacin 481 and carnobacteriocin B2, respectively.

The CbnTP fusion protein was heterologously overexpressed in *E. coli*. Pilot studies were performed by Dr. Marco van Belkum to determine optimal expression conditions. However, despite exploring a range of temperatures (20°C to 37°C), various concentrations of inducer (0.1 mM to 1.0 mM final concentration of IPTG), and different *E. coli* host strains, it appeared as though CbnTP was only expressed as inclusion bodies. It should be noted that LagD, CvaB and MesDp were also expressed as, and purified from, inclusion bodies (56, 220, 228).

#### 4.2.2.a. Purification of CbnTP from inclusion bodies

After overexpressing the fusion protein, the cells were lysed and the pellet was solubilized with urea. After centrifugation to remove cell debris, CbnTP was isolated and purified using Ni-NTA affinity chromatography. Various renaturation techniques were tried, including dialysis, rapid dilution and on-column refolding.

For refolding by rapid dilution or dialysis, the denatured CbnTP was first eluted from the Ni-NTA column with imidazole. For rapid dilution, 5 mL of the protein solution was slowly added (dropwise, over 60 min) to 30 mL of rapidly stirring buffer. This reduced the urea from 6 M to 0.9 M. However, significant precipitation was observed after the process was complete. Alternatively, the concentration of urea was reduced by slow dialysis of the protein solution (4 × 24 h) against buffer with sequentially less urea (4 M, 2 M, 1 M and 0 M). Again, substantial precipitation was observed when the concentration of urea was lowered beyond 4 M. In both cases, the heterogeneous mixture was centrifuged to remove the precipitate and the supernatant was concentrated and tested for proteolytic activity. SDS-PAGE of the supernatant indicated that the purified CbnTP was of the correct molecular weight and was isolated in high purity.

Alternatively, on-column refolding was attempted prior to elution of the CbnTP with imidazole. Over 1.5 h, the amount of urea in the wash buffer was slowly reduced from 6 M to 1 M, in the presence of 20% glycerol and 500 mM NaCl to help stabilize the protein. CbnTP was then eluted with imidazole. To concentrate the protein, remove imidazole and do a buffer exchange, a

concentrating tube was used. SDS-PAGE indicated that CbnTP had been isolated in high purity. Unfortunately, in all cases, the CbnTP purified from inclusion bodies showed no proteolytic activity toward pCbnB2 / pCbnB2<sub>RP</sub> (described below, in section 4.2.3). This is likely due to improper refolding of the protease.

#### **4.2.2.b. Purification of CbnTP from soluble protein**

After the failed attempts to purify active protein from inclusion bodies, the expression conditions for CbnTP were re-evaluated by Dr. Marco van Belkum. By lowering the temperature significantly (to 10°C), a very small amount of soluble protein was observed by SDS-PAGE analysis (Fig. 47). Thus, a large-scale (4 L prep) overexpression and purification with these new conditions was performed. The host strain was grown at 37°C with shaking, until the OD<sub>600</sub> reached ~0.6, after which the cultures were placed in an ice-water bath to rapidly cool them and slow growth. After inducing protein expression with IPTG, cultures were incubated at low temperature (10°C) for an additional 20 h.

Following cell lysis, CbnTP was purified in a two-step process. First, CbnTP was purified by Ni-NTA affinity chromatography. SDS-PAGE analysis indicated that several contaminating bands co-eluted with CbnTP, as shown in Fig. 44A. These contaminants could not be removed by extending the wash step, or by using a prolonged gradient elution. Thus, fractions containing CbnTP were combined, concentrated to ~2 mL and further purified by size-exclusion chromatography. In this second purification, the higher molecular contaminants were adequately separated from CbnTP, although a few additional, lower-weight

contaminants (likely degradation products) were observed (Fig. 44B).

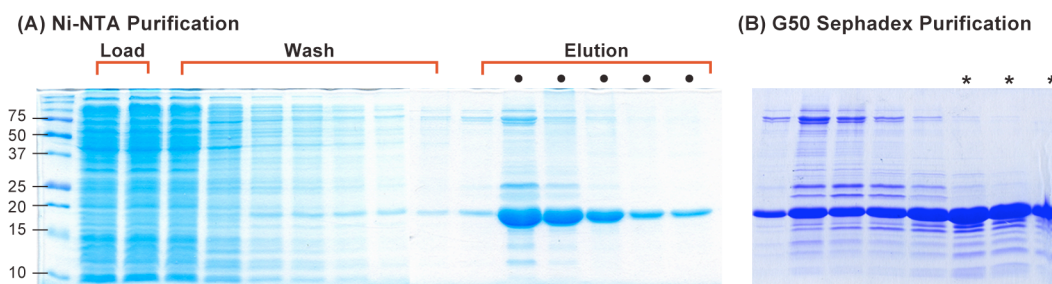


**FIG. 44.** Purification of CbnTP as soluble protein. (A) Ni-NTA affinity chromatography. The load, wash (every other fraction) and elution phases of the purification are shown. Lanes marked with circles were combined, concentrated and used in the next purification. (B) Size-exclusion chromatography. Lanes marked with asterisks were combined and concentrated. Molecular weights are indicated.

In most protein purifications, protease inhibitors are added to the lysis and purification buffers to prevent degradation of the desired protein. However, since our desired protein was itself a protease, the purification was done in the absence of protease inhibitors. In the purification of PEP (the peptidase domain of ComA), Ishii *et al.* reported that protease inhibitors did not affect the subsequent activity of their protease (223). Nonetheless, without prior knowledge regarding the activity of CbnTP, we opted to not use protease inhibitors.

CbnTP was successfully purified as soluble protein, but the purification was finicky. CbnTP had a tendency to precipitate out of solution, resulting in a continual loss of protein. This problem was also reported for the purification of PEP (223). Interestingly, it appeared as though precipitation was facilitated by the presence of the high-molecular weight contaminants. After removal of these proteins by size-exclusion chromatography, CbnTP appeared more stable. Typically, 6-8 mg of CbnTP was purified from 4 L of culture.

### 4.2.3. Peptidase activity of CbnTP

To establish the proteolytic activity of CbnTP, the purified protein was incubated with its substrate, pCbnB2 / pCbnB2<sub>-RP</sub>. Digestion reactions were performed at room temperature or 37°C for 12-18 h. Controls consisting of just the protease and just the substrate were also subjected to the same conditions. Reaction progress was monitored by MALDI-TOF. Since cleavage of pCbnB2 would liberate CbnB2, spot-on-lawn activity testing was also used as a method of bacteriocin detection, using *C. divergens* LV13 as the indicator organism.

As already mentioned, CbnTP isolated from inclusion bodies failed to cleave the substrate. However, CbnTP purified as soluble protein did exhibit proteolytic activity. In general, digestions were done with an enzyme: substrate ratio of 1:1 or 1:2 (mol/mol). Fig. 45 shows the MALDI-TOF traces and activity profile for a typical digest reaction, revealing that the leader peptide of pCbnB2/pCbnB2<sub>-RP</sub> has been cleaved by CbnTP, liberating active bacteriocin.

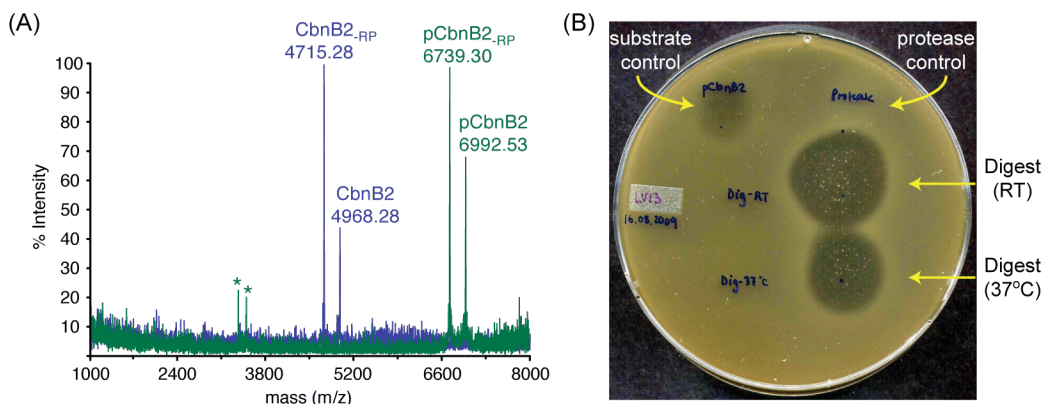


**FIG. 45.** MALDI-TOF and activity testing to determine the proteolytic activity of CbnTP toward pCbnB2. (A) Overlay of the MALDI-TOF traces of the substrate control (in green) and the digest reaction (12 h, RT; in blue). The doubly charged ions of pCbnB2 and pCbnB2<sub>-RP</sub> are identified with asterisks. In the digest reaction, the substrate has been cleaved, yielding CbnB2 / CbnB2<sub>-RP</sub>. The leader peptide ( $m/z=2043$ ) is not visible in this trace. (B) Antimicrobial activity of the controls (substrate and protease, 10  $\mu$ L each) and digestion reactions (RT and 37°C, 10  $\mu$ L each) against *C. divergens* LV13. The small zone of clearing around the substrate control is due to the minimal activity of pCbnB2, whereas the large zones of inhibition surrounding the digest reaction spots indicate the presence of active bacteriocin (CbnB2).

CbnTP was subjected to a variety of different buffer and salt conditions (to facilitate crystallization studies). Each time, the activity of CbnTP was monitored. Since the focus of this study was the purification of active protein for structural studies, detailed enzymatic characterization of CbnTP was not performed.

#### 4.2.4. Construction of Cys $\rightarrow$ Ser mutants of CbnTP

Five different Cys $\rightarrow$ Ser mutants were designed to systematically replace the four cysteine residues (positions 15, 19, 55 and 63) of CbnTP with serine residues. As such, single, double, triple and quadruple point mutants were prepared, corresponding to CbnTP.M1, CbnTP.M2, CbnTP.M3 (and CbnTP.M5), and CbnTP.M4, respectively (Fig. 46).

		15	19			55	63	
<b>CbnTP</b>	12	EKD	CGVAC	IAMILK	KYKSEV	PIHKLRE	LSGTSLE	GTSPPF
								GLKNC
								IEKLG
								FDCQ
								AV 66
<b>CbnTP.M1</b>	12	EKDS	GVAC	IAMILK	KYKSEV	PIHKLRE	LSGTSLE	GTSPPF
								GLKNC
								IEKLG
								FDCQ
								AV 66
<b>CbnTP.M2</b>	12	EKDS	GVAS	IAMILK	KYKSEV	PIHKLRE	LSGTSLE	GTSPPF
								GLKNS
								IEKLG
								FDCQ
								AV 66
<b>CbnTP.M3</b>	12	EKDS	GVAS	IAMILK	KYKSEV	PIHKLRE	LSGTSLE	GTSPPF
								GLKNS
								IEKLG
								FDCQ
								AV 66
<b>CbnTP.M4</b>	12	EKDS	GVAS	IAMILK	KYKSEV	PIHKLRE	LSGTSLE	GTSPPF
								GLKNC
								IEKLG
								FDCQ
								AV 66
<b>CbnTP.M5</b>	12	EKDS	GVAS	IAMILK	KYKSEV	PIHKLRE	LSGTSLE	GTSPPF
								GLKNS
								IEKLG
								FDCQ
								AV 66

**FIG. 46.** Cys→Ser mutants of CbnTP. Cysteine residues and serine residues (introduced as mutations) are highlighted in yellow and blue, respectively. The numbers before and after the sequences refer to the position of the first and last amino acid, respectively.

CbnTP.M1 is predicted to be the active site mutant and was constructed to facilitate structural studies of pCbnB2 bound to its [inactive] receptor. The other cysteine residues were mutated to serines to assist in crystallization efforts, as cysteine residues located on the surface of proteins have been shown to impede crystallization by participating in multimer formation (231). It is not known if the other cysteines in CbnTP are located on the surface, but the mutants were prepared nonetheless.

The mutants were constructed using site-directed mutagenesis using the primers listed in Table 7. Plasmids were propagated in either *E. coli* XL1-Blue or *E. coli* JM109 strains, both of which produce dam-methylated DNA. To prepare the first mutant (CbnTP.M1), the pQE60.CbnTP vector was amplified by PCR using original pQE60.CbnTP DNA (isolated from *E. coli* JM109) as a template and primers LAM19 and LAM20, which were specific for the *cbnTP* gene and introduced the C15S mutation. Following PCR, parental DNA was digested with the enzyme *DpnI*, which specifically cleaves dam-methylated and hemimethylated DNA (232). The remaining vector DNA (pQE60.CbnTP.M1) was transformed into *E. coli* XL1-Blue competent cells. Plasmid DNA was isolated and clones were sequenced to verify the mutation.

**TABLE 7.** Primers used for site-directed mutagenesis of CbnTP

Primer	Sequence <sup>a</sup>	Mutation
LAM19	5'—CAGCAAGATGAGAAAAGATTCAGGTGTTGCATGTATCGCAATG—3'	C15S
LAM20	5'—CATTGCGATACATGCAACACCTGAATCTTTCTCATCTTGCTG—3'	C15S *
LAM21	5'—GATGAGAAAAGATTCAGGTGTTGCATCAATCGCAATGATTTTAAAG—3'	C19S
LAM22	5'—CTTTAAAATCATTGCGATTGATGCAACACCTGAATCTTTCTCATC—3'	C19S *
LAM23	5'—CCATTTGGGTAAAAAATTCAAATTGAAAAATTAGGTTTTGATTGC—3'	C55S
LAM24	5'—GCAATCAAACCTAATTTTTCAATTGAATTTTTTAACCCAAATGG—3'	C55S *
LAM25	5'—GAAAAATTAGGTTTTGATTCAACAAGCTGTTCAAGCAGATCAAG—3'	C63S
LAM26	5'—CTTGATCTGCTTGAACAGCTTGTGAATCAAACCTAATTTTTTC—3'	C63S *

<sup>b</sup>Nucleotides encoding the mutation are underlined; \* complimentary strand.

The second mutant (CbnTP.M2) was prepared in a similar fashion, except that primers LAM21 and LAM22 were used to introduce the C19S mutation and plasmid pQE60.CbnTP.M1 (with C15S) was used as template DNA. The third and fifth mutants (CbnT.M3 and CbnTP.M5) were subsequently prepared using pQE60.CbnTP.M2 DNA as a template and primers LAM23/LAM24 (C55S mutations) or LAM25/LAM26 (C63S mutation), respectively. The final mutant, CbnTP.M4 was prepared using pQE60.CbnTP.M3 DNA as a template and primers LAM25 and LAM26 (C63S). For protein expression, *E. coli* M15[pREP4] was used as the host strain as it permits tightly regulated, high-level expression.

To determine if the CbnTP mutants would be expressed as soluble protein, or as inclusion bodies, they were grown under the same conditions used to obtain soluble CbnTP (described above). Unfortunately, SDS-PAGE analysis indicated that like CbnTP, the mutants were expressed almost entirely as inclusion bodies (Fig. 47). CbnTP.M1 showed the greatest amount of soluble protein, albeit

minimal. Virtually no soluble protein was observed from the other mutants. Although these results were disappointing, it is likely that adequate amounts of CbnTP.M1 can be isolated from a large-scale (*i.e.*: 4 L) protein preparation.

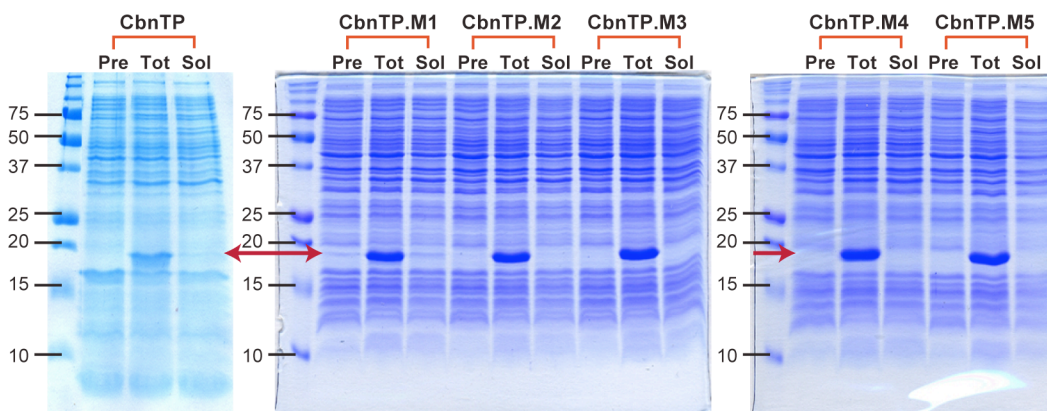


**FIG. 47.** 15% SDS-PAGE analysis of expression of CbnTP and mutants (M1-M5). The red arrow indicates the position of the expected protein. The pre-induction control (Pre), total (Tot) and soluble (Sol) protein samples are indicated. Molecular weight standards are identified.

### 4.3. Conclusions & Future Directions

The N-terminal 164 amino acids of CbnT, the ABC-transporter for carnobacteriocin B2, was successfully overexpressed and purified as a His<sub>6</sub>-tagged protein, following a two-step purification strategy. Using a previously developed system, the precursor peptide for carnobacteriocin B2 was overexpressed as a maltose binding protein fusion. Following cleavage with Factor Xa and HPLC purification, pCbnB2, and a truncated derivative (termed pCbnB2<sub>-RP</sub>) were obtained. When pCbnB2 and pCbnB2<sub>-RP</sub> were incubated with CbnTP, mass spectral analysis of the reaction mixture revealed that both pCbnB2 and pCbnB2<sub>-RP</sub> were cleaved after the Gly(-2) –Gly(-1) site, yielding three peptide fragments, two of which corresponded to CbnB2 and CbnB2<sub>-RP</sub>, and the other

which corresponded to the leader peptide. In addition, the activity of the digestion mixture against a CbnB2 sensitive strain revealed that active bacteriocin was produced. These results clearly demonstrate that the N-terminal domain of CbnTP is involved in recognition and proteolytic processing of the prepeptide. Crystallographic studies of CbnTP are currently underway, in collaboration with Dr. Jiang Yin in the group of Professor Michael James (Department of Biochemistry, University of Alberta).

A series of five Cys→Ser mutants of CbnTP were cloned as His<sub>6</sub>-tagged fusions and screened for protein production. While most of the mutants show almost no soluble protein production, the predicted active site mutant C15S (CbnTP.M1) shows soluble protein at levels similar to that of CbnTP. Future work will involve the large scale overexpression and purification of this mutant, as well as testing its activity against pCbnB2 to confirm the role of C15 as the active site cysteine. Crystallographic studies of this mutant with pCbnB2 will provide a detailed picture of how the leader peptides of the Gly-Gly motif interact with the proteolytic domains of their dedicated ABC-transporters. Such a “picture” will clarify the role of the conserved residues within the leader peptides, and ultimately reveal how these systems exert their remarkable specificity.

## **Chapter 5. Testing the activity of LAB bacteriocins against Gram-negative pathogens**

### **5.1. Background**

#### **5.1.1. Drawbacks to the utility of LAB bacteriocins in food preservation and as human therapeutics**

In chapter one, the use of LAB bacteriocins as natural food preservatives was discussed. Indeed, the bacteriocins hold great potential in this area: they are highly active against numerous food spoilage pathogens and are generally stable across a wide pH and temperature range. As mentioned, many LAB bacteria are already used as probiotics and starter cultures for numerous food products. The application of LAB bacteriocins as therapeutics is also a widely studied area. Their potent activity, GRAS status and multi-faceted mode of action make them ideal candidates as human therapeutics. However, despite the potential that bacteriocins possess, there remains one major drawback to the utility of these peptides for use in food-preservation or as therapeutics: most LAB bacteriocins are unable to kill Gram-negative pathogens such as *E. coli*, *Salmonella* and *Pseudomonas* species (4-6, 9, 104). The following sections will discuss why Gram-negative bacteria are unaffected by LAB bacteriocins and how the activity of LAB bacteriocins can be extended to this class of pathogens.

#### **5.1.2. Gram-negative bacteria and LAB bacteriocins**

Gram-positive and Gram-negative bacteria differ in the structure of their cell walls. As described in chapter 1, the cell wall of Gram-positive bacteria is composed of the cytoplasmic membrane, surrounded by a thick, protective layer

of peptidoglycan (Fig. 1). Gram-negative bacteria have an inner membrane and a cell wall similar to that of the Gram-positives (although with a much thinner layer of peptidoglycan), but they have an additional protective barrier: the outer membrane (OM). The OM is composed of a phospholipid bilayer (the inner leaflet), surrounded by a highly ordered network of lipids and polysaccharides referred to as lipopolysaccharides (LPS). The LPS layer forms a tight shield, or outer leaflet, which encases the cell (Fig. 48) (233).

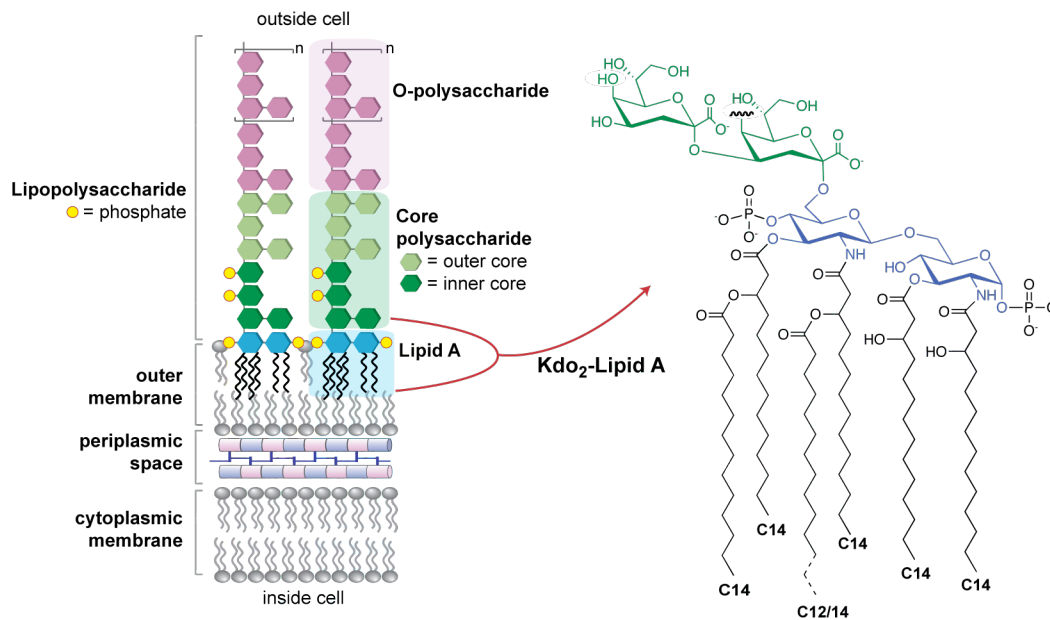


**FIG. 48.** The cell wall of Gram-negative bacteria and the chemical structure of Kdo<sub>2</sub>-Lipid A, the fundamental LPS constituent of Gram-negative bacteria. The phosphorylated glucosamine sugars of Lipid A are colored blue and the lipid tails are in black. The Kdo sugar moieties of the inner core are colored green and the outermost O-polysaccharide (O-antigen) component is colored pink. The chemical structure of Kdo<sub>2</sub>-Lipid A adapted from Raetz et al. (234).

The OM of Gram-negative cells acts as an impenetrable barrier to many compounds, including antibiotics, hydrophobic compounds, detergents and dyes (235). Small, hydrophilic compounds can passively traverse the OM via water-

filled channels, formed by porin proteins. However, larger molecules must be actively translocated across the OM by membrane-associated proteins (235).

As illustrated in Fig. 48, LPS molecules are composed of three main components: lipid A, a core oligosaccharide and an O-polysaccharide (or O-antigen) (233). Typically, lipid A is a phosphorylated glucosamine disaccharide, with multiple lipid chains (generally 14 carbons in length) that help anchor the LPS molecules in the phospholipid bilayer of the OM. Lipid A is responsible for many of the endotoxic properties of LPS (233, 234). The core oligosaccharide (divided into an inner and outer core) is covalently attached to Lipid A and consists of a series of variable sugar units. Almost all Gram-negative bacteria possess LPS molecules that contain the modified sugar 3-deoxy-D-mannooctulosonic acid (Kdo) within the inner core (234). The chemical structure of the Kdo<sub>2</sub>-Lipid A moiety is illustrated in Fig. 48. The outermost surface of the LPS molecule is the O-polysaccharide. The composition of these carbohydrate chains is strain dependent and related to the virulence and antigenic properties of the organism (234).

The Kdo<sub>2</sub>-Lipid A structure, as well as the inner core of the LPS molecule, makes the OM impenetrable to hydrophobic compounds. Numerous anionic phosphate and carboxylate groups are found within this region of LPS. These groups are stabilized by divalent cations, particularly Ca<sup>2+</sup> and Mg<sup>2+</sup> (235). However, it has been shown that if these cations are removed from the LPS layer, the integrity of the OM is jeopardized. It has been well established that chelating agents, such as EDTA, lead to the destabilization of the outer membrane. Upon

chelation of cations, LPS molecules (up to 50%) are released from the OM, exposing the underlying phospholipid bilayer of the OM (235).

Although Gram-negative cells are impenetrable to LAB bacteriocins, they are not insensitive to these peptides. Numerous studies have demonstrated that LAB bacteriocins exhibit antimicrobial activity toward Gram-negative bacteria in the presence of chelating agents (*i.e.*: EDTA, citrate or lactoferrin) or other treatments that compromise the integrity of the OM, such as osmotic shock, temperature variation (heat-shock or rapid chilling), pH variation, pulsed electric fields (PEF) and high hydrostatic pressure (HHP) (2, 5, 7, 9, 83).

Of the bacteriocins, the efficacy of nisin against numerous food spoilage and pathogenic strains of *E. coli*, *Salmonella* and *Pseudomonas* in combination with OM destabilizing treatments, has been widely studied. For example, it has been well documented that nisin, in combination with EDTA (236-243), osmotic shock (244), or temperature variation (245-248) leads to a reduction in populations of Gram-negative bacteria. However, the killing effect of nisin is not uniform and appears to vary between species and strain. It has been reported that in general, *Salmonella* spp. are least affected by nisin treatment (237). The efficacy of nisin (in combination with EDTA) in *in situ* studies is typically much less, compared to *in vitro* studies (5, 7), suggesting that components of food products may interfere with the binding of nisin (or EDTA) to its targets, or facilitate the degradation of nisin by exposure to alkaline conditions or proteolytic enzymes (7).

Besides nisin, a variety of other bacteriocins have been investigated for their activity against Gram-negatives under OM stressing conditions. Although not an exhaustive list, the other bacteriocins tested include other lantibiotics (Pep5), circular bacteriocins (enterocin AS-48 and gassericin A), type IIa bacteriocins (pediocin PA-I, sakacin P, curvacin A, enterocin A), type IIb two-component bacteriocins (brochocin C) and type IIc miscellaneous bacteriocins (enterocin B). Table 8 summarizes the observed effect of various LAB bacteriocins on Gram-negative bacteria when used in conjunction with OM stressing conditions.

As seen in Table 8, it appears as though several LAB bacteriocins are able to exert a killing effect against Gram-negative pathogens, insofar as the OM is weakened. Interestingly, of the bacteriocins that have been tested, there is some discrepancy regarding the activity of the type IIa bacteriocins: some studies report no killing effect in the presence of EDTA (241), whereas other do (249, 250). As described in chapter three, the activity of the type IIa bacteriocins is receptor mediated, and it is believed that the  $EII_t^{man}$  permease of the mannose phosphotransferase system (man-PTS) is the receptor. Although Gram-negative bacteria also contain such transport systems, amino acid differences in the  $EII_t^{man}$  permease may render the type IIa bacteriocins ineffective against these bacteria. In contrast, the receptor molecule for nisin (lipid II) is highly conserved across prokaryotes. As such, if nisin can access the cytoplasmic membrane, it will most likely display a killing effect.

**TABLE 8.** The efficacy of LAB bacteriocins against Gram-negative pathogens

Bacteriocin	Observed Effect	Ref.
<b><i>In combination with EDTA</i></b>		
Nisin	Significant reduction in population of <i>E. coli</i> , <i>Pseudomonas</i> and <i>Salmonella</i> cells observed. Growth inhibition appears to be strain dependent. Synergy not observed for <i>in situ</i> studies with meat (239, 251) or 2% UHT milk (238), but was observed with cantaloupe and melons (252).	(238-241, 243, 248, 250-254)
Brochocin C	Significant reduction (>2 log) in <i>E. coli</i> and <i>Salmonella</i> populations	(241)
Pediocin PA-1	Conflicting reports – one study reports no reduction (<0.2 log) in <i>E. coli</i> and <i>Salmonella</i> populations (241), whereas another states that a reduction in Gram-negative populations was observed (249).	(241, 249)
Sakacin P	Enhanced activity toward <i>E. coli</i> and <i>Salmonella</i> cells.	(250)
AS-48	<i>Salmonella</i> growth greatly reduced after 6 h of EDTA (50 mM) and AS-48 treatment (concentration dependent). <i>E. coli</i> O157:H7 strains showed sensitivity to AS-48 (concentration dependent).	(255, 256)
Enterocins A,B	In the presence of EDTA, enterocins displayed minimal growth inhibition toward <i>Salmonella</i>	(257)
<b><i>In combination with other chelating agents or chemical additives</i></b>		
Nisin	When used in combination with lactoferrin, a synergistic effect against <i>E. coli</i> O157:H7 was observed.	(258)
Gassericin A	When used in combination with glycine, growth inhibition of <i>Achromobacter denitrificans</i> and <i>Pseudomonas aeruginosa</i> was observed	(259)
Enterocins A,B	In the presence of lactate, enterocins displayed minimal growth inhibition toward <i>Salmonella</i>	(257)
<b><i>In combination with osmotic shock</i></b>		
Nisin	<i>E. coli</i> cells showed sensitivity to nisin. Efflux of radiolabelled cytoplasmic components detected	(244)
<b><i>In combination with temperature variation (heat-shock, chilling)</i></b>		
Nisin	Rapid chilling in the presence of nisin reduced <i>E. coli</i> , <i>Salmonella</i> and <i>Pseudomonas</i> populations (concentration dependent).	(245-247)
AS-48	The viability of sub-lethally heated (60°C, 3-5 min) <i>Salmonella</i> and <i>E. coli</i> O157:H7 cells was greatly reduced (concentration and time dependent).	(255, 256)
Enterocins A,B	Although temperature greatly influenced the growth of <i>Salmonella</i> , the presence of enterocins had little effect	(257)
<b><i>In combination with pH variation (acidic and alkaline conditions)</i></b>		
AS-48	Significant LRF of <i>E. coli</i> O157:H7 and <i>Salmonella</i> strains was observed when AS-48 was administered at pH 5 and 8	(255, 256)

<sup>a</sup> LRF: Log Reduction Factor

Thus, in the presence of OM destabilizing treatments, it is likely that many LAB bacteriocins can access the cytoplasmic membrane of Gram-negative bacteria and cause cell death, as long their activity is not dependent on a receptor molecule specific to Gram-positive organisms. However, destabilization of the OM may not be the *only* way for bacteriocins to gain access to their Gram-negative enemies. The following section will highlight how Gram-negative bacteria can be “tricked” into actively transporting lethal peptides, and the possible extension of this trickery to LAB bacteriocins.

### **5.1.3. The bacteriocins of Gram-negative organisms**

Although the OM of Gram-negative bacteria provides excellent protection from the surrounding environment, it comes at a cost. Many essential nutrients and solutes are unable to traverse the OM and therefore, must be actively transported in. In this regard, the acquisition of ferrous, soluble iron is a constant struggle for most bacteria (260). To meet this challenge, many bacteria synthesize siderophores, which are small molecules that chelate iron with high affinity (260). Siderophores complex  $\text{Fe}^{3+}$ , which is subsequently reduced inside the cell. Figure 49 illustrates three different types of siderophores. Ferrichrome (Fig. 49A) is a hexapeptide siderophore, comprised of three glycine and three modified ornithine residues. The hydroxamate groups (of the modified ornithines) are involved in coordination to iron (261, 262). Enterobactin (Fig. 49B) is an example of a catecholate-based siderophore (260). Enterobactin, which binds iron with a

$K_a$  of  $10^{52} \text{ M}^{-1}$ , has the strongest affinity for iron of the known siderophores (263).

Aerobactin (Fig. 49C) is an example of a citrate-based siderophore (264).

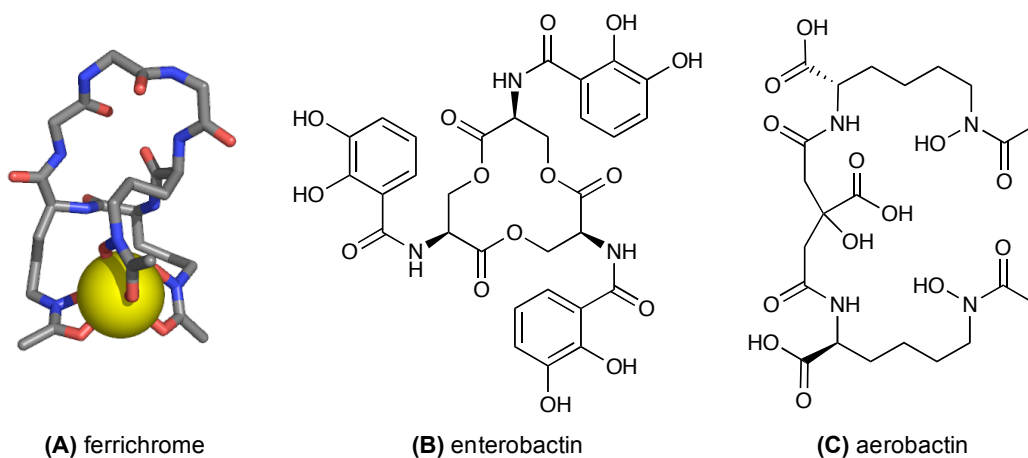


**FIG. 49.** Structures of various siderophores, used by bacteria to complex iron. (A) Ferrichrome is a hexapeptide, comprised of four glycine and three ornithine residues, whose side chains chelate iron (shown in yellow). (B) Structure of enterobactin. (C) Structure of aerobactin.

Upon chelation with iron, these siderophore complexes are then actively transported into cells, after which the siderophore is degraded to release the iron. Three main iron uptake systems have been reported: (1) FhuA, which recognizes hydroxamate siderophores such as ferrichrome; (2) FepA, Cir and Fiu which recognize catecholate siderophores such as enterobactin; and (3) FecA which recognizes hydroxycarboxylates, such as citrate (260). These OM recognition proteins are coupled to either the Tol or TonB energy transducing systems, which are anchored in the inner membrane (260). Although these systems are essential for iron-uptake, they are also the "Achilles' heel" of many Gram-negative bacteria, as will be described shortly.

The bacteriocins produced by Gram-negative bacteria are a heterogeneous group of peptides and proteins and include the microcins and colicins made by

enterobacteria. The mode of action of these bacteriocins is broad, including pore formation, inhibition of cell wall biosynthesis, inhibition of protein synthesis and degradation of DNA and RNA (192). In order for the microcins or colicins to kill their targets, they must first traverse the OM. It is well documented that these bacteriocins are actively translocated across the OM, using the same transport machinery intended to bring in iron-siderophore complexes (192). Although the details of bacteriocin translocation across the OM is not fully understood, there are three main steps involved: (1) binding to a specific OM receptor; (2) translocation via the Tol or TonB pathways; and (3) exertion of cytotoxicity, either directly on the inner membrane (pore formation) or in the cytoplasm (for nuclease-type colicins) (192).

The microcins (Mcc) are particularly interesting in this regard. Unlike the large colicins, the microcins are small (<10 kDa), hydrophobic peptides that display a broad range of post-translational modifications (265), such as simple disulfide formation (ColV and MccL) (219, 266, 267), cyclization (MccJ25) (268-270), modification of the peptide backbone to include thiazole and oxazole rings (MccB17) (271, 272), and covalent attachment of siderophore-mimicking moieties (MccE492m) (273). Currently, fourteen different microcins have been reported, seven of which have been structurally characterized (265). In some cases, only the primary amino acid sequence is known (ColV), and in other cases, extensive structural studies have revealed the 3D structure of the microcin (as for MccJ25) (268, 269). The microcins are subdivided into two subclasses. Class I contains the small (< 3.5 kDa), highly modified microcins and class II contains

the larger (60-90 aa) microcins, which are further divided into the unmodified and modified types (265). Table 9 lists the seven microcins that have been structurally characterized.

**TABLE 9.** The microcins produced by enterobacteria: their modifications, recognition and import into target cells, and mode of action.

<b>Microcin</b>	<b>Posttranslational Modification</b>	<b>OM receptor; Import</b>	<b>Cytotoxicity</b>
<b><i>Class I</i></b>			
MccB17	43 aa; Backbone modified to include 4 thiazole and 4 oxazole rings (271, 272)	OmpF; SbmA (274)	Inhibits DNA gyrase (275)
MccC7/C51	7 aa; N-formylated, covalently linked to AMP via phosphoramidate bond (276, 277)	unknown	Inhibits tRNA <sup>Asp</sup> synthetase (278, 279)
MccJ25	21 aa; cyclization between G1 and E8 carboxylate, lasso structure (268-270)	FhuA; Ton-ExbBD, SbmA (273)	Inhibits RNA polymerase (280, 281)
<b><i>Class II</i></b>			
ColV (MccV)	88 aa; disulfide loop (76-87) (219, 266)	Cir; Ton-ExbBD, SdaC (282)	Pore formation (283)
MccL	90 aa; 2 disulfide loops (29-33) and (78-89) (267)	Unknown, but likely the same as ColV (265)	Likely pore formation
MccE492m	84 aa; linear trimer of DHBS* linked to C-terminus via $\beta$ -D-glucose (273)	FepA, Cir and Fiu; Ton-ExbBD (273)	Pore formation (requires the manYZ proteins of the man-PTS) (284)
MccM	77 aa; proposed to have similar modification as MccE492m (265)	FepA, Cir and Fiu; Ton-ExbBD (265)	unknown

\* DHBS: N-(2,3-dihydroxybenzoyl)-L-serine

It is well documented that resistance to microcin activity is correlated to mutations in the FhuA or FepA/Cir/Fiu proteins, and the TonB system, suggesting that the microcins utilize the iron-uptake machinery of their target cells (265). In addition, microcin production is up-regulated in response to iron-deficient conditions. Furthermore, it has been shown that while several of the class II

microcins (such as MccE492m and MccM) are active in their unmodified form (ie: lacking their covalently attached siderophore mimic), their activity is dramatically enhanced when the peptide has been modified, suggesting that these modifications provide increased affinity with their OM receptors (265). Thus, the microcins utilize molecular-mimicry to trick target cells into actively transporting them across the OM.

#### 5.1.4. Objectives

As described in the previous section, it is the siderophore-mimicking moieties of the microcins that are recognized by receptor proteins in the OM, providing them access to target cells. Once inside, the microcin is able to exert its lethal effect. If LAB bacteriocins were engineered (either chemically or genetically) to incorporate siderophore mimics, would the same “Trojan Horse” approach transport them across the OM? Before such endeavors are undertaken, it is necessary to evaluate the activity of a variety of LAB bacteriocins against typical Gram-negative pathogens. The project herein described is the “proof of concept” for the development of modified LAB bacteriocins. Using EDTA as the means to bypass the OM, six different bacteriocins, were investigated for their killing effect against *E. coli* DH5 $\alpha$ , *P. aeruginosa* ATCC 14207 and *S. typhimurium* ATCC 23564. The bacteriocins were selected from a variety of classes (lantibiotics, type IIa, type IIb, circular). The testing strategy and killing effects of these bacteriocins is reported.

## 5.2. Results & Discussion

### 5.2.1. Bacteriocins used in this study

Three different lantibiotics were investigated: nisin, gallidermin and lactacin 3147. Nisin is the most well characterized LAB bacteriocin. Its potent activity arises from its dual mode of action. Firstly, it binds to lipid II, the precursor to peptidoglycan and inhibits cell wall biosynthesis. Secondly, it forms pores in the cytoplasmic membrane. As already mentioned, many reports have shown that nisin is active against *E. coli*, *Salmonella* and *Pseudomonas* when used in combination with EDTA. As such, nisin would serve as a “control” bacteriocin for our testing.

Gallidermin is another member of the lantibiotics. Although its N-terminus is structurally similar to nisin, gallidermin’s amino acid sequence is significantly shorter than that of nisin. Comparison of the NMR solution structures shows that gallidermin is only 30 Å in length (285), compared to 50 Å for nisin (53). Mode of action studies have revealed that gallidermin can act as a pore former, but not to the same extent as nisin – a fact that can be understood in light of the differences in length (53). However, it has also been shown that gallidermin binds more strongly than nisin to lipid II and that it also binds to lipid I (the precursor to Lipid II), which inhibits the synthesis of lipid II (53). It has been shown that both nisin and gallidermin exhibit very little cytotoxic effect on erythrocytes and intestinal epithelial cells (107), a key feature if these bacteriocins are to be developed into therapeutic agents. Both nisin and gallidermin are

commercially available, and were obtained as such. Nisin required further purification by RP-HPLC prior to use.

Lacticin 3147 is a two-component lantibiotic, comprised of the LtnA1 and LtnA2 peptides (17, 18). The two peptides act synergistically to exert their effect. Like nisin and gallidermin, lacticin 3147 has a dual mode of action: LtnA1 binds to lipid II, after which LtnA2 docks onto LtnA1 and the complex inserts into the membrane, resulting in inhibition of cell wall biosynthesis as well as pore formation (72, 73). Following a procedure developed in our laboratory by Dr. Nathaniel Martin and modified by Lara Silkin, LtnA1 and LtnA2 were isolated from the producer organism (17). However, significant oxidation, which diminishes antimicrobial activity, plagued the purification. It was discovered that oxidation of the peptides occurred when they were partially concentrated, following HPLC purification. To circumvent this problem, the purified peptides were concentrated to dryness by rotary evaporation, then redissolved in acidic water (0.1% TFA) prior to freezing and lyophilizing. Periodically, the stock solutions of LtnA1 and LtnA2 were examined by MALDI-TOF to determine if oxidation was occurring, but none was detected.

Piscicolin 126 is a type IIa bacteriocin. It has a narrow spectrum of activity and is highly active against *L. monocytogenes*, but displays no activity toward Gram-negative cells (24, 25). The efficacy of the type IIa bacteriocins against Gram-negative bacteria is unclear. In 1992, Kalchayanand *et al.* reported that pediocin PA-1/AcH inhibited the growth of *E. coli* following sublethal stresses (248). It was also reported that the activities of sakacin P and curvacin A

toward *Salmonella* and *E. coli* could be enhanced by a combination of pH and NaCl treatment, or with EDTA (250). However, in 1999 it was reported by Gao *et al.* that pediocin PA-1 in combination with EDTA had no significant effect on *E. coli* or *Salmonella* spp. (241). Since we had an expression system for PisA, we decided to study this type IIa bacteriocin. The expression and purification of PisA has already been described in chapter 3.

Carnocyclin A (CclA) is a member of the circular bacteriocins. Many of the features of CclA, including its spectrum of activity, stability, ion-channel properties and three-dimensional structure, have been described in chapter 2. Interestingly, another member of this family of bacteriocins, namely enterocin AS-48, is known to be active against certain Gram-negative bacteria. When used in combination with EDTA or other OM destabilizing factors, the activity of AS-48 is enhanced and can be extended to other Gram-negative bacteria. Similarly, it has been shown that gassericin A, another circular bacteriocin, is active against Gram-negative food-spoilage bacteria in the presence of glycine, which is known to inhibit cell wall biosynthesis.

Lastly, we examined a member of the type IId (leaderless) bacteriocins. Enterocin 710C is a two-peptide bacteriocin, comprised of Ent7A and Ent7B. Both peptides are active on their own, but display enhanced activity when used together. Ent7A and Ent7B are N-formylated and have a broad spectrum of activity, including activity against some strains of *E. coli* as well as *Brevundimonas diminuta*, an opportunistic Gram-negative bacterium that infects

immuno-suppressed hosts (manuscript in submission). The Ent7A and Ent7B peptides, purified by Xiaoji Liu, were tested as a mixture.

### 5.2.2. Testing strategy

Initially, a well-plate assay was designed to allow the facile testing of bacteriocins against the target strains by monitoring bacterial growth spectrophotometrically. The bacterial cultures were mixed with bacteriocin solutions (of varying concentrations) in the absence and presence of EDTA (10 mM final concentration). Initially, the bacteriocins nisin and subtilisin A (not described above) were tested against *E. coli* DH5 $\alpha$  and *P. aeruginosa* ATCC 14207. The plates were incubated overnight and the OD<sub>600</sub> recorded. However, results indicated that EDTA was lethal to the cell cultures: the addition of 10 mM EDTA to the cells, even in the absence of bacteriocin, inhibited cell growth.

An alternate testing strategy, based on the method described by Stevens (243), was developed wherein cells were treated with a testing solution (consisting of bacteriocin with or without EDTA) for 60 min, after which the testing solution was removed. To do so, the cells were harvested by centrifugation, and the supernatant (i.e.: the testing solution) was discarded. The cells were resuspended, serially diluted and plated out. Following incubation, colony-forming units (cfu) were enumerated and the effect of the testing solution determined. Preliminary experiments were conducted to determine if a 20 mM EDTA treatment for 60 min would be deleterious to the test organisms. The cfu of the cells treated with EDTA were compared to the cfu of the cells treated with

only cell buffer and the log reduction factor (LRF) for the effect of EDTA was determined. The results indicated that EDTA did not significantly inhibit bacterial growth (LRF < 1).

### 5.2.3. Testing results

Each of the bacteriocins was tested against *E. coli* DH5 $\alpha$ , *Pseudomonas aeruginosa* ATCC 14207 and *Salmonella typhimurium* ATCC 23564. The results are illustrated in Figure 50 and reveal that in the absence of EDTA (grey bars), none of the bacteriocins were capable of inhibiting bacterial growth (<1 LRF). Similarly, EDTA treatment had little effect on bacterial growth, with LRF generally less than one (left-most blue bar for each bacteriocin). However, in the presence of 20 mM EDTA, most of the bacteriocins exerted killing effects against at least one of the Gram-negative strains. In general, bacteriocin activity was strain dependent, and greater activity was observed at higher bacteriocin concentrations. As seen in Fig. 50, there is variation in the initial number of cfu across the various experiments. This is simply a reflection that experiments were performed on a different days, utilizing cell cultures with slightly different initial cell densities. Cells were generally harvested when the OD<sub>600</sub> of the cell culture was ~0.1, but this ranged from 0.08 – 0.13. Each experiment (testing one bacteriocin against one organism) typically required the preparation and plating of 80 samples: 10 bacteriocin testing solutions (5 with EDTA, 5 without)  $\times$  four dilutions per test  $\times$  2 (for testing in duplicate). As such, it was impractical to perform more than one experiment per day.

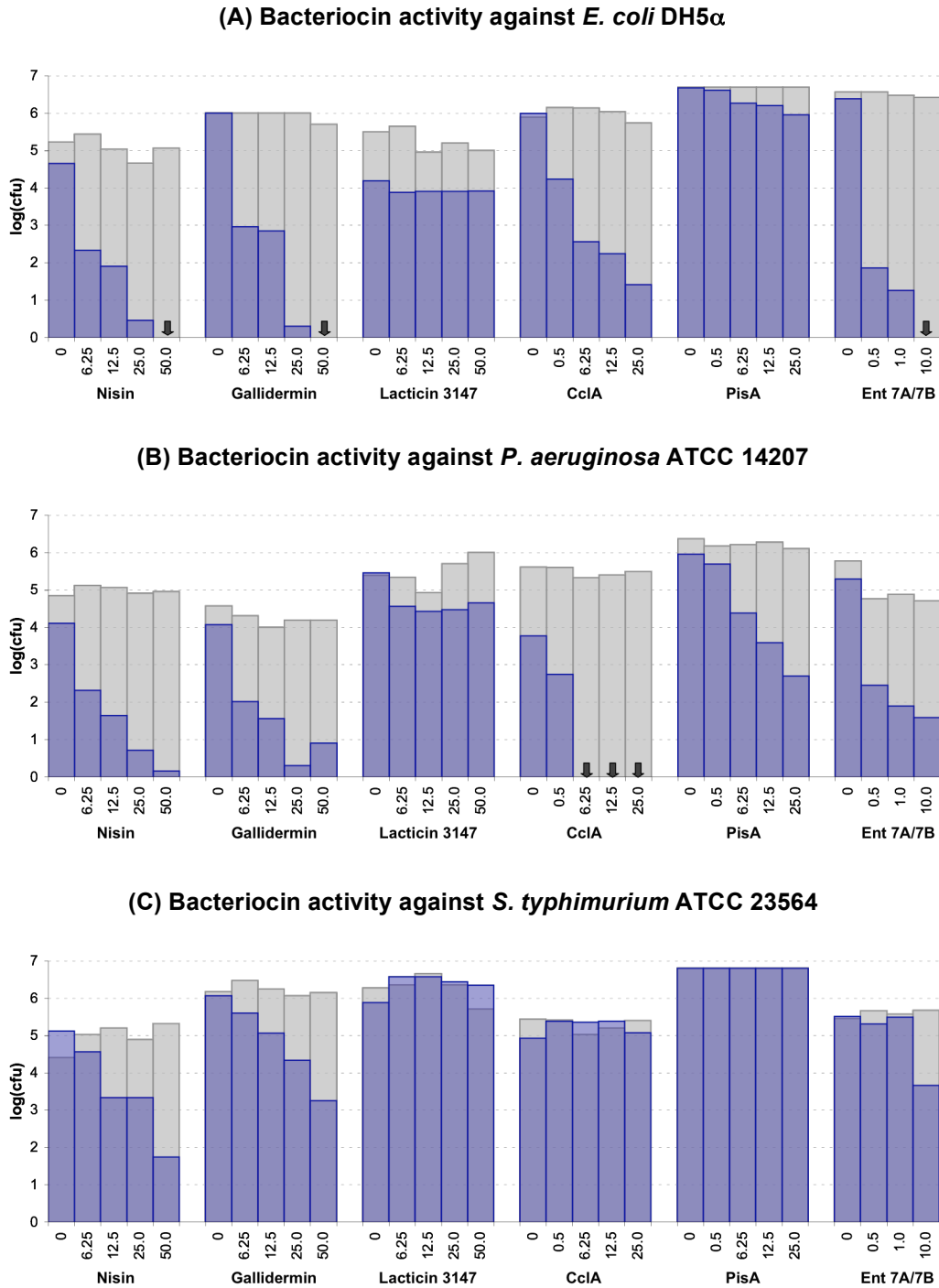


**FIG. 50.** The effect of LAB bacteriocins on the growth of Gram-negative bacteria in the absence and presence of 20 mM EDTA. The vertical axis indicates the log(cfu) after treatment of the bacteria for 1 h with bacteriocin in the absence (grey bars) or presence (blue bars) of 20 mM EDTA. The six different bacteriocins that were tested are listed along the horizontal axis, along with their respective concentrations (in  $\mu\text{M}$ ). (A) Results with *E. coli* DH5 $\alpha$ . (B) Results with *P. aeruginosa* ATCC 14207. (C) Results with *S. typhimurium* ATCC 23564. Black arrows indicate that no cfu were observed, at any of the dilutions.

For *E. coli* DH5 $\alpha$  (Fig. 50A), in the presence of EDTA, enterocins 7A/7B had the greatest effect, followed by nisin, gallidermin and CclA. Neither lacticin 3147 nor PisA had a significant effect on reduction of cfu (LRF < 1). Our results with nisin are in agreement with previous findings. PisA is a type IIa bacteriocin and as mentioned above, literature reports on the activity of different type IIa bacteriocins (in combination with OM destabilization treatments) are varied. Our findings support those of Gao and co-workers (241), who saw no significant effect of pediocin PA-1 against *E. coli* under similar testing conditions.

In the case of *P. aeruginosa* ATCC 14207 (Fig. 50B), in the presence of EDTA, CclA exhibited the most dramatic effect, with complete inhibition at the concentrations listed. Enterocins 7A/7B, nisin and gallidermin exhibited similar effects, followed by PisA. Lacticin 3147 was the least effective at inhibiting growth.

The results of testing against *S. typhimurium* ATCC 23564 are displayed in Fig. 50C. Again, EDTA had little effect on bacterial growth. Although enterocins 7A/7B, nisin and gallidermin did reduce bacterial growth, it was marginal compared to the effects on *E. coli* and *Pseudomonas*. Lacticin 3147, CclA and PisA had no effect on bacterial growth.

In general, PisA displayed little activity toward the Gram-negative pathogens. This may result from the necessity for a species-specific, membrane bound receptor for the type IIa bacteriocins. As discussed earlier in this chapter, it has been shown that the activity of the type IIa bacteriocins is receptor mediated: differences in the EII<sub>t</sub><sup>man</sup> permeases of Gram-negative bacteria, compared to those

of Gram-positive bacteria, may account for the ineffectiveness of the type IIa bacteriocins against Gram-negative pathogens, even in the presence of EDTA.

In contrast to the type IIa bacteriocins, the lantibiotics nisin and gallidermin are known to be broad-spectrum antimicrobial agents. They elicit their activity through a dual mode of action: upon binding to lipid II, they inhibit cell wall biosynthesis and cause pore formation. As mentioned previously, although gallidermin cannot always form pores in the cytoplasmic membrane, its antimicrobial activity is just as potent as that of nisin (53). Recently, it has been revealed that upon binding to lipid II, several lantibiotics are able to sequester lipid II from the septal site of actively dividing cells, thus impeding cell division (74). It has been suggested that the extreme antimicrobial activity of gallidermin may be explained by this sequestration mechanism. Our results reveal that both nisin and gallidermin were lethal to Gram-negative bacteria, in the presence of EDTA, and displayed similar levels of activity.

Surprisingly, lacticin 3147 did not display the same trend as nisin and gallidermin. In fact, even though lacticin 3147 is proposed to have a similar mode of action to that of nisin and gallidermin, it exhibited the weakest activity of the six bacteriocins tested. As described in chapter one, the LtnA1 peptide of lacticin 3147 is known to bind to lipid II, after which the LtnA2 peptide docks onto the complex and pore formation ensues (72). Structurally, the LtnA1 peptide fits within the family of “type B lantibiotics” and as such, it has been suggested that the binding of LtnA1 to lipid II is more akin to that of mersacidin with lipid II (48), compared to nisin with lipid II. The binding of mersacidin to lipid II

involves the terminal GlcNAc sugar of lipid II, in addition to the MurNAc and pyrophosphate moieties, and the binding between mersacidin and lipid II is strongly enhanced by the presence of calcium ions (286). Recently, it was demonstrated that the presence of  $\text{Ca}^{2+}$  was crucial for the binding of LtnA1 with lipid II, and for the antimicrobial activity of lacticin 3147, whereas the interaction of nisin with lipid II (and its subsequent antimicrobial activity) was unaffected (286). In the same study, it was also shown that in the absence of  $\text{Ca}^{2+}$ , the interaction between the LtnA1 and LtnA2 peptides was disrupted. Since EDTA chelates calcium ions, it is likely that the experimental conditions used in this study “inactivated” lacticin 3147. By effectively removing calcium ions from solution, the complexation of LtnA1 and lipid II was obstructed, as was the interaction between LtnA1 and LtnA2. As such, only minimal antimicrobial activity was observed. However, this does not mean that lacticin 3147 is ineffective against Gram-negative pathogens. Indeed, if an alternate OM destabilizing strategy was employed (such as heat-shock, or pH treatment), it is likely that a killing effect would be observed.

In summary, the different bacteriocins exhibited different levels of activity against the three bacterial strains that were tested. In addition, the effect of a particular bacteriocin was not uniform across the three bacteria. This is in agreement with literature reports, as is our finding that *Salmonella* is the least affected by the combined treatment of bacteriocin and EDTA.

### 5.3. Conclusions & Future Directions

This work has revealed that in general, LAB bacteriocins are effective antimicrobial agents against Gram-negative pathogens, in so far as they can access the cytoplasmic membrane. Current work in our laboratory is aimed at chemically linking siderophore mimics, such as agrobactin (a catechol-spermidine siderophore) and pyochelin (a siderophore produced by various strains of *P. aeruginosa*) onto the lantibiotic gallidermin (graduate work of Sabesan Yoganathan). Similarly, genetic modification of the enterocins 7A and 7B structural genes to incorporate a C-terminal ColV domain is also underway (graduate work of Xiaoji Liu, supervisor Dr. Lynn McMullen, Department of Agricultural Food and Nutritional Science, University of Alberta). Upon completion, these modified bacteriocins will be evaluated for their ability to gain entry into, and ultimately kill Gram-negative pathogens. If successful, application of this methodology will allow for the engineering of a vast arsenal of antimicrobial peptides to combat Gram-negative bacterial infections.

## Chapter 6. Experimental Procedures

### 6.1. General methods for protein production and purification

#### 6.1.1. Plasmids, bacterial strains and culture conditions

The various plasmids and bacterial strains utilized in this study are listed in subsequent sections, in Tables 10, 11 and 12. All biological experiments were performed under sterile conditions. Materials and solutions were either autoclaved (121°C, 15 min) or filter sterilized (0.22 µm) prior to use. Cultures were incubated with an Innova 4330 Refrigerated incubator shaker. Unless otherwise stated, *E. coli* strains were propagated in Luria-Bertani (LB) broth (Difco) and grown at 37°C, with shaking (200–250 rpm). Unless otherwise stated, *Carnobacterium* spp. were propagated in All Purpose Tween (APT) broth (Difco) and incubated at 25°C, without aeration. When required, growth media contained the appropriate antibiotic(s): ampicillin (100–200 µg/mL), erythromycin (200 µg/mL) and kanamycin (25 µg/mL) for *E. coli*. For *Carnobacterium* spp., erythromycin (5 µg/mL) was used as a selection marker. Solid agar plates were prepared by the addition of 1.5 % granulated agar (w/v) (Difco) to the broth media. Bacteria were maintained as frozen stock cultures at -80°C, and stored in either LB broth (for *E. coli*) supplemented with 20% glycerol, or APT broth (for *Carnobacterium* spp.) supplemented with 20% glycerol. Unless otherwise stated, percentage concentration implies v/v.

### **6.1.2. Centrifugation**

Unless otherwise stated, solutions were centrifuged with either a Beckman J2-21 or a Sorvall RC-5B Refrigerated SuperSpeed centrifuge. For small volumes (samples with < 1.5 mL), solutions were centrifuged with an Eppendorf 5415D centrifuge (at RT), or a Galaxy 16DH (VWR) centrifuge (at 4°C).

### **6.1.3. General approach for the expression of recombinant proteins**

Recombinant proteins were expressed in various *E. coli* host strains, grown in either LB (Difco) or 2 × YT (Difco) broth with the required antibiotics. Overnight starter cultures were prepared in 5 mL of media and incubated at 37°C for 16–18 h. Flasks containing 500 mL of prewarmed media (in 2 L flasks) were inoculated (1%) with the starter cultures and incubated until the OD<sub>600</sub> was ~0.5 (unless otherwise stated). Protein expression was induced by the addition of IPTG, at an appropriate concentration (expression dependent; details to follow). Following induction, cultures were further incubated at the appropriate temperatures and lengths of time as required for protein expression. Cells were harvested by centrifugation (11,300 × g, 15-20 min, 4°C) and pellets were stored at -80°C until further use, unless stated otherwise.

### **6.1.4. Cell lysis**

#### **6.1.4.a. Freeze thaw & sonication**

After harvesting the cells, cell pellets were resuspended in an appropriate resuspension buffer (~50 mL), transferred into 50 mL centrifuge bottles and

stored at  $-20^{\circ}\text{C}$ . Prior to lysis, tubes were chilled at  $-80^{\circ}\text{C}$  for 1 h. A small amount of lysozyme ( $\sim 10$  mg) was added to each tube and the tubes were then placed in an ice-water bath. After completely thawing ( $\sim 60$  min), the solution was subjected to two more cycles of freeze-thaw as follows: the solution was rapidly frozen by placing the tubes in a  $-78^{\circ}\text{C}$  EtOH-dry ice bath for  $\sim 20$  min and then thawed by placement in an ice-water bath for  $\sim 60$  min. Cells were lysed by 3 rounds of sonication, using a Branson Sonifier 450 (20 pulses; Duty Cycle: 80%; Output control: 6 for 3 pulses, then 8 for 17 pulses) using a prechilled medium tip. Between each round, the samples and the sonicator tip were placed in an ice-water bath for 1 min. Following sonication, the suspension was centrifuged ( $27,200 \times g$ , 30 min,  $4^{\circ}\text{C}$ ) to prepare the cleared lysate.

#### **6.1.4.b. Cell disrupter**

Cells were resuspended in an appropriate buffer ( $\sim 10$  mL/gram wet weight, unless otherwise stated). Cells were lysed with a Constant Systems Cell Disrupter, model TS (Constant Systems, Ltd.) operating at 20 kpsi. Following lysis, the suspension was centrifuged ( $27,200 \times g$ , 30 min,  $4^{\circ}\text{C}$ ) to prepare the cleared lysate.

#### **6.1.5. Spot-on-lawn activity assays**

Spot-on-lawn assays (183) were performed to monitor bacteriocin activity and guide the development of purification strategies. For growth media, either APT or LB broth was used, depending on the indicator organism. When

necessary, antibiotics were added to the growth media. For testing, 10 mL of sterile, soft agar (0.75% w/v agar) containing the appropriate growth media was heated in boiling water, until molten. After cooling to touch, the soft agar was inoculated with an overnight culture of an indicator organism (1%) and overlaid on a bed of solid agar (1.5% w/v agar). Solutions to be tested, including appropriate controls, were spotted (10  $\mu$ L) onto the agar and allowed to air dry. Plates were incubated overnight at the appropriate temperatures and examined for halos of growth inhibition.

### **6.1.6. Protein purification**

#### **6.1.6.a. Amylose XAD-16**

Amberlite XAD-16 resin (Aldrich) was used to remove hydrophobic components from culture supernatant. Typically, 60–100 g of resin was used per purification. Prior to use, the resin was prewashed in 100 mL of IPA (1 h, 4°C). The slurry was then transferred to a 2.5  $\times$  50 cm column and rinsed with 1 L of H<sub>2</sub>O at a flow rate of 5 mL/min using a peristaltic pump (Econo Pump, Bio-Rad). After loading the supernatant, the column was washed with 500 mL of 30% ethanol. Peptides were eluted from the column by washing with increasing concentrations of IPA (500 mL per wash). The final elution was with 500 mL of 70% IPA pH 2. All purification steps were performed at 4°C and spot-on-lawn activity assays were performed on all fractions to monitor the elution of bacteriocins.

#### **6.1.6.b. Megabond C<sub>18</sub> solid-phase extraction**

Megabond C<sub>18</sub> solid phase extraction cartridges (Varian) were used for desalting and to further separate hydrophobic components. Prior to use, the cartridges were preconditioned with 50 mL of methanol and 50 mL of H<sub>2</sub>O. After loading the sample, the column was washed consecutively with 50 mL of H<sub>2</sub>O, 30% ethanol and 30% acetonitrile. Peptides were eluted from the column by washing with increasing concentrations of IPA (50–60 mL). The final elution was always with 70% IPA pH 2 (60–100 mL). All purification steps were performed at room temperature and spot-on-lawn activity assays were performed on all fractions to monitor the elution of bacteriocins.

#### **6.1.6.c. RP-HPLC**

The final step of purification for most peptides required RP-HPLC. Both C<sub>8</sub> and C<sub>18</sub> columns (either semi-preparative or preparative scale) were routinely used. The specific details (column, solvents and method) for the different purifications that were performed will be provided in subsequent sections. HPLC was performed on Beckman System Gold machines (analytical or preparative), equipped with 32karat software, or on Varian Prostar Model 210 machines (analytical or preparative).

#### **6.1.6.d. Cation exchange chromatography**

SP-Sepharose (Pharmacia) was used for cation exchange chromatography. 20 mL of slurry (50% suspension in 20% EtOH) was transferred to a 2.5 × 50 cm

column and packed at a flow rate of 2 mL/min. The column was run at a flow rate of 1 mL/min for all other purposes. Prior to each use, the column was regenerated with 1 M NaCl for 30 min and then equilibrated with an appropriate running buffer, until both the  $UV_{280}$  and conductivity traces stabilized. After sample loading, the column was washed with running buffer until the  $UV_{280}$  had stabilized. Elution of protein(s) was achieved by washing the column with elution buffer (500 mM NaCl in running buffer) and monitoring the  $UV_{280}$ . Column elution was deemed complete after the conductivity increased and stabilized. Purification was performed at 4°C.

#### **6.1.6.e. Size exclusion chromatography**

A 100 mL Sephadex G50 Fine (Pharmacia) column was used for size-exclusion chromatography. Resin (~9 g) was swollen in an appropriate buffer for 3 h at 4°C. The resin was transferred to a column (1.6 × 50 cm) and packed at a flow rate of 2 mL/min. For purification of proteins, the column was operated at 0.2 mL/min, corresponding to ~525 min total run time. Prior to use, the resin was equilibrated with the desired running buffer. Typically, 2-4 mL of sample was loaded (2-4% column volume). 20 min fractions were collected and the  $UV_{280}$  was monitored. Purification was performed at 4°C.

#### **6.1.6.f. Amylose affinity chromatography**

Amylose resin (New England Biolabs) was used for the purification of maltose binding protein fusions. 50 mL of resin (in 20% EtOH) was transferred to

a 2.5 × 50 cm column and packed at a flow rate of 2 mL/min. The column was run at a flow rate of 1 mL/min for all other purposes. The column was washed with 250 mL of column buffer (20 mM Tris-Cl pH 7.4, 200 mM NaCl, 1 mM EDTA, 1 mM NaN<sub>3</sub>, 1 mM DTT) prior to use. After loading cell-free extract (diluted to 300 mL in column buffer), the column was washed with 700-800 mL of column buffer. Elution of the fusion protein was achieved by washing the column with elution buffer (10 mM maltose in column buffer) and monitoring the UV<sub>280</sub>. 5 mL fractions were collected using an automatic fraction collector. Immediately following usage, the column was regenerated by washing with 150 mL H<sub>2</sub>O, 150 mL 0.1 % (w/v) SDS, 50 mL H<sub>2</sub>O and 250 mL of column buffer. Purification was performed at 4°C. Amylose columns were typically reused 8 times before discarding the resin.

#### **6.1.6.g. Ni-NTA affinity chromatography**

Ni-NTA Superflow resin (Qiagen) was used for the purification of His<sub>6</sub>-tagged fusion proteins. Typically, 1 mL of slurry (50% suspension in 30% EtOH) was used for every 4-6 mL of cell free lysate. His<sub>6</sub>-tagged proteins were purified under native or denaturing conditions. The specific details (buffer compositions and column methods) will be described in subsequent sections.

#### **6.1.7. Factor Xa digestion**

Factor Xa (purchased from New England Biolabs, PROzyme or Pierce) was used to cleave fusion proteins bearing a Factor Xa cleavage site (IEGR).

Fusion proteins were either dialyzed against Factor Xa buffer (20 mM Tris-Cl pH 7.4–8.0, 100 mM NaCl, 2 mM CaCl<sub>2</sub>), or redissolved in this buffer, to a concentration of ~ 1–2 mg/mL. Pilot studies were performed to determine the optimal amount of Factor Xa, temperature and duration required for digestion of fusion proteins. When necessary, AEBSF (final conc. 0.1 mM) was added to the digestion mixture to inhibit Factor Xa and halt the cleavage reaction. The specific details for each digestion will be described in subsequent sections.

### **6.1.8. Protein electrophoresis**

#### **6.1.8.a. SDS-PAGE**

Proteins were resolved with 10%, 12% or 15% (w/v) acrylamide SDS-PAGE gels, with 4% stacking gels. Protein samples were mixed with either 2 × Laemmli Sample Buffer (Bio-Rad) or 6 × sample buffer [0.42 M Tris-Cl pH 6.8, 30% (v/v) glycerol, 10% (w/v) SDS, 0.6 M DTT, 0.2 mg bromophenol blue], and then heated to 100°C for 3–5 min. Electrophoresis was done at a constant voltage of 50 V for approximately 30 min, until the bands had compressed, and then at 150–200 V until the dye front neared the bottom of the gel. Gels were visualized with either coomassie stain (0.1% w/v coomassie R-250, 40% EtOH, 10% acetic acid), followed by destaining (10% EtOH, 7.5% acetic acid) or with either Bio-Safe Coomassie stain (Bio-Rad) or GelCode Blue stain (Pierce), and destained with water. Protein standards (Bio-Rad) were run to allow for molecular weight determination of proteins.

#### **6.1.8.b. Tris-Tricine SDS-PAGE**

Small peptides (< 10 kDa) were resolved on either 16.5% or 20% (w/v) acrylamide Tris-Tricine gels (287), with 4% stacking gels. Samples were mixed with either 2 × Tris-Tricine Sample Buffer (Bio-Rad) or 6 × sample buffer, and then heated to 100°C for 3–5 min unless otherwise stated. Electrophoresis was done at a constant voltage of 50 V for approximately 30 min, until the bands had compressed, and then at 150 V for 2-3 hours, until the dye front neared the bottom of the gel. Visualization of the gels was the same as for SDS-PAGE gels. Polypeptide SDS-PAGE standards (Bio-Rad) were run to allow for molecular weight determination of peptides.

#### **6.1.8.c. Western blots**

After running SDS-PAGE or Tris-Tricine gels, the proteins were electrophoretically transferred (100 V, 1 h) to a 0.22 µm nitrocellulose membrane (Bio-Rad) in transfer buffer (25 mM Tris, 192 mM glycine, 20% MeOH). Ponceau S stain (0.5% Ponceau S (Sigma) in 1% acetic acid) was used to visualize the transferred proteins. The membrane was blocked for 1 h in TBS-T solution (20 mM Tris-Cl, 136 mM NaCl, 0.1% Tween-20) containing 5% (w/v) fat-free milk powder (Carnation). The membrane was then incubated for 1 h with gentle rocking, in a 1:5000 dilution of Anti-His<sub>6</sub>-Peroxidase antibody (400 U/mL, Roche Diagnostics) in TBS-T solution. The membrane was rinsed three times with TBS-T solution, and then in a final rinse of TBS solution (20 mM Tris-Cl, 136 mM NaCl). The membrane was incubated in 1.2 mL of freshly prepared

chemiluminescence detection reagent (SuperSignal West Femto Maximum Sensitivity Substrate; Pierce, Thermo Scientific) for 2 min and then developed (0.5 – 5 min) onto autoradiography film (Kodak).

### **6.1.9. Protein quantification**

#### **6.1.9.a. Spectrophotometric quantification**

Protein concentrations were determined by measuring the  $UV_{280}$ , using a BioMate 3 Spectrophotometer (Thermo Scientific), with a path length of 1 cm. Molar extinction coefficients were calculated using the program ProtParam (151) available on the ExPASy Proteomics Server. Protein concentration was then calculated using Beer's Law:

$$c = \frac{A}{b\epsilon} \quad (\text{eq. 1})$$

where  $c$  is the concentration (mol/L),  $A$  is the UV absorbance at 280 nm,  $b$  is the path length (cm) and  $\epsilon$  is the molar extinction coefficient ( $L \text{ mol}^{-1} \text{ cm}^{-1}$ ).

#### **6.1.9.b. BCA colorimetric analysis**

Protein concentrations were also determined via the bicinchoninic acid (BCA) protein assay, using the BCA Protein Assay Kit, purchased from Pierce (Thermo Scientific). The assay was performed according to the manufacturer's instructions, with bovine serum albumin as a protein standard.

### **6.1.10. Protein characterization**

#### **6.1.10.a. Mass spectrometry**

Peptides were analyzed by matrix-assisted laser desorption ionization time-of-flight (MALDI-TOF) mass spectrometry. Spectra were recorded in positive ion mode, with an acceleration of 20 kV in the presence of a nitrogen laser ( $\lambda = 337$  nm), using a Perspective Biosystems Voyager Elite MALDI-TOF mass spectrometer, operating in reflectron mode with delayed extraction. The two-layer method (288), with either 3,5-dimethoxy-4-hydroxycinnamic acid (sinapinic acid) or  $\alpha$ -cyano-4-hydroxycinnamic acid (HCCA) as the matrix, was used for all samples. Samples were acidified prior to analysis. Samples containing high concentrations of salts were either rinsed with 0.1% TFA ( $2 \times 5$   $\mu$ L) or cleaned with ZipTip pipette tips (ZipTip <sub>$\mu$ -C18</sub>, Millipore) according to the manufacturer's instructions, prior to data acquisition.

#### **6.1.10.b. Circular dichroism**

All circular dichroism (CD) measurements were made on an OLIS DSM 17CD spectrophotometer (Bogart, GA) in a thermally controlled quartz cell with a 0.02 cm pathlength. The instrument calibration was checked against a 1 mg/mL solution of D-10-camphorsulfonic acid. The bandwidth was set at 2.0 nm. Data was collected every 1 nm and are the average of ten scans. Baseline spectra of the appropriate solvent system were subtracted from the sample spectra prior to calculating molar ellipticities. Point-by-point integration was performed as a function of the high voltage readings on the photomultiplier detectors. Results are

expressed in units of molar ellipticity ( $\text{deg cm}^2 \text{dmol}^{-1}$ ) and plotted against the wavelength.

#### **6.1.10.c. NMR**

NMR experiments were acquired on a variety of spectrometers, at three different locations. In the Department of Chemistry (University of Alberta), spectra were recorded on a Varian Inova 600 MHz spectrometer, equipped with a triple-resonance HCN probe, or an a Varian VNMR5 500 MHz spectrometer equipped with a  $^1\text{H}$ - $^{19}\text{F}$  Z-gradient probe capable of  $^{19}\text{F}$  direct detection. At the National High Field Nuclear Magnetic Resonance Centre (NANUC, University of Alberta) spectra were acquired on a Varian 800 MHz spectrometer, equipped with a triple-resonance HCN cold probe, by Dr. Ryan McKay. At the Quebec/Eastern Canada High Field NMR Facility (McGill University) spectra were acquired on Varian Inova 500 MHz and 800 MHz spectrometers equipped with triple-resonance HCN cold probes, by Dr. Tara Sprules.

## **6.2. General methodologies for genetic manipulations**

### **6.2.1. Plasmids, bacterial strains and culture conditions**

The various plasmids and bacterial strains used for genetic manipulations are listed in subsequent sections, in Tables 10, 11 and 12. Bacteria were maintained as frozen stock cultures at  $-80^\circ\text{C}$ , and stored in either LB broth (for *E. coli*) supplemented with 20% glycerol, or APT broth (for *Carnobacterium spp.*) supplemented with 20% glycerol. Prior to use, *E. coli* strains were subcultured in

5 mL of LB broth and incubated 37°C, 250 rpm, whereas *Carnobacterium spp.* were subcultured in 10 mL of APT broth and incubated at 25°C, without aeration, unless otherwise stated. When required, growth media contained the appropriate antibiotic(s) as follows. For *E. coli*, ampicillin (100–200 µg/mL), erythromycin (200 µg/mL) and kanamycin (25 µg/mL) were used as selection markers. For *Carnobacterium spp.*, erythromycin (5 µg/mL) was used as a selection marker. Solid agar plates were prepared by the addition of 1.5 % granulated agar (w/v) to the broth media. Unless otherwise stated, percentage concentration implies v/v.

### 6.2.2. Reagents and stock solutions

All genetic manipulations and biological experiments were performed under sterile conditions. All materials were autoclaved (121°C, 15 min) prior to use and all solutions were either autoclaved or filter sterilized (22 µm filter), unless otherwise stated. Ampicillin (Aldrich), kanamycin (Invitrogen) and erythromycin (Sigma) were used as antibiotic selection markers. Stock solutions of ampicillin (50 mg/mL) and kanamycin (10 mg/mL) were prepared by dissolving the antibiotic in H<sub>2</sub>O, followed by filter sterilization. Erythromycin (50 mg/mL) stock solutions were prepared by dissolving the antibiotic in 95% EtOH. Ampicillin stocks were stored at -80°C, whereas kanamycin and erythromycin stocks were stored at 4°C.

Restriction enzymes *Bam*HI, *Bgl*III, *Cla*I, *Dpn*I, *Eco*RI, *Hind*III, *Nco*I, *Pst*I and *Sac*I were purchased from Invitrogen, whereas *Bsp*HI was purchased from New England Biolabs. Restriction enzyme digests were performed according to

the manufacturers' instructions. All ligations were done with T4 DNA ligase (Invitrogen), according to the manufacturer's instructions. dATP, dCTP, dGTP and dTTP stocks were purchased from Invitrogen.

Oligonucleotide primers were ordered from Integrated DNA Technologies and were purified by either standard desalting, or PAGE purification by the manufacturer. Primers were resuspended in water (100 – 200  $\mu\text{L}$ ). After determining concentration of the DNA, 10  $\mu\text{M}$  dilutions were prepared. All primer solutions were stored at  $-20^{\circ}\text{C}$ .

### 6.2.3. Polymerase chain reaction (PCR)

DNA amplification by PCR was performed with either an Eppendorf Mastercycler Gradient or a Techgene PCR machine. In general, reaction volumes of 50  $\mu\text{L}$  were prepared. Unless otherwise stated, the concentration of primers was 10  $\mu\text{M}$ , and the dNTP mixture consisted of all four nucleotide bases at a concentration of 10 mM each. Unless otherwise stated, the amount of template used was between 10 and 50 ng. A variety of different polymerase enzymes were used and the specific PCR reaction and cycling conditions are listed below.

**Taq (Invitrogen):** PCR reaction (50  $\mu\text{L}$ ): 5  $\mu\text{L}$  of 10  $\times$  PCR buffer, 1  $\mu\text{L}$  of dNTP mix, 1.5  $\mu\text{L}$  of 50 mM  $\text{MgCl}_2$ , 1  $\mu\text{L}$  of Primer A, 1  $\mu\text{L}$  of Primer B, 1  $\mu\text{L}$  template DNA, 0.2  $\mu\text{L}$  *Taq* (1 U), 39.3  $\mu\text{L}$   $\text{H}_2\text{O}$ . Cycling conditions: (1)  $94^{\circ}\text{C}$  for 3 min; (2) 30 cycles of  $94^{\circ}\text{C}$  for 45 s,  $55^{\circ}\text{C}$  for 30 s,  $72^{\circ}\text{C}$  for 90 s; (3) final extension  $72^{\circ}\text{C}$  for 10 min; (4) hold  $4^{\circ}\text{C}$ .

**Platinum<sup>®</sup> Taq (Invitrogen):** PCR reaction (50  $\mu$ L): 5  $\mu$ L of 10  $\times$  PCR buffer, 1  $\mu$ L of dNTP mix, 1.5  $\mu$ L of 50 mM MgCl<sub>2</sub>, 1  $\mu$ L of Primer A, 1  $\mu$ L of Primer B, 1  $\mu$ L template DNA, 0.2  $\mu$ L Platinum<sup>®</sup> Taq (1 U), 39.3  $\mu$ L H<sub>2</sub>O. Cycling conditions: (1) 94°C for 30 s; (2) 30 cycles of 94°C for 45 s, 55°C for 30 s, 72°C for 60 s per kb of PCR product; (3) final extension 72°C for 10 min; (4) hold 4°C.

**Platinum<sup>®</sup> Taq High Fidelity (Invitrogen):** PCR reaction (50  $\mu$ L): 5  $\mu$ L of 10  $\times$  PCR buffer, 1  $\mu$ L of dNTP mix, 2  $\mu$ L of 50 mM MgSO<sub>4</sub>, 1  $\mu$ L of Primer A, 1  $\mu$ L of Primer B, 1  $\mu$ L template DNA, 0.2  $\mu$ L Platinum<sup>®</sup> Taq High Fidelity (1 U), 38.8  $\mu$ L H<sub>2</sub>O. Cycling conditions: (1) 94°C for 30 s; (2) 30 cycles of 94°C for 30 s, 55°C for 30 s, 68°C for 60 s per kb of PCR product; (3) final extension 68°C for 10 min; (4) hold 4°C.

**PfuUltra High Fidelity (Stratagene):** PCR reaction (50  $\mu$ L): 5  $\mu$ L of 10  $\times$  PCR buffer, 1.25  $\mu$ L of dNTP mix, 1  $\mu$ L of Primer A, 1  $\mu$ L of Primer B, 1  $\mu$ L of template DNA, 1  $\mu$ L PfuUltra High Fidelity (2.5 U), 39.75  $\mu$ L of H<sub>2</sub>O. Cycling conditions: (1) 95°C for 2 min; (2) 30 cycles of 95°C for 30 s, 55°C for 30s, 72°C for 60 s; (3) final extension 72°C for 10 min; (4) hold 4°C.

**PfuTurbo (Stratagene):** PCR reaction (50  $\mu$ L): 5  $\mu$ L of 10  $\times$  PCR buffer, 1  $\mu$ L of dNTP mix, 1  $\mu$ L of Primer A (125 ng/ $\mu$ L), 1  $\mu$ L of Primer B (125 ng/ $\mu$ L), ~50 ng template DNA, 1  $\mu$ L PfuTurbo (2.5 U), H<sub>2</sub>O up to 50  $\mu$ L. Cycling conditions: (1) 95°C for 30 s; (2) 16 cycles of 95°C for 30 s, 55°C for 60s, 68°C for 4 min; (3) final extension 68°C for 10 min; (4) hold 4°C.

#### **6.2.4. Agarose gel electrophoresis**

Agarose gels (1–2% w/v, depending on size of PCR product) were prepared with Ultra-Pure Agarose (Invitrogen) and TBE (45 mM Tris-borate, 2 mM EDTA), and were stained with either ethidium bromide (1% of 0.5 µg/mL stock, Bio-Rad) or SYBR<sup>®</sup>Safe gel stain (1/10,000 dilution of DMSO stock, Invitrogen). DNA was mixed with 6 × sample buffer (10 mM Tris-Cl pH 7.6, 0.03% bromophenol blue, 0.03% xylene cyanol, 60% glycerol, 60 mM EDTA) prior to loading onto the gel. Gels were run at 80–100 V. Gels stained with EtBr were visualized under UV light, whereas gels stained with SYBR<sup>®</sup>Safe were visualized with a Dark Reader Transilluminator (Clare Chemical Research).

#### **6.2.5. Quantification of DNA**

DNA concentration was determined spectrophotometrically at 260 nm using a BioMate 3 Spectrophotometer. For oligonucleotide stock solutions, a 0.5% dilution of the oligonucleotide was prepared and placed in a 1 mL quartz cuvette. For all other DNA solutions, either 2% or 5% dilutions of the DNA were prepared and a 100 µL quartz micro-cuvette was used for absorbance readings.

#### **6.2.6. Purification of DNA following PCR or restriction digest reactions**

Following PCR and restriction enzyme digests, DNA was purified with either the QIAquick<sup>™</sup> PCR Purification Kit or the QIAquick<sup>™</sup> Gel Extraction Kit, according to the manufacturers' instructions.

### 6.2.7. Isolation of crude DNA for use as a template for PCR

A culture of the desired cells was grown in 5 mL of broth, with the appropriate antibiotics. For *E. coli*, LB broth was used and cultures were incubated at 37°C, 250 rpm. For *Carnobacterium spp.*, APT broth was used and cultures were grown at 25°C, without aeration. After 18–20 h of growth, 200 µL of cell culture was transferred to a microcentrifuge tube and the cells harvested by centrifugation (16,000 × g, 5 min, RT). The supernatant was discarded and the cells were rinsed twice, by the addition of 200 µL of H<sub>2</sub>O followed by centrifugation (16,000 × g, 5 min, RT). The supernatant was discarded and the cells were resuspended in 100 µL H<sub>2</sub>O and then boiled for 15 min. The crude lysate, with the DNA, was stored at -20°C.

### 6.2.8. Purification of plasmid DNA on a mini-preparative scale

Two methods were used for the purification of plasmid DNA on a mini-preparative scale.

**Method 1: Alkaline-Lysis & phenol/chloroform extraction.** Isolation of plasmid DNA was performed as described by Sambrook and Russell (289). Overnight cultures were grown in 5 mL of media, with the appropriate antibiotic(s). For *E. coli*, cultures were propagated in LB broth and incubated at 37°C, 250 rpm. For *Carnobacterium spp.*, APT broth was used and cultures were grown at 25°C without aeration. After 18–20 h of growth, ~1.5 mL samples were transferred to microcentrifuge tubes, centrifuged (16,000 × g, 5 min, RT) and the supernatant discarded. The cells were rinsed by resuspending the cell pellets in

100  $\mu\text{L}$  of  $\text{H}_2\text{O}$  and repeating the centrifugation. The cell pellets were resuspended in 200  $\mu\text{L}$  of ice-cold Solution A (50 mM Tris-Cl pH 8.0, 10 mM EDTA). The cells were then lysed by the alkaline lysis method as follows. 200  $\mu\text{L}$  of Solution B (0.2 M NaOH, 1% SDS) was added and the tubes were inverted 6 times. 200  $\mu\text{L}$  of ice-cold Solution C (3 M potassium acetate, 11.5% acetic acid) was added and the tubes were inverted 6 times to facilitate precipitation of proteins and chromosomal DNA. After centrifugation (16,000  $\times g$ , 15 min, 4°C) the supernatant was transferred to new microcentrifuge tubes containing 200  $\mu\text{L}$  of chloroform: isoamyl alcohol (24:1) and 200  $\mu\text{L}$  buffer-saturated phenol. The tubes were vortexed and centrifuged (16,000  $\times g$ , 6 min, 4°C). The aqueous layer (containing the plasmid DNA) was transferred to a new microcentrifuge tube containing 400  $\mu\text{L}$  of chloroform: isoamyl alcohol (24:1). After vortexing, the tubes were again centrifuged (16,000  $\times g$ , 6 min, 4°C) and the aqueous layer (~180  $\mu\text{L}$ ) was removed and transferred to new tubes. To precipitate the purified DNA, 20  $\mu\text{L}$  of 3M sodium acetate (pH 5.2) and 500  $\mu\text{L}$  of 95% EtOH were added and the tubes chilled for at least 1 h at -20°C. The DNA was pelleted by centrifugation (16,000  $\times g$ , 20 min, 4°C). After careful removal of the supernatant, the pellets were washed twice by addition of 400  $\mu\text{L}$  of ice-cold 70% EtOH, followed by centrifugation (16,000  $\times g$ , 5 min, 4°C) and careful removal of the supernatant. The DNA was dried under vacuum, using a benchtop Savant SpeedVac Concentrator. The purified DNA was dissolved in 5  $\mu\text{L}$   $\text{H}_2\text{O}$  and stored at -20°C.

**Method 2: Commercially available Miniprep Kits.** Plasmid DNA was also purified by using either the GeneJET™ Plasmid Miniprep Kit (Fermentas) or the QIAprep Miniprep Kit (Qiagen), and following the manufacturers' instructions. In brief, cell cultures were grown as described in the previous section and plasmid purification was achieved by alkaline lysis of cell pellets, followed by adsorption of DNA on a silica spin column. After washing, the immobilized DNA was eluted from the spin columns with 30–50  $\mu$ L of elution buffer (10 mM Tris-Cl, pH 8.5) and stored at  $-20^{\circ}\text{C}$ .

### 6.2.9. Large scale purification of plasmid DNA

Two methods were used for the purification of plasmid DNA on a large-preparative scale:

**Method 1: Alkaline-Lysis & EtBr/CsCl Density Gradient.** An overnight culture of the desired *E. coli* clone was grown in 5 mL of LB broth containing ampicillin (200  $\mu\text{g}/\text{mL}$ ) at  $37^{\circ}\text{C}$ , 250 rpm.  $2 \times 200$  mL of fresh LB broth containing ampicillin (200  $\mu\text{g}/\text{mL}$ ) was inoculated (1%) with overnight culture and incubated at  $37^{\circ}\text{C}$ , 250 rpm for 24 h. The 400 mL of cell culture was divided into two centrifuge bottles (250 mL) and the cells harvested by centrifugation ( $9820 \times g$ , 20 min,  $4^{\circ}\text{C}$ ). The cell pellet in each bottle was resuspended in 20 mL of STE washing solution (100 mM NaCl, 10 mM Tris, 1 mM EDTA). After centrifugation ( $9820 \times g$ , 5 min,  $4^{\circ}\text{C}$ ), the cell pellet in each bottle was resuspended in 8 mL of Solution A (50 mM glucose, 25 mM Tris-Cl pH 8.0, 10 mM EDTA). Degradation of the cell wall was facilitated by addition of 40 mg of

lysozyme (5 mg/mL) and the mixture was incubated at 37°C for 30 min. 16 mL of freshly prepared Solution B (0.2 M NaOH, 1% SDS) was added to each bottle and the mixture was swirled gently until it became clear (no longer than 5 min). To precipitate proteins and chromosomal DNA, 12 mL of Solution C (3 M sodium acetate, 11.5% v/v acetic acid) was added to each bottle and incubated (5 min, RT). Following centrifugation (9820 × g, 15 min, 4°C), the supernatant from both bottles was divided into 4 × 30 mL centrifuge bottles. To precipitate the DNA, 10 mL of 2-propanol was added to each bottle and the mixture was incubated (10 min, RT). The DNA was pelleted by centrifugation (17,400 × g, 15 min, 20°C). The pellets were rinsed three times with 5 mL of 70% EtOH and then dried under vacuum for 10 min. 3 mL of H<sub>2</sub>O was added to each bottle and the solutions were warmed to 37°C for 20 min to dissolve the DNA. The contents of the four bottles were combined into two bottles and 6 g of CsCl was added to each bottle. The solutions were transferred to 2 × 5 mL ultracentrifuge bottles, each containing 300 µL of ethidium bromide (10 mg/mL solution). Following ultracentrifugation (49,000 rpm Beckman Type 70.1 Ti rotor, 20 h, 20°C), the DNA was visualized under long-wave UV light and the lower band (corresponding to plasmid DNA) was removed with a Pasteur pipette and transferred into a clean tube. To remove ethidium bromide, the solution was washed five times with 1.5 mL of isoamyl alcohol. Removal of CsCl was achieved by dialysis against 500 mL of TE buffer (4 mM Tris, 2 mM EDTA) for 2.5 h (with three exchanges). The DNA solution was aliquoted into four microcentrifuge tubes (~450 µL per tube) Pure DNA was obtained by phenol-chloroform extraction and precipitation as described above.

**Method 2: Commercially available Midi-prep Kits.** Plasmid DNA was also purified by using the HiSpeed Midiprep Kit (Qiagen), and following the manufacturers' instructions. The purified DNA was eluted from the QIAprecipitator with 500  $\mu$ L of elution buffer (10 mM Tris-Cl, pH 8.5) and stored at  $-20^{\circ}\text{C}$ .

## 6.2.10. Preparation of competent *E. coli* cells

### 6.2.10.a. Electrocompetent cells (*E. coli* JM109)

An overnight culture of *E. coli* JM109 was grown in 5 mL of LB broth, at  $37^{\circ}\text{C}$ , 250 rpm for 16–18 h. 100 mL of fresh LB broth was inoculated with the overnight culture (1%) and incubated at  $37^{\circ}\text{C}$ , 250 rpm until the  $\text{OD}_{600}$  was  $\sim 0.5$ . The culture was chilled on ice for 30 min and the cells were harvested by centrifugation ( $4000 \times g$ , 15 min,  $4^{\circ}\text{C}$ ). The supernatant was discarded and the cell pellet was rinsed with successive washes of 100 mL of ice cold water, 50 mL ice cold water and 2 mL 10% ice cold glycerol. Following the final rinse, the cell pellet was resuspended to a final volume of 0.2 mL with 10% ice-cold glycerol (289). The cells were immediately aliquoted into chilled microcentrifuge tubes (50  $\mu$ L per tube) and stored at  $-80^{\circ}\text{C}$ .

### 6.2.10.b. Heat-shock competent cells

*E. coli* BL21(DE3) competent cells were purchased from Stratagene or prepared by Dr. Tara Sprules. *E. coli* BL21 competent cells were prepared by Dr.

Sandra Marcus. *E. coli* XL1-Blue supercompetent cells were purchased from Stratagene.

#### **6.2.10.c. Chemically competent cells**

*E. coli* M15[pREP4] cells and *E. coli* JM109 cells were made competent by use of the Fermentas TransformAid™ Bacterial Transformation Kit, according to the manufacturers' instructions.

#### **6.2.11. Preparation of electrocompetent *Carnobacterium* spp.**

Cells from *Carnobacterium* spp. were made electrocompetent in the same manner as described above for *E. coli* except for the following changes. *Carnobacterium* spp. were grown in APT media, at 25°C without aeration. Rather than 10% glycerol, electroporation buffer was used (10% glycerol, 0.5 M sucrose, 2.5 mM potassium phosphate pH 6.0, and 1 mM MgCl<sub>2</sub>) to wash and resuspend the cell pellets (290).

#### **6.2.12. Transformation of *E. coli***

##### **6.2.12.a. Electroporation**

50 µL of electrocompetent *E. coli* JM109 cells were thawed on ice. 1–2 µL of DNA was added to the cells and the mixture was transferred to a prechilled electroporation cuvette (0.2 cm gap) and held on ice for five minutes. The cells were transformed using a Gene Pulser Electroporator (Bio-Rad) at 1.0 kV and 800 Ω resistance. 1 mL of fresh LB broth was added to the cuvette after

electroporation and the mixture transferred to a microcentrifuge tube. The culture was incubated at 37°C for 60 min and then streaked onto fresh LB agar plates, containing the appropriate antibiotic(s) and incubated at 37°C for 16–24 h.

#### **6.2.12.b. Heat-shock**

50 µL of competent *E. coli* cells were thawed on ice and transferred to a pre-chilled 14 mL polypropylene culture tube. 1–2 µL of DNA was added to the cells, swirled gently to ensure dispersion, and the mixture was incubated on ice for five minutes. The mixture was placed in a 42°C water bath for either 45 s (*E. coli* XL1-Blue supercompetent cells), 90 s (*E. coli* BL21(DE3) competent cells) or 2 min (*E. coli* BL21 competent cells) and then chilled on ice for an additional 2 min. 500 µL of fresh LB was added to the culture tube and incubated at 37°C for 60 min. The cells were streaked onto fresh LB agar plates, containing the appropriate antibiotic(s) and incubated at 37°C for 16–24 h.

#### **6.2.12.c. Chemical treatment**

*E. coli* M15[prep4] and *E. coli* JM109 cells were made chemically competent immediately before use, as described above. For each transformation, 50 µL of cells were added to 1–2 µL of pre-chilled DNA, in a microcentrifuge tube. The mixture was incubated on ice for 5 min, after which 1 mL of fresh LB broth was added and the culture incubated at 37°C for 60 min. The cells were streaked onto fresh LB agar plates, containing the appropriate antibiotic(s) and incubated at 37°C for 16–24 h.

### 6.2.13. Transformation of *Carnobacterium* spp.

Electrocompetent *Carnobacterium* spp. cells were transformed in the same manner as described above for *E. coli*, except with the following changes. Following electroporation, the cells were resuspended in 1 mL of APT broth, supplemented with 0.5 M sucrose and incubated at 25°C for 60 min. The cells were streaked out onto fresh APT agar plates, containing appropriate antibiotics and 0.5 M sucrose, and incubated at 25°C for 5–6 d.

### 6.2.14. Screening for desired clones

Following transformation, clones were screened to determine if they contained the desired insert. This required two steps: isolation of DNA and PCR:

**Step 1: DNA Isolation.** Individual colonies were subcultured in 5 mL of LB broth and incubated at 37°C, 16–28 h (for *E. coli*) or 10 mL of APT broth and incubated at 25°C, 24 h (for *Carnobacterium* spp.), with appropriate antibiotics. Plasmid DNA was isolated as either crude DNA or purified on a mini-preparative scale.

**Step 2: DNA Amplification.** The isolated DNA was used as the template in a PCR reaction, using a primer pair that allowed for amplification of the desired gene. A positive control, utilizing template DNA known to contain the desired gene, was also performed. PCR reactions were performed with either *Taq*, Platinum<sup>®</sup> *Taq* or Platinum<sup>®</sup> *Taq* High Fidelity enzymes, as described above (section 6.2.3). Following PCR, 5 µL of each PCR reaction, as well as the control,

were separated on an agarose gel and visualized with either EtBr or SYBR<sup>®</sup>Safe (section 6.2.4), allowing for identification of successful clones.

#### **6.2.15. DNA sequencing**

DNA was sequenced with the BigDye Terminator v3.1 Cycle Sequencing Kit (Applied Biosystems) and electrophoresed on an ABI 3730 DNA Analyzer (Applied Biosystems) at the Molecular Biology Services Unit (Biological Services, University of Alberta). Sequencing reactions consisted of 2  $\mu$ L sequencing buffer (200 mM Tris-Cl pH 9, 5 mM MgCl<sub>2</sub>), 1 pmol primer, 200–300 ng template DNA, 2  $\mu$ L BigDye premix and water, to a final volume of 10  $\mu$ L. The mixture was then subjected to the following PCR conditions: 30 cycles of 96°C for 30 s, 50°C for 15 s, 60°C for 60 s. The DNA was purified by sodium acetate / ethanol precipitation by transferring the reaction mixture to a microcentrifuge tube containing 10  $\mu$ L of water, 2  $\mu$ L of sodium acetate/EDTA buffer and 80  $\mu$ L of ice cold 95% EtOH. The mixture was vortexed and incubated on ice for a minimum of 15 min. The DNA was pelleted by centrifugation (16,000  $\times$  g, 15 min, 4°C), washed with 1 mL of ice-cold 70% EtOH and dried under vacuum for ~10 min. Sequences were inspected manually.

### **6.3. Experimental procedures for the structural studies of carnocyclin A**

#### **6.3.1. Plasmids, bacterial strains and culture conditions**

The plasmids and bacterial strains used in this study are listed in Table 10. Indicator organisms used to probe the antimicrobial spectrum of CclA are listed in Table 2. All biological experiments were performed under sterile conditions. All materials and solutions were autoclaved (121°C, 15 min) prior to use, except for erythromycin, which was filter sterilized. Gram-positive strains were grown in APT, except for *S. aureus*, which required Tryptic Soy Broth (TSB; Difco). Gram-positive strains were incubated at 25°C, except for *C. maltaromaticum* UAL26, which was grown at 16°C. All Gram-negative organisms were grown in LB media at 37°C, with shaking at 200 rpm for liquid cultures. If necessary, antibiotics were added to growth media. All strains were maintained as frozen stocks at -80°C in the presence of 20% glycerol. Unless otherwise stated, percentage concentration implies v/v.

**TABLE 10.** Plasmids and bacterial strains used in the study of CclA

Plasmid or Strain	Relevant Characteristics*	Ref. or Source
pMAL <sup>TM</sup> -c2X	Amp <sup>r</sup> , <i>lacI</i> , <i>lacZα</i> and <i>malE</i> expression vector, 6.6 kb	NEB
pMG36e	Expression vector, Em <sup>r</sup> , 3.6 kb	(291)
pQE60	Expression vector, Amp <sup>r</sup> , 3.4 kb	Qiagen
pMAL.FXA.pCclA	pMAL <sup>TM</sup> -c2X containing <i>malE.FXA.cclA</i> fusion	This study
pQE60.FXA.pCclA	pQE60 containing <sup>Met</sup> <i>His<sub>6</sub>.FXA.cclA</i> fusion	This study
pQE60.pCclA	pQE60 containing <sup>Met</sup> <i>His<sub>6</sub>.cclA</i> fusion	This study
pMG36e.pCclA.M1	pMG36e containing <i>cclA</i> , <i>His<sub>6</sub></i> between I6 and A7	This study
pMG36e.pCclA.M2	pMG36e containing <i>cclA</i> , <i>His<sub>6</sub></i> between L22 and T23	This study
pMG36e.pCclA.M3	pMG36e containing <i>cclA</i> , <i>His<sub>6</sub></i> between G33 and V34	This study
pMG36e.pCclA.M4	pMG36e containing <i>cclA</i> , <i>His<sub>6</sub></i> between Q52 and G53	This study
<i>E. coli</i> BL21	<i>E. coli</i> B F <sup>-</sup> <i>dcm ompT hsdS</i> (r <sub>B</sub> <sup>-</sup> m <sub>B</sub> <sup>-</sup> ) <i>gal</i> ; general purpose expression strain that lacks the <i>lon</i> protease and <i>ompT</i> outer membrane protease	Stratagene
<i>E. coli</i> JM109	E14 <sup>-</sup> (McrA <sup>-</sup> ) <i>recA1 endA1 gyrA96 thi-1 hsdR17</i> (r <sub>K</sub> <sup>-</sup> m <sub>K</sub> <sup>+</sup> ) <i>supE44 relA1 Δ(lac-proAB)</i> [F' <i>traD36 proAB lacI<sup>f</sup>ZΔM15</i> ]; general purpose strain for cloning and propagating plasmids	(134)
<i>Carnobacterium maltaromaticum</i> UAL307	PisA, CbnB1, CbnBM1 and CclA producer	Lab collection

\* FXA denotes the Factor Xa recognition sequence (IEGR)

### 6.3.2. Isolation and purification of CclA

Dr. Sylvie Garneau initially isolated the bacteriocins produced by *C. maltaromaticum* UAL307. Her purification strategies allowed for the isolation and identification of PisA, CbnB1/CbnBM1 and an additional, unknown bacteriocin (CclA). For the current study, the purification strategy was optimized for the isolation of CclA. Overnight cultures of *C. maltaromaticum* UAL307 were grown in 10 mL of APT broth and incubated at 25°C for 21–24 h. 1 L of fresh APT was inoculated (1%) with the overnight culture and incubated at 25°C for 24 h. The culture was centrifuged (11,300 × g, 10 min, 4°C) to remove the cells and the supernatant was applied to a column of Amberlite XAD-16 resin (100 g, 2.5 ×

50 cm) at a flow rate of 5 mL/min. The column was then washed consecutively with 500 mL of 30% ethanol, 40% IPA, 70% IPA and 70% IPA pH 2. All fractions were tested in spot-on-lawn assays against *C. divergens* LV13 and *C. maltaromaticum* UAL26. CclA was found to elute with 70% IPA pH 2, while PisA and CbnB1 were identified in the 40% IPA fraction. The CclA containing fraction was concentrated to ~10 mL by rotary evaporation and then loaded onto a Megabond C<sub>18</sub> cartridge. The column was washed consecutively with 50 mL of H<sub>2</sub>O, 30% ethanol, 30% acetonitrile, 40% IPA, 70% IPA and eluted with ~100 mL of 70% IPA pH 2. Again, the fractions were analyzed by spot-on-lawn activity tests against *C. divergens* LV13 and *C. maltaromaticum* UAL26 and CclA was found in the 70% IPA pH 2 elution. This fraction was concentrated, lyophilized, resuspended in ~5 mL of H<sub>2</sub>O and subjected to RP-HPLC, using a semi-preparative C<sub>8</sub> column (Vydac 208TP510, 5 µM particle size, 10 × 250 mm), using either a Beckman System Gold or Varian Prostar HPLC. IPA (0.1% TFA) and H<sub>2</sub>O (0.1% TFA) were used as solvents, according to the following gradient: (1) hold at 40% IPA for 8 min; (2) increase to 86% IPA over 30 min; (3) increase to 100% IPA over 2 min; (4) hold at 100% IPA for 2 min; (5) decrease to 40% IPA over 1 min; (6) hold at 40% IPA for 6 min. The method employed 200 µL injections, a flow rate of 1 mL/min and detection at 220 nm. CclA eluted as a sharp peak with a retention time of ~32 min, and was identified by MALDI-TOF. After purification of the whole sample, the CclA fractions were combined, concentrated, lyophilized and stored at -20°C.

### 6.3.3. Isolation and purification of [<sup>13</sup>C, <sup>15</sup>N]CclA

For NMR studies, CclA was prepared as a doubly labeled [<sup>13</sup>C, <sup>15</sup>N]CclA sample by growing the producer organism in isotopically enriched Celtone-CN Complete Media (Cambridge Isotope Laboratories, Andover MA). Purification of [<sup>13</sup>C, <sup>15</sup>N]CclA was identical to that of the unlabelled bacteriocin.

### 6.3.4. Confirming the purity and antimicrobial activity of CclA

CclA samples were mixed with an equal volume of 2 × Tris-Tricine sample buffer and loaded onto a 16.5% Tris-Tricine gel (287). Polypeptide SDS-PAGE standards (Bio-Rad) were also mixed with sample buffer and heated at 100°C for 5 min before loading onto the gel. After electrophoresis, half the gel was stained with Bio-Safe Coomassie stain (Bio-Rad) and then destained with water. The other half of the gel, to be used in activity testing, was soaked in water overnight, placed on a bed of agar and then overlaid with soft agar containing the indicator organism *C. divergens* LV13 (1% inoculum). The plate was incubated overnight and examined for halos of growth inhibition.

### 6.3.5. Antimicrobial spectrum of CclA

The antimicrobial spectrum of CclA was examined by performing spot-on-lawn activity assays of purified CclA against a variety of Gram-positive and Gram-negative organisms (listed in Table 2). Soft agar was inoculated with the indicator organism (1%) and overlaid on a bed of solid agar. A 10 µL sample of CclA (250 µM) was spotted onto the agar and allowed to air dry. Plates were

incubated overnight at the appropriate temperatures and examined for halos of growth inhibition.

### **6.3.6. Stability of CclA**

#### **6.3.6.a. Effect of temperature**

Aliquots of CclA were incubated for one hour at -80°C, -20°C, 0°C, 25°C, 50°C, 75°C, and 100°C, and also autoclaved (121°C, 15 min). Following incubation, samples were placed on ice and then tested for activity in a critical dilution assay (spot-on-lawn) (292) with *C. divergens* LV13 as the indicator organism. Tests were repeated twice.

#### **6.3.6.b. Effect of pH**

To determine the effect of pH on CclA, aliquots of the purified bacteriocin were adjusted to pH 2, 4, 5, 6, 7, 8, 10 and 12 in 10 mM Tris buffer, using HCl or NaOH. Samples were incubated at 4°C for 24 hours and then neutralized. Bacteriocin activity was determined in a critical dilution assay (spot-on-lawn) with *C. divergens* LV13 as the indicator organism. Tests were repeated twice.

#### **6.3.6.c. Effect of proteolytic enzymes**

CclA was treated with a variety of proteases. The protease, pH conditions and ratios of enzyme to bacteriocin (w/w) are listed as follows: trypsin (pH 7.5, 1:200), papain (pH 6.2, 10:1), chymopapain (pH 6.2, 8:1), pepsin (pH 2, 8:1), protease type VIII (pH 7.5, 1:1), endoproteinase Glu-C (pH 8.0, 1:20),

endoproteinase Asp-N (pH 8.0, 1:40),  $\alpha$ -chymotrypsin (pH 7.8, 1:40) and thermolysin (pH 8.0, 1:5). All samples were incubated at 37°C for a minimum of 3 h, except for thermolysin, which was heated to 65°C in a water bath for 60 min. Following treatment, samples were either tested for activity with spot-on-lawn assays (using *C. divergens* LV13 as the indicator) or examined by MALDI-TOF mass spectrometry to detect fragmentation of the peptide. All enzymes were obtained from Sigma except for endoproteinase Asp-N (Boehringer Mannheim), trypsin (Promega) and  $\alpha$ -chymotrypsin (Roche).

### **6.3.7. Amino acid sequence of CclA**

#### **6.3.7.a. Edman sequencing**

Peptides fragments were generated by enzymatic digestion of CclA. These fragments were purified by RP-HPLC by Dr. Paul Semchuk, at the Institute for Biomolecular Design (University of Alberta), and were subjected to Edman sequencing at the Michael Smith Laboratory, Protein Sequencing and Peptide Mapping Unit (University of British Columbia) using an Applied Biosystems Procise sequencer.

#### **6.3.7.b. Tandem mass spectrometry**

Dr. Randy Whittal and Jing Zheng performed the MS/MS analysis of CclA. CclA was digested with trypsin (Promega Sequencing Grade) or  $\alpha$ -chymotrypsin (Roche) for 2 to 3 hours, or with a 15 min tryptic digest followed by a 3 h chymotryptic digest. All digestion reactions were done in 50 mM

$\text{NH}_4\text{HCO}_3$  (pH 8.5) at room temperature and an enzyme to peptide ratio of 1:40 (w/w). The resulting fragments were analyzed via LC MS/MS on a nanoAcquity UPLC (Waters, MA) coupled with a Q-TOF-Premier mass spectrometer (Micromass, UK / Waters, MA). The fragments were separated using a linear water/acetonitrile gradient (0.1% formic acid) on a nanoAcquity column (3  $\mu\text{m}$  Atlantis dC<sub>18</sub>, 100 Å pore size, 75  $\mu\text{m}$  ID  $\times$  15 cm) (Waters, MA) at a flow rate of 350 nL/min, with an in-line Symmetry column (5  $\mu\text{m}$  C<sub>18</sub>, 180  $\mu\text{m}$  ID  $\times$  20 mm) (Waters, MA) as a loading/desalting column. Alternatively, digest fragments were purified by RP-HPLC, infused to the Q-TOF using nano-electrospray and the collision energy was varied to produce the MS/MS spectra. The Q-TOF was calibrated with the MS/MS spectrum of glu-fibrinopeptide. The mass spectra were manually *de novo* sequenced to generate a proposed linear peptide sequence and confirmed using the software PEAKS (Bioinformatics Solutions, Waterloo, ON) (293). Exact mass measurements of the intact peptide and peptide fragments were obtained with a Bruker Apex Qe 9.4T FTICR-MS equipped with the Apollo II dual MALDI / electrospray source. The  $[\text{M}+5\text{H}]^{5+}$  peak of the intact peptide was analyzed by electrospray ionization (ESI) and calibrated internally with bovine insulin. The peptide fragments were analyzed by MALDI, using HCCA as the matrix and calibrated with sodium cationized polyethylene glycol with *trans*-2-[3-(4-*tert*-butylphenyl)-2-methyl-2-propenylidene]malononitrile (Fluka) as matrix.

### 6.3.8. Circular dichroism of CclA

Wayne Moffat performed the CD analysis of CclA. The CD spectrum of CclA (at a concentration of 0.5 mg/mL), was recorded in 100% H<sub>2</sub>O or in 50% trifluoroethanol (TFE) / 50% H<sub>2</sub>O, at 20°C. Data were collected every 1 nm and were the average of five scans. The  $\alpha$ -helical content of the peptide was calculated according to the molar ellipticity at 222 nm, using the following equation (294):

$$\text{Percentage helicity} = \frac{-[\theta_{222\text{nm}}] + 3000}{39,000} \times 100\% \quad (\text{eq. 2})$$

### 6.3.9. Stereochemical analysis of CclA

#### 6.3.9.a. Hydrolysis and derivatization of CclA

With the assistance of summer student Michael Kreuzer, CclA was hydrolyzed to its constituent amino acids by addition of 6 N HCl (5 mL) to 6.2 mg of purified peptide, in a 15 mL pressure vessel. The vessel was heated to 110°C for 18 h. After cooling, the hydrolysate was dried under a stream of argon. The amino acids were subsequently derivatized to their pentafluoropropanamide isopropyl esters in preparation for chiral GC-MS as follows. 1.5 mL of acetyl chloride (Sigma) was added to 5 mL of cold 2-propanol, which was then added dropwise to the dried hydrolysate. The mixture was sealed and heated to 100°C for 45 min, dried under a stream of argon and then cooled in an ice bath. 3 mL of dichloromethane and 1 mL of pentafluoropropionic anhydride (Sigma) were added and the mixture was sealed and heated to 110°C for 15 min. After cooling, the mixture was dried under a stream of argon.

### 6.3.9.b. Preparation of standards

Sets of (L)- and (D)- amino acid derivatives were also prepared as follows. Approximately 0.02 mmol of the following (L)-amino acids were mixed together: Ala, Asn, Asp, Glu, Gln, Ile, Leu, Lys, Phe, Ser, Thr, Tyr and Val. Gly was also added. The mixture was treated with 3 mL of 0.2 N HCl for 5 min at 100°C and then dried under argon. The mixture was then derivatized in the same manner as described for CclA. A standard set of (D)-amino acids was prepared in the same fashion. Upon hydrolysis and derivatization, Asn and Asp were converted to the same compound, as were Glu and Gln.

### 6.3.9.c. GC-MS

With the assistance of summer student Michael Kreuzer, the derivatized amino acid samples were analyzed by GC-MS, using an Alltech Heliflex Chirasil-Val capillary column (50 m × 0.25 mm × 0.16 μm) running at a head pressure of 17 psi helium. The samples were dissolved in 100 μL of dichloromethane. 1/100 dilutions of the samples were prepared, also with dichloromethane, and 1 μL injections were used. The method started with an initial oven temperature of 30°C, followed by an immediate ramp to 90°C at a rate of 15°C/min. From 90°C, the temperature increased to 180°C at a rate of 4°C/min, with a final hold for 15 minutes. With this method, every amino acid in both the (L)- and (D)- standards gave complete resolution. When mixed together, the (L)- and (D)- enantiomers for each amino acid (except Asn/Asp) separated, with the (D)- enantiomer displaying a shorter retention time than the (L). In the case of Asn/Asp, the peak broadened

when the enantiomers were mixed, but could not be separated into two individual peaks. It was also found that (D)-Val and (L)-Thr co-eluted, as did (D)-Ser and (L)-Ile (see Fig. 12B). However, this co-elution was not a problem as the mass spectrometry profiles of these peaks could clearly distinguish between the different amino acids.

### **6.3.10. Oligomeric state of CclA**

#### **6.3.10.a. NMR studies**

To examine the effect of pH and salt on the association state of CclA, a series of titrations were performed and the resulting  $^{15}\text{N}$  HSQC spectra were acquired. The pH of the NMR sample ( $\sim 1$  mM  $[^{13}\text{C},^{15}\text{N}]\text{CclA}$ ) was adjusted to values ranging from 3 to 8 by addition of HCl or NaOH. Similarly, the effect of salt was examined by addition of NaCl (up to 500 mM) to the NMR sample (pH 5.9). NMR spectra were recorded on a Varian Inova 600 MHz spectrometer, equipped with a triple-resonance HCN probe.

#### **6.3.10.b. Dynamic light scattering (DLS)**

Dynamic light scattering (DLS) experiments were performed using a DynaPro Titan system (Wyatt Technology, Santa Barbara CA) with a  $90^\circ$  scattering angle. CclA samples (1 mM) at pH values of 3, 5, 6 and 8 were tested. Data were collected and analyzed with the program DYNAMICS (manufacturer's software). A minimum of 50 measurements was obtained for each sample, from

which the hydrodynamic radius and corresponding molecular weight were determined. BSA was used a protein standard.

### 6.3.11. NMR spectroscopy of [ $^{13}\text{C}$ , $^{15}\text{N}$ ]CclA

[ $^{13}\text{C}$ , $^{15}\text{N}$ ]CclA was dissolved in 20 mM sodium phosphate (pH 5.9) in 90%  $\text{H}_2\text{O}$ :10%  $\text{D}_2\text{O}$  to a final concentration of  $\sim 1$  mM. To prevent sample degradation 1 mM EDTA, 1 mM  $\text{NaN}_3$ , and protease inhibitors (Roche Applied Science, Laval PQ) were added. 100  $\mu\text{M}$  DSS was added for referencing. NMR spectra were acquired on a Varian Inova 600 MHz spectrometer, equipped with a triple-resonance HCN probe and z-axis pulsed-field gradients. For backbone chemical shift assignments, the following experiments were performed:  $^{15}\text{N}$  HSQC,  $^{15}\text{N}$  TOCSY-HSQC, HNCOC, CBCA(CO)NH, HNCACB. For side chain assignments, the sample was lyophilized and dissolved in an equivalent volume of 100%  $\text{D}_2\text{O}$  (repeated twice to ensure exchange of labile protons) and the following experiments were performed:  $^{13}\text{C}$  HCCH-TOCSY,  $^{13}\text{C}$  HSQC (full and aliphatic),  $^1\text{H}$  TOCSY (aromatic region) and  $^1\text{H}$  COSY (aromatic region). Structural restraints were obtained from the following experiments:  $^{15}\text{N}$  NOESY-HSQC,  $^{13}\text{C}$  NOESY-HSQC,  $^1\text{H}$  NOESY (aromatic region) and HNHA. Data were processed with NMRPipe (295) and analyzed with NMRView (296). Data were multiplied by a  $90^\circ$  shifted sine-bell squared function in all dimensions. Indirect dimensions were doubled by linear prediction and zero-filled to the nearest power of two prior to Fourier transformation.

### 6.3.12. Structure calculations

The structure of CclA was calculated with CYANA 2.1 (142), using NOE restraints obtained from the  $^{15}\text{N}$ - and  $^{13}\text{C}$ - edited NOESY- HSQC and  $^1\text{H}$  NOESY experiments and angle restraints derived from analysis of the HNHA experiment and from the program TALOS (143). A combination of manually and automatically assigned NOEs were used and calibrated within CYANA according to their intensities. After seven rounds of calculation (10,000 steps per round), a total of 657 NOE restraints, 43  $^3J_{\text{HNH}\alpha}$  coupling constants and 98 dihedral angle restraints were used in the final calculation. The 20 lowest energy conformations, with no NOE violations of  $> 0.3 \text{ \AA}$  and no residues in the disallowed region of the Ramachandran plot, were chosen as representative of the solution structure of CclA. Coordinates for CclA have been deposited in the PDB data bank (code 2KJF) and chemical shift assignments have been deposited in the BioMagRes Bank (code 16319). Electrostatic surface calculations were computed with the program APBS (297) and figures were generated with PyMOL.

### 6.3.13. Fluorine NMR

CclA was dissolved in 90%:10%  $\text{H}_2\text{O}$ :  $\text{D}_2\text{O}$  to a concentration of 1 mM. The pH of the sample was 3.8, due to residual TFA following HPLC purification. The sample was titrated with NaF (adjusted to pH 3.8) by addition of 0.5, 1, 1.5, 2 and 3 molar equivalents of NaF. The resulting 1D fluorine spectra were monitored by NMR, on a Varian VNMRS 500 MHz spectrometer equipped with a  $^1\text{H}$ - $^{19}\text{F}$  Z-

gradient probe capable of  $^{19}\text{F}$  direct detection. Control experiments with NaF and TFA in the absence of protein were performed (pH 3.80).

#### **6.3.14. Examining the lysine side chains of CclA by NMR**

$[^{13}\text{C},^{15}\text{N}]\text{CclA}$  was dissolved in 90%  $\text{H}_2\text{O}$ :10%  $\text{D}_2\text{O}$  to a final concentration of 1.5 mM and DSS was added for referencing. The pH was measured to be 3.7, due to residual trifluoroacetate in the lyophilized peptide. An  $^{15}\text{N}$  HSQC was acquired at 25°C, with the carrier position shifted to 45 ppm and the spectral window restricted to 55 ppm. Three, out of the five, lysine amino groups were visible and were assigned on the basis of a modified  $^{15}\text{N}$  TOCSY-HSQC (utilizing a 65 ms DIPSI spinlock applied with a gammaB1 of 8 kHz) and  $^{15}\text{N}$  NOESY-HSQC experiment. For both experiments, only the first XY plane ( $^1\text{H}$ ,  $^1\text{H}$ ) was acquired. 0.5 molar equivalents of NaF was added to the sample and the same NMR experiments were performed. Spectra were acquired at NANUC, on a Varian 800 MHz spectrometer, equipped with a triple-resonance HCN cold probe and z-axis pulsed-field gradients. Data were processed with NMRPipe (295) and NMRView (296).

#### **6.3.15. Secondary structure analysis and homology modeling of the other circular bacteriocins**

The secondary structure of the circular bacteriocins was predicted with both the Jpred3 (149) and PSIPred (150) protein structure prediction servers. To allow for the possibility of secondary structure across the N- and C- termini, each sequence was submitted twice, as follows (Fig. 51). In the first instance, the

regular linear sequence was submitted and from the output, coil regions were identified (Fig. 51A). The sequence was then swapped so that a coil region would become the new N-terminus, and the former N-terminal residues were added to the C-terminus of the sequence (Fig. 51B). This modified sequence was then submitted for secondary structure analysis (Fig. 51C).

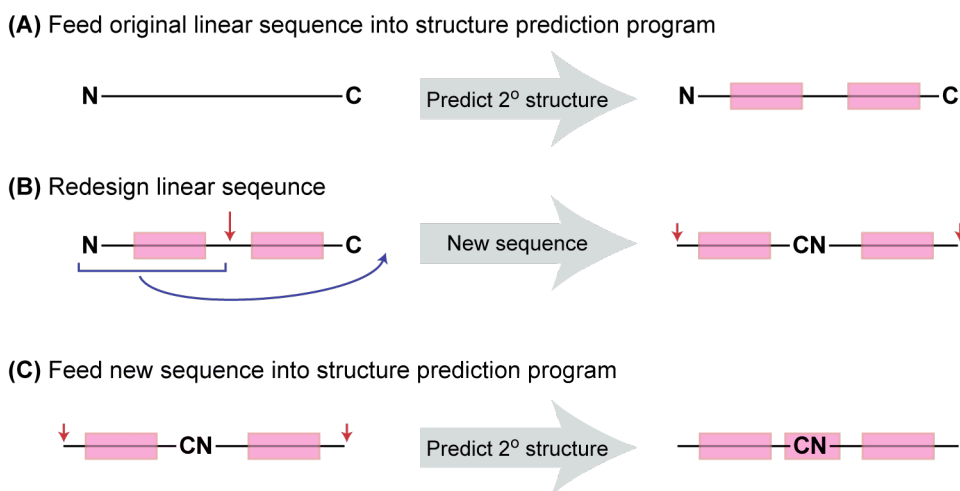


**FIG. 51.** Predicting the secondary structure of the circular bacteriocins and allowing for structural elements to encompass the N- and C- termini. (A) Predicted secondary structure based on the original linear sequence. (B) Redesigning the linear sequence so that unstructured regions become the new N- and C- termini. (C) Predicting the secondary structure of the “new” linear sequence. Pink boxes indicate regions that are predicted to display secondary structure.

For homology modeling, the sequences of AS-48, CclA, circularin A, uberolysin and lactocyclicin Q were aligned with ClustalW (144). The sequences were imported into Deep View Swiss-Pdb Viewer (298) and were fitted onto the structure of either AS-48 (pdb code 1E68) or CclA, according to the Clustal W alignment. The models were then submitted to the Swiss-Model Server for further refinement (298).

### 6.3.16. Purification of pCclA as a MalE fusion protein

WISEST student Anna King participated in the construction and overexpression of the MalE.pCclA fusion protein.

#### 6.3.16.a. Construction of pMAL.FXA.pCclA

Using total genomic DNA from *C. maltaromaticum* UAL307 (isolated by Dr. Marco van Belkum), the *cclA* structural gene was amplified by PCR, with primers LAM4A (5'–ATATCGAGCTCGAACAACAACAATAACAATAACAACCTCGGGATCGAGGGAAGGATGTTATATGAATTAGTTGCATATG–3') and LAM5 (5'–ATATGGATCCTTATAATTGAATTGCTTTTTTTATTCC–3'), which contained the *SacI* and *BamHI* restriction sites, respectively (underlined). In addition, primer LAM4A introduced a Factor Xa recognition sequence (in green) on the N-terminal side of the *cclA* structural gene. The PCR reaction (2 × 50 µL) consisted of: 10 µL of 10 × PCR buffer, 2.5 µL of dNTP mix, 2 µL of LAM4A, 2 µL of LAM5, 1 µL of template, 2 µL of *PfuUltra* High Fidelity (5 U) and 80.5 µL H<sub>2</sub>O. Cycling conditions: (1) 95°C for 2 min; (2) 30 cycles of 95°C for 30 s, 55°C for 30s, 72°C for 60 s; (3) final extension 72°C for 10 min; (4) hold 4°C. Amplification of DNA was confirmed by agarose gel electrophoresis and the PCR product was purified with the QIAquick™ PCR Purification Kit.

The PCR product was cloned into the pMAL™-c2X vector by performing a double digestion, followed by ligation. The vector had previously been digested with *SacI* and *BamHI*, and purified, by Dr. Marco van Belkum. The PCR product was digested as follows: 2 µg of DNA was digested with 1 µL of *SacI* (10 U) and

1  $\mu\text{L}$  of *Bam*HI (10 U) in 5  $\mu\text{L}$  of NEBuffer 4 (NEB) and 5  $\mu\text{L}$  of  $\text{H}_2\text{O}$ . The mixture was incubated at 37°C for 3 h, and DNA was purified with the QIAquick™ PCR Purification Kit. For the ligation reaction, 50 ng of PCR product, ~10 ng of vector DNA, 0.5  $\mu\text{L}$  of T4 DNA Ligase (0.5 U), 1  $\mu\text{L}$  of 5 × Ligase Reaction Buffer, and  $\text{H}_2\text{O}$  (final volume of 5  $\mu\text{L}$ ) were mixed together and incubated at room temperature for 1.5 h. 2.5  $\mu\text{L}$  of the reaction mixture was used to transform *E. coli* JM109 cells via electroporation. The transformed cells were streaked onto LB agar plates (100  $\mu\text{g}/\text{mL}$  ampicillin) and incubated at 37°C. Several colonies were subcultured and their crude DNA was isolated. The clones were screened by PCR and several successful transformants were identified. One of the clones was further subcultured and its plasmid DNA purified with the QIAprep™ Miniprep Kit (Qiagen). The clone was then sequenced in the forward direction with primer LGMALE (5'–GGTCGTCAGACTGTCGATGAAGCC–3') and in the reverse direction with primer LGM13PUC (5'–CGCCAGGGTTTTCC CAGTCACGAC–3'). No mutations were detected. The purified plasmid was also used to transform *E. coli* BL21 cells via the Heat-Shock method. The clones were maintained as frozen stocks at -80°C, in LB broth supplemented with 20% glycerol.

#### **6.3.16.b. Overexpression and purification of MalE.pCclA**

Overnight cultures of the clone harbouring plasmid pMAL.FXA.pCclA were grown in 5 mL of LB broth (100  $\mu\text{g}/\text{mL}$  ampicillin, 0.2% (w/v) glucose) at 37°C for 16–18 h, 200 rpm. 1 L of fresh LB broth (100  $\mu\text{g}/\text{mL}$  ampicillin, 0.2%

(w/v) glucose) was inoculated (1%) with the overnight cultures and incubated at 37°C, 200 rpm until the OD<sub>600</sub> reached ~0.5. IPTG was added (to a final concentration of 0.3 mM) and the cultures were incubated for an additional 4 h. The cells were harvested by centrifugation (11,300 × g, 20 min, 4°C) and stored at -20°C.

The cells were resuspended in 150 mL amylose column buffer (20 mM Tris-Cl pH 7.2, 100 mM NaCl, 1 mM EDTA, 1 mM NaN<sub>3</sub>, 1 mM DTT), containing three complete EDTA-Free, protease inhibitors cocktail tablets (Roche Diagnostic). Cells were lysed using the cell disrupter, operating at 20 kpsi. After centrifugation (27,200 × g, 30 min, 4°C), the cleared lysate was diluted to 300 mL with amylose column buffer and loaded onto an amylose column at 1 mL/min. The column was washed with 600 mL amylose column buffer, after which the fusion protein was eluted by addition of 10 mM maltose to the buffer. Fractions containing the eluted protein (as shown by the UV<sub>280</sub> trace and SDS-PAGE analysis) were combined, transferred to dialysis tubing (MWCO 12 – 14 kDa) and dialyzed against 3.5 L of H<sub>2</sub>O (4°C, refreshed 3 times, 4 h each). The protein solution was then frozen (-20°C, then -80°C), lyophilized and stored at -20°C.

#### **6.3.16.c. Factor Xa digestion of Male.pCclA**

An initial pilot experiment was performed to examine the cleavage of the fusion protein. The fusion protein was resuspended in Factor Xa buffer (20 mM Tris-Cl pH 7.4, 100 mM NaCl, 2 mM CaCl<sub>2</sub>) to a concentration of 1 mg/mL. 1% Factor Xa (w/w) was added and the digestion proceeded at room temperature.

Aliquots were removed and quenched with acid after 4, 8, 20 and 24 h and analyzed by MALDI-TOF mass spectrometry. According to MALDI-TOF, the cleavage appeared complete by 4 hours. However, very little pCclA ( $m/z$  6418) was observed. Instead, smaller mass units were observed ( $m/z$  2862, 3547), suggesting the likelihood of secondary cleavage and overdigestion.

Additional pilot experiments were performed, in which the amount of Factor Xa was reduced to either 0.5% or 0.25% (w/w), the reaction temperature was reduced to 4°C. Aliquots were removed every 30 min (up to 4 h), acidified and analyzed by MALDI-TOF. Again, little to no pCclA was detected, although MALDI-TOF indicated that the fusion protein had been fully cleaved after 30–60 min. The same pilot experiments were repeated, but with the addition of 50% TFE to the digestion buffer. However, in this case, MALDI-TOF indicated that no digestion had occurred (even at 4 h), likely due to the inhibition of the Factor Xa by TFE.

Nonetheless, a large-scale digestion was performed, wherein 25 mg of MalE.pCclA (1 mg/mL solution) was cleaved with 0.4% Factor Xa (w/w). After 1 h, MALDI-TOF showed no remaining fusion protein and virtually no pCclA. Nonetheless, HPLC purification was attempted as follows:

**Method 1:** Purification with a  $C_{18}$  semipreparative column (Vydac 218TP510, 300 Å, 5 µm particle size, 10 × 250 mm) on a Varian Prostar HPLC. MeCN (0.1% TFA) and H<sub>2</sub>O (0.1% TFA) were used as solvents, according to the following gradient: (1) hold at 20% MeCN for 5 min; (2) increase to 50% MeCN over 15 min; (3) increase to 70% MeCN over 3 min; (4) decrease to 20% MeCN

over 1 min; (5) hold at 40% MeCN for 9 min. The method employed 1.0 mL injections, a flow rate of 3 mL/min and detection at 220 nm.

**Method 2:** Purification with a C<sub>18</sub> preparative column (Vydac 218TP1022, 300 Å, 10 µm particle size, 22 × 250 mm) on a Beckman System Gold HPLC. MeCN (0.1% TFA) and H<sub>2</sub>O (0.1% TFA) were used as solvents, according to the following gradient: (1) hold at 20% MeCN for 5 min; (2) increase to 86% MeCN over 20 min; (3) increase to 100% MeCN over 1 min; (4) hold at 100% MeCN for 2 min; (5) decrease to 20% MeCN over 1 min; (6) hold at 20% MeCN for 6 min. The method employed 2.0 mL injections, a flow rate of 10 mL/min and detection at 220 nm.

In both cases, 5 min fractions were collected, concentrated and lyophilized. After resuspending in a minimal volume of H<sub>2</sub>O (0.1% TFA), all fractions were analyzed by MALDI-TOF. pCclA could not be identified in any fraction.

### 6.3.17. Purification of pCclA as His<sub>6</sub>-tagged fusion protein

Since pCclA could not be successfully isolated following Factor Xa digestion of the MalE-fusion protein, a different strategy was adopted. Rather than using the bulky MalE affinity tag, a His<sub>6</sub>-tag was used. Two different constructs were prepared: one that incorporated a Factor Xa cleavage site between the His<sub>6</sub>-tag and the *cclA* structural gene, and another without the cleavage site.

### 6.3.17.a. Construction of pQE60.FXA.pCclA

Using plasmid pMAL.FXA.pCclA as a template, the *cclA* structural gene was amplified by PCR, with forward primer LAM16 (5'–ATATGAAATTCATTA AAGAGGAGAAATTAACCATGCATCACCATCACCATCACATCGAGGG AAGGATGTTATATGAATTAGTTGCATAT–3') and reverse primer LAM18 (5'–ATATAAAGCTTTAATAATTGAATTGCTTTTTTTTATTCC–3') that contained the *EcoRI* and *HindIII* restrictions sites, respectively (underlined). LAM16 also incorporated the His<sub>6</sub>-tag (bolded) and Factor Xa recognition sequence (in green). The PCR reaction (2 × 50 µL) consisted of: 10 µL of 10 × PCR buffer, 2 µL of dNTP mix, 2 µL of LAM16, 2 µL of LAM18, 2 µL of template, 2 µL of *PfuUltra* High Fidelity (5 U) and 80 µL H<sub>2</sub>O. Cycling conditions: (1) 95°C for 2 min; (2) 30 cycles of 95°C for 30 s, 55°C for 30s, 72°C for 60 s; (3) final extension 72°C for 10 min; (4) hold 4°C. Amplification of DNA was confirmed by agarose gel electrophoresis and the PCR product was purified with the QIAquick™ PCR Purification Kit.

The PCR product was cloned into the pQE60 expression vector by performing a double digestion, followed by ligation. The PCR product and vector were digested separately as follows: 2 µg of DNA was digested with 1 µL of *EcoRI* (10 U) and 1 µL of *HindIII* (10 U) in 5 µL of React Buffer 2 (Invitrogen) and H<sub>2</sub>O (final volume of 50 µL). The mixtures were incubated at 37°C for 4 h, and DNA was purified with the QIAquick™ PCR Purification Kit. For the ligation reaction, 25 ng of PCR product, 75 ng of vector DNA, 0.5 µL of T4 DNA Ligase (0.5 U), 1 µL of 5 × Ligase Reaction Buffer, and H<sub>2</sub>O (final volume of 5

μL) were mixed together and incubated at room temperature for 1 h. 2.5 μL of the reaction mixture was used to transform *E. coli* JM109 cells via electroporation. The transformed cells were streaked onto LB agar plates (150 μg/mL ampicillin) and incubated at 37°C. Several colonies were subcultured and their plasmid DNA purified with the QIAprep Miniprep Kit (Qiagen). The clones were screened by PCR and successful transformants were identified. Two of the clones (16.5 and 16.6) were sequenced in the forward and reverse directions using primers QE60F2 (5'–CATAAAAATTTATTTGCTTTGTG–3') and LAM18, respectively. No mutations were detected. The clones were maintained as frozen stocks at -80°C, in LB broth supplemented with 20% glycerol.

#### **6.3.17.b. Construction of pQE60.pCclA**

Plasmid pQE60.pCclA was cloned in exactly the same way as plasmid pQE60.FXA.pCclA, except that forward primer LAM17 (5'–ATATGAATTCAT TAAAGAGGAGAAATTAACCATGCAT**CACCATCACCATCACATGTTAT** ATGAATTAGTTGCATAT–3') was used in place of primer LAM16 for the amplification of the *cclA* structural gene. Primer LAM17 included the *EcoRI* restriction site (underlined) and His<sub>6</sub>-tag (bolded), but did not contain the Factor Xa recognition site. One clone (17.4) was sequenced (as described above) and no mutations were detected. The clone was maintained as a frozen stock at -80°C, in LB broth supplemented with 20% glycerol.

**6.3.17.c. Pilot expression of clone 16.5 (<sup>Met</sup>His<sub>6</sub>.FXa.pCclA)**

Pilot studies to examine protein expression were performed by summer student Erika Steels. The parameters that were investigated were incubation temperature and concentration of inducer. An overnight culture of clone 16.5 (expressing <sup>Met</sup>His<sub>6</sub>.FXa.pCclA) was grown in 5 mL LB broth (150 µg/mL ampicillin) at 37°C, 250 rpm. Two flasks, with 50 mL of fresh LB (150 µg/mL ampicillin) were inoculated (1%) with the overnight culture and incubated at either 30°C or 37°C, 250 rpm until the OD<sub>600</sub> reached ~0.5. After removing 1 mL for pre-induction samples, cultures from each flask were aliquoted (4 × 5 mL) into sterile test tubes and IPTG was added (final concentrations of 0.1, 0.3, 0.5 and 1.0 mM), as illustrated in Fig. 52. The tubes were incubated for an additional two hours, at either 30°C or 37°C, 250 rpm.

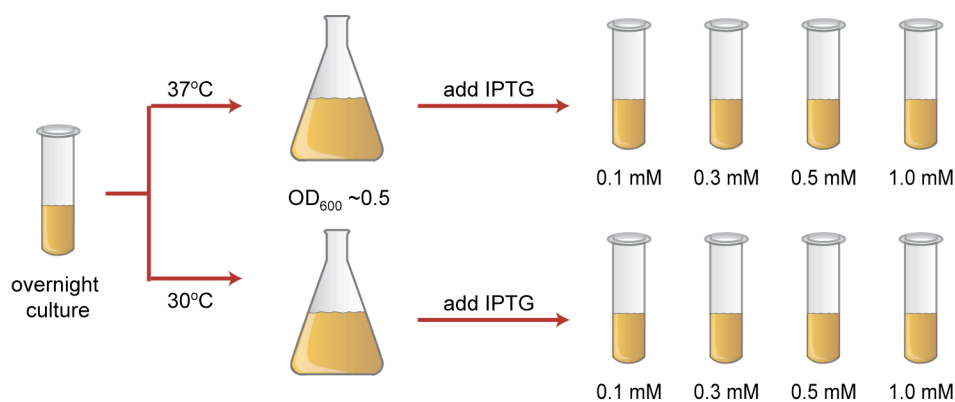


**FIG. 52.** Pilot expression of clone 16.5 to examine the effect of different growth temperatures and IPTG concentrations.

Samples for SDS-PAGE analysis were prepared as follows. 1 mL samples of the cultures were centrifuged (16,000 × g, 5 min, RT) and the cell pellets were resuspended in 200 µL of H<sub>2</sub>O. After addition of 50 µL PopCulture<sup>®</sup> Reagent

(Novagen) and 0.5  $\mu$ L Lysonase™ (Novagen), the samples were incubated for 10 min at room temperature. For the “total protein” fraction, 40  $\mu$ L of the cell lysate was mixed with 40  $\mu$ L of sample buffer (2  $\times$  Tris-Tricine sample buffer). The remaining lysate was centrifuged. For the “soluble protein” fraction, 40  $\mu$ L of the supernatant was mixed with 40  $\mu$ L of sample buffer. For the “pellet protein” (i.e.: inclusion bodies), the pellet was resuspended in 40  $\mu$ L of sample buffer. The pre-induction samples were prepared by centrifuging the 1 mL of cell culture and resuspending the pellet directly in 40  $\mu$ L of sample buffer. Samples were resolved on a 16.5% Tris-Tricine gel and visualized with GelCode stain (Pierce). Proteins were also analyzed by Western blot.

#### **6.3.17.d. Pilot expression of clone 17.4 (<sup>Met</sup>His<sub>6</sub>pCclA)**

The pilot expression of clone 17.4 (expressing <sup>Met</sup>His<sub>6</sub>pCclA) was performed in a similar fashion to that of clone 16.4, expect for the following changes: only overexpression at 37°C, with IPTG concentrations of 0.5 and 1.0 mM were tested. Protein samples were prepared with 6  $\times$  sample buffer and resolved on a 15% SDS-PAGE gel.

### **6.3.18. Construction of internally tagged His<sub>6</sub> pCclA mutants**

#### **6.3.18.a. pMG36e.pCclA.M1 – His<sub>6</sub> between I6 and A7**

Using plasmid pQE60-pCclA as a template, the *cclA* structural gene was amplified by PCR, with forward primer LAM6 (5'–ATATCTGCAGAGGAGG AAAAAAAAAATGTTATATGAATTAGTTGCATATGGTATCCATCACCATC

**ACCATCACGCACAAGGTACAGCTGAAAAGGTT**–3’) and reverse primer LAM7 (5’–ATATAAAGCTTTTATAATTGAATTGCTTTTTTTTATTCC–3’), which contained the *Pst*I and *Hind*III restriction sites, respectively (underlined). Primer LAM6 also incorporated the internal His<sub>6</sub>-tag (bolded). The PCR reaction (2 × 50 µL) consisted of: 10 µL of 10 × PCR buffer, 2 µL of dNTP mix, 2 µL of LAM6, 2 µL of LAM7, 2 µL of template, 2 µL of *PfuUltra* High Fidelity (5 U) and 80 µL H<sub>2</sub>O. Cycling conditions: (1) 95°C for 2 min; (2) 30 cycles of 95°C for 30 s, 55°C for 30s, 72°C for 60 s; (3) final extension 72°C for 10 min; (4) hold 4°C. Amplification of DNA was confirmed by agarose gel electrophoresis and the PCR product was purified with the QIAquick™ PCR Purification Kit.

The PCR product was cloned into the pMG36e vector by performing a double digestion, followed by ligation. The PCR product was digested as follows: 2 µg of DNA was digested with 1 µL of *Pst*I (10 U) and 1 µL of *Hind*III (10 U) in 5 µL of 10 × React Buffer 2 (Invitrogen) and H<sub>2</sub>O (final volume of 50 µL). The mixture was incubated at 37°C for 3 h, and DNA was purified with the QIAquick™ PCR Purification Kit. The plasmid DNA had previously been cut and purified (described in section 6.4.2.a). For the ligation, 20 ng of PCR product, 80 ng of vector DNA, 1 µL of T4 DNA Ligase (1 U), 2 µL of 5 × Ligase Reaction Buffer, and H<sub>2</sub>O (final volume of 10 µL) were mixed together and incubated at room temperature for 1 h. 2.5 µL of the reaction mixture was used to transform *E. coli* JM109 cells via electroporation. The transformed cells were streaked onto LB agar plates (200 µg/mL erythromycin) and incubated at 37°C. Several colonies were subcultured and their plasmid DNA purified with the QIAprep™ Miniprep

Kit (Qiagen). The clones were screened by PCR and successful transformants were then sequenced in the forward direction using primer SG (5'–CGGTTACTTTGGATTTTGTGA –3'). Unfortunately, no transformants containing the correct insert were obtained.

#### 6.3.18.b. pMG36e.pCclA.M4 – His<sub>6</sub> between Q52 and G53

Mutant 4 (pMG36e.pCclA.M4) was constructed in the same manner as mutant 1 (pMG36e.pCclA.M1), except that different primers were utilized. Forward primer LAM14 (5'–ATATCTGCAGAGGAGGAAAAAAAAATGTTATATGAA–3') included the *Pst*I restriction site (underlined), whereas reverse primer LAM15 (5'–ATATAAGCTTTTATAATTGAATTGCTTTTTTTTATTCC**GTGATGGT**GATGGT**GATGTTGTTTAGCAATTGCTGCTTTAAC**–3') included the *Hind*III restriction site (underlined), as well as the internal His<sub>6</sub>-tag (bolded). Sequencing of transformants indicated that the desired insert had been successfully incorporated.

Plasmid pMG36e.pCclA.M4 was subsequently transformed into *C. maltaromaticum* UAL307. The cells were made electrocompetent and transformed with 1 µL of plasmid DNA via electroporation. The cells were streaked onto APT agar plates (5 µg/mL erythromycin), supplemented with 0.5 M sucrose and incubated at 25°C for 5–6 d. Colonies were subcultured in 10 mL of APT broth (5 µg/mL erythromycin), incubated at 25°C for 24 h and then maintained as frozen stocks at -80°C, in APT broth supplemented with 20% glycerol.



were mixed together and subjected to the following cycling conditions: (1) 95°C for 2 min; (2) 7 cycles of 95°C for 20 s, 46°C for 60s, 72°C for 30 s; (3) hold 24°C. Then, 1 µL of LAM8 and 1 µL LAM11 were added and the following cycling conditions were used: (1) 95°C for 2 min; (2) 35 cycles of 95°C for 20 s, 50°C for 20s, 72°C for 30 s; (3) final extension 72°C for 3 min; (4) hold 10°C. Amplification of DNA was confirmed by agarose gel electrophoresis and the PCR product was purified with the QIAquick™ PCR Purification Kit.

The pCclA.M2 PCR product was cloned into the pMG36e vector and transformed into *E. coli* JM109 in the same manner as described above for pCclA.M1. After identification and sequencing of successful transformants, plasmid pQE60.pCclA.M2 was then transformed into *C. maltaromaticum* UAL307 cells, as described for plasmid pQE60.pCclA.M4.

#### 6.3.18.d. pMG36e-pCclA.M3 – His<sub>6</sub> between G33 and V34

Recombinant PCR was also used to prepare the pCclA.M3 insert, in exactly the same way as pCclA.M2 was prepared, except that two different primers were used. To prepare M3.A, reverse primer LAM12 (5'–GACGTGATG **GTGATGGT**GATGCCACCCAAAATTGAAATAATAGA–3') was used in place of LAM9. This primer incorporated the internal His<sub>6</sub>-tag (bolded), but at a different position. To prepare M3.B, forward primer LAM13 (5'–GGGCATCAC **CATCACCATCAC**GTACAGTCGGTTTATCAGGTGTC–3') was used in place of LAM10. The pCclA.M3 PCR product was cloned into the pMG36e

vector and transformed into both *E. coli* JM109 and *C. maltaromaticum* UAL307 cells, as described above.

### 6.3.19. Pilot expression of pCclA mutants

Overnight cultures of *C. maltaromaticum* UAL307 harbouring the mutant plasmids were grown in 10 mL of APT broth (5 µg/mL erythromycin) at 24°C for 18–24 h. Flasks containing 50 mL of fresh APT (5 µg/mL erythromycin) were inoculated (1%) with the overnight cultures and incubated for an additional 24 h at room temperature. The wild-type strain was also cultured in this manner, except without erythromycin in the growth media. The cultures were then centrifuged (11,300 × g, 20 min, 4°C) and both the supernatant and cell pellets were analyzed. 50 µL of supernatant was mixed with 50 µL 2 × Tris-Tricine sample buffer. The cell pellet (from 1 mL of culture) was resuspended in 100 µL of H<sub>2</sub>O and 100 µL of 2 × Tris-Tricine sample buffer.

The samples were analyzed by Tris-tricine gel electrophoresis (16.5% gel) and Western blot. The supernatant was partially purified by hydrophobic interaction chromatography, as follows. The supernatant was loaded onto a Megabond C<sub>18</sub> cartridge (prewashed with MeOH and H<sub>2</sub>O). The column was washed with 50 mL of 30% EtOH and 30% MeCN, before eluting the peptides with 60 mL of 70% IPA pH2. This fraction was concentrated and lyophilized. The partially purified peptides were resuspended in H<sub>2</sub>O (0.1% TFA) and analyzed by MALDI-TOF and 16.5% Tris-Tricine gel electrophoresis.

## 6.4. Experimental procedures for the investigation of the type IIa bacteriocins, their immunity proteins & mode of action

### 6.4.1. Plasmids, bacterial strains and culture conditions

The plasmids and bacterial strains used in this study are listed in Table 11.

Biological experiments were performed as previously described (section 6.3.1).

Unless otherwise stated, percentage concentration implies v/v.

**TABLE 11.** Plasmids and bacterial strains used for the study of PisA, PisI and the EII<sub>t</sub><sup>man</sup> permease

Plasmid or Strain	Relevant Characteristics <sup>c</sup>	Ref. or Source
pMG36e	Expression vector, Em <sup>r</sup> , 3.6 kb	(291)
pMAL <sup>TM</sup> -c2X	Amp <sup>r</sup> , <i>lacI</i> , <i>lacZα</i> and <i>malE</i> expression vector, 6648 bp	NEB
pQE60	Expression vector, Amp <sup>r</sup> , 3.4 kb	Qiagen
pREP4	Constitutive expression of <i>lac</i> repressor protein, Kan <sup>r</sup> ;	Qiagen
pMG36e.PisI	pMG36e containing <i>pisI</i>	This study
<sup>a</sup> pMAL-PisA	pMAL <sup>TM</sup> -c2X containing <i>malE-FXA-pisA</i> (without leader peptide sequence) fusion	This study
<sup>a</sup> pMAL-PisI	pMAL <sup>TM</sup> -c2X containing <i>malE-FXA-pisI</i> fusion	This study
pMV12	pQE60 containing <i>mptC</i> , His <sub>6</sub> -tag (C)	This study
pQE60.mptAB	pQE60 containing <i>mptAB</i> , His <sub>6</sub> -tag (C)	This study
<sup>b</sup> pMV24	pQE60 containing <i>mptD</i> , His <sub>6</sub> -tag (C)	This study
<i>E. coli</i> K12 TB1	F <sup>-</sup> <i>ara Δ(lac-proAB) [Φ80dlac Δ(lacZ)M15] rpsL(Str<sup>R</sup>) thi hsdR</i>	NEB
<i>E. coli</i> BL21(DE3)	F <sup>-</sup> <i>ompT hsdS(r<sub>B</sub><sup>-</sup> m<sub>B</sub><sup>-</sup>) dcm<sup>+</sup> Tet<sup>r</sup> gal λ(DE3)</i> ; bacteriophage DE3 lysogen carrying the T7 RNA polymerase gene controlled by the <i>lacUV5</i> promoter; general purpose expression host	Stratagene
<i>E. coli</i> JM109	E14(McrA) <i>recA1 endA1 gyrA96 thi-1 hsdR17 (r<sub>K</sub><sup>-</sup>m<sub>K</sub><sup>+</sup>) supE44 relA1 Δ(lac-proAB) [F<sup>+</sup> <i>traD36 proAB lacI<sup>q</sup>ZΔM15]</i>; general purpose strain for cloning and propagating plasmids</i>	(134)
<i>E. coli</i> M15[pREP4]	M15 phenotype: NaI <sup>S</sup> , Str <sup>S</sup> , Rif <sup>S</sup> , Thi <sup>-</sup> , Lac <sup>-</sup> , Ara <sup>+</sup> , Gal <sup>+</sup> , Mtl <sup>-</sup> , F <sup>-</sup> , RecA <sup>+</sup> , Uvr <sup>+</sup> , Lon <sup>+</sup> ; with pREP4 plasmid, used for tightly regulated expression	Qiagen
<i>Carnobacterium maltaromaticum</i> UAL26	Plasmid-free, PisA producer	(24)
<i>C. divergens</i> LV13	Wild-type divergicin A producer, PisA sensitive	(128)
<i>C. piscicola</i> LV17C	Plasmid-free, PisA sensitive	(127)

<sup>a</sup> prepared by Dr. Lucas Gursky; <sup>b</sup> prepared by Dr. Marco van Belkum; <sup>c</sup> FXA denotes the Factor Xa recognition sequence (IEGR)

## 6.4.2. Heterologous expression of *PisI*

### 6.4.2.a. Construction of pMG36e.*PisI*

Using crude DNA isolated from *C. maltaromaticum* UAL26 as a template, the *pisI* gene was amplified by PCR using primers LAM2 (5'–ATATAAAGCTTCTAATATCCATATCTAATATTGGA–3') and LAM3 (5'–ATTATATCTGCAGAATAATTAAGGAGTGATATTTTATGGG–3'), containing the *HindIII* and *PstI* restriction sites, respectively (underlined). The PCR reaction mixture (50  $\mu$ L) contained 5  $\mu$ L of 10  $\times$  PCR buffer, 1.25  $\mu$ L of dNTP mix, 1  $\mu$ L of LAM2, 1  $\mu$ L of LAM3, 1  $\mu$ L of template DNA, 1  $\mu$ L *PfuUltra* High Fidelity (2.5 U), and 39.75  $\mu$ L of H<sub>2</sub>O. Cycling conditions: (1) 95°C for 2 min; (2) 30 cycles of 95°C for 30 s, 55°C for 30s, 72°C for 60 s; (3) final extension 72°C for 10 min; (4) hold 4°C. Amplification of DNA was confirmed by agarose gel electrophoresis and the PCR product was purified with the QIAquick™ PCR Purification Kit. The pMG36e vector was isolated from *E. coli* JM109 harbouring this plasmid, using the HiSpeed Plasmid Midi Kit (Qiagen).

The PCR product was then cloned into the *PstI* and *HindIII* site of the pMG36e vector by performing double digestions, followed by ligation. The PCR product was digested as follows: 2  $\mu$ g of PCR product was digested with 1  $\mu$ L *PstI* (10 U) and 1  $\mu$ L *HindIII* (10 U), in 5  $\mu$ L of 10  $\times$  React 2 buffer (Invitrogen) and H<sub>2</sub>O (final volume 50  $\mu$ L). The pMG36e vector was digested in a similar fashion, except that 1  $\mu$ g of plasmid DNA was digested. The digestion reactions were incubated at 37°C for 3 h, and DNA was purified with the QIAquick™ PCR Purification Kit. For the ligation reaction, 50 ng of PCR product, 50 ng of vector

DNA, 0.5  $\mu\text{L}$  of T4 DNA Ligase (0.5 U) and 1.25  $\mu\text{L}$  of 5  $\times$  Ligase Reaction Buffer were mixed together (final volume of 6.75  $\mu\text{L}$ ) and incubated at room temperature for 2 h. 2.5  $\mu\text{L}$  of the reaction mixture was then used to transform *E. coli* JM109 cells via electroporation. The transformed cells were streaked onto LB agar plates (200  $\mu\text{g}/\text{mL}$  erythromycin) and incubated at 37°C for 16–18 h. Several colonies were subcultured, and their crude DNA was isolated and screened by PCR to identify successful transformants. Prior to sequencing, it was necessary to obtain pure plasmid DNA. As such, 4 successful transformants (clones M1, S2, S4 and S7) were subcultured and their DNA was purified using the HiSpeed Plasmid Midi Kit (Qiagen). The DNA was precipitated by the addition of 3M sodium acetate (40  $\mu\text{L}$ ) and 1 mL of 95% EtOH. The DNA was chilled overnight at 4°C, after which the DNA was pelleted by centrifugation (16,000  $\times$  g, 20 min, 4°C). The pellets were washed twice with 400  $\mu\text{L}$  of ice-cold 70% EtOH, dried under vacuum, redissolved in H<sub>2</sub>O and stored at -20°C. The transformants M1, S2, S4 and S7 were then sequenced in the forward direction, using primer SG (5'–CGGTTACTTTGGATTTTTGTGA –3'). Clones successfully incorporating the *pisI* gene were identified.

Plasmid pMG36e.PisI was transformed into two PisA sensitive strains, *C. maltaromaticum* LV13 and LV17C. Both strains were made electrocompetent and transformed with 2.5  $\mu\text{L}$  of plasmid DNA (clone S2) via electroporation. The cells were streaked onto APT agar plates (5  $\mu\text{g}/\text{mL}$  erythromycin), supplemented with 0.5 M sucrose and incubated at 25°C for 5–6 d. Colonies were subcultured in 10 mL of APT broth (5  $\mu\text{g}/\text{mL}$  erythromycin), incubated at 25°C for 24 h and

then maintained as frozen stocks at  $-80^{\circ}\text{C}$ , in APT broth supplemented with 20% glycerol.

#### **6.4.2.b. Activity testing**

The activity of purified PisA (purification described below, in section 6.4.5) was tested against wild-type *C. divergens* LV13 and *C. piscicola* LV17C, as well as *C. divergens* LV13 and *C. piscicola* LV17C harbouring the pMG36e.PisI plasmid. For the growth and testing of the mutant strains, erythromycin (5  $\mu\text{g}/\text{mL}$ ) was added to the media. Overnight cultures were grown in 10 mL of APT broth and incubated at  $25^{\circ}\text{C}$  for 24 h. Soft APT agar was inoculated (1%) with the overnight cultures and overlaid on a bed of hard APT agar. Starting with a stock solution of PisA (250  $\mu\text{M}$ ), serial two-fold dilutions were prepared, by dilution with  $\text{H}_2\text{O}$ . In total, eight dilutions were prepared. 10  $\mu\text{L}$  of each solution, including the stock, was then spotted onto the plates and allowed to dry. The plates were incubated at  $25^{\circ}\text{C}$  for 24 h and examined for zones of growth inhibition.

### **6.4.3. Construction of fusion proteins**

#### **6.4.3.a. pMAL-PisA**

Dr. Lucas Gursky prepared the pMAL-PisI plasmid and transformed it into *E. coli* K12 TB1 (156). As this strain is not amenable for growth in minimal media, it was decided that *E. coli* BL21(DE3) could be used as an alternate host strain. An overnight culture of *E. coli* K12 TB1 with the pMAL-PisI plasmid was

grown in 5 mL of LB broth (200 µg/mL ampicillin), at 37°C, 250 rpm. Plasmid DNA was isolated from 4 mL of culture, using the QIAprep™ Miniprep Kit (Qiagen). *E. coli* BL21(DE3) competent cells (Stratagene) were transformed with 1 µL of plasmid DNA, according to the manufacturer's protocol. Clones were subcultured and maintained as frozen stocks at -80°C in LB broth supplemented with 20% glycerol.

#### **6.4.3.b. pMAL-PisI**

Dr. Lucas Gursky also prepared the pMAL-PisI plasmid and transformed it into *E. coli* K12 TB1 (156). To facilitate overexpression of the MalE-PisA fusion protein in minimal media, the plasmid was isolated and transformed into *E. coli* BL21(DE3) competent cells, in the same manner as described above for pMAL-PisA.

#### **6.4.4. Purification of PisI, [<sup>13</sup>C,<sup>15</sup>N]PisI and [<sup>15</sup>N]PisI**

##### **6.4.4.a. Overexpression and purification of MalE-PisI**

Growth conditions for the overexpression of the MalE-PisI fusion protein, using *E. coli* TB1 K12 with plasmid pMAL-PisI, were initially worked out by Dr. Karen Kawulka. For production of unlabelled protein, LB broth was used, whereas Celtone-CN rich media (Spectra Stable Isotopes) was used for the production of [<sup>13</sup>C,<sup>15</sup>N] labeled protein. To reduce the costs associated with preparation of isotopically enriched proteins, M9 minimal media was used to propagate *E. coli* BL21(DE3) cells. To prepare <sup>13</sup>C,<sup>15</sup>N-enriched protein,

$(^{15}\text{NH}_4)_2\text{SO}_4$  and  $[\text{U-}^{13}\text{C}]\text{-D-glucose}$  (99% isotopic purity, Cambridge Isotope Laboratories) were used as the sole nitrogen and carbon sources, respectively. For  $^{15}\text{N}$ -enriched protein,  $(^{15}\text{NH}_4)_2\text{SO}_4$  and unlabelled glucose were used. The M9 minimal media was prepared as follows: for 500 mL of media, 100 mL of 5 × M9 salts (0.043 M NaCl, 0.11 M  $\text{KH}_2\text{PO}_4$  and 0.25 M  $\text{Na}_2\text{HPO}_4 \cdot 7\text{H}_2\text{O}$ ) was diluted with 400 mL of milli-Q water and sterilized. The following components were then added (all filter sterilized): 5 mL of 20% glucose, 1.25 mL of 20%  $(\text{NH}_4)_2\text{SO}_4$ , 1 mL of 1M  $\text{MgSO}_4$ , 0.5 mL of 0.1 M  $\text{CaCl}_2$ , 50  $\mu\text{L}$  10 mM  $\text{FeSO}_4$  and 50  $\mu\text{L}$  10 mg/mL thiamine.

Regardless of the strain, overnight cultures were prepared in 5 mL of LB broth (100  $\mu\text{g}/\text{mL}$  ampicillin) and incubated at 37°C, 200 rpm for 16–18 h. The desired media (either LB broth, Celtone-CN or M9 minimal media; 100  $\mu\text{g}/\text{mL}$  ampicillin) was then inoculated (1%) with the overnight cultures and the cultures were grown at 37°C, 200 rpm. When the  $\text{OD}_{600}$  reached  $\sim 0.5$ , overexpression of the recombinant protein was induced by the addition of IPTG (final conc. 0.3 mM) and the cultures were incubated for an additional three hours. The cells were harvested by centrifugation (11,300 × g, 20 min, 4°C), resuspended in  $\sim 75$  mL amylose column buffer (20 mM Tris-HCl pH 7.4, 200 mM NaCl, 1 mM EDTA, 1 mM  $\text{NaN}_3$ , 1 mM DTT) containing two complete EDTA-Free, protease inhibitors tablets (Roche Diagnostics) and stored at -80°C. Cell lysis was achieved by the addition of lysozyme ( $\sim 10$  mg) and three consecutive freeze-thaw cycles, followed by sonication. The resulting solution was centrifuged (27,200 × g, 30 min, 4°C) and the lysate was diluted to 300 mL with column buffer and applied to

a column of amylose resin. The column was washed with amylose column buffer and the fusion protein was eluted with column buffer containing 10 mM maltose. The resulting protein solution was dialyzed against water, lyophilized and stored at  $-80^{\circ}\text{C}$  until further use.

#### **6.4.4.b. Digestion with Factor Xa**

PisI was cleaved from MalE using Factor Xa. 0.5% (w/w) of Factor Xa was added to a 1 mg/mL solution of the fusion protein in digestion buffer (20 mM Tris-HCl pH 8.0, 100 mM NaCl, 2 mM  $\text{CaCl}_2$ ). The mixture was allowed to digest at room temperature for 18 hours. AEBSF was then added to the solution (final concentration of 0.1 mM) to irreversibly inhibit the enzyme and prevent secondary cleavage.

#### **6.4.4.c. Cation exchange**

Following the cleavage reaction, the solution was dialyzed (MWCO 6000–8000 Da) against 1 L of column buffer (50 mM sodium phosphate pH 6.8, 20 mM NaCl,  $4^{\circ}\text{C}$ , refreshed 3 times, 4 h each) to remove excess NaCl. Alternatively, buffer exchange was performed with a concentrating tube ( $5000 \times g$ ,  $4^{\circ}\text{C}$ , MWCO 5K, Amicon), according to the manufacturer's instructions. The solution was then applied to a column of SP-Sepharose, equilibrated with column buffer, and monitored by  $\text{UV}_{280}$ . After the Factor Xa and MalE components had passed through the column, PisI was eluted by increasing the concentration of NaCl in the column buffer to 500 mM. The purity of the fractions containing PisI

was confirmed by SDS-PAGE electrophoresis and MALDI-TOF mass spectrometry.

#### **6.4.4.d. RP-HPLC**

PisI was further purified by RP-HPLC, using a C<sub>18</sub> preparative column (Vydac 218TP1022, 300 Å, 10 µm particle size, 22 × 250 mm) on a Varian Prostar HPLC. MeCN (0.1% TFA) and H<sub>2</sub>O (0.1% TFA) were used as solvents, according to the following gradient: (1) hold at 40% MeCN for 4 min; (2) increase to 70% MeCN over 13 min; (3) hold at 70% MeCN; (4) decrease to 40% MeCN over 1 min; (5) hold at 40% MeCN for 4 min. The method employed 1.0-2.0 mL injections, a flow rate of 10 mL/min and detection at 220 nm. PisI eluted as a single peak, with a retention time of 12 min, as identified by MALDI-TOF mass spectrometry.

#### **6.4.5. Purification of PisA and [<sup>15</sup>N]PisA**

##### **6.4.5.a. Overexpression and purification of MalE-PisA**

*E. coli* BL21(DE3) cells harboring the plasmid pMAL-PisA were grown at 37°C, 200 rpm in either LB broth or M9 minimal media with (<sup>15</sup>NH<sub>4</sub>)<sub>2</sub>SO<sub>4</sub> as the sole nitrogen source, with ampicillin (100 µg/mL). Overexpression and purification of the MalE-PisA fusion protein was done in the same manner as previously described for MalE-PisI.

#### 6.4.5.b. Digestion with Factor Xa

PisA was cleaved from MalE with Factor Xa. During initial studies, it was discovered that PisA precipitated out of solution. Thus, the salt concentration of the Factor Xa buffer solution was increased to 150 mM NaCl. The fusion protein was dissolved (1 mg/mL) in buffer (20 mM Tris-HCl pH 8.0, 150 mM NaCl, 2 mM CaCl<sub>2</sub>) and 0.5% (w/w) Factor Xa was added. Digestion was complete after eight hours at room temperature, as indicated by MALDI-TOF. Pilot studies revealed that PisA was prone to secondary cleavage if exposed to Factor Xa for too long (> 8 h), thus AEBSF was added (final conc. 0.1 mM) to inhibit the enzyme and prevent secondary cleavage.

#### 6.4.5.c. RP-HPLC

PisA was purified by RP-HPLC using a C<sub>18</sub> preparative column (Vydac 218TP1022, 300 Å, 10 µm particle size, 22 × 250 mm) on a Varian Prostar HPLC. MeCN (0.1% TFA) and H<sub>2</sub>O (0.1% TFA) were used as solvents, according to the following gradient: (1) hold at 20% MeCN for 5 min; (2) increase to 50% MeCN over 15 min; (3) increase to 70% MeCN over 3 min; (4) decrease to 20% MeCN over 1 min; (5) hold at 20% MeCN for 4 min. The method employed 1.0-2.0 mL injections, a flow rate of 10 mL/min and detection at 220 nm. AEBSF, PisA and MalE eluted as a single peaks, with retention times of 13.6 min, 17.5 min and 21.5 min, respectively. The identity of PisA and MalE were confirmed by MALDI-TOF mass spectrometry. Purified PisA was concentrated by rotary evaporation, lyophilized and stored at -80°C.

#### 6.4.6. Circular dichroism

Wayne Moffat acquired the CD data for PisA and PisI. Concentrations of 0.5 mg/mL were used for both PisA and PisI, corresponding to 0.11 mM and 0.045 mM respectively. In the first set of experiments (aqueous conditions), both PisA and PisI were dissolved in buffer consisting of 20 mM sodium phosphate pH 6.0, 1 mM EDTA and 1 mM NaN<sub>3</sub>. In the second set of experiments, PisA and PisI were dissolved in 50% TFE in aqueous buffer (same as above). For both sets of experiments, baseline spectra of the appropriate solvent system were subtracted from the sample spectra prior to calculating molar ellipticities. Results were expressed in units of molar ellipticity (deg cm<sup>2</sup> dmol<sup>-1</sup>) and plotted against the wavelength.

#### 6.4.7. NMR spectroscopy of [<sup>15</sup>N]PisI and [<sup>13</sup>C,<sup>15</sup>N]PisI

NMR samples contained ~0.5 mM protein in 90% H<sub>2</sub>O/10% D<sub>2</sub>O or 100% D<sub>2</sub>O, 20 mM sodium phosphate (pH 5.9), 1 mM EDTA, 1 mM NaN<sub>3</sub> and 50 μM 2,2-dimethyl-2-silapentane-5-sulfonate sodium salt (DSS). A high quality D<sub>2</sub>O-matched Shigemi NMR tube was used. NMR spectra were acquired at 25°C on Varian Inova 500 MHz and 800 MHz spectrometers equipped with triple-resonance HCN cold probes and z-axis pulsed-field gradients. The following experiments were used for backbone and side-chain <sup>1</sup>H, <sup>13</sup>C, and <sup>15</sup>N resonance assignments: <sup>15</sup>N HSQC, <sup>15</sup>N TOCSY-HSQC, <sup>15</sup>N NOESY-HSQC, HNHA, HNCACB, CBCA(CO)NH, C(CO)NH, <sup>13</sup>C HSQC, <sup>13</sup>C HCCH-TOCSY, <sup>13</sup>C HCCH-COSY, <sup>13</sup>C NOESY-HSQC. NMR spectra were processed using

NMRPIPE (295) and analyzed with NMRView (296). Data were multiplied by a 90° shifted sine-bell squared function in all dimensions. Indirect dimensions were doubled by linear prediction and zero-filled to the nearest power of two prior to Fourier transformation.

#### 6.4.8. Structure calculations

NOE restraints were obtained from the <sup>15</sup>N- and <sup>13</sup>C- edited NOESY-HSQC experiments and  $\phi$  angle restraints were derived from analysis of the diagonal-peak to cross-peak intensity ratio in the HNHA experiment. The structure of PisI was calculated by using the CANDID module in the program CYANA 2.1 (142), using a combination of manually and automatically assigned NOEs (manual inspection of the peaks was necessary due to the presence of degraded material). Peaks were calibrated according to their intensities. A family of 100 random structures was generated and subjected to simulated annealing, with 10 000 torsion angle dynamic steps. After seven rounds of calculation, 2627 of the initial 2915 peaks were assigned. After accounting for symmetric peaks, a total of 1725 upper distance restraints and 76  $\phi$  dihedral angles were used in the final round of calculations. The twenty lowest energy conformations (no NOE violations of  $>0.3$  Å with no residues in the disallowed region of the Ramachandran plot) were chosen as representative of the solution structure of PisI. The backbone rmsd for residues 13-92 was 0.56 Å. Structural statistics were calculated with CYANA (142) and MOLMOL (299). Figures were generated with PyMOL, PDB2PQR (300), APBS (297) and MOLMOL. Coordinates have been

deposited in the PDB data bank, with the accession code 2K19. Chemical shift assignments have been deposited under BMRB accession number 15763.

#### **6.4.9. Titration of [<sup>15</sup>N]PisA with PisI**

##### **6.4.9.a. Aqueous conditions**

[<sup>15</sup>N]PisA was dissolved in the same buffer used for the NMR studies of PisI (described above) to a concentration of 0.7 mM, as estimated by UV<sub>280</sub>. The <sup>15</sup>N HSQC spectrum of [<sup>15</sup>N]PisA was recorded in the presence of 0, 0.5, 1.0 and 2.0 molar equivalents of unlabelled PisI. Spectra were acquired at 25°C on a Varian Inova 600 MHz spectrometer, equipped with a triple-resonance HCN probe. NMR spectra were processed and analyzed as described above.

##### **6.4.9.b. 50% TFE**

To induce helicity in the bacteriocin, [<sup>15</sup>N]PisA was dissolved in 50% TFE / aqueous buffer as follows: [<sup>15</sup>N]PisA was initially dissolved in aqueous buffer (40 mM sodium phosphate pH 6.0, 2 mM EDTA, 2 mM NaN<sub>3</sub> and 100 μM DSS). An equivalent volume of *d*<sub>3</sub>-TFE was then added. The concentration of [<sup>15</sup>N]PisA was estimated to be 0.6 mM by UV<sub>280</sub>. The <sup>15</sup>N HSQC spectrum of [<sup>15</sup>N]PisA was recorded in the presence of 0 and 1.1 molar equivalents of unlabelled PisI (also prepared in the same 50% TFE / aqueous buffer). NMR spectra were processed and analyzed as described above.

#### 6.4.10. Construction of pMV24

With the assistance of Dr. Marco van Belkum, *mptC* was cloned into the pQE60 vector. Using genomic DNA, purified from *Listeria monocytogenes* EGD-e (isolated by Dr. Sandra Marcus) as a template, the *mptC* gene was amplified by PCR using primers MVB5 (5'–ATATCCATGGATTAAGAGGAGAATAAT TATGTCTGTCATATCAATAATTTTAG–3') and MVB6 (5'–ATATAAAGCTT **AGTGATGGT**GATGGT**GATG**ATAGTCGTTTAATATATCGCC–3'), which contained the *Nco*I and *Hind*III restriction sites, respectively (underlined). Primer MVB6 also incorporated a C-terminal His<sub>6</sub>-tag (bolded). The PCR reaction mixture (2 × 50 µL) consisted of 10 µL 10 × PCR buffer, 4 µL of MgSO<sub>4</sub>, 2 µL dNTP mix, 1 µL MVB5, 1 µL of MVB6, 1 µL of template DNA, 0.5 µL of Platinum<sup>®</sup> *Taq* High Fidelity, and 80.5 µL H<sub>2</sub>O. Cycling conditions: (1) 94°C for 30 s; (2) 35 cycles of 94°C for 30 s, 55°C for 30 s, 68°C for 60 s; (3) final extension 68°C for 10 min; (4) hold 4°C. Amplification of DNA was confirmed with agarose gel electrophoresis, stained with EtBr. The PCR product was purified with the QIAquick<sup>™</sup> PCR Purification Kit.

The PCR product was then cloned into the *Nco*I and *Hind*III site of the pQE60 vector by performing double digestions, followed by ligation. The PCR product was digested as follows: 15 µL of PCR product (~2 µg) was digested with 1 µL *Nco*I (10 U) and 1 µL *Hind*III (10 U), in 5 µL of 10 × React 2 buffer (Invitrogen) and H<sub>2</sub>O (up to 50 µL). The pQE60 vector was digested in a similar fashion, except that 1 µg of plasmid DNA was digested. The digestion reactions were incubated at 37°C for 2.5 h. The DNA was purified by phenol-chloroform

extraction followed by sodium acetate / EtOH precipitation. The purified DNA was resuspended in 5  $\mu$ L of H<sub>2</sub>O.

For the ligation reaction, 1.5  $\mu$ L of PCR product, 1.5  $\mu$ L of vector DNA, 0.5  $\mu$ L of T4 DNA Ligase (0.5 U), 1  $\mu$ L of 5  $\times$  Ligase Reaction Buffer and 0.5  $\mu$ L of H<sub>2</sub>O were mixed together (final volume of 5  $\mu$ L) and incubated at room temperature for 2 h. 3  $\mu$ L of the reaction mixture was used to transform chemically competent *E. coli* JM109 cells, via the Fermentas TransformAid™ Kit. The transformed cells were streaked onto LB agar plates (100  $\mu$ g/mL ampicillin) and incubated at 37°C for 24 h. Eleven different colonies were subcultured, and their plasmid DNA was purified via the alkaline-lysis & phenol/chloroform extraction method, followed by sodium acetate / EtOH precipitation. The clones were screened by PCR and two (clones 5 and 6) were identified as successful transformants.

A large-scale DNA purification was performed on clone 5, using the Alkaline-Lysis & EtBr/CsCl Density Gradient method (section 6.2.9, Method 1). The DNA was sequenced in the forward direction, using primers SM91 (5'–CGC ATGTACATTAATTGGTCTCG–3') and SM92 (5'–GTATGGCTATCGGTGGA GGAATGG–3'), and in the reverse direction using primer MVB11 (5'–GTCCAT CAAGTGAACAATTGG–3'). However, inspection of the sequence revealed a mutation within the His<sub>6</sub>-tag. Therefore, plasmid DNA from clone 6 was isolated, using the QIAprep™ Miniprep Kit (Qiagen). The DNA was sequenced in the forward direction, using primers SM91 and SM92, and in the reverse direction,

using primers MVB6 and MVB11. Sequence results revealed that clone 6 had the correct insert.

Chemically competent *E. coli* M15[prep4] cells were subsequently transformed with 1  $\mu$ L of plasmid DNA from clone 6. Colonies were subcultured in 5 mL of LB (100  $\mu$ g/mL ampicillin and 25  $\mu$ g/mL kanamycin) and incubated at 37°C, 250 rpm for 16 h, after which stock cultures were prepared and stored at -80°C, in LB broth supplemented with 20% glycerol.

#### 6.4.11. Construction of pQE60.mptAB

To clone *mptAB* into the pQE60 vector, neither the *Nco*I nor *Bam*HI restriction sites could be used, as both recognition sequences appeared within the *mptAB* structural gene. Therefore, an alternative approach was taken: *mptAB* was amplified using a primer that would incorporate the restriction site for *Bsp*HI (at the 5' position of the gene). Upon digestion, this would generate a sticky end complementary to the *Nco*I site of the pQE60 vector. Thus, *mptAB* was amplified by PCR using the same template as for *mptC* (see above), but with forward primer LAMB (5'–ATATTCATGAATTAAGAGGAGAATAATTATGGTAGGAATTATCCTCGCA–3') and reverse primer LAMC (5'–ATATAGATCTTTAGTGATGGTGATGGTGATGTTGTGTCTTTAATTCGTGTTTTG–3'), containing the *Bsp*H1 and *Bgl*III restriction sites, respectively (underlined). Primer LAMC also introduced a C-terminal His<sub>6</sub>-tag (bolded). The PCR reaction mixture (2  $\times$  50  $\mu$ L) consisted of 10  $\mu$ L 10  $\times$  PCR buffer, 4  $\mu$ L of MgSO<sub>4</sub>, 2  $\mu$ L dNTP mix, 1  $\mu$ L LAMB, 1  $\mu$ L of LAMC, 1  $\mu$ L of template DNA, 0.5  $\mu$ L of Platinum<sup>®</sup> *Taq* High

Fidelity, and 80.5  $\mu\text{L}$   $\text{H}_2\text{O}$ . Cycling conditions: (1) 94°C for 30 s; (2) 30 cycles of 94°C for 30 s, 55°C for 30 s, 68°C for 60 s per kb of PCR product; (3) final extension 68°C for 10 min; (4) hold 4°C. Amplification of DNA was confirmed with agarose gel electrophoresis, stained with EtBr. The PCR product was purified with the QIAquick™ PCR Purification Kit.

The PCR product was then cloned into the *NcoI* and *BglIII* site of the pQE60 vector by performing a double digestion, followed by ligation. The PCR product was digested as follows: 200 ng of PCR product was first digested with 1  $\mu\text{L}$  of *BspHI* (10 U) in 4  $\mu\text{L}$  of 10  $\times$  React 2 buffer (Invitrogen) and  $\text{H}_2\text{O}$  (up to 40  $\mu\text{L}$ ), for 2 h at 37°C. Then, 1  $\mu\text{L}$  of 10  $\times$  React 2 buffer (Invitrogen), 2.5  $\mu\text{L}$  of 1 M NaCl, 1  $\mu\text{L}$  of *BglIII* (10 U) and 5.5  $\mu\text{L}$   $\text{H}_2\text{O}$  was added (final volume of 50  $\mu\text{L}$ ) and the mixture incubated for an additional 2 h at 37°C. The pQE60 vector was digested as follows: 2  $\mu\text{g}$  of plasmid was digested with 1  $\mu\text{L}$  of *NcoI* (10 U), 1  $\mu\text{L}$  of *BglIII* (10 U) in 5  $\mu\text{L}$  of 10  $\times$  React 3 buffer (Invitrogen) and  $\text{H}_2\text{O}$  (up to 50  $\mu\text{L}$ ), for 4 h at 37°C. The digested DNA was purified by phenol-chloroform extraction and sodium acetate / EtOH precipitation. For the ligation reaction, 30–50 ng of PCR product and 30–50 ng of vector DNA were mixed with 2  $\mu\text{L}$  of 5  $\times$  Ligase Reaction Buffer, 1  $\mu\text{L}$  of T4 DNA Ligase (1 U) and  $\text{H}_2\text{O}$  (to a final volume of 10  $\mu\text{L}$ ) and incubated at room temperature for 2 h.

The reaction mixture (2.5–5 $\mu\text{L}$ ) was used to transform chemically competent *E. coli* JM109 or *E. coli* M15[pREP4] cells, via the Fermentas TransformAid™ Kit. The transformed cells were streaked onto LB agar plates containing the appropriate antibiotics and incubated at 37°C for 24 h. Colonies

were subcultured, plasmid DNA was purified by the alkaline lysis & phenol-chloroform extraction method, followed by sodium acetate / EtOH precipitation, and then screened by PCR. Several attempts to clone *mptAB* into the pQE60 vector were attempted and a total of 96 transformants were screened. However, no successful clones were identified.

#### **6.4.12. Pilot studies on the overexpression of IIC and IID**

Plasmid pVM12, overexpressing the IID protein as a His<sub>6</sub>-fusion, was prepared by Dr. Marco van Belkum and transformed into *E. coli* M15[pREP4] cells, as described above. Pilot experiments to determine if the IIC and IID proteins would be overexpressed were conducted as follows. Overnight cultures of *E. coli* M15[pREP4] with plasmid pMV24 (for IIC) were grown in 5 mL of LB broth (100 µg/mL ampicillin and 25 µg/mL kanamycin) and incubated at 37°C, 250 rpm for 16–18 h. Two flasks containing 50 mL of fresh LB broth (100 µg/mL ampicillin and 25 µg/mL kanamycin) were inoculated (1%) with the overnight cultures and incubated at 37°C, 250 rpm. When the OD<sub>600</sub> reached ~0.5, a 1 mL pre-induction sample was removed, and different amounts of IPTG were added to each flask, corresponding to final IPTG concentration of 0.5 mM and 1 mM. The flasks were incubated for an additional 3 h, after which 1 mL samples were removed. The same experiments were conducted using *E. coli* M15[pREP4] with plasmid pMV12 (for IID). It was noted that after addition of IPTG (and induction of protein overexpression), the OD<sub>600</sub> of the cell culture expression IID decreased.

Samples for SDS-PAGE were prepared as previously described (section 6.3.17.c), except that after centrifugation, the pellets were resuspended in 100  $\mu$ L of H<sub>2</sub>O, and samples were mixed with 6  $\times$  SDS-PAGE sample buffer. The samples were analyzed on a 10% SDS-PAGE gel and also by Western blot.

Summer student Erika Steels performed additional experiments with *E. coli* cells expressing IIC (with plasmid pMV24) to examine levels of protein expression at either 30°C or 37°C, with 0.1, 0.3, 0.5 or 1.0 mM IPTG (see Fig. 51 for a schematic of the pilot experiments). Pilot experiments were conducted in the same manner as described in section 6.3.17.c. Samples for SDS-PAGE were prepared as previously described (section 6.3.17.c) except that samples were mixed with 2  $\times$  SDS-PAGE sample buffer. The samples were analyzed on a 15% SDS-PAGE gel and also by Western blot.

## **6.5. Experimental procedures for the *in vitro* studies of the peptidase domain of CbnT**

### **6.5.1. Plasmids, bacterial strains and culture conditions**

The plasmids and bacterial strains used in this study are listed in Table 12. Biological experiments were performed as previously described (section 6.3.1). Unless otherwise stated, percentage concentration implies v/v.

**TABLE 12.** Plasmids and bacterial strains used for the study of CbnTP and CbnTP mutants

Plasmid or Strain	Relevant Characteristics <sup>c</sup>	Ref. or Source
pREP4	Constitutive expression of <i>lac</i> repressor protein, Kan <sup>r</sup> ;	Qiagen
pQE60	Expression vector, Amp <sup>r</sup> , 3.4 kb	Qiagen
<sup>a</sup> pLQP	pMAL <sup>TM</sup> -c2X containing the <i>malE-FXA-pCbnB2</i> fusion	(211)
<sup>b</sup> pQE60.CbnTP	pQE60 containing <i>CbnTP</i> (164 N-terminal aa)- <i>His<sub>6</sub></i> fusion	This Study
pQE60.CbnTP.M1	pQE60 containing <i>CbnTP</i> (164 N-terminal aa)- <i>His<sub>6</sub></i> fusion, C15S	This study
pQE60.CbnTP.M2	pQE60 containing <i>CbnTP</i> (164 N-terminal aa)- <i>His<sub>6</sub></i> fusion, C15S C19S	This study
pQE60.CbnTP.M3	pQE60 containing <i>CbnTP</i> (164 N-terminal aa)- <i>His<sub>6</sub></i> fusion, C15S, C19S, C55S	This study
pQE60.CbnTP.M4	pQE60 containing <i>CbnTP</i> (164 N-terminal aa)- <i>His<sub>6</sub></i> fusion, C15S, C19S, C55S, C63S	This study
pQE60.CbnTP.M5	pQE60 containing <i>CbnTP</i> (164 N-terminal aa)- <i>His<sub>6</sub></i> fusion, C15S, C19S, C63S	This study
<i>E. coli</i> XL1-Blue	<i>recA1 endA1 gyrA96 thi-1 hsdR17 supE44 relA1 lac</i> [F <sup>+</sup> <i>proAB lacI<sup>q</sup>Z ΔMI5 Tn10(Tet<sup>r</sup>)</i> ]	Stratagene
<i>E. coli</i> BL21(DE3)	F <sup>-</sup> <i>ompT hsdS</i> (r <sub>B</sub> <sup>-</sup> m <sub>B</sub> <sup>-</sup> ) <i>dcm</i> <sup>+</sup> Tet <sup>r</sup> gal λ(DE3); bacteriophage DE3 lysogen carrying the T7 RNA polymerase gene controlled by the <i>lacUV5</i> promoter; general purpose expression host	Stratagene
<i>E. coli</i> JM109	E14(Mcr <sup>A</sup> ) <i>recA1 endA1 gyrA96 thi-1 hsdR17</i> (r <sub>K</sub> <sup>-</sup> m <sub>K</sub> <sup>+</sup> ) <i>supE44 relA1 Δ(lac-proAB)</i> [F <sup>+</sup> <i>traD36 proAB lacI<sup>q</sup>ZΔMI5</i> ]; general purpose strain for cloning and propagating plasmids	(134)
<i>E. coli</i> M15[pREP4]	M15 phenotype: NaI <sup>S</sup> , Str <sup>S</sup> , Rif <sup>S</sup> , Thi <sup>-</sup> , Lac <sup>-</sup> , Ara <sup>+</sup> , Gal <sup>+</sup> , Mtl <sup>-</sup> , F <sup>-</sup> , RecA <sup>+</sup> , Uvr <sup>+</sup> , Lon <sup>+</sup> ; with pREP4 plasmid, used for tightly regulated expression	Qiagen
<i>Carnobacterium divergens</i> LV13	Wild-type divergicin A producer, CbnB2 sensitive	(128)

<sup>a</sup> prepared by Dr. Luis Quadri; <sup>b</sup> prepared by Dr. Marco van Belkum; <sup>c</sup> FXA denotes the Factor Xa recognition sequence (IEGR)

## 6.5.2. Purification of pCbnB2

### 6.5.2.a. Overexpression and purification of Male-pCbnB2

50 μL of *E. coli* BL21(DE3) competent cells were transformed with 2 μL of plasmid pLQP (211) using heat-shock treatment. The cells were streaked onto LB agar plates (200 μg/mL ampicillin) and incubated at 37°C for ~20 h. Single colonies were picked and used to inoculate culture tubes containing 5 mL of LB

broth (200 µg/mL ampicillin). The tubes were incubated at 37°C, 200 rpm for 16–18 h. Four flasks containing 500 mL of LB broth (150 µg/mL ampicillin), were inoculated (1%) with the overnight cultures and incubated at 37°C, 200 rpm. When the OD<sub>600</sub> reached 0.45, IPTG (final concentration of 0.3 mM) was added to each flask and the cultures were incubated for an additional 3 h at 37°C, 200 rpm. The cells were harvested by centrifugation (11,300 × g, 20 min, 4°C).

The cell pellets were resuspended in 200 mL of amylose column buffer (20 mM Tris-Cl pH 7.2, 100 mM NaCl, 1 mM EDTA, 1 mM NaN<sub>3</sub>, 1 mM DTT), containing four complete EDTA-Free, protease inhibitors cocktail tablets (Roche Diagnostic). Cells were lysed using the cell disrupter, operating at 20 kpsi. After centrifugation (27,200 × g, 30 min, 4°C), the cleared lysate was diluted to 300 mL with amylose column buffer and loaded onto an amylose column at 1 mL/min. The column was washed with 600 mL amylose column buffer, after which the fusion protein was eluted by addition of 10 mM maltose to the buffer. Fractions containing the eluted protein (as shown by the UV<sub>280</sub> trace and SDS-PAGE analysis) were combined, transferred to dialysis tubing (MWCO 12 – 14 kDa) and dialyzed against 3.5 L of H<sub>2</sub>O (4°C, refreshed 3 times, 4 h each). The protein solution was then frozen (-20°C, then -80°C), lyophilized and stored at -20°C. Approximately 225 mg of fusion protein was obtained from 2 L of culture.

#### **6.5.2.b. Factor Xa Digestion of MalE-pCbnB2**

Initial attempts to digest MalE-pCbnB2 with Factor Xa were done following literature procedure (153, 211). The fusion protein was resuspended in

Factor Xa buffer (20 mM Tris-Cl pH 7.4, 100 mM NaCl, 1 mM CaCl<sub>2</sub>), to yield a 2 mg/mL solution. Digestion proceeded by the addition of 1% (w/w) Factor Xa and incubating the mixture at room temperature, overnight (~12 h) with gentle rocking. However, severe overdigestion of pCbnB2 was observed by MALDI-TOF under these conditions. The digest was repeated, using 0.3% Factor Xa (w/w) and digesting overnight (~12 h) at room temperature, but again, severe overdigestion was observed.

A pilot study was then performed to determine the optimal amount of enzyme and length of time required for the digestion to proceed without overdigestion. The fusion protein was dissolved in Factor Xa buffer at a concentration of 1 mg/mL. Two different digestions were prepared: Digest A contained 0.5% (w/w) Factor Xa, and Digest B contained 1% (w/w) Factor Xa. The digests were incubated at room temperature. At times 2 h, 4 h, 6 h and 12 h, 50 µL aliquots were removed from each sample, quenched by acidification and stored at -20°C. The samples were analyzed by MALDI-TOF and SDS-PAGE. Following the pilot experiment, it was decided to digest the fusion protein (dissolved in Factor Xa buffer, 1 mg/mL) with 0.5% (w/w) Factor Xa for 3.5 h at room temperature.

#### **6.5.2.c. RP-HPLC purification**

pCbnB2 was purified by RP-HPLC using a preparative C<sub>18</sub> column (Vydac 218TP1022, 10 µm particle size, 22 × 250 mm), on a Varian Prostar HPLC. MeCN (0.1% TFA) and H<sub>2</sub>O (0.1% TFA) were used as solvents, according to the

following gradient: (1) 5 min at 20% MeCN; (2) increase to 60% MeCN over 20 min; (3) decrease to 20% over 1 min; (4) hold at 20% MeCN for 4 min. The method employed 2.0 mL injections, a flow rate of 10 mL/min and detection at 220 nm. Both the pCbnB2 and MalE proteins were isolated as single peaks, with retention times of 17.8 min and 22 min, respectively. MALDI-TOF analysis showed that pCbnB2 was isolated as a mixture of the full-length peptide (residues 1-66) and a truncated peptide (residues 1-64). This truncation product was previously reported by Sprules *et al.* (153). Fractions containing the purified pCbnB2 were combined, concentrated by rotary evaporation and lyophilized. From 38 mg of fusion protein, 2.2 mg of pCbnB2 was obtained, corresponding to a yield of ~41%. The pCbnB2 was dissolved in water to a concentration of 200  $\mu$ M, aliquoted into smaller volumes, and stored at -20°C.

### 6.5.3. Purification of CbnTP from inclusion bodies

#### 6.5.3.a. Overexpression conditions

Dr. Marco van Belkum prepared plasmid pQE60.CbnTP to express the peptidase domain of CbnT as a His<sub>6</sub>-tagged fusion protein. As such, the 5' part of the *cbnT* gene (encoding for the first 164 aa of CbnT) was amplified by PCR, with incorporation of a C-terminal His<sub>6</sub>-tag, and cloned into the pQE60 expression vector. Overnight cultures of *E. coli* M15[pREP4] with plasmid pQE60.CbnTP were grown in 5 mL of LB broth (150  $\mu$ g/mL ampicillin and 25  $\mu$ g/mL kanamycin) at 37°C, 200 rpm for 16–18 h. Two flasks, each containing 500 mL of 2 × YT broth (150  $\mu$ g/mL ampicillin and 25  $\mu$ g/mL kanamycin), were

inoculated (1%) with the overnight cultures and incubated at 37°C, 200 rpm. When the OD<sub>600</sub> reached 0.55, IPTG (final conc. of 0.1 mM) was added to each flask and the cultures were incubated for an additional 3 h at 37°C, 200 rpm. The cells were harvested by centrifugation (11,300 × g, 20 min, 4°C), and the cell pellets stored at -20°C.

### 6.5.3.b. Purification of inclusion bodies

Two different methods were used to purify CbnTP from inclusion bodies:

**Method 1.** The cell were resuspended in lysis buffer (~4 mL/gram wet weight; 100 mM Tris-Cl pH 7.0, 5 mM EDTA, 5 mM DTT, 5 mM benzamidine•HCl) and lysed by 2 passes through the cell disrupter, operating at 20 kpsi. The suspension was centrifuged (22,000 × g, 60 min, 4°C) and the supernatant was discarded. The pellet was washed multiple times with wash buffer (~5 mL/gram wet weight cells; 100 mM Tris-Cl pH 7.0, 5 mM EDTA, 5 mM DTT, 2 M urea, 2% Triton X-100), followed by centrifugation. For the final wash, the pellet was resuspended in wash buffer without urea and Triton X-100. Inclusion bodies were then extracted by resuspending the pellet in extraction buffer (2 mL/gram wet weight; 100 mM sodium sulfate, 10 mM Tris-Cl , 8 M urea, pH 8.0), followed by centrifugation (28,000 × g, 60 min, 4°C). The supernatant was incubated with Ni-NTA resin (1 mL resin slurry per mL of protein solution) for 30 min at room temperature. The mixture was transferred to a column (1.6 × 20 cm) and packed at 1 mL/min. The column was then washed with 20 mL of wash buffer (100 mM sodium sulfate, 10 mM Tris-Cl, 6 M urea,

500 mM NaCl, 20% glycerol, pH 6.3). The protein was eluted by the addition of 250 mM imidazole (250 mM) to the wash buffer. The flow thru, wash fractions and elution fractions were analyzed on a 15% SDS-PAGE gel.

**Method 2: Modified Qiagen Protocol.** This was performed by summer student Victor Dong. The cells were resuspended in resuspension buffer (~4 mL/gram wet weight; 50 mM sodium phosphate pH 8.0, 300 mM NaCl, 10 mM imidazole, 5 mM DTT, 5 mM EDTA), lysed with the cell disrupter and centrifuged (22,000 × g, 60 min, 4°C). To solubilize inclusion bodies, the pellet was resuspended in extraction buffer (5 mL/gram wet weight; 100 mM sodium phosphate, 10 mM Tris-Cl, 8 M urea, pH 8.0), followed by centrifugation (10,000 × g, 30 min, 4°C). 5 mL of Ni-NTA resin was added to the supernatant and the mixture was incubated for 30 min (4°C) and then transferred to a column (1.6 × 20 cm) and packed at 1 mL/min. The column was washed with 2 × 4 mL of wash buffer (100 mM sodium phosphate, 10 mM Tris-Cl, 8 M urea, pH 6.3). The protein was eluted with wash buffer at reduced pH as follows: 2 × 5 mL at pH 5.9 and then 2 × 5 mL at pH 4.5. The flow thru, wash fractions and elution fractions were analyzed on a 15% SDS-PAGE gel.

### 6.5.3.c. Refolding attempts

To refold the denatured CbnTP, three different methods were tried:

**Method 1: Dialysis.** The eluted protein was transferred to dialysis tubing (MWCO 6000–8000 Da) and dialyzed against 4 L of buffer (50 mM sodium phosphate pH 7.5, 50 mM sodium sulfate, 1 mM DTT) containing 4 M urea (for

24 h), 2 M urea (for 24 h), 1 M urea (for 24 h) and 0 M urea (for 24 h), respectively. Significant precipitation of the protein was observed when the concentration of urea was lower than 4 M. The precipitate was pelleted out by centrifugation and the supernatant was concentrated with a concentrating tube (5000 × g, 4°C, MWCO 5K, Amicon).

**Method 2: Rapid Dilution.** This was performed by summer student Victor Dong. 5 mL of eluted protein was drawn into a syringe. Over the course of 60 min, the protein was added dropwise to 30 mL of rapidly stirring buffer (50 mM sodium phosphate pH 7.5, 50 mM sodium sulfate, 1 mM DTT), at 4°C. A significant amount of precipitate formed during the process. The precipitate was pelleted out by centrifugation and the supernatant was concentrated with a concentrating tube (5000 × g, 4°C, MWCO 5K, Amicon).

**Method 3: On-column refolding.** Prior to elution, the Ni-NTA column was washed with 5 × 15 mL portions of wash buffer containing 5 M, 4 M, 3 M, 2 M and 1 M urea, respectively, at 1 mL/min. The His<sub>6</sub>-tagged protein was then eluted by washing the column with 4 × 15 mL of running buffer containing 50 mM, 100 mM, 150 mM and 250 mM imidazole, respectively. All fractions (washes and elutions) were analyzed on a 15% SDS-PAGE gel. To remove imidazole, perform a buffer exchange (into 50 mM sodium phosphate pH 7.5, 50 mM sodium sulfate, 1 mM DTT) and concentrate the eluted protein, a concentrating tube was used (5000 × g, 4°C, MWCO 5K, Amicon).

#### 6.5.3.d. Activity of CbnTP isolated from inclusion bodies

The purified and refolded CbnTP samples were mixed with pCbnB2 and incubated overnight (~12 h) at room temperature. CbnTP and pCbnB2 controls were also subjected to the same conditions. The samples were analyzed by MALDI-TOF and activity testing. For MALDI-TOF, samples were acidified and desalted by zip-tipping (ZipTip<sub>μ-C18</sub>, Millipore). For spot-on-lawn activity testing, APT soft agar containing the indicator organism *C. divergens* LV13 was overlaid on a bed of hard agar. 10 μL of the digest and control samples were spotted onto the plate and allowed to dry. The plate was incubated overnight at room temperature and inspected for zones of inhibition.

#### 6.5.4. Purification of CbnTP as soluble protein

##### 6.5.4.a. Overexpression conditions

An overnight culture of *E. coli* M15[pREP4] bearing the plasmid pQE60.CbnTP was grown in 50 mL of LB broth (200 μg/mL ampicillin and 25 μg/mL kanamycin) at 37°C, 250 rpm for 16–18 h. A total of 4 L of 2 × YT (200 μg/mL ampicillin and 25 μg/mL kanamycin), divided into 8 × 500 mL, was inoculated (1%) with the overnight culture. When the OD<sub>600</sub> reached 0.5–0.8, the flasks were placed in an ice-bath for 20 min, after which IPTG (final conc. of 0.5 mM) was added to induce protein expression. The cultures were incubated at 10°C, 250 rpm for 20 h. The cells were harvested by centrifugation (11,300 × g, 20 min, 4°C) and stored at -80°C. From 4 L of culture, ~20 g of wet weight of cells was obtained.

#### 6.5.4.b. Purification of soluble protein

The cells were resuspended in lysis buffer (3 mL/gram wet weight cells; 50 mM sodium phosphate pH 8.0, 300 mM NaCl, 10 mM imidazole). No protease inhibitors were used in the purification to avoid potential inactivation of the desired protein. The cells were lysed with the cell disrupter, operating at 20 kpsi and the suspension was centrifuged ( $27,200 \times g$ , 30 min, 4°C). Ni-NTA resin (50% slurry) was added to the cleared lysate (~1 mL slurry/ 7–9 mL lysate) and the mixture was incubated for 60 min at 4°C with gentle rocking. The mixture was transferred to a column (1.6 × 20 cm) and the resin packed at 1.5 mL/min. The column was then washed with wash buffer (50 mM sodium phosphate pH 8.0, 300 mM NaCl, 20 mM imidazole) until the UV<sub>280</sub> trace showed that no more proteins were washing off the column (typically about 70 min). The desired protein was then eluted over 60 min by washing the column for 3 × 20 min with wash buffer containing 125 mM, 250 mM and 500 mM imidazole. 5 min fractions were collected during the wash and elution steps. The flow thru, wash fractions and elution fractions were analyzed on a 15% SDS-PAGE gel. Fractions containing the desired protein were combined and concentrated to ~2 mL, using a concentrating tube ( $5000 \times g$ , 4°C, MWCO 5K, Amicon).

The concentrated protein solution was then applied to a G50 Sephadex size exclusion column to desalt, perform a buffer exchange and further purify CbnTP from co-eluting contaminants. The column was operated at 0.2 mL/min and 20 min fractions were collected. The running buffer consisting of 10 mM Tris-Cl pH 7.5, 150 mM sodium sulfate, 1 mM DTT. Fractions containing protein

(as shown by  $UV_{280}$ ) were analyzed on a 15% SDS-PAGE gel. Fractions showing the desired protein in highest purity were combined and concentrated ( $5000 \times g$ ,  $4^{\circ}C$ , MWCO 5K, Amicon). Protein concentration was determined by BCA analysis and the protein was sent to collaborators for crystal screening.

#### **6.5.4.c. Activity of CbnTP isolated as soluble protein**

The proteolytic activity of CbnTP (isolated as soluble protein) toward pCbnB2 was examined as described above (section 6.5.3.d). Following digestion, MALDI-TOF and activity testing were used to analyze the digest reactions. When multiple samples of CbnTP were being tested, the concentrations of CbnTP were normalized prior to testing.

#### **6.5.5. Construction of CbnTP mutants**

Five different Cys→Ser mutants of CbnTP were constructed using site-directed mutagenesis. Primers were designed to be ~40 bp in length, with the site of mutation located in the center of the primer, and with a GC content of ~40%. Primers were dissolved in 100  $\mu$ L  $H_2O$  and the concentration of each was determined. The primers were then diluted to 125 ng/ $\mu$ L with  $H_2O$ .

##### **6.5.5.a. Construction of pQE60.CbnTP.M1**

Plasmid pQE60.CbnTP was purified by growing *E. coli* JM109 with plasmid pQE60.CbnTP in 5 mL of LB broth (200  $\mu$ g/mL ampicillin) at  $37^{\circ}C$ , 250 rpm for 16–18 h. A 1 mL sample of cell culture was harvested by centrifugation

(16,000 × g, 5 min, RT) and the plasmid isolated with the GeneJET™ Plasmid Miniprep Kit (Fermentas). The C15S mutation (underlined) was introduced using primer pair LAM19 (5'-CAGCAAGATGA GAAAGATTCAGGTGTTGCATGT ATCGCAATG-3') and LAM20 (5'-CATTGCGATACATGCAACACCTGAAT CTTTCTCATCTTGCTG-3'). The PCR reaction (50 μL) contained 5 μL of 10 × buffer, 3 μL of template (57 ng), 1 μL of LAM19 (125 ng), 1 μL of LAM20 (125 ng), 1 μL dNTPs, 1 μL *PfuTurbo* (2.5 U) and 38 μL H<sub>2</sub>O. Cycling conditions are the same as previously described (section 6.2.3). After the PCR reaction was complete, 4 μL of *DpnI* (20 U) was added, the mixture was pipetted up and down, centrifuged (16,000 × g, 1 min, RT) and then incubated at 37°C for 60 min. *E. coli* XL1-Blue supercompetent cells were transformed with 2 μL of DNA by the heat-shock method. The mixture was streaked onto LB agar plates (200 μg/mL ampicillin) and incubated at 37°C for 20 h. Four colonies were subcultured in 5 mL of LB broth (200 μg/mL ampicillin) and incubated at 37°C, 250 rpm for 16 h. Plasmid DNA was isolated from each culture using the GeneJET™ Plasmid Miniprep Kit (Fermentas). Each clone was sequenced in the forward direction, using primer QE60F2 (5'-CATAAAAATTTATTTGCTTTGTG-3') and clones successfully incorporating the mutation were identified. Purified plasmid DNA from one of the successful clones was then transformed into chemically competent *E. coli* M15[pREP4] cells, using the Fermentas TransformAid™ Kit. Colonies were subcultured in 5 mL of LB (200 μg/mL ampicillin and 25 μg/mL kanamycin) and incubated at 37°C, 250 rpm for 16 h. Stock cultures were

prepared in LB broth, supplemented with 20% glycerol and stored at -80°C. This plasmid contained the C15S mutation of CbnTP.

#### 6.5.5.b. Construction of pQE60.CbnTP.M2

Using plasmid pQE60.CbnTP.M1 (isolated in the previous step) as a template for PCR, the C19S mutation (underlined) was introduced using primer pair LAM21 (5'–GATGAGAAAGATTCAGGTGTTGCATCAATCGCAATGATTTTAAAG–3') and LAM22 (5'–CTTTAAAATCATTGCGATTGATGCAACACCTGAATCTTTCTCATC–3'). The PCR reaction (50 µL) contained 5 µL of 10 × buffer, 1 µL of template (50 ng), 1 µL of LAM21 (125 ng), 1 µL of LAM22 (125 ng), 1 µL dNTPs, 1 µL *PfuTurbo* (2.5 U) and 40 µL H<sub>2</sub>O. Cycling conditions are the same as previously described. The subsequent *DpnI* digestion, transformation into *E. coli* XL1-Blue supercompetent cells, subculturing, sequencing of clones, and transformation into *E. coli* M15[pREP4] competent cells are the same as reported above. This plasmid contained the C15S and C19S mutations of CbnTP.

#### 6.5.5.c. Construction of pQE60.CbnTP.M3

Using plasmid pQE60.CbnTP.M2 (isolated in the previous step) as a template for PCR, the C55S mutation (underlined) was introduced using primer pair LAM23 (5'–CCATTTGGGTTAAAAAATTCAATTGAAAAATTAGGTTT TGATTGC–3') and LAM24 (5'–GCAATCAAAACCTAATTTTTCAATTGAATTTTTTAACCCAAATGG–3'). The PCR reaction (50 µL) contained 5 µL of 10 ×

buffer, 1  $\mu$ L of template (50 ng), 1  $\mu$ L of LAM23 (125 ng), 1  $\mu$ L of LAM24 (125 ng), 1  $\mu$ L dNTPs, 1  $\mu$ L *PfuTurbo* (2.5 U) and 40  $\mu$ L H<sub>2</sub>O. Cycling conditions are the same as previously described. The subsequent *DpnI* digestion, transformation into *E. coli* XL1-Blue supercompetent cells, subculturing, sequencing of clones, and transformation into *E. coli* M15[pREP4] competent cells are the same as reported above. This plasmid contained the C15S, C19S and C55S mutations of CbnTP.

#### 6.5.5.d. Construction of pQE60.CbnTP.M4

Using plasmid pQE60.CbnTP.M3 (isolated in the previous step) as a template for PCR, the C63S mutation (underlined) was introduced using primer pair LAM25 (5'–GAAAAATTAGGTTTTGATTCACAAGCTGTTCAAGCAGATCAAG–3') and LAM26 (5'–CTTGATCTGCTTGAACAGCTTGTGAATCAAAACCTAATTTTTTC–3'). The PCR reaction contained 5  $\mu$ L of 10  $\times$  buffer, 1  $\mu$ L of template (50 ng), 1  $\mu$ L of LAM23 (125 ng), 1  $\mu$ L of LAM24 (125 ng), 1  $\mu$ L dNTPs, 1  $\mu$ L *PfuTurbo* (2.5 U) and 40  $\mu$ L H<sub>2</sub>O. Cycling conditions are the same as previously described. The subsequent *DpnI* digestion, transformation into *E. coli* XL1-Blue supercompetent cells, subculturing and sequencing of clones, and transformation in *E. coli* M15[prep4] is the same as reported above. This plasmid contained the C15S, C19S, C55S and C63S mutations of CbnTP.

#### 6.5.5.e. Construction of pQE60.CbnTP.M5

Using plasmid pQE60.CbnTP.M2 as a template for PCR, the C63S mutation (underlined) was introduced using primer pair LAM25 (5'–GAAAAAT TAGGTTTTGATTCACAAGCTGTTCAAGCAGATCAAG–3') and LAM26 (5'–CTTGATCTGCTTGAACAGCTTGTGAATCAAAACCTAATTTTTC–3'). The PCR reaction (50  $\mu$ L) contained 5  $\mu$ L of 10  $\times$  buffer, 1  $\mu$ L of template (50 ng), 1  $\mu$ L of LAM23 (125 ng), 1  $\mu$ L of LAM24 (125 ng), 1  $\mu$ L dNTPs, 1  $\mu$ L *PfuTurbo* (2.5 U) and 40  $\mu$ L H<sub>2</sub>O. Cycling conditions are the same as previously described. The subsequent *DpnI* digestion, transformation into *E. coli* XL1-Blue supercompetent cells, subculturing, sequencing of clones, and transformation into *E. coli* M15[pREP4] competent cells are the same as reported above. This plasmid contained the C15S, C19S and C63S mutations of CbnTP.

#### 6.5.6. Pilot Expression of CbnTP Mutants

Overnight cultures of *E. coli* M15[pREP4] containing the mutant plasmids were grown in 5 mL of LB broth (200  $\mu$ g/mL ampicillin and 25  $\mu$ g/mL kanamycin) and incubated at 37°C, 250 rpm for 16–18 h. Flasks containing 50 mL of 2  $\times$  YT broth (200  $\mu$ g/mL ampicillin and 25  $\mu$ g/mL kanamycin) were inoculated (1%) with the overnight cultures and incubated at 37°C, 250 rpm until the OD<sub>600</sub> reached ~0.8. Flasks were placed in an ice-bath for 20 min, 1 mL pre-induction samples were removed and IPTG (final conc. of 0.5 mM) was added to induce protein expression. The cultures were incubated at 10°C, 250 rpm for 20 h.

Samples for SDS-PAGE were prepared as previously described (section 6.3.17.c), except that after centrifugation, the pellets were resuspended in 100  $\mu$ L of H<sub>2</sub>O, and samples were mixed with 6  $\times$  SDS-PAGE sample buffer. Samples were resolved on a 15% SDS-PAGE gel and visualized with Coomassie stain.

## **6.6. Experimental procedures for testing the activity of LAB bacteriocins against Gram-negative pathogens**

### **6.6.1. Reagents, bacterial strains and culture conditions**

All solutions and materials used in this study were sterilized prior to use, either by autoclaving (121°C, 15 min) or filter sterilization (0.22  $\mu$ m). Cell buffer was comprised of 50 mM Tris-Cl pH 7.2, 4 mM CaCl<sub>2</sub>, 100 mM NaCl and 0.1% gelatin. Solutions containing EDTA and cell buffer were prepared by diluting 0.5 M EDTA (pH 8.0) to 80 mM and 40 mM in cell buffer. Three Gram-negative strains were used for testing in this study: *E. coli* DH5 $\alpha$ , *Pseudomonas aeruginosa* ATCC 14207 and *Salmonella typhimurium* ATCC 23564. Bacteria were grown in LB broth at 37°C, 250 rpm and on LB agar plates (1.5% agar) at 37°C. Bacterial cultures were maintained as frozen stocks at -80°C, in LB broth supplemented with 20% glycerol.

### **6.6.2. Preparation of bacteriocin testing solutions**

#### **6.6.2.a. General description of testing solutions**

The testing was designed so that equivalent volumes of bacterial culture and bacteriocin testing solutions would be mixed. As such, the testing solutions were prepared at twice their desired final concentrations. Two sets of testing

solutions were prepared for each bacteriocin: Set A was prepared without EDTA and Set B with EDTA. For Set A, bacteriocin stock solutions were diluted with cell buffer. For Set B, the same bacteriocin stock solutions were diluted with cell buffer containing EDTA, resulting in a concentration of 40 mM EDTA. Table 13 lists the bacteriocins that were used in this study and the various concentrations of the testing solutions.

**TABLE 13.** Concentrations of the various bacteriocin test solutions

Bacteriocin	Set A (no EDTA)					Set B (with 40 mM EDTA)				
	1	2	3	4	5	1E	2E	3E	4E	5E
[CclA] $\mu\text{M}$	0	1	12.5	25	50	0	1	12.5	25	50
[Enterocin 710C] $\mu\text{M}$	0	1	2	10	--	0	1	2	10	--
[Gallidermin] $\mu\text{M}$	0	12.5	25	50	100	0	12.5	25	50	100
[Lacticin] $\mu\text{M}$	0	12.5	25	50	100	0	12.5	25	50	100
[Nisin] $\mu\text{M}$	0	12.5	25	50	100	0	12.5	25	50	100
[PisA] $\mu\text{M}$	0	1	12.5	25	50	0	1	12.5	25	50

For bacteriocins prone to oxidation (nisin, gallidermin and lacticin 3147), MALDI-TOF analysis and spot-on-lawn activity testing (against known indicator strains) was periodically performed on stock solutions to monitor for oxidation and subsequent loss of antimicrobial activity.

#### 6.6.2.b. CclA

CclA was purified as previously described (section 6.3.2). A 200  $\mu\text{M}$  stock solution of CclA was prepared by dissolving the lyophilized sample in water. This stock solution was then used to prepare the 2 sets of testing solutions with the concentrations listed in Table 13.

### 6.6.2.c. Enterocin 710C (Ent7A & Ent7B)

Enterocins 7A and Ent 7B were purified by graduate student Xiaoji Liu. A 200  $\mu\text{M}$  stock solution of each peptide was prepared by dissolving the HPLC-purified samples in water. Equivalent volumes of each solution were mixed to prepare a 200  $\mu\text{M}$  stock solution of enterocin 710C (100  $\mu\text{M}$  Ent 7A + 100  $\mu\text{M}$  Ent 7B). This stock solution was used to prepare 2 sets of testing solutions with the concentrations listed in Table 13.

### 6.6.2.d. Gallidermin

Gallidermin ( $\geq 90\%$  purity) was purchased (Axxora) and a 200  $\mu\text{M}$  stock solution prepared by dissolving the lyophilized peptide in water. This stock solution was then used to prepare the 2 sets of testing solutions with the concentrations listed in Table 13.

### 6.6.2.e. Lacticin 3147

Lacticin 3147 was obtained by growing the producer organism and isolating the bacteriocin (peptides LtnA1 and LtnA2) from culture supernatant, as described by Martin, *et al.* (17). Overnight cultures of *L. lactis* subsp. *lactis* MG1363 were grown in 10 mL of M17 broth (supplemented with 10% lactose), at 30°C for 24 h. 4  $\times$  1 L volumes of modified tryptone-yeast broth were inoculated (1%) with the overnight cultures and incubated at 30°C for 24 h. The modified tryptone-yeast media contained (per 800 mL): 2.5 g tryptone, 5.0 g yeast, 1.5 g D/L methionine, 50 mg  $\text{MnSO}_4 \cdot \text{H}_2\text{O}$  and 125 mg  $\text{MgSO}_4$ . Prior to sterilization, the

media was preclarified by passing it through a column (2.5 × 50 cm) of Amberlite XAD-16 resin (75 g), which had been prewashed with IPA and water. A total of 3.2 L of media was prepared in this manner, divided into 4 × 1 L bottles (800 mL per bottle) and then autoclaved (121°C, 15 min). Separate solutions of 10% D-glucose and 20% β-glycerophosphate were also prepared and autoclaved. 100 mL of each of these solutions was then added to the 800 mL of media.

After 24 h of growth, 50 g of ammonium sulfate and 75 mg of DTT was added to each bottle and incubated for an additional 30 min. The cultures were centrifuged (11,300 × g, 20 min, 4°C) to harvest the cells and precipitated proteins. The pellets were combined and resuspended in 250 mL of 70% IPA pH 2 (+1 mM DTT). The mixture was stirred for 3 h at 4°C and then centrifuged (11,300 × g, 20 min, 4°C) to remove cell debris. The supernatant was concentrated to ~50 mL by rotary evaporation and then loaded onto a Megabond C<sub>18</sub> column. The column was washed with successive washes (60 mL each) of water (+ 1mM DTT), 30% EtOH (+1 mM DTT) and 60 mL of 24% IPA (+1mM DTT). The bacteriocins were eluted with 100 mL of 70% IPA pH 2 (+1 mM DTT). The eluted sample was concentrated under rotary evaporation, transferred to a 15 mL falcon tube and lyophilized.

The sample was redissolved in ~10 mL of 24% IPA (+1 mM DTT) and sonicated for ~15 min. Insoluble material was pelleted out by centrifugation (20 min) with a tabletop centrifuge (IEC Clinical Centrifuge; Damon). The supernatant was transferred to a clean 15 mL falcon tube. The sample was purified by RP-HPLC, using a preparative C<sub>18</sub> column (Vydac 218TP1022, 10 μm

particle size, 22 × 250 mm) using a Varian Prostar HPLC. IPA (0.1% TFA) and H<sub>2</sub>O (0.1% TFA) were used as solvents, according to the following gradient: (1) 5 min at 24% IPA; (2) increase to 44% IPA over 20 min; (3) decrease to 24% over 0.5 min; (4) hold at 24% IPA for 5 min. The method employed 1.0 mL injections, a flow rate of 12 mL/min and detection at 220 nm. Both the LtnA1 and LtnA2 peptides were isolated as single peaks, with retention times of ~17 min and ~23 min, respectively. The LtnA2 peak was generally shorter and broader than that of LtnA1. The eluted samples were immediately frozen on dry ice. Initially, helium was continuously bubbled through the solvents to prevent oxidation of the peptides. However, it was later discovered that this was unnecessary, as the peptides were stable under HPLC conditions and instead, oxidation was occurring after concentrating the sample. Following HPLC, the purified LtnA1 and LtnA2 samples were rotovapped to dryness, immediately redissolved in 0.1% TFA, frozen and placed on the lyophilizer until completely dry. If the samples were not rotovapped to dryness (i.e.: concentrated to a few mL) prior to lyophilization, significant oxidation of the peptides was observed by MALDI-TOF. The identity of LtnA1 and LtnA2 was confirmed by MALDI-TOF (Fig. 53).

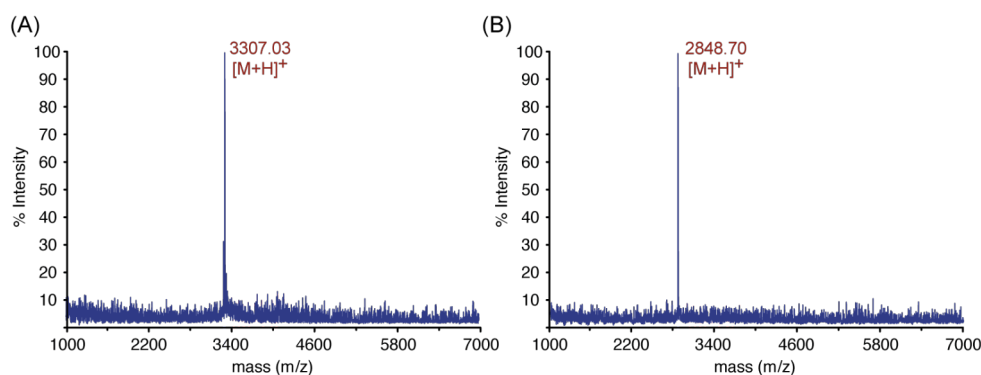


**FIG. 53.** MALDI-TOF traces of purified lacticin 3147. (A) LtnA1 (B) LtnA2.

Following purification, a 200  $\mu\text{M}$  stock solution of each peptide was prepared by dissolving the lyophilized peptides in water. Equivalent volumes of each solution were then mixed to prepare a 200  $\mu\text{M}$  stock solution of lacticin 3147 (100  $\mu\text{M}$  LtnA1 + 100  $\mu\text{M}$  LtnA2). This stock solution was used to prepare 2 sets of testing solutions with the concentrations listed in Table 13.

#### **6.6.2.f. Nisin A**

A 2.5% preparation of nisin A was purchased (Sigma) and HPLC-purified by graduate student Lara Silkin. A 200  $\mu\text{M}$  stock solution of nisin was prepared by dissolving the lyophilized sample in water. This stock solution was used to prepare 2 sets of testing solutions with the concentrations listed in Table 13.

#### **6.6.2.g. PisA**

PisA was purified as previously described (section 6.4.5), by summer student Erika Steels. A 400  $\mu\text{M}$  stock solution was prepared by dissolving the lyophilized peptide in water. A 100  $\mu\text{M}$  stock solution was prepared by dilution with cell buffer, and used to prepare 2 sets of testing solutions with the concentrations listed in Table 13.

#### **6.6.2.h. Subtilosin A**

Subtilosin A was purified by Dr. Karen Kawulka (41, 42). A 100  $\mu\text{M}$  stock solution was prepared by dissolving the lyophilized peptide in water.

Subtilosin A was only used in the in-solution testing, as described in the following section (6.6.3.a).

### **6.6.3. Testing procedure**

#### **6.6.3.a. In-solution testing**

Overnight cultures of *E. coli* DH5 $\alpha$  and *P. aeruginosa* ATCC 14207 were prepared by inoculating 5 mL of LB broth with stock culture and incubating for 16-18 h at 37°C, 250 rpm. Flasks with 50 mL of fresh LB broth were inoculated with the overnight cultures (1%) and incubated at 37°C, 250 rpm until the OD<sub>600</sub> was approximately 0.2. 100  $\mu$ M stock solutions of nisin and subtilosin A, and a 500  $\mu$ M stock solution of EDTA were prepared.

Testing was performed using 12 wells of a 96-well plate (columns 1-6, rows I and II, see Table 14), as follows. For both rows, 100  $\mu$ L of LB broth was added to column 1 and 100  $\mu$ L of cell culture was added to columns 2-6. For both rows, 100  $\mu$ L of water was added to columns 1 and 2, which would serve as the negative (no growth) and positive (normal growth) controls, respectively. To both rows, a combination (100  $\mu$ L total) of the bacteriocin stock solution and water was added to each well in columns 3, 4, 5 and 6 to generate a final bacteriocin concentration of 50  $\mu$ M, 25  $\mu$ M, 12.5  $\mu$ M and 6.25  $\mu$ M, respectively. To row II, 4  $\mu$ L of EDTA solution was added to wells in columns 2-6. This resulted in a final concentration of 10 mM EDTA, with minimal dilution of the bacteriocins (< 2% dilution). Table 14 displays the volumes (in  $\mu$ L) of all the solutions added, where

C, B, W, E and LB refer to cell culture, bacteriocin stock solution, water, EDTA stock solution and LB broth, respectively. Tests were repeated in duplicate.

**TABLE 14.** Layout of well-plate and testing solutions for in-solution bacteriocin testing against Gram-negative pathogens

	<b>1</b> <b>blank</b>	<b>2</b> <b>culture</b> <b>only</b>	<b>3</b> <b>50 <math>\mu</math>M</b>	<b>4</b> <b>25 <math>\mu</math>M</b>	<b>5</b> <b>12.5 <math>\mu</math>M</b>	<b>6</b> <b>6.25 <math>\mu</math>M</b>
<b>I</b>		C - 100	C - 100	C - 100	C - 100	C - 100
	LB - 100	B - 0	B - 100	B - 50	B - 25	B - 12.5
	W - 100	W - 100	W - 0	W - 50	W - 75	W - 67.5
		E - 0	E - 0	E - 0	E - 0	E - 0
<b>II</b>		C - 100	C - 100	C - 100	C - 100	C - 100
	LB - 100	B - 0	B - 100	B - 50	B - 25	B - 12.5
	W - 100	W - 100	W - 0	W - 50	W - 75	W - 67.5
		E - 4	E - 4	E - 4	E - 4	E - 4

*C*: cell culture; *B*: bacteriocin stock solution; *W*: water; *E*: EDTA stock solution; *LB*: LB broth. All numbers refer to volumes, in  $\mu$ L.

Four plates were set-up: two for testing nisin, and 2 for testing subtilisin A against *E. coli* DH5 $\alpha$  and *P. aeruginosa* ATCC 14207. The plates were incubated for 16–18 h at 37°C. The contents of each well were resuspended by pipetting up and down and air bubbles popped with a syringe tip. The OD<sub>600</sub> of each well was read with a plate reader, using column 1 as a reference. The OD<sub>600</sub> was then plotted as a function of bacteriocin concentration.

### 6.6.3.b. Colony counting method

An alternate testing method was developed, based on the method described by Stevens *et al.* (243). Overnight cultures of *E. coli*, *P. aeruginosa* or *S. typhimurium* were prepared by inoculating 5 mL of LB broth with the frozen stock and incubating for 16-18 h at 37°C, 250 rpm. 50 mL of fresh LB broth was

inoculated with the overnight culture (1%) and incubated at 37°C, 250 rpm until the OD<sub>600</sub> was approximately 0.1, corresponding to a cell density of  $\sim 1 \times 10^7$  cfu/mL. To prepare the bacteria for testing, 2.4 mL of the culture was centrifuged (16,000  $\times$  g, 5 min, RT) and the pellet rinsed with 2.4 mL of cell buffer. The cells were resuspended in 2.4 mL of fresh cell buffer. 100  $\mu$ L of cell culture was placed into 1.5 mL microcentrifuge tubes and then 100  $\mu$ L of bacteriocin test solution (see Table 13) was added. The tubes were vortexed to ensure efficient mixing, and then incubated at 37°C for 1 h. To remove the testing solution (bacteriocin with/without EDTA), the cells were harvested by centrifugation (16,000  $\times$  g, 5 min, RT) and the pellet was rinsed once with 100  $\mu$ L of fresh cell buffer. The cells were resuspended in 100  $\mu$ L of fresh cell buffer and serial dilutions ( $10^{-1}$ ,  $10^{-2}$  and  $10^{-3}$ ) were prepared by diluting 10  $\mu$ L of cell culture with 90  $\mu$ L of fresh cell buffer. 85  $\mu$ L of each suspension ( $10^0$ ,  $10^{-1}$ ,  $10^{-2}$  and  $10^{-3}$ ) was then streaked on LB agar plates. Following incubation at 37°C for  $\sim 20$  h, the plates were examined and colony forming units (cfu) were counted. Each bacteriocin was tested in duplicate (except for enterocin 710C). In cases where results were anomalous (*i.e.*: dilution series didn't make sense, no growth observed, too much growth observed) tests were repeated until consistent results were obtained.

#### **6.6.4. Analysis of cfu data**

Plates containing fewer than  $\sim 500$  cfu were counted in full. For plates containing more than 500 cfu, but discernable colonies, the plate was segmented (into 1/2, 1/4 or 1/8) and this portion was counted and used to estimate the total

number of cfu on the plate. The  $\log_{10}(\text{cfu})$  for each plate was calculated. To determine the effect of a treatment (exposure to bacteriocin, EDTA or combination), the log reduction factor (LRF) was calculated according to equation 3. LRF values less than 1 were considered insignificant.

$$LRF = \log(\text{cfu}_{\text{no treatment}}) - \log(\text{cfu}_{\text{treatment}}) \quad (\text{eq. 3})$$

## Chapter 7. References

- (1) van Belkum, M. J., and Stiles, M. E. (2000) Nonlantibiotic antibacterial peptides from lactic acid bacteria, *Nat. Prod. Rep.* *17*, 323-335.
- (2) Parada, J. L., Caron, C. R., Medeiros, A. B. P., and Soccol, C. R. (2007) Bacteriocins from lactic acid bacteria: Purification, properties and use as biopreservatives, *Braz. Arch. Biol. Techn.* *50*, 521-542.
- (3) Cintas, L. M., Casaus, M. P., Herranz, C., Nes, I. F., and Hernández, P. E. (2001) Review: Bacteriocins of lactic acid bacteria, *Food Sci. Technol. Int.* *7*, 281-305.
- (4) Gillor, O., Etzion, A., and Riley, M. A. (2008) The dual role of bacteriocins as anti- and probiotics, *Appl. Microbiol. Biotechnol.* *81*, 591-606.
- (5) Deegan, L. H., Cotter, P. D., Hill, C., and Ross, P. (2006) Bacteriocins: Biological tools for bio-preservation and shelf-life extension, *Int. Dairy J.* *16*, 1058-1071.
- (6) Cotter, P. D., Hill, C., and Ross, R. P. (2005) Bacteriocins: Developing innate immunity for food, *Nat. Rev. Microbiol.* *3*, 777-788.
- (7) Gálvez, A., Abriouel, H., López, R. L., and Ben Omar, N. (2007) Bacteriocin-based strategies for food biopreservation, *Int. J. Food Microbiol.* *120*, 51-70.
- (8) Eijsink, V. G. H., Axelsson, L., Diep, D. B., Håvarstein, L. S., Holo, H., and Nes, I. F. (2002) Production of class II bacteriocins by lactic acid

- bacteria; an example of biological warfare and communication, *Antonie Leeuwenhoek* 81, 639-654.
- (9) Chen, H., and Hoover, D. G. (2003) Bacteriocins and their food applications, *Compr. Rev. Food Sci. F.* 2, 82-100.
- (10) Tagg, J. R., Dajani, A. S., and Wannamaker, L. W. (1976) Bacteriocins of Gram-positive bacteria, *Bacteriol. Rev.* 40, 722-756.
- (11) Klaenhammer, T. R. (1988) Bacteriocins of Lactic-Acid Bacteria, *Biochimie* 70, 337-349.
- (12) Nes, I. F., Yoon, S. S., and Diep, W. B. (2007) Ribosomally synthesized antimicrobial peptides (Bacteriocins) in lactic acid bacteria: A review, *J. Food Sci. Biotechnol.* 16, 675-690.
- (13) Klaenhammer, T. R. (1993) Genetics of bacteriocins produced by lactic acid bacteria, *FEMS Microbiol. Rev.* 12, 39-85.
- (14) Maqueda, M., Sánchez-Hidalgo, M., Fernández, M., Montalbán-López, M., Valdivia, E., and Martínez-Bueno, M. (2008) Genetic features of circular bacteriocins produced by Gram-positive bacteria, *FEMS Microbiol. Rev.* 32, 2-22.
- (15) Mattick, A. T. R., and Hirsch, A. (1944) A Powerful Inhibitory Substance produced by Group *N* Streptococci, *Nature* 154, 551-551.
- (16) Kellner, R., Jung, G., Hörner, T., Zähler, H., Schnell, N., Entian, K. D., and Götz, F. (1988) Gallidermin - a New Lanthionine-Containing Polypeptide Antibiotic, *Eur. J. Biochem.* 177, 53-59.

- (17) Martin, N. I., Sprules, T., Carpenter, M. R., Cotter, P. D., Hill, C., Ross, R. P., and Vederas, J. C. (2004) Structural characterization of lacticin 3147, a two-peptide lantibiotic with synergistic activity, *Biochemistry* *43*, 3049-3056.
- (18) McAuliffe, O., Hill, C., and Ross, R. P. (2000) Each peptide of the two-component lantibiotic lacticin 3147 requires a separate modification enzyme for activity, *Microbiology* *146*, 2147-2154.
- (19) Bierbaum, G., Brötz, H., Koller, K. P., and Sahl, H. G. (1995) Cloning, Sequencing and Production of the Lantibiotic Mersacidin, *FEMS Microbiol. Lett.* *127*, 121-126.
- (20) Brötz, H., Bierbaum, G., Markus, A., Molitor, E., and Sahl, H. G. (1995) Mode of Action of the Lantibiotic Mersacidin: Inhibition of Peptidoglycan Biosynthesis via a Novel Mechanism, *Antimicrob. Agents Chemother.* *39*, 714-719.
- (21) Benedict, R. G., Dvonch, W., Shotwell, O. L., Pridham, T. G., and Lindenfelser, L. A. (1952) Cinnamycin, an antibiotic from *Streptomyces cinnamoneus* nov. sp., *Antibiot. Chemother.* *2*, 591-594.
- (22) Hastings, J. W., Sailer, M., Johnson, K., Roy, K. L., Vederas, J. C., and Stiles, M. E. (1991) Characterization of leucocin A UAL187 and cloning of the bacteriocin gene from *Leuconostoc gelidum*, *J. Bacteriol.* *173*, 7491-7500.
- (23) Marugg, J. D., Gonzalez, C. F., Kunka, B. S., Ledebøer, A. M., Pucci, M. J., Toonen, M. Y., Walker, S. A., Zoetmulder, L. C. M., and Vandenberg,

- P. A. (1992) Cloning, expression, and nucleotide-sequence of genes involved in production of pediocin PA-1, a bacteriocin from *Pediococcus acidilactici* PAC1.0, *Appl. Environ. Microbiol.* 58, 2360-2367.
- (24) Gursky, L. J., Martin, N. I., Derksen, D. J., van Belkum, M. J., Kaur, K., Vederas, J. C., Stiles, M. E., and McMullen, L. M. (2006) Production of piscicolin 126 by *Carnobacterium maltaromaticum* UAL26 is controlled by temperature and induction peptide concentration, *Arch. Microbiol.* 186, 317-325.
- (25) Jack, R. W., Wan, J., Gordon, J., Harmark, K., Davidson, B. E., Hillier, A. J., Wettenhall, R. E. H., Hickey, M. W., and Coventry, M. J. (1996) Characterization of the chemical and antimicrobial properties of piscicolin 126, a bacteriocin produced by *Carnobacterium piscicola* JG126, *Appl. Environ. Microbiol.* 62, 2897-2903.
- (26) Nissen-Meyer, J., Holo, H., Håvarstein, L. S., Sletten, K., and Nes, I. F. (1992) A Novel Lactococcal Bacteriocin Whose Activity Depends on the Complementary Action of Two Peptides, *J. Bacteriol.* 174, 5686-5692.
- (27) Anderssen, E. L., Diep, D. B., Nes, I. F., Eijsink, V. G. H., and Nissen-Meyer, J. (1998) Antagonistic activity of *Lactobacillus plantarum* C11: Two new two-peptide bacteriocins, plantaricins EF and JK, and the induction factor plantaricin A, *Appl. Environ. Microbiol.* 64, 2269-2272.
- (28) Holo, H., Nilssen, O., and Nes, I. F. (1991) Lactococcin A, a New Bacteriocin from *Lactococcus lactis* subsp. *cremoris*: Isolation and Characterization of the Protein and Its Gene, *J. Bacteriol.* 173, 3879-3887.

- (29) Cintas, L. M., Casaus, P., Holo, H., Hernandez, P. E., Nes, I. F., and Håvarstein, L. S. (1998) Enterocins L50A and L50B, two novel bacteriocins from *Enterococcus faecium* L50, are related to staphylococcal hemolysins, *J. Bacteriol.* 180, 1988-1994.
- (30) Cintas, L. M., Casaus, P., Herranz, C., Håvarstein, L. S., Holo, H., Hernández, P. E., and Nes, I. F. (2000) Biochemical and genetic evidence that *Enterococcus faecium* L50 produces enterocins L50A and L50B, the *sec*-dependent enterocin P, and a novel bacteriocin secreted without an N-terminal extension termed enterocin Q, *J. Bacteriol.* 182, 6806-6814.
- (31) Pütsep, K., Brändén, C. I., Boman, H. G., and Normark, S. (1999) Antibacterial peptide from *H-pylori*, *Nature* 398, 671-672.
- (32) Brede, D. A., Faye, T., Johnsborg, O., Odegård, I., Nes, I. F., and Holo, H. (2004) Molecular and genetic characterization of propionicin F, a bacteriocin from *Propionibacterium freudenreichii*, *Appl. Environ. Microbiol.* 70, 7303-7310.
- (33) Joerger, M. C., and Klaenhammer, T. R. (1986) Characterization and Purification of Helveticin J and Evidence for a Chromosomally Determined Bacteriocin Produced by *Lactobacillus helveticus* 481, *J. Bacteriol.* 167, 439-446.
- (34) Nilsen, T., Nes, I. F., and Holo, H. (2003) Enterolysin A, a cell wall-degrading bacteriocin from *Enterococcus faecalis* LMG 2333, *Appl. Environ. Microbiol.* 69, 2975-2984.

- (35) Hickey, R. M., Twomey, D. P., Ross, R. P., and Hill, C. (2003) Production of enterolysin A by a raw milk enterococcal isolate exhibiting multiple virulence factors, *Microbiology* 149, 655-664.
- (36) Uguen, M., and Uguen, P. (2002) The LcnC homologue cannot replace LctT in lactacin 481 export, *FEMS Microbiol. Lett.* 208, 99-103.
- (37) Samyn, B., Martínez-Bueno, M., Devreese, B., Maqueda, M., Gálvez, A., Valdivia, E., Coyette, J., and Van Beeumen, J. (1994) The cyclic structure of the enterococcal peptide antibiotic AS-48, *FEBS Lett.* 352, 87-90.
- (38) Kemperman, R., Kuipers, A., Karsens, H., Nauta, A., Kuipers, O., and Kok, J. (2003) Identification and characterization of two novel clostridial bacteriocins, circularin A and closticin 574, *Appl. Environ. Microbiol.* 69, 1589-1597.
- (39) Kawai, Y., Saito, T., Kitazawa, H., and Itoh, T. (1998) Gassericin A; an uncommon cyclic bacteriocin produced by *Lactobacillus gasseri* LA39 linked at N- and C-terminal ends, *Biosci. Biotechnol. Biochem.* 62, 2438-2440.
- (40) Leer, R. J., van der Vossen, J. M. B. M., van Giezen, M., van Noort, J. M., and Pouwels, P. H. (1995) Genetic analysis of acidocin B, a novel bacteriocin produced by *Lactobacillus acidophilus*, *Microbiology* 141, 1629-1635.
- (41) Babasaki, K., Takao, T., Shimonishi, Y., and Kurahashi, K. (1985) Subtilosin A, a new antibiotic peptide produced by *Bacillus subtilis* 168: Isolation, structural analysis, and biogenesis, *J. Biochem.* 98, 585-603.

- (42) Kawulka, K. E., Sprules, T., Diaper, C. M., Whittal, R. M., McKay, R. T., Mercier, P., Zuber, P., and Vederas, J. C. (2004) Structure of subtilisin A, a cyclic antimicrobial peptide from *Bacillus subtilis* with unusual sulfur to  $\alpha$ -carbon cross-links: Formation and reduction of  $\alpha$ -thio- $\alpha$ -amino acid derivatives, *Biochemistry* 43, 3385-3395.
- (43) Kawulka, K., Sprules, T., McKay, R. T., Mercier, P., Diaper, C. M., Zuber, P., and Vederas, J. C. (2003) Structure of subtilisin A, an antimicrobial peptide from *Bacillus subtilis* with unusual posttranslational modifications linking cysteine sulfurs to  $\alpha$ -carbons of phenylalanine and threonine, *J. Am. Chem. Soc.* 125, 4726-4727.
- (44) Zheng, G., Yan, L. Z., Vederas, J. C., and Zuber, P. (1999) Genes of the *sbo-alb* locus of *Bacillus subtilis* are required for production of the antilisterial bacteriocin subtilisin, *J. Bacteriol.* 181, 7346-7355.
- (45) Sebei, S., Zendo, T., Boudabous, A., Nakayama, J., and Sonomoto, K. (2007) Characterization, *N*-terminal sequencing and classification of cerein MRX1, a novel bacteriocin purified from a newly isolated bacterium: *Bacillus cereus* MRX1, *J. Appl. Microbiol.* 103, 1621-1631.
- (46) Huang, T., Geng, H., Miyyapuram, V. R., Sit, C. S., Vederas, J. C., and Nakano, M. M. (2009) Isolation of a Variant of Subtilisin A with Hemolytic Activity, *J. Bacteriol.* 191, 5690-5696.
- (47) Chatterjee, C., Paul, M., Xie, L. L., and van der Donk, W. A. (2005) Biosynthesis and mode of action of lantibiotics, *Chem. Rev.* 105, 633-683.

- (48) Bierbaum, G., and Sahl, H. G. (2009) Lantibiotics: Mode of Action, Biosynthesis and Bioengineering, *Curr. Pharm. Biotechnol.* *10*, 2-18.
- (49) Asaduzzaman, S. M., and Sonomoto, K. (2009) Lantibiotics: Diverse activities and unique modes of action, *J. Biosci. Bioeng.* *107*, 475-487.
- (50) Nagao, J. I., Asaduzzaman, S. M., Aso, Y., Okuda, K., Nakayama, J., and Sonomoto, K. (2006) Lantibiotics: Insight and foresight for new paradigm, *J. Biosci. Bioeng.* *102*, 139-149.
- (51) Cotter, P. D., Hill, C., and Ross, R. P. (2005) Bacterial lantibiotics: Strategies to improve therapeutic potential, *Curr. Protein Pept. Sci.* *6*, 61-75.
- (52) Brötz, H., Josten, M., Wiedemann, I., Schneider, U., Götz, F., Bierbaum, G., and Sahl, H. G. (1998) Role of lipid-bound peptidoglycan precursors in the formation of pores by nisin, epidermin and other lantibiotics, *Mol. Microbiol.* *30*, 317-327.
- (53) Bonelli, R. R., Schneider, T., Sahl, H. G., and Wiedemann, I. (2006) Insights into in vivo activities of lantibiotics from gallidermin and epidermin mode-of-action studies, *Antimicrob. Agents Chemother.* *50*, 1449-1457.
- (54) Willey, J. M., and van der Donk, W. A. (2007) Lantibiotics: Peptides of diverse structure and function, *Annu. Rev. Microbiol.* *61*, 477-501.
- (55) Levensgood, M. R., Patton, G. C., and van der Donk, W. A. D. (2007) The leader peptide is not required for post-translational modification by lactacin 481 synthetase, *J. Am. Chem. Soc.* *129*, 10314-10315.

- (56) Håvarstein, L. S., Diep, D. B., and Nes, I. F. (1995) A Family of Bacteriocin ABC Transporters Carry out Proteolytic Processing of Their Substrates Concomitant with Export, *Mol. Microbiol.* 16, 229-240.
- (57) Draper, L. A., Ross, R. P., Hill, C., and Cotter, P. D. (2008) Lantibiotic immunity, *Curr. Protein Pept. Sci.* 9, 39-49.
- (58) Qiao, M. Q., Immonen, T., Koponen, O., and Saris, P. E. J. (1995) The Cellular Location and Effect on Nisin Immunity of the NisI Protein from *Lactococcus lactis* N8 Expressed in *Escherichia coli* and *L. lactis*, *FEMS Microbiol. Lett.* 131, 75-80.
- (59) Koponen, O., Takala, T. M., Saarela, U., Qiao, M. Q., and Saris, P. E. J. (2004) Distribution of the NisI immunity protein and enhancement of nisin activity by the lipid-free NisI, *FEMS Microbiol. Lett.* 231, 85-90.
- (60) Takala, T. M., Koponen, O., Qiao, M. Q., and Saris, P. E. J. (2004) Lipid-free NisI: interaction with nisin and contribution to nisin immunity via secretion, *FEMS Microbiol. Lett.* 237, 171-177.
- (61) Stein, T., Heinzmann, S., Solovieva, I., and Entian, K. D. (2003) Function of *Lactococcus lactis* nisin immunity genes *nisI* and *nisFEG* after coordinated expression in the surrogate host *Bacillus subtilis*, *J. Biol. Chem.* 278, 89-94.
- (62) Breukink, E., and de Kruijff, B. (2006) Lipid II as a target for antibiotics, *Nat. Rev. Drug Discov.* 5, 321-332.

- (63) de Kruijff, B., van Dam, V., and Breukink, E. (2008) Lipid II: A central component in bacterial cell wall synthesis and a target for antibiotics, *Prostaglandins Leukot. Essent. Fatty Acids* 79, 117-121.
- (64) Martin, N. I., and Breukink, E. (2007) The expanding role of lipid II as a target for antibiotics, *Future Microbiol.* 2, 513-525.
- (65) Labischinski, H., Goodell, E. W., Goodell, A., and Hochberg, M. L. (1991) Direct Proof of a "More-Than-Single-Layered" Peptidoglycan Architecture of *Escherichia coli* W7: a Neutron Small-Angle Scattering Study, *J. Bacteriol.* 173, 751-756.
- (66) Chatterjee, A. N., and Perkins, H. R. (1966) Compounds Formed between Nucleotides Related to Biosynthesis of Bacterial Cell Wall and Vancomycin, *Biochem. Biophys. Res. Commun.* 24, 489-494.
- (67) Molinari, H., Pastore, A., Lian, L. Y., Hawkes, G. E., and Sales, K. (1990) Structure of Vancomycin and a Vancomycin D-Ala-D-Ala Complex in Solution, *Biochemistry* 29, 2271-2277.
- (68) Perkins, H. R. (1969) Specificity of Combination between Mucopeptide Precursors and Vancomycin or Ristocetin, *Biochem. J.* 111, 195-205.
- (69) Sheldrick, G. M., Jones, P. G., Kennard, O., Williams, D. H., and Smith, G. A. (1978) Structure of vancomycin and its complex with acetyl-D-alanyl-D-alanine, *Nature* 271, 223-225.
- (70) Hsu, S. T. D., Breukink, E., Tischenko, E., Lutters, M. A. G., de Kruijff, B., Kaptein, R., Bonvin, A., and van Nuland, N. A. J. (2004) The nisin-

- lipid II complex reveals a pyrophosphate cage that provides a blueprint for novel antibiotics, *Nat. Struct. Mol. Biol.* *11*, 963-967.
- (71) Chan, W. C., Leyland, M., Clark, J., Dodd, H. M., Lian, L. Y., Gasson, M. J., Bycroft, B. W., and Roberts, G. C. K. (1996) Structure-activity relationships in the peptide antibiotic nisin: Antibacterial activity of fragments of nisin, *FEBS Lett.* *390*, 129-132.
- (72) Wiedemann, I., Böttiger, T., Bonelli, R. R., Wiese, A., Hagge, S. O., Gutschmann, T., Seydel, U., Deegan, L., Hill, C., Ross, P., and Sahl, H. G. (2006) The mode of action of the lantibiotic lactacin 3147 - a complex mechanism involving specific interaction of two peptides and the cell wall precursor lipid II, *Mol. Microbiol.* *61*, 285-296.
- (73) Morgan, S. M., O'Connor, P. M., Cotter, P. D., Ross, R. P., and Hill, C. (2005) Sequential actions of the two component peptides of the lantibiotic lactacin 3147 explain its antimicrobial activity at nanomolar concentrations, *Antimicrob. Agents Chemother.* *49*, 2606-2611.
- (74) Hasper, H. E., Kramer, N. E., Smith, J. L., Hillman, J. D., Zachariah, C., Kuipers, O. P., de Kruijff, B., and Breukink, E. (2006) An alternative bactericidal mechanism of action for lantibiotic peptides that target lipid II, *Science* *313*, 1636-1637.
- (75) Brötz, H., Bierbaum, G., Leopold, K., Reynolds, P. E., and Sahl, H. G. (1998) The lantibiotic mersacidin inhibits peptidoglycan synthesis by targeting lipid II, *Antimicrob. Agents Chemother.* *42*, 154-160.

- (76) Brötz, H., Bierbaum, G., Reynolds, P. E., and Sahl, H. G. (1997) The lantibiotic mersacidin inhibits peptidoglycan biosynthesis at the level of transglycosylation, *Eur. J. Biochem.* 246, 193-199.
- (77) Wiedemann, I., Breukink, E., van Kraaij, C., Kuipers, O. P., Bierbaum, G., de Kruijff, B., and Sahl, H. A. (2001) Specific binding of nisin to the peptidoglycan precursor lipid II combines pore formation and inhibition of cell wall biosynthesis for potent antibiotic activity, *J. Biol. Chem.* 276, 1772-1779.
- (78) Hasper, H. E., de Kruijff, B., and Breukink, E. (2004) Assembly and stability of nisin-Lipid II pores, *Biochemistry* 43, 11567-11575.
- (79) Breukink, E., van Heusden, H. E., Vollmerhaus, P. J., Swiezewska, E., Brunner, L., Walker, S., Heck, A. J. R., and de Kruijff, B. (2003) Lipid II is an intrinsic component of the pore induced by nisin in bacterial membranes, *J. Biol. Chem.* 278, 19898-19903.
- (80) van Heusden, H. E., de Kruijff, B., and Breukink, E. (2002) Lipid II induces a transmembrane orientation of the pore-forming peptide lantibiotic nisin, *Biochemistry* 41, 12171-12178.
- (81) Breukink, E., Wiedemann, I., van Kraaij, C., Kuipers, O. P., Sahl, H. G., and de Kruijff, B. (1999) Use of the cell wall precursor lipid II by a pore-forming peptide antibiotic, *Science* 286, 2361-2364.
- (82) McAuliffe, O., Ryan, M. P., Ross, R. P., Hill, C., Breuwer, P., and Abee, T. (1998) Lacticin 3147, a broad-spectrum bacteriocin which selectively dissipates the membrane potential, *Appl. Environ. Microbiol.* 64, 439-445.

- (83) Drider, D., Fimland, G., Héchard, Y., McMullen, L. M., and Prévost, H. (2006) The continuing story of class IIa bacteriocins, *Microbiol. Mol. Biol. Rev.* 70, 564-582.
- (84) Ennahar, S., Sashihara, T., Sonomoto, K., and Ishizaki, A. (2000) Class IIa bacteriocins: biosynthesis, structure and activity, *FEMS Microbiol. Rev.* 24, 85-106.
- (85) Quadri, L. E. N., Sailer, M., Terebiznik, M. R., Roy, K. L., Vederas, J. C., and Stiles, M. E. (1995) Characterization of the protein conferring immunity to the antimicrobial peptide carnobacteriocin B2 and expression of carnobacteriocins B2 and BM1, *J. Bacteriol.* 177, 1144-1151.
- (86) Dayem, M. A., Fleury, Y., Devilliers, G., Chaboisseau, E., Girard, R., Nicolas, P., and Delfour, A. (1996) The putative immunity protein of the Gram-positive bacteria *Leuconostoc mesenteroides* is preferentially located in the cytoplasm compartment, *FEMS Microbiol. Lett.* 138, 251-259.
- (87) Fimland, G., Eijsink, V. G. H., and Nissen-Meyer, J. (2002) Comparative studies of immunity proteins of pediocin-like bacteriocins, *Microbiology* 148, 3661-3670.
- (88) Fimland, G., Johnsen, L., Dalhus, B., and Nissen-Meyer, J. (2005) Pediocin-like antimicrobial peptides (class IIa bacteriocins) and their immunity proteins: biosynthesis, structure, and mode of action, *J. Pept. Sci.* 11, 688-696.

- (89) Maqueda, M., Gálvez, A., Martínez-Bueno, M., Sanchez-Barrena, M. J., González, C., Albert, A., Rico, M., and Valdivia, E. (2004) Peptide AS-48: Prototype of a New Class of Cyclic Bacteriocins, *Curr. Protein Pept. Sci.* 5, 399-416.
- (90) Kalmokoff, M. L., Cyr, T. D., Hefford, M. A., Whitford, M. F., and Teather, R. M. (2003) Butyrivibriocin AR10, a new cyclic bacteriocin produced by the ruminal anaerobe *Butyrivibrio fibrisolvens* AR10: characterization of the gene and peptide, *Can. J. Microbiol.* 49, 763-773.
- (91) Kawai, Y., Kusnadi, J., Kemperman, R., Kok, J., Ito, Y., Endo, M., Arakawa, K., Uchida, H., Nishimura, J., Kitazawa, H., and Saito, T. (2009) DNA Sequencing and Homologous Expression of a Small Peptide Conferring Immunity to Gassericin A, a Circular Bacteriocin Produced by *Lactobacillus gasseri* LA39, *Appl. Environ. Microbiol.* 75, 1324-1330.
- (92) Kawai, Y., Saito, T., Suzuki, M., and Itoh, T. (1998) Sequence analysis by cloning of the structural gene of gassericin A, a hydrophobic bacteriocin produced by *Lactobacillus gasseri* LA39, *Biosci. Biotechnol. Biochem.* 62, 887-892.
- (93) Kemperman, R., Jonker, M., Nauta, A., Kuipers, O. P., and Kok, J. (2003) Functional analysis of the gene cluster involved in production of the bacteriocin circularin A by *Clostridium beijerinckii* ATCC 25752, *Appl. Environ. Microbiol.* 69, 5839-5848.
- (94) Martínez-Bueno, M., Maqueda, M., Gálvez, A., Samyn, B., Van Beeumen, J., Coyette, J., and Valdivia, E. (1994) Determination of the gene sequence

- and the molecular structure of the enterococcal peptide antibiotic AS-48, *J. Bacteriol.* 176, 6334-6339.
- (95) Wirawan, R. E., Swanson, K. M., Kleffmann, T., Jack, R. W., and Tagg, J. R. (2007) Uberolysin: a novel cyclic bacteriocin produced by *Streptococcus uberis*, *Microbiology* 153, 1619-1630.
- (96) Martínez-Bueno, M., Valdivia, E., Gálvez, A., Coyette, J., and Maqueda, M. (1998) Analysis of the gene cluster involved in production and immunity of the peptide antibiotic AS-48 in *Enterococcus faecalis*, *Mol. Microbiol.* 27, 347-358.
- (97) Gálvez, A., Maqueda, M., Martínez-Bueno, M., and Valdivia, E. (1991) Permeation of bacterial cells, permeation of cytoplasmic and artificial membrane vesicles, and channel formation on lipid bilayers by peptide antibiotic AS-48 *J. Bacteriol.* 173, 886-892.
- (98) Gálvez, A., Maqueda, M., Martínez-Bueno, M., and Valdivia, E. (1989) Bactericidal and Bacteriolytic Action of Peptide Antibiotic AS-48 against Gram-Positive and Gram-Negative Bacteria and Other Organisms, *Res. Microbiol.* 140, 57-68.
- (99) Ennahar, S., Sonomoto, K., and Ishizaki, A. (1999) Class IIa bacteriocins from lactic acid bacteria: Antibacterial activity and food preservation, *J. Biosci. Bioeng.* 87, 705-716.
- (100) Gálvez, A., Lopez, R. L., Abriouel, H., Valdivia, E., and Ben Omar, N. (2008) Application of bacteriocins in the control of foodborne pathogenic and spoilage bacteria, *Crit. Rev. Biotechnol.* 28, 125-152.

- (101) Cleveland, J., Montville, T. J., Nes, I. F., and Chikindas, M. L. (2001) Bacteriocins: safe, natural antimicrobials for food preservation, *Int. J. Food Microbiol.* 71, 1-20.
- (102) Guinane, C. M., Cotter, P. D., Hill, C., and Ross, R. P. (2005) Microbial solutions to microbial problems; lactococcal bacteriocins for the control of undesirable biota in food, *J. Appl. Microbiol.* 98, 1316-1325.
- (103) Settanni, L., and Corsetti, A. (2008) Application of bacteriocins in vegetable food biopreservation, *Int. J. Food Microbiol.* 121, 123-138.
- (104) Helander, I. M., vonWright, A., and Mattila-Sandholm, T. M. (1997) Potential of lactic acid bacteria and novel antimicrobials against gram-negative bacteria, *Trends Food Sci. Technol.* 8, 146-150.
- (105) Parisien, A., Allain, B., Zhang, J., Mandeville, R., and Lan, C. Q. (2008) Novel alternatives to antibiotics: bacteriophages, bacterial cell wall hydrolases, and antimicrobial peptides, *J. Appl. Microbiol.* 104, 1-13.
- (106) Rossi, L. M., Rangasamy, P., Zhan, J., Qiu, X. Q., and Wu, G. Y. (2008) Research advances in the development of peptide antibiotics, *J. Pharm. Sci.* 97, 1060-1070.
- (107) Maher, S., and McClean, S. (2006) Investigation of the cytotoxicity of eukaryotic and prokaryotic antimicrobial peptides in intestinal epithelial cells in vitro, *Biochem. Pharmacol.* 71, 1289-1298.
- (108) Silkin, L., Hamza, S., Kaufman, S., Cobb, S. L., and Vederas, J. C. (2008) Spermicidal Bacteriocins: Lacticin 3147 and Subtilosin A, *Bioorg. Med. Chem. Lett.* 18, 3103-3106.

- (109) Martin-Visscher, L. A., van Belkum, M. J., Garneau-Tsodikova, S., Whittall, R. M., Zheng, J., McMullen, L. M., and Vederas, J. C. (2008) Isolation and characterization of carnocyclin A, a novel circular bacteriocin produced by *Carnobacterium maltaromaticum* UAL307, *Appl. Environ. Microbiol.* 74, 4756-4763.
- (110) Gong, X. D., Martin-Visscher, L. A., Nahirney, D., Vederas, J. C., and Duszyk, M. (2009) The circular bacteriocin, carnocyclin A, forms anion-selective channels in lipid bilayers, *BBA-Biomembranes* 1788, 1797-1803.
- (111) Martin-Visscher, L. A., Gong, X. D., Duszyk, M., and Vederas, J. C. (2009) The Three-dimensional Structure of Carnocyclin A Reveals That Many Circular Bacteriocins Share a Common Structural Motif, *J. Biol. Chem.* 284, 28674-28681.
- (112) Craik, D. J., Daly, N. L., Saska, I., Trabi, M., and Rosengren, K. J. (2003) Structures of naturally occurring circular proteins from bacteria, *J. Bacteriol.* 185, 4011-4021.
- (113) Craik, D. J. (2009) Circling the enemy: cyclic proteins in plant defence, *Trends Plant Sci.* 14, 328-335.
- (114) Craik, D. J. (2006) Chemistry - Seamless proteins tie up their loose ends, *Science* 311, 1563-1564.
- (115) Kawai, Y., Kemperman, R., Kok, J., and Saito, T. (2004) The circular bacteriocins gassericin A and circularin A, *Curr. Protein Pept. Sci.* 5, 393-398.

- (116) Sawa, N., Zendo, T., Kiyofuji, J., Fujita, K., Himeno, K., Nakayama, J., and Sonomoto, K. (2009) Identification and Characterization of Lactocyclicin Q, a Novel Cyclic Bacteriocin Produced by *Lactococcus* sp. Strain QU 12, *Appl. Environ. Microbiol.* 75, 1552-1558.
- (117) Gillon, A. D., Saska, I., Jennings, C. V., Guarino, R. F., Craik, D. J., and Anderson, M. A. (2008) Biosynthesis of circular proteins in plants, *Plant J.* 53, 505-515.
- (118) Daly, N. L., Rosengren, K. J., and Craik, D. J. (2009) Discovery, structure and biological activities of cyclotides, *Adv. Drug Deliver. Rev.* 61, 918-930.
- (119) Ireland, D. C., Colgravel, M. L., Nguyencong, P., Daly, N. L., and Craik, D. J. (2006) Discovery and characterization of a linear cyclotide from *Viola odorata*: Implications for the processing of circular proteins, *J. Mol. Biol.* 357, 1522-1535.
- (120) Saska, I., Gillon, A. D., Hatsugai, N., Dietzgen, R. G., Hara-Nishimura, I., Anderson, M. A., and Craik, D. J. (2007) An asparaginyl endopeptidase mediates *in vivo* protein backbone cyclization, *J. Biol. Chem.* 282, 29721-29728.
- (121) González, C., Langdon, G. M., Bruix, M., Gálvez, A., Valdivia, E., Maqueda, M., and Rico, M. (2000) Bacteriocin AS-48, a microbial cyclic polypeptide structurally and functionally related to mammalian NK-lysin, *Proc. Natl. Acad. Sci. USA* 97, 11221-11226.

- (122) Sánchez-Barrena, M. J., Martínez-Ripoll, M., Gálvez, A., Valdivia, E., Maqueda, M., Cruz, V., and Albert, A. (2003) Structure of bacteriocin AS-48: From soluble state to membrane bound state, *J. Mol. Biol.* 334, 541-549.
- (123) Jiménez, M. A., Barrachi-Saccilotto, A. C., Valdivia, E., Maqueda, M., and Rico, M. (2005) Design, NMR characterization and activity of a 21-residue peptide fragment of bacteriocin AS-48 containing its putative membrane interacting region, *J Pept Sci* 11, 29-36.
- (124) Kawai, Y., Ishii, Y., Arakawa, K., Uemura, K., Saitoh, B., Nishimura, J., Kitazawa, H., Yamazaki, Y., Tateno, Y., Itoh, T., and Saitoh, T. (2004) Structural and functional differences in two cyclic bacteriocins with the same sequences produced by lactobacilli, *Appl. Environ. Microbiol.* 70, 2906-2911.
- (125) Quadri, L. E. N., Sailer, M., Roy, K. L., Vederas, J. C., and Stiles, M. E. (1994) Chemical and genetic characterization of bacteriocins produced by *Carnobacterium piscicola* LV17B, *J. Biol. Chem.* 269, 12204-12211.
- (126) van Belkum, M. J., Hayema, B. J., Jeeninga, R. E., Kok, J., and Venema, G. (1991) Organization and Nucleotide Sequences of two Lactococcal Bacteriocin Operons, *Appl. Environ. Microbiol.* 57, 492-498.
- (127) Ahn, C., and Stiles, M. E. (1990) Plasmid-associated bacteriocin production by a strain of *Carnobacterium piscicola* from meat, *Appl. Environ. Microbiol.* 56, 2503-2510.

- (128) Worobo, R. W., van Belkum, M. J., Sailer, M., Roy, K. L., Vederas, J. C., and Stiles, M. E. (1995) A signal peptide secretion-dependent bacteriocin from *Carnobacterium divergens*, *J. Bacteriol.* 177, 3143-3149.
- (129) Franz, C. M. A. P., Worobo, R. W., Quadri, L. E. N., Schillinger, U., Holzapfel, W. H., Vederas, J. C., and Stiles, M. E. (1999) Atypical genetic locus associated with constitutive production of enterocin B by *Enterococcus faecium* BFE 900, *Appl. Environ. Microbiol.* 65, 2170-2178.
- (130) Ryan, M. P., Rea, M. C., Hill, C., and Ross, R. P. (1996) An application in cheddar cheese manufacture for a strain of *Lactococcus lactis* producing a novel broad-spectrum bacteriocin, lacticin 3147, *Appl. Environ. Microbiol.* 62, 612-619.
- (131) Schillinger, U., Kaya, M., and Lücke, F. K. (1991) Behavior of *Listeria monocytogenes* in meat and its control by a bacteriocin-producing strain of *Lactobacillus sake*, *J. Appl. Bacteriol.* 70, 473-478.
- (132) Héchard, Y., Dérijard, B., Letellier, F., and Cenatiempo, Y. (1992) Characterization and purification of mesentericin Y105, an anti-*Listeria* bacteriocin from *Leuconostoc mesenteroides*, *J. Gen. Microbiol.* 138, 2725-2731.
- (133) González, C. F., and Kunka, B. S. (1987) Plasmid-associated bacteriocin production and sucrose fermentation in *Pediococcus acidilactici*, *Appl. Environ. Microbiol.* 53, 2534-2538.

- (134) Yanisch-Perron, C., Vieira, J., and Messing, J. (1985) Improved M13 phage cloning vectors and host strains: nucleotide sequences of the M13mp18 and pUC19 vectors, *Gene* 33, 103-119.
- (135) Miteva, M., Andersson, M., Karshikoff, A., and Otting, G. (1999) Molecular electroporation: a unifying concept for the description of membrane pore formation by antibacterial peptides, exemplified with NK-lysin, *FEBS Lett.* 462, 155-158.
- (136) Hille, B. (1992) *Ionic channels of excitable membranes*, 2nd ed., Sinauer Associates Inc, Sunderland, Mass.
- (137) Kaur, K., Andrew, L. C., Wishart, D. S., and Vederas, J. C. (2004) Dynamic relationships among type IIa bacteriocins: Temperature effects on antimicrobial activity and on structure of the C-terminal amphipathic  $\alpha$  helix as a receptor-binding region, *Biochemistry* 43, 9009-9020.
- (138) Gallagher, N. L. F., Sailer, M., Niemczura, W. P., Nakashima, T. T., Stiles, M. E., and Vederas, J. C. (1997) Three-dimensional structure of leuocin A in trifluoroethanol and dodecylphosphocholine micelles: Spatial location of residues critical for biological activity in type IIa bacteriocins from lactic acid bacteria, *Biochemistry* 36, 15062-15072.
- (139) Uteng, M., Hauge, H. H., Markwick, P. R. L., Fimland, G., Mantzilas, D., Nissen-Meyer, J., and Muhle-Goll, C. (2003) Three-dimensional structure in lipid micelles of the pediocin-like antimicrobial peptide sakacin P and a sakacin P variant that is structurally stabilized by an inserted C-terminal disulfide bridges, *Biochemistry* 42, 11417-11426.

- (140) Wang, Y. J., Henz, M. E., Gallagher, N. L. F., Chai, S. Y., Gibbs, A. C., Yan, L. Z., Stiles, M. E., Wishart, D. S., and Vederas, J. C. (1999) Solution structure of carnobacteriocin B2 and implications for structure-activity relationships among type IIa bacteriocins from lactic acid bacteria, *Biochemistry* 38, 15438-15447.
- (141) Wishart, D. S., and Sykes, B. D. (1994) The  $^{13}\text{C}$  Chemical-Shift Index: A simple method for the identification of protein secondary structure using  $^{13}\text{C}$  chemical-shift data, *J. Biomol. NMR* 4, 171-180.
- (142) Güntert, P., Mumenthaler, C., and Wüthrich, K. (1997) Torsion angle dynamics for NMR structure calculation with the new program DYANA, *J. Mol. Biol.* 273, 283-298.
- (143) Cornilescu, G., Delaglio, F., and Bax, A. (1999) Protein backbone angle restraints from searching a database for chemical shift and sequence homology, *J. Biomol. NMR* 13, 289-302.
- (144) Larkin, M. A., Blackshields, G., Brown, N. P., Chenna, R., McGettigan, P. A., McWilliam, H., Valentin, F., Wallace, I. M., Wilm, A., Lopez, R., Thompson, J. D., Gibson, T. J., and Higgins, D. G. (2007) Clustal W and clustal X version 2.0, *Bioinformatics* 23, 2947-2948.
- (145) Holm, L., Kääriäinen, S., Rosenström, P., and Schenkel, A. (2008) Searching protein structure databases with DaliLite v.3, *Bioinformatics* 24, 2780-2781.
- (146) Ahn, V. E., Leyko, P., Alattia, J. R., Chen, L., and Privé, G. G. (2006) Crystal structures of saposins A and C, *Protein Sci.* 15, 1849-1857.

- (147) Hecht, O., van Nuland, N. A., Schleinkofer, K., Dingley, A. J., Bruhn, H., Leippe, M., and Grotzinger, J. (2004) Solution structure of the pore-forming protein of *Entamoeba histolytica*, *J. Biol. Chem.* 279, 17834-17841.
- (148) Liepinsh, E., Andersson, M., Ruyschaert, J. M., and Otting, G. (1997) Saposin fold revealed by the NMR structure of NK-lysin, *Nat. Struct. Biol.* 4, 793-795.
- (149) Cole, C., Barber, J. D., and Barton, G. J. (2008) The Jpred 3 secondary structure prediction server, *Nucleic Acids Res.* 36, W197-W201.
- (150) McGuffin, L. J., Bryson, K., and Jones, D. T. (2000) The PSIPRED protein structure prediction server, *Bioinformatics* 16, 404-405.
- (151) Gasteiger, E., Hoogland, C., Gattiker, A., Duvaud, S., Wilkins, M. R., Appel, R. D., and Bairoch, A. (2005) Protein identification and analysis tools on the ExPASy server, in *The Proteomics Protocols Handbook* (Walker, J. M., Ed.) pp 571-607, Humana Press.
- (152) Lai, C. Z., Koseoglu, S. S., Lugert, E. C., Boswell, P. G., Rábai, J., Lodge, T. P., and Bühlmann, P. (2009) Fluorous Polymeric Membranes for Ionophore-Based Ion-Selective Potentiometry: How Inert Is Teflon AF?, *J. Am. Chem. Soc.* 131, 1598-1606.
- (153) Sprules, T., Kawulka, K. E., Gibbs, A. C., Wishart, D. S., and Vederas, J. C. (2004) NMR solution structure of the precursor for carnobacteriocin B2, an antimicrobial peptide from *Carnobacterium piscicola*: Implications

- of the  $\alpha$ -helical leader section for export and inhibition of type IIa bacteriocin activity, *Eur. J. Biochem.* 271, 1748-1756.
- (154) van Belkum, M. J., Worobo, R. W., and Stiles, M. E. (1997) Double-glycine-type leader peptides direct secretion of bacteriocins by ABC transporters: Colicin V secretion in *Lactococcus lactis*, *Mol. Microbiol.* 23, 1293-1301.
- (155) Sánchez-Hidalgo, M., Martínez-Bueno, M., Fernández-Escamilla, A. M., Valdivia, E., Serrano, L., and Maqueda, M. (2008) Effect of replacing glutamic residues upon the biological activity and stability of the circular enterocin AS-48, *J Antimicrob Chemother* 61, 1256-1265.
- (156) Martin-Visscher, L. A., Sprules, T., Gursky, L. J., and Vederas, J. C. (2008) Nuclear magnetic resonance solution structure of PisI, a group B immunity protein that provides protection against the type IIa bacteriocin piscicolin 126, PisA, *Biochemistry* 47, 6427-6436.
- (157) Eijsink, V. G. H., Skeie, M., Middelhoven, P. H., Brurberg, M. B., and Nes, I. F. (1998) Comparative studies of class IIa bacteriocins of lactic acid bacteria, *Appl. Environ. Microbiol.* 64, 3275-3281.
- (158) Savadogo, A., Ouattara, C. A. T., Bassole, I. H. N., and Alfred, S. A. (2006) Bacteriocins and lactic acid bacteria - a minireview, *African Journal of Biotechnology* 5, 678-683.
- (159) Fimland, G., Blingsmo, O. R., Sletten, K., Jung, G., Nes, I. F., and NissenMeyer, J. (1996) New biologically active hybrid bacteriocins constructed by combining regions from various pediocin-like bacteriocins:

- The C-terminal region is important for determining specificity, *Appl. Environ. Microbiol.* *62*, 3313-3318.
- (160) Fimland, G., Eijsink, V. G. H., and Nissen-Meyer, J. (2002) Mutational analysis of the role of tryptophan residues in an antimicrobial peptide, *Biochemistry* *41*, 9508-9515.
- (161) Fimland, G., Jack, R., Jung, G., Nes, I. F., and Nissen-Meyer, J. (1998) The bactericidal activity of pediocin PA-1 is specifically inhibited by a 15-mer fragment that spans the bacteriocin from the center toward the C terminus, *Appl. Environ. Microbiol.* *64*, 5057-5060.
- (162) Fimland, G., Johnsen, L., Axelsson, L., Brurberg, M. B., Nes, I. F., Eijsink, V. G. H., and Nissen-Meyer, J. (2000) A C-terminal disulfide bridge in pediocin-like bacteriocins renders bacteriocin activity less temperature dependent and is a major determinant of the antimicrobial spectrum, *J. Bacteriol.* *182*, 2643-2648.
- (163) Johnsen, L., Fimland, G., and Meyer, J. N. (2005) The C-terminal domain of pediocin-like antimicrobial peptides (class IIa bacteriocins) is involved in specific recognition of the C-terminal part of cognate immunity proteins and in determining the antimicrobial spectrum, *J. Biol. Chem.* *280*, 9243-9250.
- (164) Haugen, H. S., Fimland, G., Nissen-Meyer, J., and Kristiansen, P. E. (2005) Three-dimensional structure in lipid micelles of the pediocin-like antimicrobial peptide curvacin A, *Biochemistry* *44*, 16149-16157.

- (165) Johnsen, L., Fimland, G., Mantzilas, D., and Nissen-Meyer, J. (2004) Structure-function analysis of immunity proteins of pediocin-like bacteriocins: C-terminal parts of immunity proteins are involved in specific recognition of cognate bacteriocins, *Appl. Environ. Microbiol.* 70, 2647-2652.
- (166) Chen, Y. H., Ludescher, R. D., and Montville, T. J. (1997) Electrostatic interactions, but not the YGNGV consensus motif, govern the binding of pediocin PA-1 and its fragments to phospholipid vesicles, *Appl. Environ. Microbiol.* 63, 4770-4777.
- (167) Kazazic, M., Nissen-Meyer, J., and Fimland, G. (2002) Mutational analysis of the role of charged residues in target-cell binding, potency and specificity of the pediocin-like bacteriocin sakacin P, *Microbiology* 148, 2019-2027.
- (168) Thompson, J. D., Higgins, D. G., and Gibson, T. J. (1994) CLUSTAL W: Improving the sensitivity of progressive multiple sequence alignment through sequence weighting, position-specific gap penalties and weight matrix choice, *Nucleic Acids Res.* 22, 4673-4680.
- (169) Aymerich, T., Holo, H., Håvarstein, L. S., Hugas, M., Garriga, M., and Nes, I. F. (1996) Biochemical and genetic characterization of enterocin A from *Enterococcus faecium*, a new antilisterial bacteriocin in the pediocin family of bacteriocins, *Appl. Environ. Microbiol.* 62, 1676-1682.
- (170) Tomita, H., Fujimoto, S., Tanimoto, K., and Ike, Y. (1996) Cloning and genetic organization of the bacteriocin 31 determinant encoded on the

- Enterococcus faecalis* pheromone responsive conjugative plasmid pYI17, *J. Bacteriol.* 178, 3585-3593.
- (171) Kawamoto, S., Shima, J., Sato, R., Eguchi, T., Ohmomo, S., Shibato, J., Horikoshi, N., Takeshita, K., and Sameshima, T. (2002) Biochemical and genetic characterization of mundticin KS, an antilisterial peptide produced by *Enterococcus mundtii* NFRI 7393, *Appl. Environ. Microbiol.* 68, 3830-3840.
- (172) Bennik, M. H. J., Vanloo, B., Brasseur, R., Gorris, L. G. M., and Smid, E. J. (1998) A novel bacteriocin with a YGNGV motif from vegetable-associated *Enterococcus mundtii*: full characterization and interaction with target organisms, *Biochim. Biophys. Acta-Biomembr.* 1373, 47-58.
- (173) Saavedra, L., Minahk, C., Holgado, A. P. D., and Sesma, F. (2004) Enhancement of the enterocin CRL35 activity by a synthetic peptide derived from the NH<sub>2</sub>-terminal sequence, *Antimicrob. Agents Chemother.* 48, 2778-2781.
- (174) Tichaczek, P. S., Vogel, R. F., and Hammes, W. P. (1994) Cloning and sequencing of *sakP* encoding sakacin P, the bacteriocin produced by *Lactobacillus sake* ITH 673, *Microbiology* 140, 361-367.
- (175) Kalmokoff, M. L., Banerjee, S. K., Cyr, T., Hefford, M. A., and Gleeson, T. (2001) Identification of a new plasmid-encoded *sec*-dependent bacteriocin produced by *Listeria innocua* 743, *Appl. Environ. Microbiol.* 67, 4041-4047.

- (176) Fremaux, C., Héchard, Y., and Cenatiempo, Y. (1995) Mesentericin Y105 gene clusters in *Leuconostoc mesenteroides* Y105, *Microbiology* 141, 1637-1645.
- (177) Simon, L., Fremaux, C., Cenatiempo, Y., and Berjeaud, J. M. (2002) Sakacin G, a new type of antilisterial bacteriocin, *Appl. Environ. Microbiol.* 68, 6416-6420.
- (178) Yildirim, Z., Winters, D. K., and Johnson, M. G. (1999) Purification, amino acid sequence and mode of action of bifidocin B produced by *Bifidobacterium bifidum* NCFB 1454, *J. Appl. Microbiol.* 86, 45-54.
- (179) Cintas, L. M., Casaus, P., Håvarstein, L. S., Hernández, P. E., and Nes, I. F. (1997) Biochemical and genetic characterization of enterocin P, a novel *sec*-dependent bacteriocin from *Enterococcus faecium* P13 with a broad antimicrobial spectrum, *Appl. Environ. Microbiol.* 63, 4321-4330.
- (180) Tichaczek, P. S., Vogel, R. F., and Hammes, W. P. (1993) Cloning and Sequencing of *curA* Encoding Curvacin A, the Bacteriocin Produced by *Lactobacillus curvatus* LTH1174, *Arch. Microbiol.* 160, 279-283.
- (181) Métivier, A., Pilet, M. F., Dousset, X., Sorokine, O., Anglade, P., Zagorec, M., Piard, J. C., Marion, D., Cenatiempo, Y., and Fremaux, C. (1998) Divercin V41, a new bacteriocin with two disulphide bonds produced by *Carnobacterium divergens* V41: primary structure and genomic organization, *Microbiology* 144, 2837-2844.
- (182) Axelsson, L. (2004) GenBank, accession no. AJ626711.

- (183) Franz, C., van Belkum, M. J., Worobo, R. W., Vederas, J. C., and Stiles, M. E. (2000) Characterization of the genetic locus responsible for production and immunity of carnobacteriocin A: the immunity gene confers cross-protection to enterocin B, *Microbiology* 146, 621-631.
- (184) O'Keeffe, T., Hill, C., and Ross, R. P. (1999) Characterization and heterologous expression of the genes encoding enterocin A production, immunity, and regulation in *Enterococcus faecium* DPC1146, *Appl. Environ. Microbiol.* 65, 1506-1515.
- (185) Kim, I. K., Kim, M. K., Kim, J. H., Yim, H. S., Cha, S. S., and Kang, S. O. (2007) High resolution crystal structure of PedB: a structural basis for the classification of pediocin-like immunity proteins, *BMC Struct. Biol.* 7.
- (186) Brurberg, M. B., Nes, I. F., and Eijsink, V. G. H. (1997) Pheromone-induced production of antimicrobial peptides in *Lactobacillus*, *Mol. Microbiol.* 26, 347-360.
- (187) Jeon, H. J., Noda, M., Matoba, Y., Kumagai, T., and Sugiyama, M. (2009) Crystal structure and mutagenic analysis of a bacteriocin immunity protein, Mun-im, *Biochem. Biophys. Res. Commun.* 378, 574-578.
- (188) Saavedra, L., de Ruiz Holgado, A., and Sesma, F. (2003) GenBank, accession no. AY398693.
- (189) Axelsson, L., and Holck, A. (1995) The genes involved in production of and immunity to sakacin A, a bacteriocin from *Lactobacillus sake* Lb706, *J. Bacteriol.* 177, 2125-2137.

- (190) Sprules, T., Kawulka, K. E., and Vederas, J. C. (2004) NMR solution structure of ImB2, a protein conferring immunity to antimicrobial activity of the type IIa bacteriocin, carnobacteriocin B2, *Biochemistry* 43, 11740-11749.
- (191) Johnsen, L., Dalhus, B., Leiros, I., and Nissen-Meyer, J. (2005) 1.6 Å crystal structure of EntA-im: A bacterial immunity protein conferring immunity to the antimicrobial activity of the pediocin-like bacteriocin enterocin A, *J. Biol. Chem.* 280, 19045-19050.
- (192) Cascales, E., Buchanan, S. K., Duché, D., Kleanthous, C., Lloubès, R., Postle, K., Riley, M., Slatin, S., and Cavard, D. (2007) Colicin biology, *Microbiol. Mol. Biol. Rev.* 71, 158-229.
- (193) Kolade, O. O., Carr, S. B., Kühlmann, U. C., Pommer, A., Kleanthous, C., Bouchcinsky, C. A., and Hemmings, A. M. (2002) Structural aspects of the inhibition of DNase and rRNase colicins by their immunity proteins, *Biochimie* 84, 439-446.
- (194) Dennis, C. A., Videler, H., Pauptit, R. A., Wallis, R., James, R., Moore, G. R., and Kleanthous, C. (1998) A structural comparison of the colicin immunity proteins Im7 and Im9 gives new insights into the molecular determinants of immunity-protein specificity, *Biochem. J.* 333, 183-191.
- (195) Osborne, M. J., Breeze, A. L., Lian, L. Y., Reilly, A., James, R., Kleanthous, C., and Moore, G. R. (1996) Three-dimensional solution structure and <sup>13</sup>C nuclear magnetic resonance assignments of the colicin E9 immunity protein Im9, *Biochemistry* 35, 9505-9512.

- (196) Chak, K. F., Safo, M. K., Ku, W. Y., Hsieh, S. Y., and Yuan, H. S. (1996) The crystal structure of the immunity protein of colicin E7 suggests a possible colicin-interacting surface, *Proc. Natl. Acad. Sci. U. S. A.* *93*, 6437-6442.
- (197) Yan, L. Z., Gibbs, A. C., Stiles, M. E., Wishart, D. S., and Vederas, J. C. (2000) Analogues of bacteriocins: Antimicrobial specificity and interactions of leucocin A with its enantiomer, carnobacteriocin B2, and truncated derivatives, *J. Med. Chem.* *43*, 4579-4581.
- (198) Dalet, K., Cenatiempo, Y., Cossart, P., Consortium, E. L. G., and Héchard, Y. (2001) A  $\sigma^{54}$ -dependent PTS permease of the mannose family is responsible for sensitivity of *Listeria monocytogenes* to mesentericin Y105, *Microbiology* *147*, 3263-3269.
- (199) Diep, D. B., Skaugen, M., Salehian, Z., Holo, H., and Nes, I. F. (2007) Common mechanisms of target cell recognition and immunity for class II bacteriocins, *Proc. Natl. Acad. Sci. U. S. A.* *104*, 2384-2389.
- (200) Gravesen, A., Ramnath, M., Rechinger, K. B., Andersen, N., Jansch, L., Héchard, Y., Hastings, J. W., and Knøchel, S. (2002) High-level resistance to class IIa bacteriocins is associated with one general mechanism in *Listeria monocytogenes*, *Microbiology* *148*, 2361-2369.
- (201) Héchard, Y., Pelletier, C., Cenatiempo, Y., and Frère, J. (2001) Analysis of  $\sigma^{54}$ -dependent genes in *Enterococcus faecalis*: a mannose PTS permease (EII<sup>Man</sup>) is involved in sensitivity to a bacteriocin, mesentericin Y105, *Microbiology* *147*, 1575-1580.

- (202) Kjos, M., Nes, I. F., and Diep, D. B. (2009) Class II one-peptide bacteriocins target a phylogenetically defined subgroup of mannose phosphotransferase systems on sensitive cells, *Microbiology* 155, 2949-2961.
- (203) Ramnath, M., Beukes, M., Tamura, K., and Hastings, J. W. (2000) Absence of a putative mannose-specific phosphotransferase system enzyme IIAB component in a leucocin A resistant strain of *Listeria monocytogenes*, as shown by two-dimensional sodium dodecyl sulfate-polyacrylamide gel electrophoresis, *Appl. Environ. Microbiol.* 66, 3098-3101.
- (204) Barabote, R. D., and Saier, M. H. (2005) Comparative genomic analyses of the bacterial phosphotransferase system, *Microbiol. Mol. Biol. Rev.* 69, 608-634.
- (205) Postma, P. W., Lengeler, J. W., and Jacobson, G. R. (1993) Phosphoenolpyruvate:Carbohydrate Phosphotransferase Systems of Bacteria, *Microbiol. Rev.* 57, 543-594.
- (206) Dalet, K., Briand, C., Cenatiempo, Y., and Héchard, Y. (2000) The *rpoN* gene of *Enterococcus faecalis* directs sensitivity to subclass IIa bacteriocins, *Curr. Microbiol.* 41, 441-443.
- (207) Robichon, D., Gouin, E., Débarbouillé, M., Cossart, P., Cenatiempo, Y., and Héchard, Y. (1997) The *rpoN* ( $\sigma_{54}$ ) gene from *Listeria monocytogenes* is involved in resistance to mesentericin Y105, an

- antibacterial peptide from *Leuconostoc mesenteroides*, *J. Bacteriol.* 179, 7591-7594.
- (208) Vu-Khac, H., and Miller, K. W. (2009) Regulation of Mannose Phosphotransferase System Permease and Virulence Gene Expression in *Listeria monocytogenes* by the EII<sub>t</sub><sup>Man</sup> Transporter, *Appl. Environ. Microbiol.* 75, 6671-6678.
- (209) Ramnath, M., Arous, S., Gravesen, A., Hastings, J. W., and Héchard, Y. (2004) Expression of *mptC* of *Listeria monocytogenes* induces sensitivity to class IIa bacteriocins in *Lactococcus lactis*, *Microbiology* 150, 2663-2668.
- (210) Soliman, W., Bhattacharjee, S., and Kaur, K. (2007) Molecular dynamics simulation study of interaction between a class IIa bacteriocin and its immunity protein, *BBA-Proteins Proteomics* 1774, 1002-1013.
- (211) Quadri, L. E. N., Yan, L. Z., Stiles, M. E., and Vederas, J. C. (1997) Effect of amino acid substitutions on the activity of carnobacteriocin B2: Overproduction of the antimicrobial peptide, its engineered variants, and its precursor in *Escherichia coli*, *J. Biol. Chem.* 272, 3384-3388.
- (212) Kotake, Y., Ishii, S., Yano, T., Katsuoka, Y., and Hayashi, H. (2008) Substrate recognition mechanism of the peptidase domain of the quorum-sensing-signal-producing ABC transporter ComA from *Streptococcus*, *Biochemistry* 47, 2531-2538.
- (213) Martín, M., Gutiérrez, J., Criado, R., Herranz, C., Cintas, L. M., and Hernández, P. E. (2007) Chimeras of mature pediocin PA-1 fused to the

- signal peptide of enterocin P permits the cloning, production, and expression of pediocin PA-1 in *Lactococcus lactis*, *J. Food Prot.* *70*, 2792-2798.
- (214) Nagao, J., Morinaga, Y., Islam, M. R., Asaduzzaman, S. M., Aso, Y., Nakayama, J., and Sonomoto, K. (2009) Mapping and identification of the region and secondary structure required for the maturation of the nukacin ISK-1 prepeptide, *Peptides* *30*, 1412-1420.
- (215) Patton, G. C., Paul, M., Cooper, L. E., Chatterjee, C., and van der Donk, W. A. (2008) The importance of the leader sequence for directing lanthionine formation in lactacin 481, *Biochemistry* *47*, 7342-7351.
- (216) Chatterjee, C., Patton, G. C., Cooper, L., Paul, M., and van der Donk, W. A. (2006) Engineering dehydro amino acids and thioethers into peptides using lactacin 481 synthetase, *Chem. Biol.* *13*, 1109-1117.
- (217) Kluskens, L. D., Kuipers, A., Rink, R., de Boef, E., Fekken, S., Driessen, A. J. M., Kuipers, O. P., and Moll, G. N. (2005) Post-translational modification of therapeutic peptides by NisB, the dehydratase of the lantibiotic nisin, *Biochemistry* *44*, 12827-12834.
- (218) Rink, R., Kuipers, A., de Boef, E., Leenhouts, K. J., Driessen, A. J. M., Moll, G. N., and Kuipers, O. P. (2005) Lantibiotic structures as guidelines for the design of peptides that can be modified by lantibiotic enzymes, *Biochemistry* *44*, 8873-8882.
- (219) Håvarstein, L. S., Holo, H., and Nes, I. F. (1994) The Leader Peptide of Colicin-V Shares Consensus Sequences with Leader Peptides That Are

- Common among Peptide Bacteriocins Produced by Gram-Positive Bacteria, *Microbiology* 140, 2383-2389.
- (220) Aucher, W., Lacombe, C., Héquet, A., Frère, J., and Berjeaud, J. M. (2005) Influence of amino acid substitutions in the leader peptide on maturation and secretion of mesentericin Y105 by *Leuconostoc mesenteroides*, *J. Bacteriol.* 187, 2218-2223.
- (221) Chen, P., Qi, F. X., Novak, J., Krull, R. E., and Caufield, P. W. (2001) Effect of amino acid substitutions in conserved residues in the leader peptide on biosynthesis of the lantibiotic mutacin II, *FEMS Microbiol. Lett.* 195, 139-144.
- (222) Ihnken, L. A. F., Chatterjee, C., and van der Donk, W. A. (2008) *In vitro* reconstitution and substrate specificity of a lantibiotic protease, *Biochemistry* 47, 7352-7363.
- (223) Ishii, S., Yano, T., and Hayashi, H. (2006) Expression and characterization of the peptidase domain of *Streptococcus pneumoniae* ComA, a bifunctional ATP-binding cassette transporter involved in quorum sensing pathway, *J. Biol. Chem.* 281, 4726-4731.
- (224) Gajic, O., Buist, G., Kojic, M., Topisirovic, L., Kuipers, O. P., and Kok, J. (2003) Novel mechanism of bacteriocin secretion and immunity carried out by lactococcal multidrug resistance proteins, *J. Biol. Chem.* 278, 34291-34298.
- (225) Otto, M., and Gotz, F. (2001) ABC transporters of staphylococci, *Res. Microbiol.* 152, 351-356.

- (226) Higgins, C. F. (1992) ABC Transporters - from Microorganisms to Man, *Annu. Rev. Cell Biol.* 8, 67-113.
- (227) Franke, C. M., Tiemersma, J., Venema, G., and Kok, J. (1999) Membrane topology of the lactococcal bacteriocin ATP-binding cassette transporter protein LcnC: Involvement of LcnC in lactococcin A maturation, *J. Biol. Chem.* 274, 8484-8490.
- (228) Wu, K. H., and Tai, P. C. (2004) Cys<sup>32</sup> and His<sup>105</sup> are the critical residues for the calcium-dependent cysteine proteolytic activity of CvaB, an ATP-binding cassette transporter, *J. Biol. Chem.* 279, 901-909.
- (229) Quinlan, R. A., Moir, R. D., and Stewart, M. (1989) Expression in *Escherichia coli* of Fragments of Glial Fibrillary Acidic Protein: characterization, assembly properties and paracrystal formation, *J. Cell Sci.* 93, 71-83.
- (230) Nagai, K., and Thogersen, H. C. (1984) Generation of  $\beta$ -globin by sequence-specific proteolysis of a hybrid protein produced in *Escherichia coli*, *Nature* 309, 810-812.
- (231) Shrimpton, C. N., Glucksman, M. J., Lew, R. A., Tullai, J. W., Margulies, E. H., Roberts, J. L., and Smith, A. I. (1997) Thiol activation of endopeptidase EC 3.4.24.15: A novel mechanism for the regulation of catalytic activity, *J. Biol. Chem.* 272, 17395-17399.
- (232) Nelson, M., and McClelland, M. (1992) Use of DNA Methyltransferase Endonuclease Enzyme Combinations for Megabase Mapping of Chromosomes, *Method Enzymol.* 216, 279-303.

- (233) Raetz, C. R. H., and Whitfield, C. (2002) Lipopolysaccharide endotoxins, *Annu. Rev. Biochem.* 71, 635-700.
- (234) Raetz, C. R. H., Reynolds, C. M., Trent, M. S., and Bishop, R. E. (2007) Lipid A modification systems in Gram-negative bacteria, *Annu. Rev. Biochem.* 76, 295-329.
- (235) Vaara, M. (1992) Agents That Increase the Permeability of the Outer-Membrane, *Microbiol. Rev.* 56, 395-411.
- (236) Belfiore, C., Castellano, P., and Vignolo, G. (2007) Reduction of *Escherichia coli* population following treatment with bacteriocins from lactic acid bacteria and chelators, *Food Microbiol.* 24, 223-229.
- (237) Boziaris, I. S., and Adams, M. R. (1999) Effect of chelators and nisin produced in situ on inhibition and inactivation of Gram negatives, *Int. J. Food Microbiol.* 53, 105-113.
- (238) Branen, J. K., and Davidson, P. M. (2004) Enhancement of nisin, lysozyme, and monolaurin antimicrobial activities by ethylenediaminetetraacetic acid and lactoferrin, *Int. J. Food Microbiol.* 90, 63-74.
- (239) Cutter, C. N., and Siragusa, G. R. (1995) Treatments with Nisin and Chelators to Reduce *Salmonella* and *Escherichia coli* on Beef, *J. Food Protec.* 58, 1028-1030.
- (240) Delves-Broughton, J. (1993) The Use of EDTA to Enhance the Efficacy of Nisin Towards Gram-Negative Bacteria, *Int. Biodeterior. Biodegrad.* 32, 87-97.

- (241) Gao, Y., van Belkum, M. J., and Stiles, M. E. (1999) The outer membrane of gram-negative bacteria inhibits antibacterial activity of brochocin-C, *Appl. Environ. Microbiol.* 65, 4329-4333.
- (242) Stevens, K. A., Klapes, N. A., Sheldon, B. W., and Klaenhammer, T. R. (1992) Antimicrobial Action of Nisin against *Salmonella typhimurium* Lipopolysaccharide Mutants, *Appl. Environ. Microbiol.* 58, 1786-1788.
- (243) Stevens, K. A., Sheldon, B. W., Klapes, N. A., and Klaenhammer, T. R. (1991) Nisin Treatment for Inactivation of *Salmonella* Species and Other Gram-Negative Bacteria, *Appl. Environ. Microbiol.* 57, 3613-3615.
- (244) Kordel, M., and Sahl, H. G. (1985) Susceptibility of bacterial, eukaryotic and artificial membranes to the disruptive action of the cationic peptides Pep 5 and nisin, *FEMS Microbiol. Lett.* 34, 139-144.
- (245) Boziaris, I. S., and Adams, M. R. (2000) Transient sensitivity to nisin in cold-shocked Gram negatives, *Lett. Appl. Microbiol.* 31, 233-237.
- (246) Boziaris, I. S., and Adams, M. R. (2001) Temperature shock, injury and transient sensitivity to nisin in Gram negatives, *J. Appl. Microbiol.* 91, 715-724.
- (247) Elliason, D. J., and Tatini, S. R. (1999) Enhanced inactivation of *Salmonella typhimurium* and verotoxigenic *Escherichia coli* by nisin at 6.5°C, *Food Microbiol.* 16, 257-267.
- (248) Kalchayanand, N., Hanlin, M. B., and Ray, B. (1992) Sublethal Injury Makes Gram-Negative and Resistant Gram-Positive Bacteria Sensitive to

- the Bacteriocins, Pediocin Ach and Nisin, *Lett. Appl. Microbiol.* 15, 239-243.
- (249) Osmanagaoglu, Ö. (2005) Sensitivity of sublethally injured Gram-negative bacteria to pediocin P, *J. Food Saf.* 25, 266-275.
- (250) Gänzle, M. G., Weber, S., and Hammes, W. P. (1999) Effect of ecological factors on the inhibitory spectrum and activity of bacteriocins, *Int. J. Food Microbiol.* 46, 207-217.
- (251) Zhang, S. S., and Mustapha, A. (1999) Reduction of *Listeria monocytogenes* and *Escherichia coli* O157 : H7 numbers on vacuum-packaged fresh beef treated with nisin or nisin combined with EDTA, *J. Food Prot.* 62, 1123-1127.
- (252) Ukuku, D. O., and Fett, W. F. (2002) Effectiveness of chlorine and nisin-EDTA treatments of whole melons and fresh-cut pieces for reducing native microflora and extending shelf-life, *J. Food Saf.* 22, 231-253.
- (253) Cutter, C. N., and Siragusa, G. R. (1995) Population Reductions of Gram-Negative Pathogens Following Treatments with Nisin and Chelators under Various Conditions, *J. Food Protec.* 58, 977-983.
- (254) Stevens, K. A., Sheldon, B. W., Klapes, N. A., and Klaenhammer, T. R. (1992) Effect of Treatment Conditions on Nisin Inactivation of Gram-Negative Bacteria, *J. Food Prot.* 55, 763-766.
- (255) Abriouel, H., Valdivia, E., Gálvez, A., and Maqueda, M. (1998) Response of *Salmonella choleraesuis* LT2 spheroplasts and permeabilized cells to the bacteriocin AS-48, *Appl. Environ. Microbiol.* 64, 4623-4626.

- (256) Ananou, S., Gálvez, A., Martínez-Bueno, M., Maqueda, M., and Valdivia, E. (2005) Synergistic effect of enterocin AS-48 in combination with outer membrane permeabilizing treatments against *Escherichia coli* O157 : H7, *J. Appl. Microbiol.* 99, 1364-1372.
- (257) Bover-Cid, S., Jofré, A., Aymerich, T., and Garriga, M. (2008) Modeling the combined effects of enterocins A and B, lactate, and EDTA on the growth of *Salmonella* at different temperatures, *Int. Microbiol.* 11, 11-16.
- (258) Murdock, C. A., Cleveland, J., Matthews, K. R., and Chikindas, M. L. (2007) The synergistic effect of nisin and lactoferrin on the inhibition of *Listeria monocytogenes* and *Escherichia coli* O157 : H7, *Lett. Appl. Microbiol.* 44, 255-261.
- (259) Arakawa, K., Kawai, Y., Iioka, H., Tanioka, M., Nishimura, J., Kitazawa, H., Tsurumi, K., and Saito, T. (2009) Effects of gassericins A and T, bacteriocins produced by *Lactobacillus gasseri*, with glycine on custard cream preservation, *J. Dairy Sci.* 92, 2365-2372.
- (260) Faraldo-Gómez, J. D., and Sansom, M. S. P. (2003) Acquisition of siderophores in Gram-negative bacteria, *Nat. Rev. Mol. Cell Biol.* 4, 105-116.
- (261) Vanderhelm, D., Baker, J. R., Engwilmot, D. L., Hossain, M. B., and Loghry, R. A. (1980) Crystal-Structure of Ferrichrome and a Comparison with the Structure of Ferrichrome-A, *J. Am. Chem. Soc.* 102, 4224-4231.
- (262) Emery, T., and Neilands, J. B. (1959) Iron-Binding Centre of Ferrichrome Compounds, *Nature* 184, 1632-1633.

- (263) Harris, W. R., and Raymond, K. N. (1979) Ferric Ion Sequestering Agents. 3. Spectrophotometric and Potentiometric Evaluation of 2 New Enterobactin Analogs: 1,5,9-N,N',N''-Tris(2,3-dihydroxybenzoyl)-cyclotriazatridecane and 1,3,5-N,N',N''-Tris(2,3-dihydroxybenzoyl)triaminomethylbenzene, *J. Am. Chem. Soc.* *101*, 6534-6541.
- (264) Budzikiewicz, H. (2005) Bacterial Citrate Siderophores, *Mini-Rev Org Chem* *2*, 119-124.
- (265) Duquesne, S., Destoumieux-Garzón, D., Peduzzi, J., and Rebuffat, S. (2007) Microcins, gene-encoded antibacterial peptides from enterobacteria, *Nat. Prod. Rep.* *24*, 708-734.
- (266) Fath, M. J., Zhang, L. H., Rush, J., and Kolter, R. (1994) Purification and Characterization of Colicin V from *Escherichia coli* Culture Supernatants, *Biochemistry* *33*, 6911-6917.
- (267) Pons, A. M., Delalande, F., Duarte, M., Benoit, S., Lanneluc, I., Sablé, S., Van Dorsselaer, A., and Cottenceau, G. (2004) Genetic analysis and complete primary structure of microcin L, *Antimicrob. Agents Chemother.* *48*, 505-513.
- (268) Bayro, M. J., Mukhopadhyay, J., Swapna, G. V. T., Huang, J. Y., Ma, L. C., Sineva, E., Dawson, P. E., Montelione, G. T., and Ebright, R. H. (2003) Structure of antibacterial peptide microcin J25: A 21-residue lariat protoknot, *J. Am. Chem. Soc.* *125*, 12382-12383.

- (269) Rosengren, K. J., Clark, R. J., Daly, N. L., Göransson, U., Jones, A., and Craik, D. J. (2003) Microcin J25 has a threaded sidechain-to-backbone ring structure and not a head-to-tail cyclized backbone, *J. Am. Chem. Soc.* *125*, 12464-12474.
- (270) Wilson, K. A., Kalkum, M., Ottesen, J., Yuzenkova, J., Chait, B. T., Landick, R., Muir, T., Severinov, K., and Darst, S. A. (2003) Structure of microcin J25, a peptide inhibitor of bacterial RNA polymerase, is a lassoed tail, *J. Am. Chem. Soc.* *125*, 12475-12483.
- (271) Bayer, A., Freund, S., and Jung, G. (1995) Posttranslational Heterocyclic Backbone Modifications in the 43-Peptide Antibiotic Microcin B17: Structure Elucidation and NMR Study of a  $^{13}\text{C}$ ,  $^{15}\text{N}$ -Labeled Gyrase Inhibitor, *Eur. J. Biochem.* *234*, 414-426.
- (272) Videnov, G., Kaiser, D., Brooks, M., and Jung, G. (1996) Synthesis of the DNA gyrase inhibitor microcin B17, a 43-peptide antibiotic with eight aromatic heterocycles in its backbone, *Angew. Chem.-Int. Edit. Engl.* *35*, 1506-1508.
- (273) Thomas, X., Destoumieux-Garzón, D., Peduzzi, J., Afonso, C., Blond, A., Birlirakis, N., Goulard, C., Dubost, L., Thai, R., Tabet, J. C., and Rebuffat, S. (2004) Siderophore peptide, a new type of post-translationally modified antibacterial peptide with potent activity, *J. Biol. Chem.* *279*, 28233-28242.
- (274) Laviña, M., Pugsley, A. P., and Moreno, F. (1986) Identification, Mapping, Cloning and Characterization of a Gene (*sbmA*) Required for

- Microcin-B17 Action on *Escherichia coli* K12, *J. Gen. Microbiol.* *132*, 1685-1693.
- (275) del Castillo, F. J., del Castillo, I., and Moreno, F. (2001) Construction and characterization of mutations at codon 751 of the *Escherichia coli gyrB* gene that confer resistance to the antimicrobial peptide microcin B17 and alter the activity of DNA gyrase, *J. Bacteriol.* *183*, 2137-2140.
- (276) Fomenko, D. E., Metlitskaya, A. Z., Péduzzi, J., Goulard, C., Katrukha, G. S., Gening, L. V., Rebuffat, S., and Khmel, I. A. (2003) Microcin C51 plasmid genes: Possible source of horizontal gene transfer, *Antimicrob. Agents Chemother.* *47*, 2868-2874.
- (277) Guijarro, J. I., González-Pastor, J. E., Baleux, F., Millán, J. L. S., Castilla, M. A., Rico, M., Moreno, F., and Delepierre, M. (1995) Chemical-Structure and Translation Inhibition Studies of the Antibiotic Microcin C7, *J. Biol. Chem.* *270*, 23520-23532.
- (278) Metlitskaya, A., Kazakov, T., Kommer, A., Pavlova, O., Praetorius-Ibba, M., Ibba, M., Krasheninnikov, I., Kolb, V., Khmel, I., and Severinov, K. (2006) Aspartyl-tRNA synthetase is the target of peptide nucleotide antibiotic Microcin C, *J. Biol. Chem.* *281*, 18033-18042.
- (279) Van de Vijver, P., Vondenhoff, G. H. M., Kazakov, T. S., Semenova, E., Kuznedelov, K., Metlitskaya, A., Van Aerschot, A., and Severinov, K. (2009) Synthetic Microcin C Analogs Targeting Different Aminoacyl-tRNA Synthetases, *J. Bacteriol.* *191*, 6273-6280.

- (280) Adelman, K., Yuzenkova, J., La Porta, A., Zenkin, N., Lee, J., Lis, J. T., Borukhov, S., Wang, M. D., and Severinov, K. (2004) Molecular mechanism of transcription inhibition by peptide antibiotic microcin J25, *Mol. Cell.* *14*, 753-762.
- (281) Mukhopadhyay, J., Sineva, E., Knight, J., Levy, R. M., and Ebright, R. H. (2004) Antibacterial peptide microcin J25 inhibits transcription by binding within and obstructing the RNA polymerase secondary channel, *Mol. Cell* *14*, 739-751.
- (282) Chehade, H., and Braun, V. (1988) Iron-Regulated Synthesis and Uptake of Colicin-V, *FEMS Microbiol. Lett.* *52*, 177-182.
- (283) Yang, C. C., and Konisky, J. (1984) Colicin V Treated *Escherichia coli* Does Not Generate Membrane-Potential, *J. Bacteriol.* *158*, 757-759.
- (284) Bieler, S., Silva, F., Soto, C., and Belin, D. (2006) Bactericidal activity of both secreted and nonsecreted microcin e492 requires the mannose permease, *J. Bacteriol.* *188*, 7049-7061.
- (285) Freund, S., Jung, G., Gutbrod, O., Folkers, G., Gibbons, W. A., Allgaier, H., and Werner, R. (1991) The Solution Structure of the Lantibiotic Gallidermin, *Biopolymers* *31*, 803-811.
- (286) Böttiger, T., Schneider, T., Martinez, B., Sahl, H. G., and Wiedemann, I. (2009) Influence of Ca<sup>2+</sup> Ions on the Activity of Lantibiotics Containing a Mersacidin-Like Lipid II Binding Motif, *Appl. Environ. Microbiol.* *75*, 4427-4434.

- (287) Schägger, H., and von Jagow, G. (1987) Tricine-sodium dodecyl sulfate-polyacrylamide gel electrophoresis for the separation of proteins in the range from 1 kDa to 100 kDa, *Anal. Biochem.* 166, 368-379.
- (288) Dai, Y. Q., Whittal, R. M., and Li, L. (1999) Two-layer sample preparation: A method for MALDI-MS analysis of complex peptide and protein mixtures, *Anal. Chem.* 71, 1087-1091.
- (289) Sambrook, J., and Russell, D. W. (2001) *Molecular Cloning: a laboratory manual*, 3rd ed., Cold Spring Harbor Laboratory Press, Cold Spring Harbor, N.Y.
- (290) van Belkum, M. J., and Stiles, M. E. (2006) Characterization of the theta-type plasmid pCD3.4 from *Carnobacterium divergens*, and modulation of its host range by RepA mutation, *Microbiology* 152, 171-178.
- (291) van de Guchte, M., van der Vossen, J. M. B. M., Kok, J., and Venema, G. (1989) Construction of a Lactococcal Expression Vector: Expression of Hen Egg White Lysozyme in *Lactococcus lactis* subsp. *lactis*, *Appl. Environ. Microbiol.* 55, 224-228.
- (292) Franz, C. M. A. P., Schillinger, U., and Holzappel, W. H. (1996) Production and characterization of enterocin 900, a bacteriocin produced by *Enterococcus faecium* BFE 900 from black olives, *Int. J. Food Microbiol.* 29, 255-270.
- (293) Ma, B., Zhang, K. Z., Hendrie, C., Liang, C. Z., Li, M., Doherty-Kirby, A., and Lajoie, G. (2003) PEAKS: powerful software for peptide *de novo*

- sequencing by tandem mass spectrometry, *Rapid Comm. Mass Spectrom.* *17*, 2337-2342.
- (294) Morrow, J. A., Segall, M. L., Lund-Katz, S., Phillips, M. C., Knapp, M., Rupp, B., and Weisgraber, K. H. (2000) Differences in stability among the human apolipoprotein E isoforms determined by the amino-terminal domain, *Biochemistry* *39*, 11657-11666.
- (295) Delaglio, F., Grzesiek, S., Vuister, G. W., Zhu, G., Pfeifer, J., and Bax, A. (1995) NMRPIPE: A multidimensional spectral processing system based on unix pipes, *J. Biomol. NMR* *6*, 277-293.
- (296) Johnson, B. A., and Blevins, R. A. (1994) NMR View: A computer program for the visualization and analysis of NMR data, *J. Biomol. NMR* *4*, 603-614.
- (297) Baker, N. A., Sept, D., Joseph, S., Holst, M. J., and McCammon, J. A. (2001) Electrostatics of nanosystems: Application to microtubules and the ribosome, *Proc. Natl. Acad. Sci. U. S. A.* *98*, 10037-10041.
- (298) Guex, N., Diemand, A., and Peitsch, M. C. (1999) Protein modelling for all, *Trends Biochem.Sci.* *24*, 364-367.
- (299) Koradi, R., Billeter, M., and Wüthrich, K. (1996) MOLMOL: A program for display and analysis of macromolecular structures, *J. Mol. Graphics* *14*, 51-55.
- (300) Dolinsky, T. J., Nielsen, J. E., McCammon, J. A., and Baker, N. A. (2004) PDB2PQR: an automated pipeline for the setup of Poisson-Boltzmann electrostatics calculations, *Nucleic Acids Res.* *32*, 665-667.

## Appendix A. NMR Solution structure of ColV

### A.1. Background

This thesis has focused exclusively on the bacteriocins produced by Gram-positive bacteria, in particular lactic acid bacteria. However, as described in chapter five, Gram-negative bacteria also produce bacteriocins, including the microcins and the colicins. In fact, the first bacteriocin ever reported was produced by *E. coli* V and hence, referred to as colicin V (1, 2). Despite its name, colicin V (ColV) is significantly smaller than other colicins, and instead, belongs to the microcin family of bacteriocins. It has subsequently been renamed microcin V (MccV), but is still commonly referred to as ColV.

Although ColV was first described in 1925, it wasn't isolated and fully characterized until 1994 (3, 4), as its purification was hindered by its instability and hydrophobic properties. However, once purified, analysis by Edman sequencing and mass spectrometry revealed that ColV is an 88 aa protein, with a disulfide bond linking C76 and C87 (4). It has been suggested that ColV may bind iron and that the C-terminal domain of the protein, in particular the cysteine residues, may play a key role in such binding (3). ColV exerts its killing action by forming pores in the cytoplasmic membrane of sensitive cells (5).

Recently, the primary sequence of microcin L (MccL) was reported and found to be remarkably similar to ColV, particularly in the C-terminus, with 87.5% identity across the last 32 residues (6). The N-terminal domain of both peptides is hydrophobic, whereas the C-terminal domain is largely hydrophilic.



in order to better understand the mechanism by which it is recognized and transported across the outer membrane of target cells.

## **A.2. Results & Discussion**

### **A.2.1. Purification of ColV**

Using the plasmid pMAL-ColV, constructed by Dr. Lucas Gursky, ColV was overexpressed as a maltose-binding fusion protein in both unlabelled and isotopically enriched media. Using the unlabelled fusion protein, the various steps required to obtain pure ColV (amylose chromatography, Factor Xa digestion and HPLC purification) were optimized. The MalE-ColV fusion protein was purified via affinity chromatography using amylose resin. To remove the MalE affinity tag from ColV, the fusion protein was treated with 1% Factor Xa (w/w) for ~12 h. During the digestion, precipitation was often observed, which resulted in a poor overall yield of the peptide. ColV was purified by RP-HPLC and its identity confirmed by MALDI-TOF.

### **A.2.2. NMR spectroscopy of ColV**

[<sup>13</sup>C,<sup>15</sup>N]ColV was initially dissolved in 90% H<sub>2</sub>O/10% D<sub>2</sub>O to a concentration of ~0.5 mM and an <sup>15</sup>N HSQC spectrum was acquired at 22°C. However, the spectrum showed poor spectral dispersion, as many of the amide resonances were either overlapped, or clustered within a narrow chemical shift range (~0.5 ppm for <sup>1</sup>H). The experiment was repeated at different temperatures (10°C and 30°C) to see if the spectra would improve. However, very little change

was observed, as illustrated in Fig. A.2A. ColV was also subjected to buffering conditions (20 mM sodium phosphate, pH 6.7), but again, no changes were observed. Poor spectral dispersion suggested that ColV was likely unstructured and random coil in aqueous conditions. Trifluoroethanol is a membrane-mimicking solvent and has been shown to induce helicity in many type IIa bacteriocins (10-14). Therefore, we added  $d_3$ -TFE to the NMR sample, to see if ColV would assume secondary structure. However, as shown in Fig. A.2B, the spectral dispersion worsened upon the addition of 15%  $d_3$ -TFE.

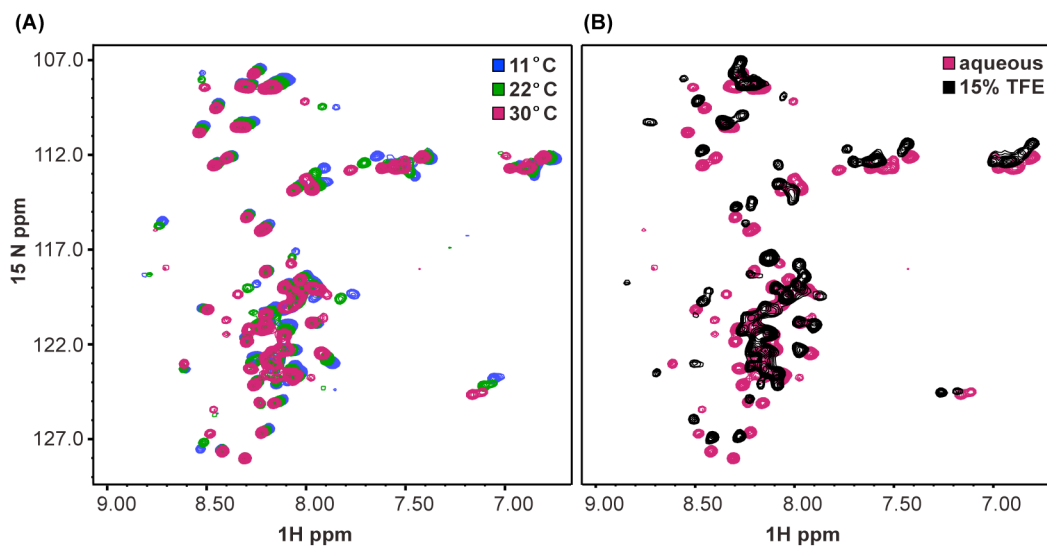


**FIG. A.2.**  $^{15}\text{N}$  HSQC spectra of ColV in aqueous and membrane-mimicking conditions. (A) The effect of temperature on spectral dispersion, in aqueous conditions. (B) Comparing the effect of aqueous and membrane-mimicking conditions on spectral dispersion (at room temperature).

Despite the high degree of overlap and likelihood that ColV was random coil, additional NMR analysis of ColV (in aqueous conditions) was performed. Using the  $^{15}\text{N}$  HSQC, HNCACB and CBCA(CO)NH experiments, most (80%) of the backbone resonances (H, HN and  $\text{C}\alpha$ ), as well as  $\text{C}\beta$ , were assigned. The

chemical shifts of the  $\beta$ -carbons of cysteine residues are known to be highly sensitive to the oxidation state of the cysteine. Typical  $C\beta$  chemical shifts for reduced and oxidized cysteines are  $28.4 \pm 2.4$  ppm and  $40.7 \pm 3.8$  ppm, respectively (15). For ColV, the  $C\beta$  chemical shifts of C76 and C87 were found to be 43.2 and 44.8 ppm, respectively, thus confirming the presence of the disulfide bond.

Unfortunately, chemical shift index (CSI) analysis (16) of the  $\alpha$ -carbons indicated that ColV was likely random coil, in agreement with our previous findings based on the  $^{15}\text{N}$  HSQC. Furthermore, of the 17 residues that could not be assigned (excluding the first residue), 11 of them resided within the C-terminal domain that is implicated in ColV uptake. Thus, we would be unable to determine any structural elements within that region. No further structural analysis of ColV was undertaken.

Since ColV acts as a pore former, we hypothesized that the hydrophobic, N-terminal domain of this peptide would adopt a helical structure. However, our results from NMR did not confirm this. In addition, secondary structure prediction, using either the Jpred3 (17) or the PSIPred (18) servers further indicates that ColV is largely unstructured.

### **A.3. Conclusions**

Colicin V, a microcin produced by *E. coli*, is the oldest known bacteriocin. It is an 88 aa peptide, whose activity depends on the presence of a N-terminal domain that causes pore formation, and a C-terminal domain required for uptake

into sensitive cells. We had hoped that the 3D structure of ColV would provide structural insight into how this bacteriocin is recognized by the Cir outer membrane receptor, and hence imported into target cells. Unfortunately, we were unable to obtain such information. It may well be that ColV only assumes defined structure when in the presence of its receptor Cir.

## A.4. Experimental Procedures

### A.4.1. Plasmids, bacterial strains and culture conditions

The plasmids and bacterial strains used in this study are listed in Table A.1. All biological experiments were performed under sterile conditions. All materials and solutions were autoclaved (121°C, 15 min) prior to use, except for ampicillin, glucose and IPTG stock solutions, which were filter sterilized. For overexpression of unlabeled protein, cultures were grown in LB broth at 37°C, 200 rpm. For overexpression of labeled protein, cultures were grown in Celtone-CN rich media (Spectra Stable Isotopes), supplemented with 5 mL of 20% glucose. Media containing ampicillin (100 µg/mL) was used for selection of transformants. Stock cultures were maintained at -80°C in LB broth supplemented with 20% glycerol.

**TABLE A.1.** Plasmids and bacterial strains used for investigation of ColV

Plasmid or Stain	Relevant Characteristics <sup>b</sup>	Ref. or Source
pMAL <sup>TM</sup> -c2X	PTAC promoter, Amp <sup>r</sup> , <i>lacI</i> , <i>lacZα</i> and <i>malE</i> expression vector, 6648 bp	NEB
<sup>a</sup> pMAL-ColV	pMAL <sup>TM</sup> -c2X containing <i>malE-FXA-colV</i> (without leader sequence) fusion	This study
<i>E. coli</i> K12 TB1	F <sup>-</sup> <i>ara</i> Δ( <i>lac-proAB</i> ) [Φ80 <i>dlac</i> Δ( <i>lacZ</i> )M15] <i>rpsL</i> (Str <sup>R</sup> ) <i>thi</i> <i>hsdR</i>	NEB

<sup>a</sup> prepared by Dr. Lucas Gursky; <sup>b</sup> FXA denotes the Factor Xa recognition sequence (IEGR)

#### A.4.2. Preparation of [<sup>13</sup>C,<sup>15</sup>N]ColV

##### A.4.2.a. Overexpression and purification of MalE-ColV

Dr. Karen Kawulka initially determined growth conditions for the overexpression of unlabeled and doubly labeled MalE-ColV. Overnight cultures of *E. coli* TB1 K12, harboring the plasmid pMAL-ColV, were grown in 5 mL of LB broth (100 µg/mL ampicillin) and incubated at 37°C, 200 rpm for 16–18 h. 3 × 500 mL of either unlabelled or labeled media (100 µg/mL ampicillin) was inoculated (1%) with the overnight culture and incubated at 37°C, 200 rpm. When the OD<sub>600</sub> reached ~0.55, IPTG (final conc. of 0.3 mM) was added and the cultures were incubated for an additional 3 h at 37°C, 200 rpm. The cells were harvested by centrifugation (11,300 × g, 20 min, 4°C) and resuspended in ~60 mL of amylose column buffer (20 mM Tris-Cl pH 7.2, 100 mM NaCl, 1 mM EDTA, 1 mM NaN<sub>3</sub>, 1 mM DTT). The suspension was transferred to 2 × 50 mL centrifuge bottles, each containing one complete EDTA-Free, protease inhibitors cocktail tablet (Roche Diagnostic). The solutions were stored at -20°C.

The cells were lysed by three cycles of freeze-thaw, followed by sonication. After centrifugation (27,200 × g, 30 min, 4°C), the cleared lysate was diluted to 300 mL with amylose column buffer and loaded onto an amylose column (50 mL resin, 2.5 × 50 cm) at 1 mL/min. The column was washed with 500 mL amylose column buffer, after which the fusion protein was eluted by addition of 10 mM maltose to the buffer. 5 min fractions were collected during the elution and the UV<sub>280</sub> was monitored. Fractions containing the eluted protein (as shown by UV<sub>280</sub>) were combined, transferred to dialysis tubing (MWCO 12 –

14 kDa) and dialyzed against 3.5 L of H<sub>2</sub>O (4°C, refreshed 3 times, 4 h each). The protein solution was then frozen (-20°C, then -80°C), lyophilized and stored at -20°C. From 1.5 L of culture, ~65 mg of labeled fusion protein was obtained

#### **A.4.2.b. Factor Xa digestion**

Pilot studies and large-scale digestions were initially performed on the unlabelled MalE-ColV fusion protein to allow for optimization of conditions. In addition, HPLC purification conditions (see below) were developed using the unlabelled digested fusion protein, before proceeding with the digestion and purification of the doubly labeled sample. MALDI-TOF and SDS-PAGE were used to monitor cleavage and purification of the proteins.

The [<sup>13</sup>C, <sup>15</sup>N]-fusion protein was resuspended in Factor Xa buffer (20 mM Tris-Cl pH 7.4, 100 mM NaCl, 1 mM CaCl<sub>2</sub>), to yield a 1 mg/mL solution. Digestion proceeded by the addition of 1% Factor Xa (w/w) and the mixture was incubated at room temperature for 8h with gentle rocking. The sample was immediately purified by HPLC.

#### **A.4.2.c. RP-HPLC purification**

After developing HPLC purification conditions using the unlabelled sample, [<sup>13</sup>C, <sup>15</sup>N]ColV was purified from [<sup>13</sup>C, <sup>15</sup>N]MalE by RP-HPLC, using a preparative C<sub>18</sub> column (Waters Nova-Pak cartridge, 300 Å pore size, 15 µm particle size), on a Varian Prostar HPLC. MeCN (0.075% TFA) and H<sub>2</sub>O (0.075% TFA) were used as solvents, according to the following gradient: (1) hold at 30%

MeCN for 5 min; (2) increase to 50% MeCN over 30 min; (3) increase to 100% MeCN over 2 min; (4) hold at 100% MeCN for 3 min; (5) decrease to 30% MeCN over 2 min; (6) hold at 30% MeCN for 8 min. The method employed 3.0 mL injections, a flow rate of 10 mL/min and detection at 220 nm. Both [ $^{13}\text{C}$ ,  $^{15}\text{N}$ ]ColV and [ $^{13}\text{C}$ ,  $^{15}\text{N}$ ]MalE were isolated as single peaks, with retention times of 23 min and 28–30 min, respectively, as identified by MALDI-TOF. To prevent oxidation, argon was bubbled through the purified [ $^{13}\text{C}$ ,  $^{15}\text{N}$ ]ColV sample and it was stored on ice. Following HPLC, the [ $^{13}\text{C}$ ,  $^{15}\text{N}$ ]ColV sample was concentrated by rotary evaporation, frozen and lyophilized. From 65 mg of fusion protein, ~1.2 mg of purified [ $^{13}\text{C}$ ,  $^{15}\text{N}$ ]ColV was obtained (~11% yield).

#### A.4.3. NMR spectroscopy of [ $^{13}\text{C}$ , $^{15}\text{N}$ ]ColV

[ $^{13}\text{C}$ ,  $^{15}\text{N}$ ]ColV was initially dissolved 90%  $\text{H}_2\text{O}$ /10%  $\text{D}_2\text{O}$ , 1 mM EDTA, 1 mM  $\text{NaN}_3$  and 50  $\mu\text{M}$  2,2-dimethyl-2-silapentane-5-sulfonate sodium salt (DSS), to a concentration of ~0.5 mM. The pH was measured to be ~5.9. A high quality  $\text{D}_2\text{O}$  matched Shigemi NMR tube was used. NMR spectra were acquired on a Varian Inova 500 MHz spectrometer equipped with a triple-resonance HCN cold probe and z-axis pulsed-field gradients. To examine the effect of temperature on spectral dispersion, a series of  $^{15}\text{N}$  HSQC experiments were recorded at 11°C, 22°C and 30°C.  $d_3$ -TFE was also added to the sample (15%) in an attempt to enhance spectral dispersion. To remove  $d_3$ -TFE, the sample was frozen and the NMR tube was placed under vacuum until all solvent had sublimed. The contents of the tube were then redissolved in an equivalent volume of 90%  $\text{H}_2\text{O}$ /10%  $\text{D}_2\text{O}$

20 mM sodium phosphate (pH 6.7), but this did not enhance spectral dispersion either. A second sample of [ $^{13}\text{C}$ , $^{15}\text{N}$ ]ColV was dissolved in 90%  $\text{H}_2\text{O}$ /10%  $\text{D}_2\text{O}$  (with EDTA,  $\text{NaN}_3$  and DSS added, as described above). For backbone  $^1\text{H}$ ,  $^{13}\text{C}$ , and  $^{15}\text{N}$  resonance assignments, the following experiments were recorded at 30°C:  $^{15}\text{N}$  HSQC, HNCACB and CBCA(CO)NH. NMR spectra were processed using NMRPIPE (19) and analyzed with NMRView (20). Data were multiplied by a 90° shifted sine-bell squared function in all dimensions. Indirect dimensions were doubled by linear prediction and zero-filled to the nearest power of two prior to Fourier transformation.

## A.5. References

- (1) Gratia, A. (1925) Sur un remarquable exemple d'antagonisme entre deux souches de Colibacille, *C. R. Soc. Biol.* 93, 1040–1041 (in French).
- (2) Fredericq, P. (1946) Sur la pluralité des récepteurs d'antibiose de *E. coli*, *C. R. Soc. Biol.* 140, 1189–1194 (in French).
- (3) Fath, M. J., Zhang, L. H., Rush, J., and Kolter, R. (1994) Purification and Characterization of Colicin V from *Escherichia coli* Culture Supernatants, *Biochemistry* 33, 6911-6917.
- (4) Håvarstein, L. S., Holo, H., and Nes, I. F. (1994) The Leader Peptide of Colicin-V Shares Consensus Sequences with Leader Peptides That Are Common among Peptide Bacteriocins Produced by Gram-Positive Bacteria, *Microbiology* 140, 2383-2389.

- (5) Yang, C. C., and Konisky, J. (1984) Colicin V Treated *Escherichia coli* Does Not Generate Membrane-Potential, *J. Bacteriol.* 158, 757-759.
- (6) Pons, A. M., Delalande, F., Duarte, M., Benoit, S., Lanneluc, I., Sablé, S., Van Dorsselaer, A., and Cottenceau, G. (2004) Genetic analysis and complete primary structure of microcin L, *Antimicrob. Agents Chemother.* 48, 505-513.
- (7) Chehade, H., and Braun, V. (1988) Iron-Regulated Synthesis and Uptake of Colicin-V, *FEMS Microbiol. Lett.* 52, 177-182.
- (8) Duquesne, S., Destoumieux-Garzón, D., Peduzzi, J., and Rebuffat, S. (2007) Microcins, gene-encoded antibacterial peptides from enterobacteria, *Nat. Prod. Rep.* 24, 708-734.
- (9) Azpiroz, M. F., and Laviña, M. (2007) Modular structure of microcin H47 and colicinV, *Antimicrob. Agents Chemother.* 51, 2412-2419.
- (10) Kaur, K., Andrew, L. C., Wishart, D. S., and Vederas, J. C. (2004) Dynamic relationships among type IIa bacteriocins: Temperature effects on antimicrobial activity and on structure of the C-terminal amphipathic  $\alpha$  helix as a receptor-binding region, *Biochemistry* 43, 9009-9020.
- (11) Martin-Visscher, L. A., Sprules, T., Gursky, L. J., and Vederas, J. C. (2008) Nuclear magnetic resonance solution structure of PisI, a group B immunity protein that provides protection against the type IIa bacteriocin piscicolin 126, PisA, *Biochemistry* 47, 6427-6436.
- (12) Sprules, T., Kawulka, K. E., Gibbs, A. C., Wishart, D. S., and Vederas, J. C. (2004) NMR solution structure of the precursor for carnobacteriocin

- B2, an antimicrobial peptide from *Carnobacterium piscicola*: Implications of the  $\alpha$ -helical leader section for export and inhibition of type IIa bacteriocin activity, *Eur. J. Biochem.* 271, 1748-1756.
- (13) Gallagher, N. L. F., Sailer, M., Niemczura, W. P., Nakashima, T. T., Stiles, M. E., and Vederas, J. C. (1997) Three-dimensional structure of leucocin A in trifluoroethanol and dodecylphosphocholine micelles: Spatial location of residues critical for biological activity in type IIa bacteriocins from lactic acid bacteria, *Biochemistry* 36, 15062-15072.
- (14) Uteng, M., Hauge, H. H., Markwick, P. R. L., Fimland, G., Mantzilas, D., Nissen-Meyer, J., and Muhle-Goll, C. (2003) Three-dimensional structure in lipid micelles of the pediocin-like antimicrobial peptide sakacin P and a sakacin P variant that is structurally stabilized by an inserted C-terminal disulfide bridges, *Biochemistry* 42, 11417-11426.
- (15) Sharma, D., and Rajarathnam, K. (2000)  $^{13}\text{C}$  NMR chemical shifts can predict disulfide bond formation, *J. Biomol. NMR* 18, 165-171.
- (16) Wishart, D. S., and Sykes, B. D. (1994) The  $^{13}\text{C}$  Chemical-Shift Index: A simple method for the identification of protein secondary structure using  $^{13}\text{C}$  chemical-shift data, *J. Biomol. NMR* 4, 171-180.
- (17) Cole, C., Barber, J. D., and Barton, G. J. (2008) The Jpred 3 secondary structure prediction server, *Nucleic Acids Res.* 36, W197-W201.
- (18) McGuffin, L. J., Bryson, K., and Jones, D. T. (2000) The PSIPRED protein structure prediction server, *Bioinformatics* 16, 404-405.

- (19) Delaglio, F., Grzesiek, S., Vuister, G. W., Zhu, G., Pfeifer, J., and Bax, A. (1995) NMRPIPE: A multidimensional spectral processing system based on unix pipes, *J. Biomol. NMR* 6, 277-293.
- (20) Johnson, B. A., and Blevins, R. A. (1994) NMR View: A computer program for the visualization and analysis of NMR data, *J. Biomol. NMR* 4, 603-614.